



*Ministero dell'Istruzione,
dell'Università e della Ricerca*



UNIVERSITÀ DEGLI STUDI DI SALERNO


Dipartimento di Ingegneria Civile

*Dottorato di Ricerca
in
Rischio e Sostenibilità
nei Sistemi dell'Ingegneria Civile, Edile ed Ambientale*

XXXIV Ciclo (2018-2022)

**APPLICATION OF MEMBRANE TECHNOLOGY
FOR FOOD INDUSTRY WASTEWATER
TREATMENT AND RESOURCE RECOVERY**

Md. Nahid Pervez


Il Tutor
Prof. Vincenzo Naddo

Co-Tutor
Prof. Ing. Tiziano Zarra



Il Coordinatore
Prof. Fernando Fraternali



“Bismillah al-Rahman al-Rahim”

In the name of Allah, the Most Gracious, the Most Merciful

CONTENTS

CONTENTS	i
LIST OF FIGURES	v
LIST OF TABLES	ix
ABSTRACT	xi
ACKNOWLEDGEMENTS	xiii
ABOUT THE AUTHOR	xiv
LIST OF PUBLICATIONS	xv
1. INTRODUCTION	1
1.1 Objectives	4
1.2 Outlines	5
2. WASTEWATER TREATMENT IN FOOD INDUSTRY	7
2.1 Characteristics of food industry wastewater	8
2.2 Membrane bioreactor	10
2.3 Pressure-Driven Membrane Filtration	12
2.4 Membrane distillation	15
2.5 Electrodialysis	17
2.6 Forward osmosis	18
2.7 Electrospun nanofiber membranes	19
2.8 Membrane fouling	24
3. RESOURCE RECOVERY FROM FOOD WASTE	26
3.1 Adsorption	29
3.2 Distillation	31
3.3 Precipitation	32
3.4 Esterification	33
3.5 Extraction	34
3.6 Gas stripping	36
3.7 Membrane contactor	36
3.8 Membrane distillation	38

3.9	Electrodialysis	39
3.10	Pervaporation	41
3.11	Forward osmosis	42
3.12	Pressure-driven membrane filtration	44
3.13	Factors affecting pressure driven membrane-assisted recovery of VFAs	47
3.13.1	Membrane material	47
3.13.2	Membrane pore size and molecular weight cut-off	49
3.13.3	Membrane charge	53
3.13.4	Membrane hydrophilicity/phobicity	53
3.13.5	VFAs concentrations	64
3.13.6	Medium pH	64
3.13.7	Operating temperature	66
3.13.8	Ionic strength	66
4.	DEVELOPMENT OF ELECTROSPUN NANOFIBER MEMBRANES FOR FOOD INDUSTRY WASTEWATER TREATMENT	73
4.1	One-step fabrication of novel polyethersulfone-based composite electrospun nanofibers membrane for food industry wastewater treatment	73
4.1.1	Introduction	73
4.1.2	Materials and methods	75
4.1.3	Results and Discussion	79
4.2	Fabrication of polyethersulfone/polyacrylonitrile electrospun nanofiber membrane for food industry wastewater treatment	94
4.2.1	Introduction	94
4.2.2	Materials and methods	97
4.2.3	Results and Discussion	99
5.	PROCESS INTENSIFICATION OF PRESSURE-DRIVEN MEMBRANE FILTRATION FOR RESOURCE RECOVERY FROM FOOD WASTE	113
5.1	Double-stage membrane-assisted anaerobic digestion process intensification for production and recovery of volatile fatty acids from food waste	113
5.1.1	Introduction	113
5.1.2	Materials and methods	115
5.1.3	Results and Discussion	120
5.2	Feasibility of nanofiltration process for high efficient recovery and concentrations of food waste-derived volatile fatty acids	137
5.2.1	Introduction	137
5.2.2	Materials and methods	139

5.2.3 Results and Discussion	142
6. CONCLUSIONS AND FUTURE PERSPECTIVE	156
REFERENCES	159

LIST OF FIGURES

Figure 1.1 Waste generation framework of the food industry.....	1
Figure 2.1 Typical representation of anaerobic MBR (AnMBR) and aerobic MBR (AMBR).....	11
Figure 2.2 Typical representation of pressure-driven membrane process.....	13
Figure 2.3. Representative diagram of membrane distillation process.	16
Figure 2.4 Conventional electrodialysis set up for wastewater treatment.....	18
Figure 2.5 Schematic diagram of Forward osmosis (FO) process	19
Figure 2.6 Electrospinning process for nanofiber membrane preparation and their uses in dyes removal.	21
Figure 3.1 (a) Production pathway of VFAs (Wainaina et al., 2019d) and (b) Application of VFAs with their market feasibility (Atasoy et al., 2018).	27
Figure 3.2 VFAs recovery by adsorption process (Reyhanitash et al., 2017).	30
Figure 3.3 VFAs recovery by the solvent extraction process (Aghapour Aktij et al., 2020b).....	35
Figure 3.4 Tentative MD process scheme for VFAs recovery (Aghapour Aktij et al., 2020b).	38
Figure 3.5 Tentative CED process scheme for VFAs recovery (Aghapour Aktij et al., 2020b).	40
Figure 3.6 Tentative PV process scheme for VFAs recovery (Khalid et al., 2019).	41
Figure 3.7 Tentative FO process scheme for VFAs recovery (Zhang et al., 2020).	43
Figure 3.8 Pressure driven membrane filtration process for VFAs recovery (Liao et al., 2018).	45
Figure 4.1 Illustration of one-step electrospinning nanofiber membrane fabrication process	77
Figure 4.2 Image of the electrospinning nanofiber membrane fabrication commercial machine.....	77
Figure 4.3 SEM images and average diameter distribution of pristine PES (a, c) and	

PES/HPC (b, d) nanofiber membranes.	80
Figure 4.4 FTIR spectra of PES and PES/HPC nanofiber membranes.	81
Figure 4.5 XRD pattern of PES and PES/HPC nanofiber membranes.	82
Figure 4.6 TGA curves of PES and PES/HPC nanofiber membranes.	83
Figure 4.7 Stress-strain curve of PES and PES/HPC nanofiber membranes.	84
Figure 4.8 Water contact angle of pristine PES (a) and PES/HPC nanofiber membranes with their surface states (c) and (d), respectively.....	85
Figure 4.9 Effect of initial concentrations on the MB adsorption capacity of PES and PES/HPC nanofiber membrane.....	86
Figure 4.10 Pseudo-first-order kinetic model and pseudo-second-order kinetic model for the MB adsorption on PES (a) and PES/HPC (b).....	87
Figure 4.11 The adsorption isotherms of MB by PES (a) and PES/HPC (b) according to Langmuir and Freundlich equations.	89
Figure 4.12 Effect of pH on the MB adsorption capacity.	91
Figure 4.13 Proposed adsorption mechanism of MB in the presence of PES/HPC nanofiber membrane.	92
Figure 4.14 Illustration of electrospun nanofiber membrane fabrication process...	97
Figure 4.15 SEM images and water contact angle of pristine PES (a, c) and PES/PAN (b, d) nanofiber membranes; insets are the diameter distribution of corresponding nanofiber membranes.	101
Figure 4.16 FTIR spectra (a), XRD patterns (b), TGA profiles (c) and stress-strain curve (d) of PES and PES/PAN nanofiber membranes.	103
Figure 4.17 Effect of pH on MB adsorption capacity (a) and zeta potential (b) of PES and PES/PAN electrospun nanofiber membranes.	105
Figure 4.18 Effect of MB concentrations on adsorption capacity of PES and PES/PAN fiber membrane.....	106
Figure 4.19 Pseudo-first-order kinetic model and pseudo-second-order kinetic model for the MB adsorption on PES (a) and PES/PAN (b).....	106
Figure 4.20 The adsorption isotherms of MB by PES (a) and PES/PAN (b) according to Langmuir and Freundlich equations.	108
Figure 4.21 (a) Effect of inorganic anions on MB adsorption capacity and (b) recyclability tests by PES and PES/PAN nanofiber membrane, respectively.	110
Figure 4.22 Proposed adsorption mechanism of MB in the presence of PES/PAN nanofiber membrane.	111
Figure 5.1 Schematic diagram of the semi-continuous immersed microfiltration membrane bioreactor.....	117
Figure 5.2 Schematic diagram of the ultrafiltration unit.....	118
Figure 5.3 Changes in the total volume of H ₂ , CH ₄ and CO ₂ during anaerobic digestion of food waste at different pH values.....	122

Figure 5.4 The profile of VFAs concentration and distribution and changes in the medium pH throughout the AD MBR experiment.. Error! Bookmark not defined.	
Figure 5.5 1) The changes in the TMP and TSS values throughout the experiment with highlights of 2) day 30 3) day 59 4) day 73 5) day 83 representing different stages of fermentation and filtration. Error! Bookmark not defined.	
Figure 5.6 UV-Vis spectra of feed (F), permeate (P) and retentate (R) upon ultrafiltration (Temperature 37°C, Pressure=5 bar) (A) and (Room temperature, Pressure=5 bar) (B).....	133
Figure 5.7 Changes in the concentrations of VFAs before and after ultrafiltration (Temperature 37°C, Pressure=5 bar) (A) and Room temperature, Pressure=5 bar (B).	134
Figure 5.8 Changes in the permeate flux during ultrafiltration of VFA-containing effluent (Temperature 37°C, Pressure=5 bar) (A) and Room temperature, Pressure=5 bar (B).....	136
Figure 5.9 Schematic diagram of the nanofiltration system.	140
Figure 5.10 Two-stage recyclability system of nanofiltration.....	141
Figure 5.11 UV-Vis spectra of DI water, feed, retentate and permeate upon nanofiltration membrane (200-300 Da) (A), and upon nanofiltration membrane (300-500 Da) (B).	146
Figure 5.12. Flux-time profile at various pH for 200-300 Da nanofiltration membrane (Temperature 20-21°C, Pressure=15 bar).....	152
Figure 5.13 Flux-time profile at various pH for 300-500 Da nanofiltration membrane (Temperature 20-21°C, Pressure=15 bar).....	153
Figure 5.14 VFAs concentration and recovery percentages for NF (a) sequencing and (b) recirculation experiments	155

LIST OF TABLES

Table 2.1: Typical characteristics of food industry wastewater (Aderibigbe et al., 2017)	9
Table 2.2: Different types of food industries wastewater characteristics.....	10
Table 2.3. Performance of pressure-driven membrane filtration for food industry wastewater treatment	13
Table 2.4 Applications of electrospun nanofiber membranes in MB removal.	23
Table 3.1 Effect of membrane characteristics on VFAs recovery (MF-UF)	Error! Bookmark not defined.
Table 3.2 Effect of membrane characteristics on VFAs recovery (NF)	Error! Bookmark not defined.
Table 3.3 Effect of membrane characteristics on VFAs recovery (RO).....	Error! Bookmark not defined.
Table 3.4 Effect of medium characteristics on VFAs recovery (MF-UF).....	Error! Bookmark not defined.
Table 3.5 Effect of medium characteristics on VFAs recovery (NF)	Error! Bookmark not defined.
Table 3.6 Effect of medium characteristics on VFAs recovery (RO).....	Error! Bookmark not defined.
Table 4.1 Kinetics parameters for MB adsorption.	88
Table 4.2 Adsorption isotherms parameters for MB.	89
Table 4.3 Comparison of the MB adsorption capacity with previously reported literature.	89
Table 4.4 Effect of NaCl concentrations and recyclability tests on MB adsorption capacity by PES and PES/HPC nanofiber membrane, respectively.....	93
Table 4.5 Kinetics parameters for MB adsorption by PES and <u>PES/PAN membranes.</u>	

.....	107
Table 4.6 Adsorption isotherms parameters for MB.	108
Table 4.7 Comparison of the MB adsorption capacity with previously reported literature.	109
Table 5.1 Characteristics of used ultrafiltration membranes.	118
Table 5.2 C/N ratios of days from different OLR values.	124
Table 5.3 Physicochemical properties of microfiltered and ultrafiltered streams (Temperature 37°C, Pressure=5 bar).	Error! Bookmark not defined.
Table 5.4 Physicochemical properties of microfiltered and ultrafiltered streams (Room temperature, Pressure=5 bar).	Error! Bookmark not defined.
Table 5.5 Characteristics of used nanofiltration membranes.	139
Table 5.6 Physicochemical parameters of nanofiltered solution (Pore size: 200-300Da, Temperature 20-21°C, Pressure=15 bar); (F= Feed, R= Retentate, P= Permeate).	Error! Bookmark not defined.
Table 5.7 Physicochemical parameters of nanofiltered solution (Pore size: 300-500Da, Temperature 20-21°C, Pressure=15 bar). ...	Error! Bookmark not defined.
Table 5.8 VFAs concentration via nanofiltration (Pore size: 200-300Da, Temperature 20-21°C, Pressure=15 bar).....	Error! Bookmark not defined.
Table 5.9 VFAs concentration via nanofiltration (Pore size: 300-500Da, Temperature 20-21°C, Pressure=15 bar).	Error! Bookmark not defined.
Table 5.10 Characteristics of VFAs compounds.	151
Table 5.11 Permeate flux rate at various pH using two nanofiltration membrane.	154

ABSTRACT

The food sector plays an important role in ensuring the general people's good health and nutritional needs by maintaining food security and food safety. This industry's scope of activities is covered by food production, postharvest management, processing, manufacturing, packing, transportation, and consumption. However, the growing worldwide population has increased the need for food, but at the same time there has been a significant increase in the output of waste generation of the food industry, which represented as an ultimate challenge. Mainly, two types of wastes, liquid waste (wastewater) and solid waste (food waste), are observed on a large scale, but by treating these wastes, various potential benefits could be obtained in terms of clean water production and resource recovery, respectively. With the emergence of wastewater treatment and resource recovery technologies, membrane process has been identified as a mainstream tool in the last few years due to its unique advantages, including high efficiency, portable facilities, economically feasible, etc. Therefore, in the current thesis, novel electrospun nanofibers membranes have been applied in treating wastewater and pressure-driven membrane filtration used for resource recovery by modulating their process intensification.

As of today, electrospun-based nanofibers membrane materials, usually with smaller diameters (less than 100 nm) and higher surface area, have been used widely to replace traditional adsorbents. Thus, the authors, using an environmentally friendly approach for eliminating methylene blue from an aqueous solution, have developed a unique electrospun nanofiber membrane made of a combination of polyethersulfone and hydroxypropyl cellulose (PES/HPC). Structures of the newly manufactured membrane were studied using SEM, FTIR, TGA, and XRD. The results show that a uniformLy-sized nanofiber with an ultrathin diameter of 168.5 nm and high mechanical stability has been observed in the membrane. Contact angle measurements have shown that the blended membrane exhibits good hydrophilicity, and excellent adsorption capacity. The highest adsorption capacity was found to be 259.74 mg/g at neutral pH under room temperature, and the pseudo-second-order model was found to be accurate. In addition, a novel

polyethersulfone/polyacrylonitrile (PES/PAN) blended electrospun nanofiber-based membrane was developed and applied for removing methylene blue from aqueous solutions. SEM results exhibited a smooth surface of the blended PES/PAN nanofiber membrane with an ultrathin diameter of 151.5 nm, much better than the pristine PES nanofiber membrane (261.5 nm). Besides, the blended PES/PAN nanofiber membrane showed a good mechanical stability and hydrophilicity nature, which are vital for adsorption study. Experimental adsorption kinetic data obeyed by the pseudo-second-order ($R^2=0.9970$) and consistent with the Langmuir isotherm model ($R^2=0.9983$) by showing the maximum adsorption capacity of 1010 mgMB/g at neutral pH and room temperature, indicating that the adsorption process occurred in a monolayer form of the membrane surface.

Additionally, the potential of organic waste streams (i.e., food waste) for the sustainable production of precursor chemicals such as volatile fatty acids (VFAs) using anaerobic digestion (AD) has received significant attention in the present days within a consortium of resource recovery. AD-derived VFAs have great market appeal if the challenges with their recovery and purification from the complex AD effluent is overcome. In this study, a novel microfiltration immersed membrane bioreactor (MBR) was used for the production of VFAs from food waste and simultaneously *in-situ* recovery of VFAs. The recovered permeate was then subjected to further purification using a side stream ultrafiltration unit. It was found that VFAs concentration (above 6 g/L) was higher for 10 kDa at pH 5.4 in ultrafiltered solution. After that, nanofiltration was carried out using two commercial nanofiltration membranes of 200-300 Da and 300-500 Da under various pH, applying constant pressure and temperature of 15 bar and 20-21°C, respectively. As noticed, the membrane with the molecular weight cut-off (MWCO) of 200-100 Da appeared to be more effective with an increased concentration of total VFAs (16.94 g/L) and recovery percentage above 90% at pH 9. Moreover, the concentration and recovery percentages of individual VFAs were further enhanced by conducting a sequential permeate recycling process, where, interestingly, recovery percentages of 100% was reached for specific acids.

Overall, the novel electrospun nanofibers membrane are promising for future food industry wastewater treatment applications with increased efficiency, while the use of pressure-driven membrane filtration as a post-treatment of anaerobically digested food waste-derived effluent could be a potential recovery pathway of VFAs-based chemicals.

ACKNOWLEDGEMENTS

To begin, I'd like to express my gratitude to my outstanding primary supervisor, Prof. Vincenzo Naddeo, for his unwavering support and guidance over the last four years. Throughout this period, his vast expertise and expert assistance have proven to be invaluable tools.

Furthermore, gratitude to my co-supervisor, Prof. Tiziano Zarra, for generously sharing his knowledge and experience. Also, Prof. Vincenzo Belgiorno, Antonio Buonerba, Paolo Napodano and all SEED members for their insights and suggestions regarding my PhD research project.

A very special thanks to Prof. Mohammad J. Taherzadeh and Dr. Amir Mahboubi for welcoming me to the Swedish Centre for Resource Recovery, University of Borås, Sweden, and giving me an outstanding opportunity to research my PhD thesis project.

Special thanks also go to Prof. Dr. Md. Mominul Islam for providing me with an opportunity to carry out my PhD research activity in the material chemistry research laboratory (MCRL), University of Dhaka, Bangladesh.

In addition, my sincere thanks go to Prof. Hongchen Song (University of Chinese Academy of Sciences), Prof. Shadi W. Hasan (Khalifa University), Prof. George K. Stylios (Heriot-Watt University), Prof. Yaping Zhao (East China Normal University), Prof. Yingjie Cai (Wuhan Textile University), Prof. Ibrahim H. Mondal (University of Rajshahi) and Prof. Pasquale Del Gaudio (University of Salerno) for their continued support on research activity and scientific discussion.

Last but not least, I am very grateful to my parents (Md. Firoj Ali Khan and Nasrin Nahar), my brother (Naim Parves Tanvir), my wife (Mst. Monira Rahman Mishu), friends, other relatives for their unconditional love and support during my research journey.

ABOUT THE AUTHOR

Md. Nahid Pervez received his BSc degree in Textile Engineering (2014) at the Southeast University (Bangladesh) under the supervision of Prof Syed Fakhrul Hassan. After that, he secured Color Root (Hubei) Scholarship to pursue his MSc studies in Textile Engineering at the Wuhan Textile University (China) in 2016. During his MSc studies, he worked on dye wastewater treatment by Fenton catalytic system in the group of Prof. Felix Y. Telegin (Ivanovo State University of Chemical Technology, Russia). Afterwards, he worked as a visiting researcher under the supervision of Prof. George K. Stylios (Heriot-Watt University, UK, 2016-2017), Prof. Aivaras Kareiva (Vilnius University, Lithuania, 2018). Currently, he is a PhD candidate at the University of Salerno (Italy) under the supervision of Prof. Vincenzo Naddeo, and he spent one-year research period under the supervision of Prof. Mohammad J. Taherzadeh (Swedish Center for resource recovery of the University of Boras, Sweden, 2020-2021) and also for two months under Prof. Mominul Islam (University of Dhaka, Bangladesh, 2021). His current research focuses on the application of new materials for environmental applications.

LIST OF PUBLICATIONS

Publications discussed in the thesis

Peer-Reviewed Journal Articles

1. **Pervez, M. N.**, Mishu, M. R., Stylios, G. K., et al. (2021) 'Sustainable treatment of food industry wastewater using membrane technology: A short review', *Water*, 13, pp. 3450. <https://doi.org/10.3390/w13233450>
 2. **Pervez, M. N.**, Mahboubi, A., Uwineza, C., et al. (2022) 'Factors influencing pressure-driven membrane-assisted volatile fatty acids recovery and purification-A review', *Science of the Total Environment*, 817, pp. 152993. <https://doi.org/10.1016/j.scitotenv.2022.152993>
 3. **Pervez, M. N.**, Bilgiç, B., Mahboubi, A., et al. (2022) 'Double-stage membrane-assisted anaerobic digestion process intensification for production and recovery of volatile fatty acids from food waste', *Science of the Total Environment*, 825, pp. 154084. <https://doi.org/10.1016/j.scitotenv.2022.154084>
 4. **Pervez, M. N.**, Talukder, M.E, Mishu, M. R., et al. (2022) 'One-step fabrication of novel polyethersulfone-based composite electrospun nanofiber membranes for food industry wastewater treatment', *Membranes*, 12(4), 413; <https://doi.org/10.3390/membranes12040413>
 5. **Pervez, M. N.**, Talukder, M.E, Mishu, M. R., et al. (2022) 'Fabrication of polyethersulfone/polyacrylonitrile electrospun nanofiber membrane for food industry wastewater treatment', *Journal of Water Process Engineering*, 47 (C), 102838, <https://doi.org/10.1016/j.jwpe.2022.102838>
 6. **Pervez, M. N.**, Mahboubi, A., Uwineza, C., et al. (2022) 'Feasibility of nanofiltration process for high efficient recovery and concentrations of food waste-derived volatile fatty acids', *Journal of Water Process Engineering*, 48 (C), 102933, <https://doi.org/10.1016/j.jwpe.2022.102933>
-

Conference Proceedings/Presentations

1. **Pervez, M. N.,** Talukder, M. E., Bounerba, A., et al. (2021) 'An investigation of the effectiveness of wastewater filtration by electrospun nanofibre membranes', *International Conference on Water, Energy & Climate Change (WECC 2021)*, Sharjah, UAE.
2. **Pervez, M. N.,** Stylios, G. K., Mishu, M. R., et al.. (2021) 'Best available technologies for wastewater treatment and resource recovery', *International Conference on Computer, Communication, Chemical, Material and Electronic Engineering (IC⁴ME²-2021)*, Rajshahi, Bangladesh.
3. **Pervez, M. N.,** Mahboubi, A., Hasan, S. W., et al. (2021) 'An overview of pressure-driven membrane technologies for a sustainable recovery of volatile fatty acids (VFAs)', *Proceedings of 17th International Conference on Environmental Science and Technology*, Athens, Greece.
4. **Pervez, M. N.,** Mahboubi, A., Hasan, S. W., et al. (2020) 'Microfiltration and ultrafiltration as efficient, sustainable pretreatment technologies for resource recovery'. *Proceedings of 3rd WaterenergyNEXUS Conference*, Djerba, Tunisia.
5. **Pervez, M. N.,** Uwineza, C., Sapmaz, T., et al. (2021) 'Strategies for the improvement of VFAs recovery in the nanofiltration process within the circular economy framework'. *Proceedings of 17th International Conference on Environmental Science and Technology*, Athens, Greece.

ADDITIONAL PUBLICATIONS

Additional works were carried out during my PhD programme at the University of Salerno.

Peer-Reviewed Journal Articles

1. **Pervez, M. N.,** Wei, Y., Sun, P., et al. (2021) ' α -FeOOH quantum dots impregnated graphene oxide hybrids enhanced arsenic adsorption: the mediation role of environmental organic ligands', *Science of The Total Environment*, 781, pp. 146726, <https://doi.org/10.1016/j.scitotenv.2021.146726>.
2. **Pervez, M. N.,** Balakrishnan, M., Hasan, S. W., et al. (2020) 'A critical review on nanomaterials membrane bioreactor (NMs-MBR) for wastewater treatment', *npj Clean Water*, 3, pp. 43. <https://doi.org/10.1038/s41545-020-00090>

-
3. Talukder, M. E., **Pervez, M.N.**, Jianming, W., et al. (2022). Ag nanoparticles immobilized sulfonated polyethersulfone/polyethersulfone electrospun nanofiber membrane for the removal of heavy metals. *Scientific Reports*, 12(1), pp. 5814. <https://doi.org/10.1038/s41598-022-09802-9>
 4. Khan, A. H., Sharholy, M., Alam, P., et al. (2022). Evaluation of cost benefit analysis of municipal solid waste management systems. *Journal of King Saud University-Science*, 34(4), pp.101997. <https://doi.org/10.1016/j.jksus.2022.101997>
 5. Jing, J., **Pervez, M. N.**, Sun, P., et al. (2021) 'Highly efficient removal of bisphenol A by a novel Co-doped LaFeO₃ perovskite/PMS system in salinity water', *Science of The Total Environment*, 801, pp. 149490. <https://doi.org/10.1016/j.scitotenv.2021.149490>.
 6. Talukder, M. E., **Pervez, M. N.**, Jianming, W., et al. (2021) 'Chitosan-functionalized sodium alginate-based electrospun nanofiber membrane for As (III) removal from aqueous solution', *Journal of Environmental Chemical Engineering*, 9, pp. 106693. <https://doi.org/10.1016/j.jece.2021.106693>.
 7. **Pervez, M. N.**, Fu, D., Wang, X., et al. (2021) 'A bifunctional α -FeOOH@GCA nanocomposite for enhanced adsorption of arsenic and photo Fenton-like catalytic conversion of As (III)', *Environmental Technology & Innovation*, 22, pp. 101437. <https://doi.org/10.1016/j.eti.2021.101437>
 8. **Pervez, M. N.**, He, W., Zarra, T., et al. (2020) 'New sustainable approach for the production of Fe₃O₄/graphene oxide-activated persulfate system for dye removal in real wastewater', *Water*, 12, pp. 733. <https://doi.org/10.3390/w12030733>.
 9. **Pervez, M. N.**, Telegin, F. Y., Cai, Y., et al. (2019) 'Efficient degradation of Mordant Blue 9 using the fenton-activated persulfate system', *Water*, 11, pp. 2532. <https://doi.org/10.3390/w11122532>
 10. Shafiq, F., Siddique, A., **Pervez, M. N.**, et al. (2021) 'Extraction of natural dye from aerial parts of Argy Wormwood based on optimized Taguchi approach and functional finishing of cotton fabric', *Materials*, 14, pp. 5850. <https://doi.org/10.3390/ma14195850>.
 11. Talukder, M. E., Alam, F., **Pervez, M. N.**, et al. (2022) 'New generation washable PES membrane face mask for virus filtration', *Nanocomposites*, 8, pp. 13-23. <https://doi.org/10.1080/20550324.2021.2008209>.
 12. Hossain, M. Y., Zhu, W., **Pervez, M. N.**, et al. (2021) 'Adsorption, kinetics, and thermodynamic studies of cacao husk extracts in waterless sustainable dyeing of cotton fabric', *Cellulose*, 28, pp. 2521–2536. <https://doi.org/10.1007/s10570-020-03662-0>.
 13. Hossain, M. Y., Zhu, W., Zhang, C., et al. (2022) 'Green and sustainable method to improve fixation of a natural functional dye onto cotton fabric using

cationic dye-fixing agent/D5 microemulsion', *Journal of Natural Fibers*, 19, pp. <https://doi.org/10.1080/15440478.2021.2024933>.

14. Lin, L., Zhu, W., Zhang, C., et al. (2021) 'Combination of wet fixation and drying treatments to improve dye fixation onto spray-dyed cotton fabric', *Scientific Reports*, 11, pp. 15403. <https://doi.org/10.1038/s41598-021-94885-z>.

15. Zhang, P., Zhu, W., Hossain, M. Y., et al. (2022) 'Towards improved performance of reactive dyeing on cotton fabric using process sensitivity analysis', *International Journal of Clothing Science and Technology*, pp. 1-19. <https://doi.org/10.1108/IJCST-03-2021-0035>,

Book Chapters

1. **Pervez, M. N., Mondal, M. I. H., Cai, Y., et al.** (2021). Textile waste management and environmental concerns. *Fundamentals of Natural Fibres and Textiles*. Sawston, United Kingdom: **ELSEVIER**. <https://doi.org/10.1016/B978-0-12-821483-1.00002-4>.
2. **Pervez, M. N., Hossain, M. Y., Talukder, M. E., et al.** (2022). Nanomaterial-based smart and sustainable protective textiles. *Protective Textiles from Natural Resources*. Sawston, United Kingdom: **ELSEVIER**. <https://www.elsevier.com/books/protective-textiles-from-natural-resources/mondal/978-0-323-90477-3>.
3. Hasan, K. M. F., **Pervez, M. N., Talukder, M. E., et al.** (2021). Community entrepreneurship and environmental sustainability of the handloom sector. *Handloom Sustainability and Culture*. Singapore: **Springer Nature Singapore Pte Ltd**. https://doi.org/10.1007/978-981-16-5967-6_2.

1. INTRODUCTION

Food is a necessary component of our daily existence. Every country's food business is fundamental and vital to its survival. Food processing is by far the most sensitive stage in order to build up a fundamental vibe that is interlinked with the food supply chain initiative, but the manufacturing of that food has a negative impact on our surroundings (Khan et al., 2021b, Sandhu et al., 2020). Our planet's ability to replenish the resources and environmental services that underpin our wealth and progress is being quickly depleted as a result of rampant mass manufacturing. In addition to harming the environment, the present food supply chain also has detrimental effects on human well-being, making it unsustainable. Among them, waste generation from food industries is generally unavoidable by-products and is considered one of the most threatened parts of the progressive civilization cycle. With the majority of liquid waste and solid waste are typically discharged from the food industry, whereby the manufacturer leading processing parts remained the original sources of wastes (Frenkel et al., 2017, Hang, 2004). Overall, the food industry waste generation framework is shown in Figure 1.1.

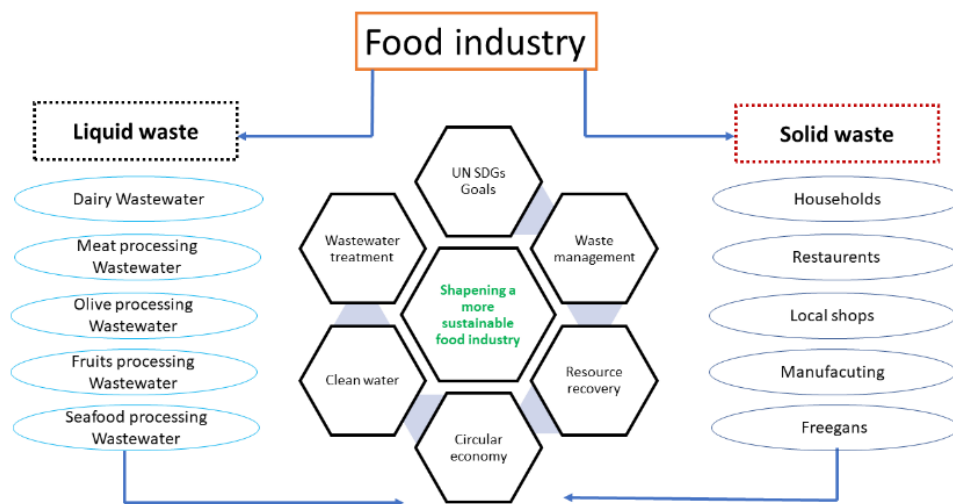


Figure 1.1 Waste generation framework of the food industry

According to the Environmental Protection Agency (EPA), the definition of liquid waste could be described by the presence of a “liquid” substance with any waste’s materials. Liquid waste is generally regarded as one of the important issues around the world because 71% of the Earth’s surface is covered by water, which means liquid waste formation is strongly associated with this criterion. There are many operations stages (temperature control, cleaning, cooking, sanitation, transportation and other auxiliary steps) in the food industry where water is a must component to run the whole chain production process, thereby a large amount of wastewater effluents are generated accordingly (Chu et al., 2013). Contaminants in wastewater may include a wide range of substances such as microbes, colloids and proteins as well as ions of heavy metals and dyestuffs. Among them, dyestuff-contaminated industrial wastewater has significantly negatively impacted water and land quality, human health, and the ecosystem. It is the most challenging compound to remove from the industrial effluent streams because of having a stable and complex structure (Pervez et al., 2020e, Morshed et al., 2020b, Pervez et al., 2019b). Notably, the food industry uses a variety of dyestuffs for their manufacturing purposes, and methylene blue (MB) is one of them. One of the most often utilized dyes in the manufacture of consumer goods like roasters, cutlery and paper sheets is MB (cationic azo dye). It may permanently harm the eyesight of people and animals alike by causing severe eye burns. Acute palpitations and wheezing may be caused by some substances, which might exacerbate lung difficulties (Pervez et al., 2021c, Jing et al., 2021b, Kaya-Özkiper et al., 2022). The investigation of suitable techniques for eliminating MB from wastewater discharge by the food sector is thus of fundamental relevance. After being treated by effective technologies from food industry wastewater, water reuse could be a great manifesto for balancing the socio-economic situation due to freshwater availability.

On the other hand, the worrisome buildup of solid waste, especially food waste (FW), is the consequence of an increasing pace of industrialization, urbanization, and poor waste management. Besides, it has the potential to hinder the progress of certain industries and whole nations toward their sustainability objectives. More than 1.3 billion tonnes of food are thrown out worldwide every year, costing the globe an estimated \$1 trillion (Goh and Jie, 2019). According to The Food and Agriculture Organization (FAO), any edible or healthy substances lost, degraded or wasted along the supply chain derived from organic waste sources such as households, kitchen and food processing operation plants are typically considered food waste (Chen et al., 2017). One of the most common strategies for dealing with food waste is anaerobic digestion (AD). AD produces biogas, which is a valuable source of energy. However, intermediate products of AD such as volatile fatty acids (VFAs) are of more market

appeal and unit value compared to biogas (Wainaina et al., 2020a, Kleerebezem et al., 2015, Lü et al., 2021). VFAs are carboxylic acids (acetic acid, propionic acid, butyric acid, valeric acid and caproic acid) containing six or fewer carbon atoms in their chain. AD-assisted waste-derived VFAs production is considered as a sustainable platform compared to the currently achieved synthetic route, i.e., fossil-based sources (Huq et al., 2021, Aydin et al., 2018). VFAs have many industrial applications from bioplastics and biofuels to cosmetics and pharmaceuticals (Agnihotri et al., 2022). However, in order to market VFAs acquired from AD, VFAs should be effectively recovered/separated (collected in pure form) from microorganism particle-riched mixed effluent and concentrated to favorable levels (Atasoy et al., 2018, Chen et al., 2021). Regardless of the great interest in the application of FW in a waste-biorefinery and the complexity involved in waste generated VFAs separation, purification and concentration from FW digestate, there is lack of available information in the application of pressure-driven membrane processes in this regard.

As of today, various approaches have been developed for the treatment of food industry wastewater and the management of food waste (Shrivastava et al., 2022, Zan et al., 2022, Yadav et al., 2022). However, some techniques are still hindered by their continuous limitations, such as low efficiency, complex setup, costly and, most importantly, environmental unsustainability is a major issue. Therefore, new technological advancements are required to manage wastewater and resource recovery from waste effectively. Recent studies have proven that membrane-based technology, which incorporates a variety of diverse and unique separation processes, provides a more holistic solution and allows for the treatment of wastewater and resource recovery owing to their superior efficiency, cost-effectiveness and operational flexibility without much affecting the water quality and waste substances (Ashraf et al., 2021, Chowdhury et al., 2021). On the one hand, electrospun nanofiber membranes have been well recognized for their tailoring properties to capture organic pollutants from wastewater. On the other hand, the pressure-driven membrane filtration process (microfiltration, ultrafiltration, nanofiltration and reverse osmosis) has long been used to recover precious materials from waste sources. Accordingly, this thesis proposed a novel way to produce clean water (wastewater treatment) and concentrated VFAs (resource recovery) by using a membrane-based process to sort out the challenges.

1.1 Objectives

Wastewater treatment has long been utilized as an essential process in terms of environmental sustainability, while the resource recovery concept is turned out to be a valuable aspect in present days. Interestingly, both are crucial domains for laboratory-scale research and industry. In this thesis, novel membranes (electrospun nanofiber membranes) are applied to treat food industry wastewater, and pressure-driven membrane filtration technology is employed for resource recovery, such as VFAs from food waste. This research scheme was designed based on the research gaps about nanofiber membranes that are not yet applied for food industry wastewater treatment and pressure-driven membrane filtration, on the other hand, process intensification of this technology has rarely been utilized for VFAs recovery from real food waste sources. Therefore, this thesis aims to fill the gap in the research area of wastewater treatment and resource recovery in the food industry by combining sustainable membrane technology and these technologies that could be applied on an industrial scale to progress for further advanced implications. For this purpose, the specific research goals can be categorized to investigate:

- **Phase A:** To explore the use of electrospun nanofibers membrane as a next-generation membrane to improve the wastewater purification process.
 - **Study I:** Development of a unique electrospun nanofiber membrane made of a combination of polyethersulfone and hydroxypropyl cellulose (PES/HPC) using an environmentally friendly approach for eliminating methylene blue from an aqueous solution.
 - **Study II:** Synthesis of a novel polyethersulfone/polyacrylonitrile (PES/PAN)-based electrospun nanofibers membrane aiming to enhance the adsorption capacity of methylene blue.
- **Phase B:** To study pressure-driven membrane filtration technology as a sustainable pathway for VFAs recovery.
 - **Study I:** Application of a microfiltration anaerobic membrane bioreactor and external ultrafiltration unit to intensify the

processing stage and produce a clear feed solution (concentration of VFAs and other compounds).

- **Study II:** Nanofiltration of actual ultrafiltered VFAs effluent collected from a semi-continuous microfiltration immersed membrane bioreactor was employed for improving the yield of VFAs.

1.2 Outlines

- **Chapter 1** introduces the background of the research topic and briefly discusses the scope and main objectives.
- **Chapter 2** provides an overview of food industry wastewater treatment, focuses on membrane technologies, identify of electrospun nanofibers membrane potential for treating food industry wastewater, challenges and future perspective were also reported.
- **Chapter 3** presents a comprehensive state of the art of volatile fatty acids and their potential in terms of market, recovery methods with a focus on pressure-driven membrane filtration, describes factors affecting pressure-driven membrane-assisted recovery of VFAs, including membrane properties and medium characteristics, and finally, challenges and future suggestions are highlighted.
- **Chapter 4** discusses the details of experimental setups, design of the testing plan, samples preparation and analytical methods of electrospun nanofiber membranes and their application towards dye removal.
- **Chapter 5** discusses the details of substrates, experimental setups, samples collection and analytical methods of pressure-driven membrane filtration and their application toward VFAs recovery.
- **Chapter 6** presents the conclusions drawn from this thesis work and provides future suggestions for the advancement of this research.

2. WASTEWATER TREATMENT IN FOOD INDUSTRY

Increased population growth and urbanization have led to water scarcity around the world. Literature data show that industrial sectors use 4 trillion cubic meters of water per annum, while the accessibility of clean water for daily human activities are estimated at around 0.01 trillion cubic meters (Awange, 2021, Tapera, 2019, Pervez et al., 2021f, Pervez et al., 2021b, Naddeo and Korshin, 2021). There is an urgent need to find new clean water supply resources from various sectors such as rainwater, saline water and wastewater. A considerable amount of industrial wastewater being directly discharged into the natural environment causes severe problems for human health and the ecosystem (Pervez et al., 2020e, Jing et al., 2021b, Naddeo, 2021, Naddeo and Liu, 2020). Therefore, industrial wastewater treatment would be a feasible solution for overcoming the freshwater shortage and contributing to our environmental sustainability development.

Food industry has been recognized as one of the major water consumers and wastewater generators among all industries. Water consumption stages include the processing of raw material and utility purposes such as washing, heating, and cooling stages (Walsh et al., 2016, Flörke et al., 2013). However, it has been pointed out that the utility part is the main contributor to large volumes of wastewater generated annually (Compton et al., 2018). Studies showed that effluents from the food processing industry contain complex compounds which are difficult to remove (Jing et al., 2021a, Sakcharoen et al., 2021), hence, requiring efficient treatment technologies. There are numerous methods that have been applied to treat food industry wastewater, such as physical-chemical systems (coagulation, filtration, evaporation, centrifugation and gravity concentration) (Barbera and Gurnari, 2018), adsorption (Sellaoui et al., 2021), Fenton oxidation (Leifeld et al., 2018, Pervez et al., 2019b), ozone (Norton and Misiewicz, 2012), microalgae cultivation (Li et al., 2019b), constructed wetlands (Sehar, 2020), UV disinfection (de Nardi et al., 2011), plasma (Patange et al., 2018), microbial fuel cells (MFCs) (Ceconet et al., 2018), etc. However, their high operation cost and the generation of secondary pollutants

have limited their applications (Valta et al., 2015, Asgharnejad et al., 2021, Morshed et al., 2020b).

Recently, there has been a growing interest in developing environmentally friendly, cost-effective, and efficient treatment systems for the treatment of food industry wastewater. Membrane processes show great potential owing to their unique advantages, such as high-quality effluents, less energy required, and easy operation (Millanar-Marfa et al., 2021). There are various types of membrane operations such as membrane bioreactors (MBRs), pressure-driven membrane filtration (microfiltration (MF), ultrafiltration (UF), nanofiltration (NF), and reverse osmosis (RO)), forward osmosis (FO), electrodialysis (ED), membrane contactors and membrane distillation (MD) (Pervez et al., 2020b). Membranes are fabricated through several methods, including phase inversion (Ng et al., 2021, Ng et al., 2020), sintering (Li et al., 2021), track-etching (Molodkina et al., 2012) and wet spinning (Zhang et al., 2015). However, these processes showed several environmental concerns, operational costs, and availability.

Meanwhile, it has been discussed in the scientific community that fabrication tuning strategy has played a vital role in improving the performance of membrane processes. Electrospinning is a versatile technique for the fabrication of nanofibers membranes with less than 100 nm (Pervez and Stylios, 2018a, Pervez and Stylios, 2018c). Electrospun membranes, generally termed as nanofibers membranes, show great promise in water treatment applications due to their outstanding features such as high surface area, mechanical robustness, small pores, porosity, and lightweight (Pervez et al., 2020f). Several studies were reported in the literature for the application of electrospun nanofibers in MBRs (Bjorge et al., 2009, Lotfikatouli et al., 2021), MF (Wang et al., 2012), UF (Dobosz et al., 2017), NF (Shen et al., 2019), RO (Zhou et al., 2019), ED (Zheng et al., 2020), MD (Deka et al., 2019), membrane contactors (Kim et al., 2022) and FO (Obaid et al., 2020).

2.1 Characteristics of food industry wastewater

It is known that several types of food processing industries are available due to the demand for diverse food choices. As a result, each industry produces a significant amount of organic-rich wastewater effluents. Examples include biological chemical oxygen (BOD), salts, fats, dyestuff, greases, oils, chemical oxygen demand (COD), total dissolved solids (TDS), and total suspended solids (TSS). Additional pollutants may be present depending on the raw materials and processing procedures. Typical characteristics of food industry wastewater are presented in Table 2.1.

Table 2.1: Typical characteristics of food industry wastewater (Aderibigbe et al., 2017)

Common parameters	Standard volume (mg/L)
Total suspended solids	50
Total nitrogen	10
Total Phosphorus	2
Biochemical oxygen demand	50
Chemical oxygen demand	250
Oil and grease	10
pH	5.5-9.0

Tentative comparison of the different food industry sectors wastewater parameters could be made by measuring their initial effluent quantity (Table 2.2). For instance, soybean processing industries generated 7 to 10 tons of wastewater in which various substances are found, such as amino acids, lipids, organic acids, vitamins, saponin, mono/oligosaccharides, whey protein, and COD amount remains 10 to 20 g/L (Qiu et al., 2019). Dairy industry produced wastewater contains high concentration of solids where 50% are found in the volatile form. The typical concentration of COD ranges between 2 to 10 g/L, whereas nutrients (phosphorus and nitrogen) were present in very low concentrations when compared to other industries (Karadag et al., 2015). Similarly, oil mill industry wastewater effluent contains very low concentration of nitrogen, while phenolic compounds (long-chain fatty acids and tannins) are present in high concentrations (Beltrán-Heredia et al., 2001). In starch processing industries, carbon, nitrogen and phosphorus (330:30:1 in molar ratio) are present in higher concentrations with COD concentration ranges from 6 to 56 g/L (Chatzipaschali and Stamatis, 2012). Besides, the wastewater effluent collected from other industries such as meat processing, winery and brewery has the same characteristics with higher content of mineral compounds (Sroka et al., 2004, Arantes et al., 2017, de Carvalho et al., 2018). However, direct discharge of food industrial wastewater effluents into the environment can cause human health problems through the interface with the microbiological process due to the presence of refractory organics and their high concentrations, which are not easy to remove using a typical treatment process (Barrera-Díaz et al., 2006, Chiacchierini et al., 2004). Thus, it is clear that the wastewater generated by all types of food industries must be treated via using highly efficient treatment processes.

Table 2.2: Different types of food industries wastewater characteristics

Sources	Main components of wastewater	Characteristics	Ref
Dairy	Proteins, detergents, lactose, and lipids	BOD= 442 mg/L COD= 8960 mg/L TDS= 253.6 mg/L pH= 7.10	(Qasim and Mane, 2013)
Olive mill	Phenols, pectin, sugars, fats, oil, salts and carbohydrates	BOD= 4426 mg/L COD= 55,730–156,000 mg/L Total phenol = 2439–8300 mg/L pH= 5.6	(Benamar et al., 2020, Değermenci et al., 2016)
Slaughterhouse	Nitrogen, sodium, potassium, calcium and fats	BOD= 1209 mg/L COD= 4221 mg/L Total nitrogen= 427 mg/L pH= 6.95	(Bustillo-Lecompte et al., 2016)
Fruits	Carbohydrates, minerals, nitrogen, phosphorus and salts	BOD= 860 mg/L COD= 919 mg/L Total nitrogen= 40 mg/L pH= 5.5-7.2	(Puchlik and Struk-Sokołowska, 2017)
Seafood	Sodium chlorides, phosphorus, nitrogen, salts, fats and grease	BOD= 3250 mg/L COD= 13180 mg/L Salts= 2–5% (w/v) pH= 5-7	(Ahmad et al., 2021)

2.2 Membrane bioreactor

Membrane bioreactor (MBR) processes have proven to be quite effective in the removal of organic and inorganic contaminants from wastewaters. It has achieved growing popularity in recent years as a result of stricter environmental regulations and an increase in water reuse policies. The widespread use of MBR is attributable to its reliability, scalability, less amount sludge generation, good efficiency, simplicity of operation, and smaller footprint (Melin et al., 2006). MBRs wastewater treatment process is accomplished using a combined biological process (organic pollutant biodegradation) and filtration unit (accountable for the separation of treated water from solids effluent through the use of a membrane panel). Typically,

anaerobic membrane bioreactors (AnMBRs) and aerobic membrane bioreactors (AMBRs) are the two categories of MBRs, which are distinguished by their arrangements and hydrodynamic regulation of permeate flux (Figure 2.1) (Al-Asheh et al., 2021). With over 30 years of experience, this technology has provided the benefits of treating wastewater, as a result, MBRs are preferred over other techniques for obtaining high quality treated wastewater, such as activated carbon adsorption, filtration, and coagulation. Meanwhile, compared to conventional MBRs, integration in MBR with other technologies such as FO-MBR, MBR-RO/NF, advanced oxidation processes (AOPs)/electrocoagulation-MBR are considered potential candidates for wastewater treatment (Goswami et al., 2018, Neoh et al., 2016).

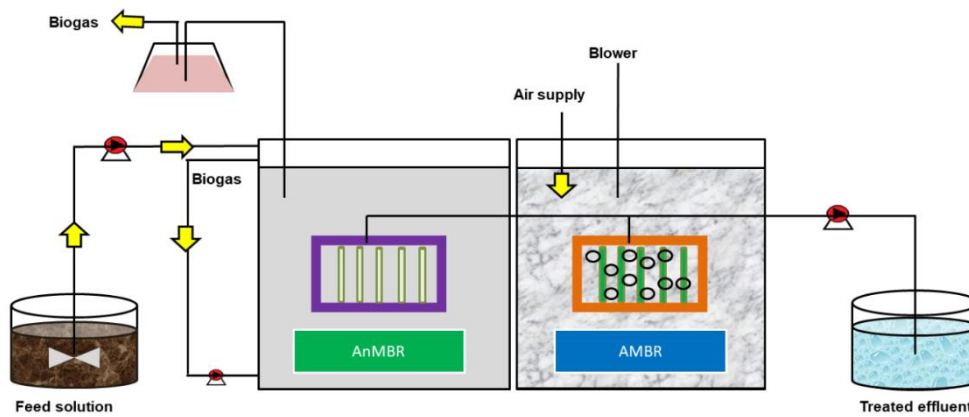


Figure 2.1 Typical representation of anaerobic MBR (AnMBR) and aerobic MBR (AMBR).

Several studies investigated the effectiveness of MBRs in treating food industries wastewater. For instance, He et al. (He et al., 2005) have treated food wastewater with an AnMBR. This study used a higher strength food wastewater since it contains a high concentration of COD (more than 1000 mg/L) and exhibited a high-efficiency COD removal rate (81–94%). It was noticed that the volumetric loading rate (VLR) influences the efficiency through which high COD removals were obtained below 4.5 kg/m³d of VLR (Wang et al., 2005, Galib et al., 2016). Mixed liquor suspended solid (MLSS) concentration also influences the performance of MBRs during the treatment of food industry wastewater. Katayon, S., et al. (Katayon et al., 2004) achieved a higher removal rate of suspended solids (99.2%) and turbidity (99.73%) at a lower concentration of MLSS. However, some studies have recently introduced a two-stage AnMBR set-up to enhance food wastewater removal efficiency regardless of the effect of the operational parameters (Acharya et al., 2006b, Acharya

et al., 2006a). This two-stage scheme was proposed because of their crucial advantages such as stability, inhibition reduction of toxic compounds resulted in higher affinity between particles and membrane surface. A recent report also demonstrated that a two-stage dynamic AnMBR could be efficient for food wastewater treatment and found that in all cases, more than 90% of MLSS and total COD were successfully removed under stable operating conditions (Mahat et al., 2021). Thus, it can be speculated that the use of designed moduled MBRs operation may prospect to improve the effluent quality of food industry discharged wastewater.

2.3 Pressure-Driven Membrane Filtration

The pressure-driven membrane filtration processes are now considered the most multifunctioning and effective technologies for wastewater reclamation, providing a number of benefits such as easy installation, rapid execution and higher efficiency. In this process, the feed stream was loaded in the filtration unit equipped with a membrane panel and required pressure exerted immediately during the operation to separate into permeate and retentate solution (Van Der Bruggen et al., 2003b). The rejection behavior of membranes is especially important in this type of operation, because it is responsible for eliminating large amounts of organic matter, micropollutants, and dyestuff from raw effluents, which results in high-quality permeate water for various uses including, soil/fertilizer growth, toilet flushing, household washing and watering gardens (Hube et al., 2020a).

Membranes are classified into MF, UF, NF and RO (Figure 2.2). In MF, membranes with larger pores typically have pores with diameters of about 10–0.1 μm and MWCOs ($>100,000$ Daltons), thereby it can be effective at removing large suspended solids, colloids, particles, and some types of bacteria. In this process, the operating pressure typically ranges from 0.1 to 2 bar. UF membranes with pore sizes ranging between 0.1 and 0.01 microns and molecular cutoff weight (MWCO) values ranging between 1000 and 100,000 Da are used. As a result, this process has the capability to retain larger compounds such as polysaccharides, emulsions, proteins and colloidal particles. The operating pressure normally ranges from 0.1 to 5 bar. NF membranes lie between the UF and RO processes where the diameters of those membranes are 0.01–0.001 μm , equivalent to 200–1000 Da MWCO. It is usually employed to remove small molecular weight molecules (divalent ions, amino acids, organic acids, glucose and sugars). This is generally carried out at pressure ranges from 5 to 30 bar. RO is by far the most effective for removing dissolved salts, inorganic contaminants and chemical substances because of their smaller pore size

in the range of 0.1-1 nm and MWCO about 100 Da. It needs higher operating pressure, which typically runs between 20 and 65 bar.

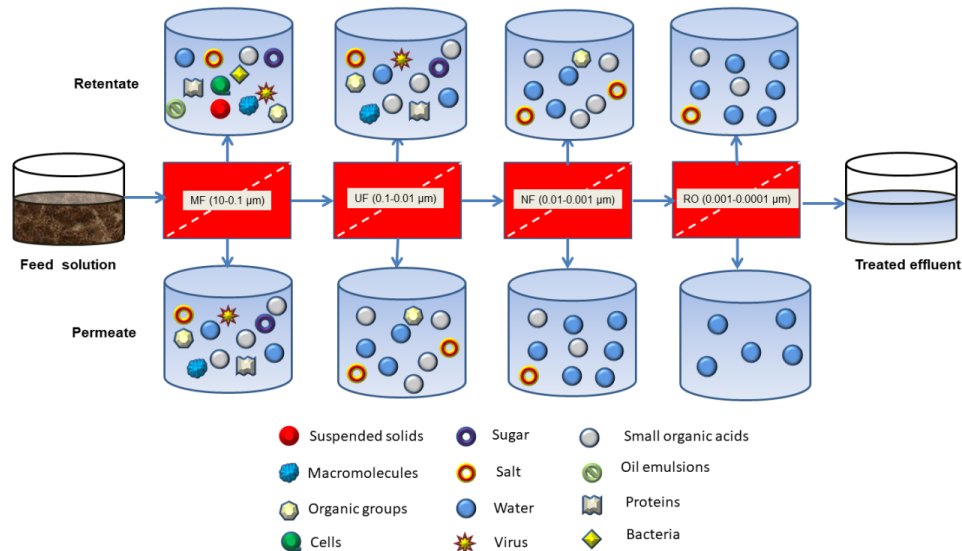


Figure 2.2 Typical representation of pressure-driven membrane process

Table 2.3. Performance of pressure-driven membrane filtration for food industry wastewater treatment

Type of membrane filtration	Source	Characteristics	Performance	Ref
MF	Dairy wastewater	BOD= 890 ± 92 mg/L COD= 3536 ± 328 mg/L Turbidity= 623 ± 140 NTU TSS= 1860 ± 220 mg/L pH= 7.3 ± 0.3	COD Removal (%) = 89 ± 2 Color Removal (%) = 93 ± 5 Turbidity Removal (%) = 98 ± 4	(Zielińska and Galik, 2017)
UF	Dairy wastewater	BOD= 890 ± 92 mg/L COD= 3536 ± 328 mg/L Turbidity= 623 ± 140 NTU TSS= 1860 ± 220 mg/L pH= 7.3 ± 0.3	COD Removal (%) = 95 ± 1 Color Removal (%) = 97 ± 6 Turbidity Removal (%) = 99 ± 5	(Zielińska and Galik, 2017)
NF	Restaurant wastewater	BOD= 816.17–1097.25 mg/L	COD Removal (%) = 99.4	(Zulaikha et al., 2014)

RO	Olive wastewater	COD= 10,356.67–16,443.33 mg/L	BOD Removal (%) = 86.8
		Turbidity= 402.67–1208 NTU	Turbidity Removal (%) = 99.9
		TSS= 1860 ± 220 mg/L	
		pH= 4.49–6.15	
		Suspended matter= 14-16 mg/L	COD Removal (%) = 99.8
		COD= 120.5–226.6 mg/L	(Ochando-Pulido et al., 2012)

Recently, greater emphasis has been made on the application of the pressure-driven membrane filtration process in food wastewater treatment (Table 2.3) (Ochando-Pulido and Martinez-Ferez, 2012, Muro et al., 2012). Generally, MF has been shown to produce particles free solutions from dairy wastewater effluents due to their larger pore size. It is known that the presence of solid particles may blockage the membrane pores, which in turn hinder the removal percentages of pollutants from the food wastewater using membrane filtration. Hence, some studies used ceramic MF membrane and found that up to 90% of solids particles could be removed from various food process industrial raw wastewater, accompanying much clear permeate effluent quality (Hart et al., 1988, Kumar et al., 2016b, Hua et al., 2007). These studies demonstrated that the MF process could be an effective pretreatment step for the next membrane filtration process, such as UF. For instance, Zielińska et al. (Zielińska and Galik, 2017) conducted an experimental study with alone MF, UF, and combined UF/MF to treat dairy wastewater. Results showed that alone MF could remove 89±2% COD while using the UF process, the removal efficiency of COD increased to 95±1%. This is attributed to the sieve retention mechanism, in which particles are retained on the membrane surface and differences observed based on MWCO. UF was found to have a higher COD removal ability due to the lower cut-off value of the UF membrane compared to the MF (Cui et al., 2010).

The observation highlights the importance of MF/UF membranes for the removal of high-molecular-weight contaminants rather than dissolved ions, whereas NF or RO would be more appropriate for ion rejection in further stages. The effluent quality turned out to be standard after being subjected to the NF process followed by the UF process. Zulaikha et al. (Zulaikha et al., 2014) treated restaurant wastewater effluent through sequential filtration from UF to NF and obtained similar removal percentages of COD (97.8%) and turbidity (9.9%). However, a significant reduction in BOD₅ and conductivity were observed under the NF operation, which indicates that the incorporation of NF membranes is potentially suitable for the production of fit-for-purpose water. In contrast to NF, RO has a high selectivity for impurities in

the water. NF membranes are well-known for their ability to reject almost all impurities in the water, particularly multivalent ions. The management of food industry wastewater through the use of RO has been investigated due to its scalability and stringent water reuse environmental regulations and standards (Ochando-Pulido et al., 2012). When comparing the removal efficiency between NF and RO, it was noticed that the maximum COD removal reached values up to 60% for NF while RO removed more than 95% of COD and multivalent ions, indicating that pore size and membrane surface charge plays a significant role in purifying effluents (Vourch et al., 2008, Coskun et al., 2010). However, having set a goal of obtaining high-quality permeate water, some observations still need to be handled properly. Among these, factors associated with NF/RO membranes and the pretreatment stage are highly recommended in RO/NF application. Moreover, when complex chemical compounds including organic acids, polyphenols, and other substances present in food industrial wastewater effluents correspond to recovery/concentration, entitled to maintain a significant benefit in the economic and environmental impact of effluents in the pressure-driven membrane filtration process (Giacobbo et al., 2017).

2.4 Membrane distillation

MD is a thermally-driven process that uses a hydrophobic membrane to separate feed and permeate solutions. MD process is operated by the difference in vapour pressure caused by the temperature variation throughout the membrane surface (Figure 2.3). The hydrophobic nature of the membrane allows only vapour to pass through, leaving liquid on the feed side and preventing it from entering the membrane pores (Alkudhiri et al., 2012, Alsebaei and Ahmad, 2020). There are a number of benefits to the MD process. It can be performed at less pressure and temperatures than the feed solution boiling point. Due to the pore volume in the microporous membrane, the MD process demands less vapour space while a traditional distillation column requires a large vapour space. It allows a very high non-volatile solvent separating factor and can also be used to concentrate aqueous solutions or to produce high purity water. It can make use of any level of low waste heat, which can then be used in conjunction with solar energy, making it a viable option for the supply of freshwater resources from brackish water in regions where a lack of available water is severe (Anvari et al., 2020, Drioli et al., 2015).

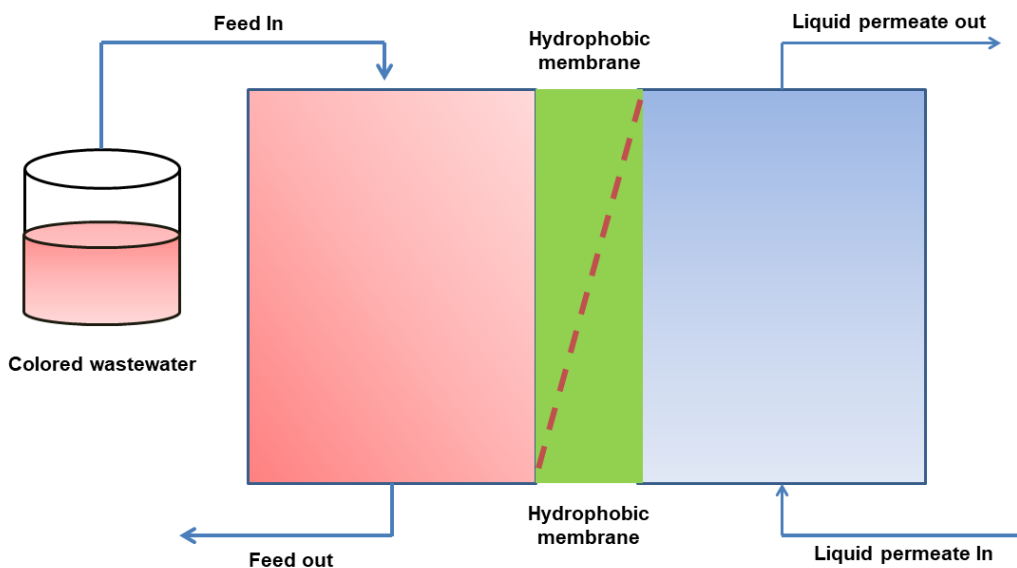


Figure 2.3. Representative diagram of membrane distillation process.

Due to these advantages, MD has received significant attention in the treatment of food industry wastewater. Researchers have developed several types of MD configurations including direct contact MD (DCMD) which has frequently been used in treating olive mill wastewater. The use of DCMD in olive mill wastewater treatment has the potential to recover the phenolic compounds in the concentrate because it is a non-destructive technique towards the phenol content (El-Abbassi et al., 2012). In DCMD system, El-Abbassi et al. (El-Abbassi et al., 2013a) used commercially available flat sheet polytetrafluoroethylene (PTFE) membranes (TF200, Gelman) having pore size around $0.2 \mu\text{m}$ to treat real olive wastewater in Morocco. Results showed that no effect was observed on the phenolic content and anti-oxidant ability when DCMD was applied at 80°C . Notably, it was discovered that PTFE membranes had a better polyphenols recovery efficiency (99%) than PVDF membranes (89%) (El-Abbassi et al., 2013a). Nevertheless, DCMD's limit on permeate flux and flux reduction remain unchanged. However, these challenges may be overcome by applying an integrated MD system such as osmotic MD (El-Abbassi et al., 2013b), MF/NF integrated MD system (Garcia-Castello et al., 2010). These studies showed that pretreatment technologies (MF/NF) play a significant role in enhancing the treatment efficiency by removing solids particles, resulting in a high permeate quality effluent.

2.5 Electrodialysis

ED, a proven technology for water desalination, acid and basic production, can reduce toxicity and separate ionic and non-ionic species from the industrial effluents under the influence of applied electric potential. In principle, the conventional ED (CED) structure consists of alternating arrangements between anode and cathode, with multiple cation exchange membrane (CCEM) and anion exchange membranes (AEM) (Figure 2.4). Anions can pass through anion membranes (AEM), however they cannot pass through membranes for cation exchange (CEM). Cations can likewise pass through a CEM and not an AEM (Luiz et al., 2017). In addition, a unique form of membrane called a bipolar is used in an ED field. Bipolar membranes are composed of cation laminate and layer of anion exchange (Huang and Xu, 2006a). These membranes, when using an electrical potential, ensure that electric charge is transported via protons and water splitting hydroxyl ions. The ED process shows a greater rate of water recovery, reduced operating cost, easier operation and membrane stability compared to RO. Therefore, the use of ED has piqued the scientific community's interest as economic and efficient technology (Al-Amshawee et al., 2020).

ED offers the food industry three distinct advantages: better food safety, increased economic competitiveness, and increased environmental friendliness. The most application of ED in the food industry covers extracting some resourceful materials from the effluents instead of only purifying the effluents. However, a few studies are focused on particular food industry wastewater treatment through the use of ED technology. In general, food wastewater contains a large amount of organic matter that is not easy to remove by applying conventional technologies. In this context, Valero et al. (Valero et al., 2015) used a laboratory-scale ED and performed a series of experiments in order to reduce the organic matter and conductivity simultaneously from real almond industry wastewater. Initial and final TOC analysis of the dilute and concentrate confirmed the movement of organic anions over the membrane. For instance, the TOC dilute solution drops from 272 to 93 mg/L, whereas for the concentrate, TOC increased from 12 to 268 mg/L, which indicates that the most organic material is transmitted through the membrane and the solution of dilution decreases both its conductivity and organic content. Besides, ED has also effectively reduced COD (85-90%) and acids and bases regeneration from salts riched food industrial effluents (Hestekin et al., 2010).

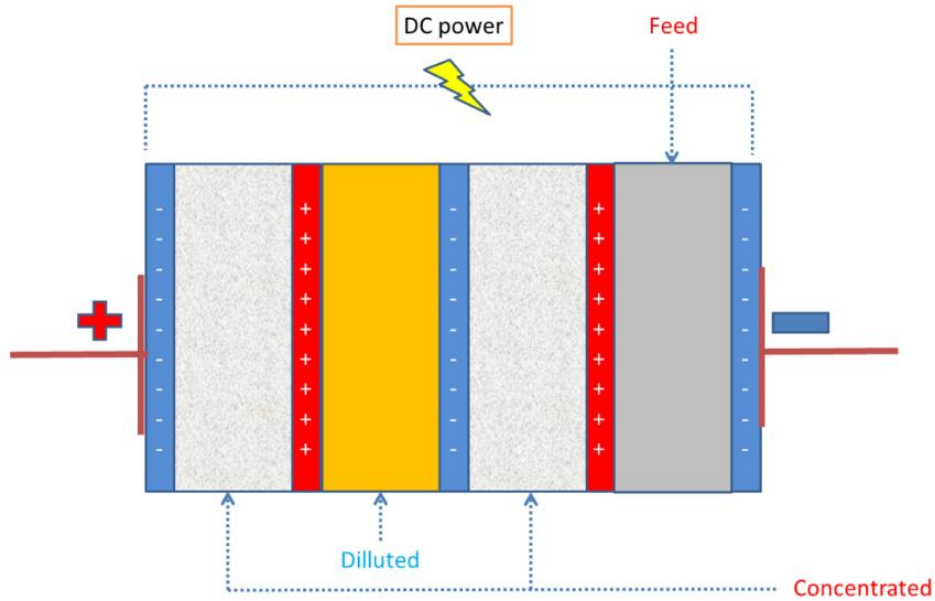


Figure 2.4 Conventional electrodesalination set up for wastewater treatment

2.6 Forward osmosis

FO is an emerging water treatment membrane-based technology, which has been widely explored in the last few decades both from academic and industrial perspectives. FO is a process by which water passes from the feed solution to the drawing solution due to osmotic pressure difference (from low to high) over a semi-permeable FO membrane, as a result this process does not require physical/hydraulic pressure during the operation. During the osmotic process, when the feed solution and draw solution reach equilibrium, water permeation is observed from the feed solution to the draw solution through the FO membrane (Figure 2.5). Because of this, the draw solution is dilute and the feed solution is concentrated throughout the procedure (Chung et al., 2012, Francis et al., 2020). The advantages of FO have been stated in the comparison to reverse osmosis (RO) processes to include fewer membrane fouling and improved energy efficiency (Zamani et al., 2015).

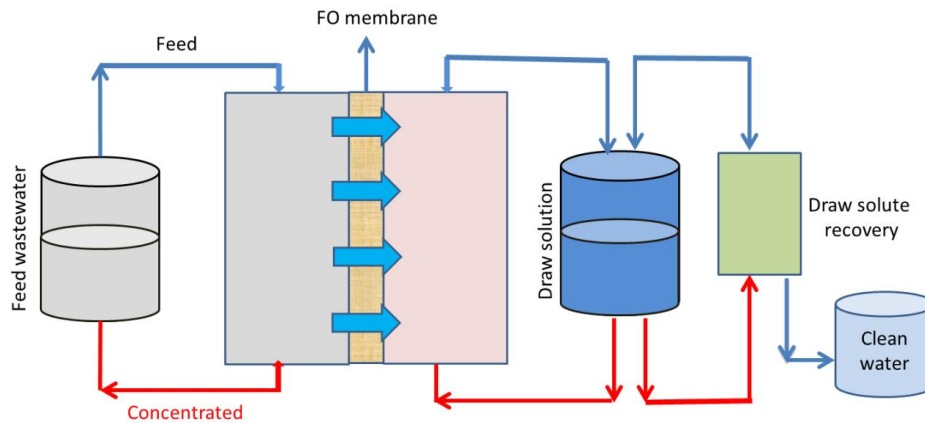


Figure 2.5 Schematic diagram of Forward osmosis (FO) process

FO membrane process is capable of removing nearly all of the dissolved ions and suspended particles in a solution. The massive reductions of solids reduced power consumption by half of the succeeding low-pressure FO process. Previously, food wastewater from different sources has been treated with FO process. For instance, Gebreyohannes et al. (Gebreyohannes et al., 2015) applied a single-step FO process to treat olive mill wastewater effluent. The FO treatment resulted in nearly complete decolorization, ion retention, and TOC and TIC rejection rates of 96% and 99%, respectively. In addition, total phenolic rejection was found to be greater than 98% in dried residue from FO streams. In parallel, the general applicability of the FO process in treating dairy and sugarcane molasses distillery wastewater effluents were also examined (Haupt and Lerch, 2018, Singh et al., 2019). The obtained results showed that 80-90% of COD has ultimately been rejected upon the use of FO. FO process is apparently shown to show potential in treating food wastewater, however, many researchers suggested that the standalone FO process is facing some challenges such as lower efficiency, less attractiveness and economic unstable. Hence, FO integrated with other competitive membrane operations such as nanofiltration, reverse osmosis, membrane distillation, and electro dialysis would be a suitable process intensification candidate by enhancing their overall performance towards the food industry wastewater purification.

2.7 Electrospun nanofiber membranes

The latest generation of membranes is known as electrospun nanofiber membranes (diameter usually less than 100 nm) and have the potential to offer an advancement

in the treatment of water and wastewater. In electrospinning, the electrostatic forces help create thinner fibers whereby a high voltage is delivered to a syringe containing polymer solution or melt that assist in collecting the fibers on the ground plate (Talukder et al., 2021d, Talukder et al., 2021b). The produced nanofiber membrane has a significant water permeability and flexibility, as well as high porosity, a large surface area to volume ratio, and high water absorption. Many different features can affect the electrospun nanofibers. The properties of polymers, solutions, and processes are typically categorized into three classes. The characteristics of polymers include the type of polymer used, its molecular weight, and the distribution of its molecular weight. The solution attributes include the type of solvent used, the rate at which the solvent evaporates, as well as the viscosity, concentration and surface tension of the solution. The parameters of the process include flow rate, voltage applied, nozzle tip-to-collector distance, room temperature, and relative humidity (Figure 2.6).

However, developing a feasible electrospinning technology capable of producing homogeneous nanofibers membranes on a wide scale remains a major issue. In this context, several scaled-up technologies have been performed in recent years. For example, Chen et al. (Chen et al., 2020) reported a continuous antibacterial electrospinning nanofibers membrane through the use of a roll-to-roll scale-up post functionalization approach. Besides, the process's capacity to scale and the technical difficulties that have been investigated to far show that free-surface technologies have great production volume up-scaling potentialities. Centrifugal electrospinning, on the other hand, has been shown to be capable of producing nanofibers with diameters as small as 100 nm. Co-axial and multi-axial technologies, on the other hand, can achieve greater material and processing flexibility and, as a result, more diverse functionalities in the resulting nanofibers. These technologies also allow for scale-up when multi-needle approaches are combined with appropriate techniques in order to deal with multi-jet instabilities (Persano et al., 2013). In addition, several companies such as Inovenso (www.inovenso.com), Mecc Co. (www.mecc.co.jp), E-Spin Nanotech (www.espinnanotech.com) and Elmarco (www.elmarco.com) have been started to produce large scale electrospun nanofiber membranes, which is effective in terms of up-scaling trend. Notably, the mass-production scale of continuous nanofiber membranes will also be potentially realizable for treating high strength food wastewater effluents.

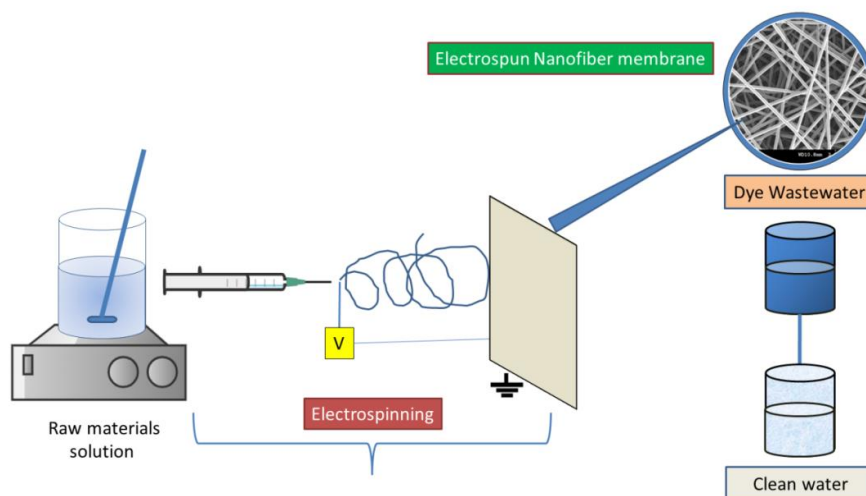


Figure 2.6 Electrospinning process for nanofiber membrane preparation and their uses in dyes removal.

The applications of electrospun nanofiber membranes are rarely utilized for the treatment of real food industry wastewater effluent. On the other hand, mostly applied in removing toxic dyes from aqueous effluent, which is also negotiable since real food industrial effluent contains this substance with a large amount. Particularly, methylene blue (MB) is a popular azo dye with a cationic nature and a good candidate for use in textile, paper, leather, cosmetics, plastics and rubber industries. Moreover, it is also used in food processing equipment preparation such as cutlery, roasters, paper plates, food packaging and food additives. However, this kind of color might be seen as a pollutant due to its adverse effects. It causes eye burns that may result in irreversible eye damage to people and animals. People with lung problems may suffer from intense palpitations or wheezing after breathing in certain substances. While consuming orally causes a hot feeling, nausea, vomiting, heavy sweating, mental confusion, and methemoglobinemia. Thus, it is worth investigating to purify MB-contained food industry wastewater effluent.

Adsorptive removal of MB through the use of electrospun nanofiber membrane has been widely investigated in recent years (Table 2.4). Adsorption refers to the process by which molecules are transferred from one fluid bulk to another on a solid surface. This might happen as a result of chemical bonding interactions (chemical sorption) and physical forces (physical sorption) (Hossain et al., 2021a). Compared to other techniques, adsorption has been proven to be superior in terms of flexibility, ease of operation, cost-effectiveness and insensitivity to harmful contaminants. In the adsorption process, the adsorbent should have a high specific surface area and

porosity, in this case, electrospun nanofiber membrane-based adsorbents exhibit high efficiency of dyes removal over conventional phase inversion membranes because of their high specific surface area and linked porosity. For example, Wang et al. (Wang et al., 2019a) prepared sodium alginate-based water-insoluble electrospun nanofiber membrane and cross-linked it with trifluoroacetic acid (TFA), glutaraldehyde vapor (GA) and calcium chloride (CaCl_2) towards MB removal. It was noticed that CaCl_2 cross-linked nanofiber showed a maximum MB adsorption capacity of 2230 mg/g, which is attributed to the high specific surface area of the membrane obtained by the cross-linking approach. In another study, Zhao et al. (Zhao et al., 2015b) developed thermal cross-linked β -cyclodextrin-based nanofibers and obtained a maximum adsorption capacity of MB with an amount of 826.45 mg/g, which was higher than pure β -cyclodextrin adsorbent (105 mg/g). The existence of $-\text{COOH}$ groups in the membrane surface influence the adsorption performances.

The surface functionalization method has been played a vital role in improving the removal capacity of MB using the electrospun nanofiber membrane. Incorporating functional groups onto the electrospun nanofiber membrane surface provided a substantial amount of active binding sites for MB adsorption. For example, the adsorption capacity of oxidized carbon nanofibers membrane was higher (MB, 168 mg/g) compared to the pristine carbon nanofibers membrane (MB, 48.8 mg/g) because of the electrostatic interactions that occurred between the electrospun nanofibers membranes (Thamer et al., 2019). Besides, plasma etching has been revealed as a green surface functionalization technology and promoted the adsorption performance of electrospun nanofibers membranes. Bai et al. (Bai et al., 2018) fabricated air plasma-assisted PLLA nanofibrous membranes and showed that electrostatic interaction was mainly responsible for the high adsorption of MB. They suggested that other electrospun nanofibers membranes could be used for further development, and plasma operations should be optimized.

The fabrication of metal-doped electrospun nanofibers membrane is now potentially be considered as a robust tool for the development of nanofibers-based heterogeneous catalysts towards MB degradation. This can be done by following either pre or post-modification strategy. For example, Shalan et al. (Shalan et al., 2021) prepared Ag/Fe co-doped cellulose acetate electrospun nanofiber using a pre-modification approach and degraded MB (more than 95%) via photocatalysis reaction. The degradation process of MB was carried out within a very short time (50 min) and exhibited good reusability capacity up to 5 cycles. Besides, the composite doped membrane showed outstanding mechanical properties. On the other, Cheng et al. (Cheng et al., 2020) used a post-surface-modified electrospun nanofiber membrane whereby they first prepared a cellulose acetate nanofiber membrane and deacetylated it through NaOH solution. Next, the deacetylated

membrane was coated with polydopamine (PDA) and immediately applied for MB removal. Results suggest that the deprotonation of the phenol group from the PDA presented a negative charge and effectively captured positively charged MB due to the electrostatic interactions force. Overall, it implies that modulation of design and fabrication strategy could be a possible perspective way to improve the performance of electrospun nanofibers membranes towards wastewater treatment.

Table 2.4 Applications of electrospun nanofiber membranes in MB removal.

Membrane materials	Membrane characteristics	Operational conditions	Adsorption capacity, q_e , max (mg/g)	Ref.
Sodium alginate (SA), poly(ethylene oxide) (PEO)	Fiber diameter = 150 nm, surface area = 13.97 m ² /g	Initial MB conc. = 200 to 1500 mg/L, V = 50 mL, pH = 6, Adsorbent weight = 20 mg	2230	(Wang et al., 2019a)
β -cyclodextrin, poly(acrylic acid) (PAA)	Fiber diameter = 20.56 nm, surface area = 34.88 m ² /g	Initial MB conc. = 40 mg/L, V = 80 mL, pH = 9, Adsorbent weight = 6 mg	826.45	(Zhao et al., 2015b)
Plasma etched poly(l-lactic acid) (PLLA)	Fiber diameter = N/A, surface area = 22.84 m ² /g	Initial MB conc. = 4 mg/L, V = 3 mL, pH = N/A, Adsorbent weight = 10 mg	8.73	(Bai et al., 2018)
Poly(vinyl alcohol) (PVA)/starch	Fiber diameter = 350–450, surface area = 45.61 m ² /g	Initial MB conc. = 250 mg/L, V = 60 mL, pH = 8.5, Adsorbent weight = 5 mg	400	(Moradi et al., 2019)
Polyacrylonitrile (PAN)	Fiber diameter = 250–300, surface area = N/A	Initial MB conc. = 25 mg/L, V = 10 mL, pH = 10, Adsorbent weight = 7 mg	72.46	(Ibupoto et al., 2018)
Hydroxypropyl- β -cyclodextrin (HP β CD) and benzoxazine monomer (BA-a)	Fiber diameter = N/A, surface area = N/A	Initial MB conc. = 10-100 mg/L, V = 5 mL, pH = N/A, Adsorbent weight = 5 mg	46	(Dogan et al., 2019)

Sericin/ cyclodextrin/poly (vinyl alcohol)	Fiber diameter = N/A, surface area = N/A	Initial MB conc. 187 = 20 mg/L, V = 80 mL, pH = 8, Adsorbent weight = 14 mg	(Zhao et al., 2015a)
Poly-L-lactic acid (pLLA), polyaniline (PANI)	Fiber diameter = 518 nm, surface area = 7.0±0.4	Initial MB conc. 239 = 250 mg/L, V = 10 mL, pH = 6, Adsorbent weight = 10 mg	(Mohammad and Atassi, 2020b)
Polyacrylonitrile (PAN), polyaniline (PANI)	Fiber diameter = 418 nm, surface area = 10.0±0.3	Initial MB conc. 398 = 250 mg/L, V= 10 mL, pH = 6, Adsorbent weight = 10 mg	(Mohammad and Atassi, 2020b)
Polyacrylonitrile (PAN)	Fiber diameter = 225 nm, surface area = N/A	Initial MB conc. 42 = 400 mg/L, V = 10 mL, pH = N/A, Adsorbent weight = 10 mg	(Haider et al., 2015b)
Ethylenediamine (EDA)-grafted polyacrylonitrile (PAN)	Fiber diameter = 230 nm, surface area = N/A	Initial MB conc. 94 = 400 mg/L, V = 10 mL, pH = N/A, Adsorbent weight = 10 mg	(Haider et al., 2015b)
Oxime grafted polyacrylonitrile (OX-g-PAN)	Fiber diameter = 231 nm, surface area = N/A	Initial MB conc. 102 = 400 mg/L, V = 10 mL, pH = 6, Adsorbent weight = 10 mg	(Haider et al., 2014)
Cellulose acetate (CA)	Fiber diameter = 752±311 nm, surface area = N/A	Initial MB conc. 45 = 30 mg/L, V = 100 mL, pH = 8, Adsorbent weight = 80 mg	(Ali et al., 2019)
Cellulose acetate (CA)/ polyaniline/ β-cyclodextrin (PANI/β-CD)	Fiber diameter = 1085±325 nm, surface area = N/A	Initial MB conc. 49 = 30 mg/L, V = 100 mL, pH = 8, Adsorbent weight = 80 mg	(Ali et al., 2019)

2.8 Membrane fouling

Membrane fouling is by far the most important phenomenon limiting the extended application of membrane separation processing in different industries. The

occurrence of membrane fouling is due to membrane pore narrowing, pore blockage, and cake layer formation on membrane surface due to the interaction of microbial metabolites, organic and inorganic substances, and microorganisms with the membrane surface (Guo et al., 2012). Membrane fouling can be irreversible or reversible fouling based on the extent of fouling and the possibility to regenerate the membrane by different membrane cleaning approaches. Irreversible and reversible fouling issues are partly cured by chemical and physical cleaning strategies, respectively (Wang et al., 2014b). For example, NF and reverse osmosis membranes are prepared from dense materials, are more susceptible to fouling, while, porous MF and UF membranes can be rather easily physically cleaned by backwashing, aeration or chemically cleaned with acid and/or base (Shirazi et al., 2010). Lately, electrospun nanofiber membranes face also fouling issues such as irreversible, reversible and biofouling. Several factors such as membrane properties, feed characteristics, operation conditions, and various foulants led to a complex fouling formation phenomenon (T. M et al., 2021a). Membrane fouling lowers membrane permeate flux and therefore limits the removal efficiency of pollutants during the processes. Membrane fouling mainly occurred by organic compounds and macromolecules like pectins, starch, glucose and other substances in food industrial wastewater effluents. The literature shows that food industrial wastewater effluents is often related to irreversible and reversible fouling phenomena, especially reversible fouling is the dominant in the potato processing wastewater treatment plant, as reported by Bouchareb et al. (Bouchareb et al., 2021). Usually, this could be managed by chemical cleaning and backwashing method, and pre-treatment stage possible be a sustainable solution. However, there is still a lack of understanding regarding the relationship between removal efficiency and fouling issues in food industrial wastewater effluents.

3. RESOURCE RECOVERY FROM FOOD WASTE

Globally an enormous amount of waste is generated on daily basis posing a serious threat to the stability socio-economic, environmental and health systems (Nizami et al., 2017). A considerable portion of these wastes is composed of organic compounds rich in nutrients which are conducive to be recovered in order to replace virgin resources. Therefore, in recent years, the scientific and industrial communities have shown great interest in different nutrient recovery approaches complying with the principles of a circular economy to build sustainable societies by turning waste into value-added products (Skaggs et al., 2018).

One of the established proficient nutrient recovery and waste remediation pathways is the anaerobic digestion (AD) process that has long been used for biogas and fertilizer production via microbial conversion of organic residues (Xu et al., 2018a, Wainaina et al., 2020c). Recent research has demonstrated that compounds of higher value and application diversity such as volatile fatty acids (VFAs), intermediate products of anaerobic digestion, could be accumulated and recovered as final products of AD rather than biogas. This is the basis of a potential platform for developing environment friendly and renewable biobased chemical precursors from waste rather than fossil sources (Chen et al., 2013). As an example, Liu et al. (Liu et al., 2018) have reported that there is nearly 3-times higher net profit in VFAs (9.12 USD/m³) production from sewage sludge than biogas (3.71 USD/m³). VFAs are short-chain saturated carboxylic acids containing six or fewer carbon atoms such as acetic, propionic and butyric acids. Other than fossil-based routes, VFAs can be produced in the midst of the anaerobic digestion process (acidogenesis and acetogenesis) using a wide range of municipal and industrial by-products, residuals and waste streams rich in organics such as food waste, agricultural residues, sewage sludge, microalgae etc. (Figure 3.1a) (Wainaina et al., 2019a, Parchami et al., 2020b). VFAs are considered as very important chemical compounds for the synthesis of olefins, esters, alcohols and aldehydes. Besides, VFAs can be applied in many research areas and industrial sectors such as bioenergy production, bioplastic synthesis, microbial fuel cells, textiles, food, cosmetics, pharmaceutical industries and as a potential carbon source for biological nutrient removal in wastewater

treatment plants (Mengmeng et al., 2009, Uyar et al., 2009, Bhatia and Yang, 2017, Zheng et al., 2010, Luo et al., 2019). Following these commercial applications clearly demonstrates the high market value and need for VFAs now and in the future (Figure 3.1b).

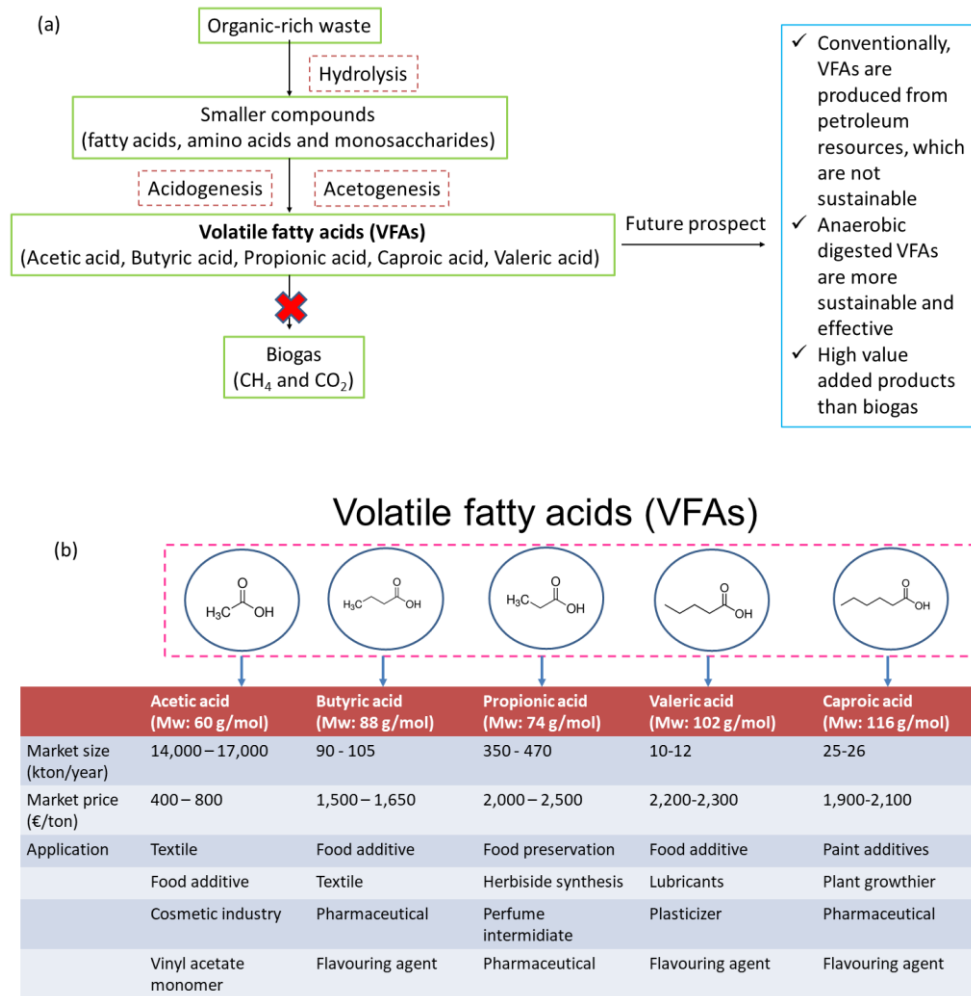


Figure 3.1 (a) Production pathway of VFAs (Wainaina et al., 2019c) and (b) Application of VFAs with their market feasibility (Atasoy et al., 2018).

Although, waste-based sources are one of the feasible platforms nowadays to achieve VFAs, it should be realized that anaerobically digested waste effluent is an unpurified complex mixture of VFAs, microorganisms, salts, proteins, lipids etc. that limit the application of the obtained solution as a purified VFA source. Moreover, in

most cases, the high water content of the AD effluent results in a dilute VFAs solution (Zhang and Angelidaki, 2015, Battista et al., 2020, Da Ros et al., 2020b). Besides, acid accumulation in anaerobic fermentation tends to inhibit the further production of VFAs, which means that the VFAs produced should be separated in real time (Yuan et al., 2019). In general, extraction of VFAs at high rate and yield from these mix liquid effluent is a challenging task. These obstacles can be tackled either through enhancement in productivity, product yield and concentration by fermentation and upstream optimizations or the application of practical and efficient separation and concentration processes (Masse et al., 2008).

The downstream or as called “post effluent treatment” for VFA recovery has gained substantial attention recently. Till present, several techniques such as adsorption (Reyhanitash et al., 2017), distillation and evaporation (Horiuchi et al., 2002), extraction (Katikaneni and Cheryan, 2002), electrodialysis (Strathmann, 2010) and pressure-driven membrane processes (Zacharof and Lovitt, 2012) have been implemented for VFAs recovery. Among them, membrane-based purification processes including microfiltration, ultrafiltration, nanofiltration, reverse osmosis and forward osmosis are regularly used to recover, purify and concentrate VFAs from mixed solutions. Membrane filtration offers many benefits such as the ease of customization and scalability, the possibility to apply for different effluents, low energy demand, minimal phase change during separation, separation specificity etc. Moreover, membrane separation technology can be integrated into any stage from fermentation to polishing the final product. The AD can be performed using anaerobic membrane bioreactors (AnMBRs) using pressure-driven membrane modules in order to produce microorganism and particle free VFAs-rich permeates (Trad et al., 2015, Wainaina et al., 2019c). Following that, ultrafiltration can be used to remove macromolecules such as lipids and proteins (e.g. enzymes) from the effluent, and nanofiltration and reverse osmosis can be employed to remove monovalent and divalent salts, and excess water (Song et al., 2018, Van der Bruggen et al., 2003a). However, membrane fouling and cleaning have always been the major hurdle in the industrial scale application of membrane separation processes.

In order to have a functional cascade of integrated membrane separation processes that assist optimal recovery, purification and concentration of VFAs from waste-derived AD effluents, it is of great importance to have a thorough knowledge of the factors affecting filtration operations. In order to guarantee long-term application of a pressure-driven membrane filtration system aimed at VFAs separation from complex media the effect of parameters such as membrane material, pore size, charge, hydrophilicity/phobicity, operating temperature, separation driving force (pressure, concentration and electrical potential), and effect of medium characteristics such as medium pH, solid content, EPS and SMP content and medium

viscosity should be clearly understood and defined (Odey et al., 2019, Rajabzadeh et al., 2012, Masse et al., 2010, Zhou et al., 2013a). However, to the knowledge of the authors, there are limited reports specifically on the factors influencing VFAs recovery from AD effluents. Till now, different techniques have been applied in VFAs recovery and purification, whereby a comprehensive analysis of the effect of determining factors involved in the membrane filtration of AD effluents for VFAs recovery is required to investigate.

3.1 Adsorption

Adsorption has been employed to capture the protonated form of diluted VFAs (neutral) from complex aqueous solutions. Usually, this process occurs through the interaction between a solid adsorbent surface (resin, activated carbon etc.) and adsorbate (VFAs molecules etc.) (Tung and King, 1994). In a recent study, Tonucci et al. (Tonucci et al., 2020) synthesized hybrid imprinted polymer-based adsorbent and tested it for the adsorption of VFAs from anaerobic effluents. Results showed that maximum VFAs adsorption capacity of $Q_e \sim 50$ mg/g (Q_e is the amount of VFAs adsorbed) was obtained and efficiently regenerated after the selective adsorption process. In this regard, the adsorbent's surface structure plays a critical role for the uptake of VFAs. The basic groups of adsorbent surfaces (alkaline surfaces) have more affinity to carboxylic acids because of the acid-base interactions but opposite results were achieved for acidic groups (El-Sayed and Bandosz, 2004). Therefore, several different types of materials, such as ion exchange resins and activated carbon, have been used for the adsorption of VFAs (Fufachev et al., 2020, Talebi et al., 2020).

Ion exchange materials could be applied together with the adsorption process in order to facilitate the recovery process whereby making a strong bond between the functional group of the ion exchange material and the ionized acid (López-Garzón and Straathof, 2014, Garcia and King, 1989). Among them, ion exchange resins have been using frequently due to their high surface area and the macroporous surface where the functional groups are mainly located. This could assist the diffusion mechanism during the adsorption process which is connected to the mass transfer characteristics scenario. In general, the adsorption process is regulated by the diffusion rate and the corresponding resin surface can act as supporting material (Kawabata et al., 1981, Fargues et al., 2010). The rate of diffusion is mainly controlled by three scenarios such as adsorption of VFAs molecules on the surface,

penetration of VFAs molecules in the surface and diffusion through the resin surface (Anderson et al., 1968, Smithells et al., 1936).

Anasthas et al. (Anasthas and Gaikar, 2001) used quaternary amino functional groups based ion exchange resin for the adsorption of acetic acid in non-aqueous phases. The sorption process interacted through the H-bonded complex formation between the functional group of resin and proton molecule of acid with the adsorption isotherm data being well fitted to the Langmuir model. Reyhanitash et al. (Reyhanitash et al., 2017) recovered VFAs from the fermented artificial wastewater by employing four types of resin-based adsorbents, which can be categorized as follows primary, secondary, tertiary amine-functionalized, and nonfunctionalized structured polystyrene-divinylbenzene resins. Initially, they conducted a batch adsorbent screening tests and found that non-functionalized adsorbent endows better adsorption capacity, while the functionalized adsorbents showed higher affinity to mineral acids. Later, they investigated a column test in the presence of non-functionalized adsorbent to determine the concentration profile of VFAs. Total recovery profile of butyric acid was enhanced ranging from 0.25 wt% to 91 wt% evaporated through a temperature-based fractionation of VFAs molecules. In the case of regeneration performance, nonfunctionalized adsorbent could be stable up to four adsorption–desorption cycles, which are of economic importance when large scale VFAs recovery using the adsorption process is targeted (Figure 3.2).

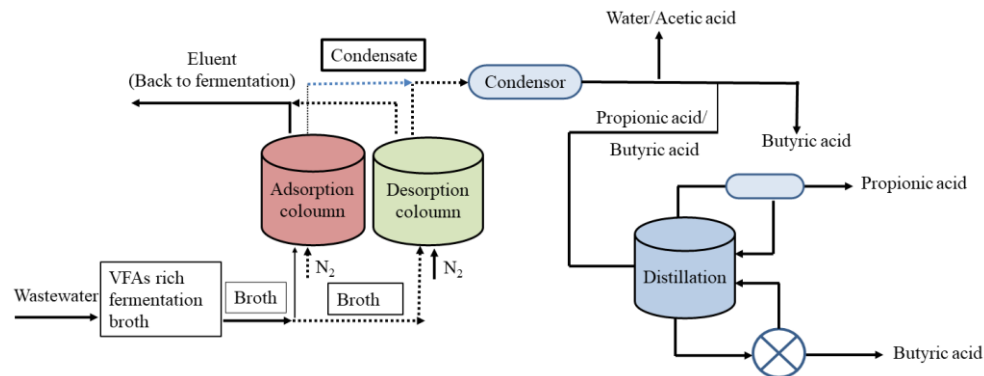


Figure 3.2 VFAs recovery by adsorption process (Reyhanitash et al., 2017).

Rebecchi et al. (Rebecchi et al., 2016) explored the VFAs recovery efficiency from an actual VFAs-rich effluent using ion exchange resins based adsorbents. Four different resins were used for the adsorption experimental purposes including primary amine, tertiary amine and quaternary amine. Results showed that tertiary amine (Ambelyst A21) resin prevails adsorption capacity from grape pomace effluent (76%) and synthetic VFAs mixtures (85%), respectively, and interestingly

this resin has a lower price compared to others. The adsorption capacity of Amberlyst A21 resin was also successfully investigated in previous studies (López-Garzón and Straathof, 2014, Li et al., 2009, Fargues et al., 2010). The desorption results were carried out with ethanol and NaOH solvents evaporation technique and ultimately around 97% of the VFAs were recovered on the desorbed surface. This work indicated that the Amberlyst A21 resin could be used for further VFAs adsorption studies from anaerobically digested effluent in an innovative approach.

In a comparative study considering activated carbon and resins for the adsorption of VFAs, the resin demonstrated a superior mixed acid adsorption capacity (74%) over activated carbon (63%) (Da Silva and Miranda, 2013, Yousuf et al., 2016, Uslu et al., 2010). The reason can be explained that the hydrophobic nature of the resin Amberlite IRA-67, attracts more acids under the pKa value of the acids, which makes them better adsorbent than activated carbon (Nielsen et al., 2010). Similarly, Eregowda et al. (Eregowda et al., 2020) conducted VFAs adsorption experiment in a batch system through anion exchange resins and compared it with that of activated carbon. This study utilized 11 anion exchange resins. Results showed that Amberlite IRA-67 adsorption capacity was fitted by the Freundlich model, which means the adsorption process is related to multilayer adsorption. , On the other hand, both the Langmuir and Freundlich model fitted the Dowex Optipore L-493 adsorption, resulting in a monolayer and multilayer related adsorption process, respectively (Saadi et al., 2015) These studies indicate that the resin-based adsorbents are preferential for VFAs adsorption purposes.

Although the adsorption process has been considered as an efficient technique for the recovery of VFAs, cost associated with the adsorption process are considerable when commercial adsorbents are needed to be recycled or regenerated (Bélafi-Bakó et al., 2004). Additionally, the presence of competing ions such as phosphate, sulfate and chloride are responsible for poor adsorption efficiency in VFA solutions resulting from the fermentation of complex organic wastes.

3.2 Distillation

Distillation is a fundamental physical separation and purification process of the components or substances from a liquid mixture. This process occurs when a liquid sample is evaporated using various boiling points and turned into a condenser through a distilled column to capture the produced vapors. Usually, the components or substances may be fully or partially separated and purified from the mixture (Lei et al., 2003, Qi et al., 2019). The distillation technique has been used commonly to

separate VFAs from various media (Demiral and Ercengiz Yildirim, 2003, Petersen et al., 2018). Regarding the application of distillation for VFA recovery, it is recommended to use distillation for the separation of VFAs from low concentration effluents as the efficiency of the VFAs separation deteriorates as highly concentrated VFA solutions reach the azeotropic point (Huang et al., 2008). For VFAs, the boiling point is considerably higher than water due to the fact that the structure of VFAs contains electrophile such as carbonyl groups (Reyhanitash et al., 2019). Various distillation approaches have been implemented to recover VFAs. Demiral et al. (Demiral and Ercengiz Yildirim, 2003) used the extractive distillation process for VFAs recovery from waste streams. They employed two solvents (adiponitrile and sulfolane) with a higher boiling point as the distillation process requires solvent-based substances to become more effective. So far, reactive distillation approach has identified as a promising technique for acid recovery (Painer et al., 2015, Komesu et al., 2015, Gangadwala et al., 2008). In this regard, Singh et al. (Singh et al., 2006, Singh et al., 2007) studied the effect of various parameters on acetic acid recovery reaching an experimental recovery of 80%. Regarding reactive distillation, Saha et al. (Saha et al., 2000) suggested that the recovery efficiency of acetic acid could be even further enhanced in the presence of an esterification distillation column. Butyric acid has reported being successfully recovered up to 89% through an ionic liquid induce short-path distillation process. This process effectively removed all the salt content resulting in the final product being mainly acids (Blahušiak et al., 2012). Generally, the distillation process requires two steps: the effluent stream dewatering and organic acid concentration. However, as the final polishing step, the remaining acid may be recovered by evaporation (Wasewar et al., 2002). Literature shows that the distillation based purification can open new processing possibilities for VFAs recovery. This process also has some disadvantages, like water is the main component of the fermentation broth with less boiling point than VFAs components, requiring a higher amount of energy, which is not economical. In addition, the concentration step is also time-consuming in the distillation process.

3.3 Precipitation

Precipitation is a conventional method that is usually applied to separate compounds from a mixture. Among them, the calcium-based precipitation process is commonly used to recover VFAs and four steps are required to obtain the final product including, a certain amount of Ca(OH)_2 or CaCO_3 added to the filtered liquid of fermentation broth under mixing conditions, then, calcium salts of VFAs have filtered away from the original aqueous liquid and exposed to H_2SO_4 in order to

release the desired amount of VFAs and finally purification added for obtaining a pure form of VFAs components (Min et al., 2011). Although environmental issues accompany the calcium precipitation process, the processing costs are higher since a large amount of H₂SO₄ and lime needed during the operation eventually increased the production budget (Wasewar et al., 2003). Followingly, King et al. (King and Starr, 1992) conducted a three-step process including extraction by solid solvent, dewatering to precipitate the acids and the collection of the acid conversion products in order to remove VFAs from water. VFAs can also be separated by using ammonia-based titration precipitating agents (Berglund et al., 1999). Moreover, the production of unwanted byproduct such as solid waste of calcium sulphate during the precipitation process has also hindered its application (Zacharof and Lovitt, 2013b).

3.4 Esterification

Another widely used VFAs recovery method is esterification. The benefits of esterification have been harvested in applications such as biodiesel production, VFA-ester compounds for fragrance and scents industry, and production of ammonium sulphate as fertilizer (Plácido and Zhang, 2018, Katikaneni and Cheryan, 2002, Ishihara, 2009). The esterification process produces ester products using an equilibrium reaction between two reactants, such as alcohols and acids. This process generally occurs in the presence of an acid catalyst and heat. Recovery of carboxylic acids using the esterification process has long been a popular method. Neumann et al. (Neumann and Sasson, 1984) used methanol esterification method for the recovery of dilute acetic acid as methyl acetate in a chemorectification column with an organic solid polymer catalyst. The reaction process was kinetically fitted with second-order for acetic acid and zero-order for methanol. One study showed that the addition of salt (CaCl₂) promoted the reaction yield when the polystyrene-supported solid acid catalyst was used under ethanol esterification (Yagyu et al., 2013). Accordingly, it was found that diarylammonium salt could catalyze the direct esterification process, which helps suppress solubility in water due to its hydrophobic nature and facilitates acetic acid recovery. Moreover, the esterification process occurred in a flow reaction system that can be pertinent to the industrial-scale operation (Igarashi et al., 2012). On the other hand, Bianchi et al. (Bianchi et al., 2003) implemented two types of experimental protocols for acetic acid esterification with alcohol: a complete evaporation condensations reaction and distillation. They have reported that the latter method was most favourable for a high amount of acetic acid recovery. Recovery of acetic acid by methyl esters

esterification from the real anaerobic fermentation broth was examined by Plácido et al. (Plácido and Zhang, 2018) and stated that 50% of acetic acid could be recovered with a VFA concentration of 800 gVFA/L while less than 10% observed at 500 gVFA/L. Besides, they noticed that ammonium sulphate salt was produced as a byproduct due to acidification of the fermentation broth that influenced plants economic growth. However, the downside is that esterification can be inhibited in the presence of a large amount of water. The adjustment of pH also can affect esterification potential as it is reported that the recovery of acetic acid without pH control (pH at about 6.5) resulted in low recovery yields of 5-20% (Horiuchi et al., 2002).

3.5 Extraction

Extraction is a well-established technique whereby two different immiscible liquids, such as water (polar compound) and an organic solvent (non-polar), are in contact with one another phases during the operation upon their relative solubilities. Besides, a net transfer reaction is observed from one phase to the other driven by chemical potential. After completing the transfer process, the solvent product is enriched with solute(s), which is known as extract substance (Kertes et al., 2009a). The extraction process has been known for more than a century to recover VFAs compounds effectively (Mostafa, 1999, Kertes et al., 2009b).

Benefiting from the extraction techniques, three extraction processes, including solvent extraction, reactive extraction and ionic liquids extraction, have been accomplished to recover VFAs so far (Figure 3.3). Solvent extraction is an efficient and economical process and uses various kinds of solvents in the aqueous phase. For instance, the use of trioctylphosphine oxide (TOPO) solvent allows an acetic acid recovery yield of 75%. TOPO can make a strong hydrogen bond with carboxylic acids in the organic phase due to its low solubility, high boiling point and good stability, and as a consequence, result in an extract phase with a higher amount of carboxylic acids (Golob et al., 1981). In another variation of recovery sources of VFAs within the solvent extraction approach, Shin et al. (Shin et al., 2009) introduced waste-derived streams sources along with an organic solvent (2-ethylhexyl alcohol) and successfully, 96.3% of acetic acid was recovered. Consistent with the above studies, several studies are also recovered acetic acid using a synthetic solvent (Chen et al., 2016, Cebreiros et al., 2017, Kim et al., 2016). However, recovery of VFAs by a green solvent in lieu of synthetic toxic solvents is of interest from the point of sustainable development goals (SDGs), for this, a recent study (Rodríguez-Llorente et al., 2019) proposed a sustainable route for the recovery of

VFAs from aqueous solution using natural solvents. Results showed that valeric and butyric acids extraction yield percentages were higher. Additionally, the authors conducted solvent stability studies by using an alkali medium.

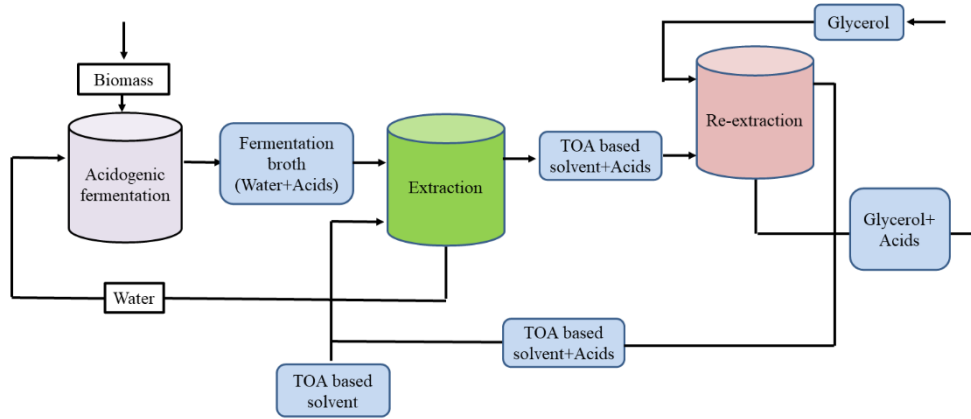


Figure 3.3 VFAs recovery by the solvent extraction process (Aghapour Aktij et al., 2020b).

On the other hand, the reactive extraction process also separates VFAs compounds from aqueous solutions using several extractants. Rasrendra et al. (Rasrendra et al., 2011) investigated the VFAs extraction efficiency from the phase splitted pyrolysis oil aqueous solution in the presence of tri-n-octylamine (TOA) and yield of 84% for acetic acid, while the extraction efficiency of acetic acid increased to more than 90% using aliphatic tertiary amines reactive extraction process (Mahfud et al., 2008). Furthermore, there is considerable research that uses triisooctylamine (Yang et al., 2013a), tri-butyl phosphate (Eda et al., 2017), trioctylamine/Octanol (Ahsan et al., 2013) and tributyl phosphate (Mukherjee and Munshi, 2020) in the reactive extraction process as effective extractants for a high amount of VFAs recovery. Finally, the extraction process has been amplified by the use of ionic liquids (ILs)-based extractants towards VFAs recovery due to their outstanding separation efficiencies, good stability and, more importantly, well fitted for the environment (López-Porfiri et al., 2020, Sprakel and Schuur, 2019, Şahin and Kurtulbaş, 2020, Cevasco and Chiappe, 2014, Wang et al., 2017). After that, Schuur's group published some potential results of acetic acid recovery by using ionic liquids medium, and they also confirmed that the extraction process is influenced hydrogen bond (Reyhanitash et al., 2016, Reyhanitash et al., 2019, Reyhanitash et al., 2015). Recently, oliveira and co-workers (Oliveira et al., 2012) have proved that phosphonium-based ILs are more amendable than traditional organic solvents in terms of VFAs recovery performances. Despite the progress of the extraction

process, this process depends on several factors, including operational parameters, raw materials availability and selection of appropriate solvents, etc. These issues must be amended constructively in order to achieve maximum output.

3.6 Gas stripping

Gas stripping is a relatively simple process, which involves gas sparging via the fermentation broth to transfer volatile compounds from the liquid state to the gaseous state to obtain the recovered products. This process has maintained Henry's law related to liquid and gas-phases concentration behaviour (Atasoy et al., 2018, Qureshi and Blaschek, 2001).

The recovery of VFAs compound from glucose fed meat anaerobic digester using gas stripping has been investigated by Li et al. (Li et al., 2015). This work conditioned their inoculum (anaerobic sludge) under an acidic medium (pH kept below 4.8), which favors VFAs accumulation since, at this pH, all VFAs compounds are found in undissociated form, and it is reported that undissociated form of VFAs must be present in the stripping process to be effective (Ramos-Suarez et al., 2021b). Results showed that at an acidic medium, the compounds of VFAs were recovered in the form of their salts with an amount of 80% butyrate and 20% acetate while only a minor portion of propionate and valerate. Interestingly, this study also demonstrated that the reduction of pH trend promoted lactic acid conversion to other valuable VFAs compounds during the fermentation process. Furthermore, a recent study (Huang et al., 2016) has shown that the gas stripping process can also be employed in another way rather than ammonia stripping directly from VFAs-riched liquid digested of swine manure using the solid-liquid separation technique. Afterwards, the total concentration of VFAs was 94.4 mg-COD/g-VS, which is promising in terms of the marketable demand for VFAs. However, the gas stripping process faces some challenges, such as needed a large volume of gases for circulation and subsequent recovery steps for adsorbents/condensers (Qureshi et al., 2014).

3.7 Membrane contactor

Membrane processes have attracted significant interest in the field of product recovery from waste-based resources due to their advantages over other extraction approaches in efficiency, time and energy-saving and sustainability (Shi et al., 2018b, Abels et al., 2013, Hube et al., 2020b, Mahboubi et al., 2016, He et al., 2012, Pervez et al., 2020g, Pervez and Stylios, 2018d, Pervez et al., 2020c). Various

membrane processes including membrane contactor, forward osmosis, membrane distillation, pervaporation, electrodialysis, microfiltration, ultrafiltration, nanofiltration and reverse osmosis have been utilized at different stages of VFAs recovery (He et al., 2012, Rongwong et al., 2018a).

Membrane contactor (MC) is an effective technique when it comes to the recovery of valuable compounds. This method realizes the separation of compounds into two phases while preventing their mixing. In other words a membrane brings two phases in contact through which the mass transfer between the phases occurs (Asfand and Bourouis, 2015). This method is mainly affected by the liquid phase characteristics (aqueous or organic) and the membrane surface properties (hydrophobicity, pore size or charge) (Drioli et al., 2005). In general, hydrophobic membranes are more preferential for resource recovery because of their good thermal stability and chemical resistance, also low energy required and large scale mass transfer ratios (Zhang et al., 2009, Rongwong and Goh, 2020). The application of MC for the recovery of VFAs has been practiced for a century. Tugtas et al. (Tugtas, 2014) used a membrane contactor for VFAs recovery in the presence of a flat membrane. Results highlighted higher selectivity of acetic acid (1.599) over water with separation occurring at a mass flux of 12.23 g/(m²h). In MC system, separation of VFAs can be affected by the medium pH. In this regard, Yesil et al. (Yesil et al., 2014) conducted the VFAs recovery experiments using polytetrafluoroethylene (PTFE) membrane contactor and they reported that higher selectivity (permeation fluxes) of VFAs could be obtained at lower pH. Among the VFAs considered, caproic acid showed better selectivity compared to other acids. Membrane contactors can be also utilized to bring gas-liquid or gas-gas phases in contact. A recent study by Aydin et al. (Aydin et al., 2018) used vapour permeation membrane contactor (VPMC) to recover mixed VFAs. They utilized three VPMC configurations including air-filled PTFE membrane with the other two being extractants (TOA or TDDA) filled PTFE membrane. The recovery percentage of VFAs were reported higher for extractants filled PTFE membrane except for acetic acid. In addition, TOA-filled membrane has also demonstrated a higher selectivity towards caproic acids, butyric acids and valeric acids (Rongwong and Goh, 2020). However, MC VFAs separation can be challenged by medium properties. It is noteworthy that the feed containing suspended particles result in lower VFAs recovery percentages (Yesil et al., 2014) and therefore suspended particles-free feed solution are the target of MC VFAs separation.

3.8 Membrane distillation

Membrane distillation (MD) is a thermally driven process whereby the vapour molecules are transported across a hydrophobic membrane. The hydrophobic property of the membrane used in the MD process allows passing gases and vapours through the membrane surface while preventing liquid transport (Figure 3.4) (Song et al., 2007). MD has various advantages over other thermal membrane separation processes such as high concentration of compounds could be retained as retentate, lower temperature requirements, larger membrane pore size and operation at atmospheric pressure. More importantly, fouling issues of the MD process could be minimized using suitable cleaning protocols since it is in direct contact with fermentation broth, while the processes such as membrane filtration or PV needed liquid steam pretreatment procedure to prevent the fouling scale (Gryta, 2008, Guillen-Burrieza et al., 2014).

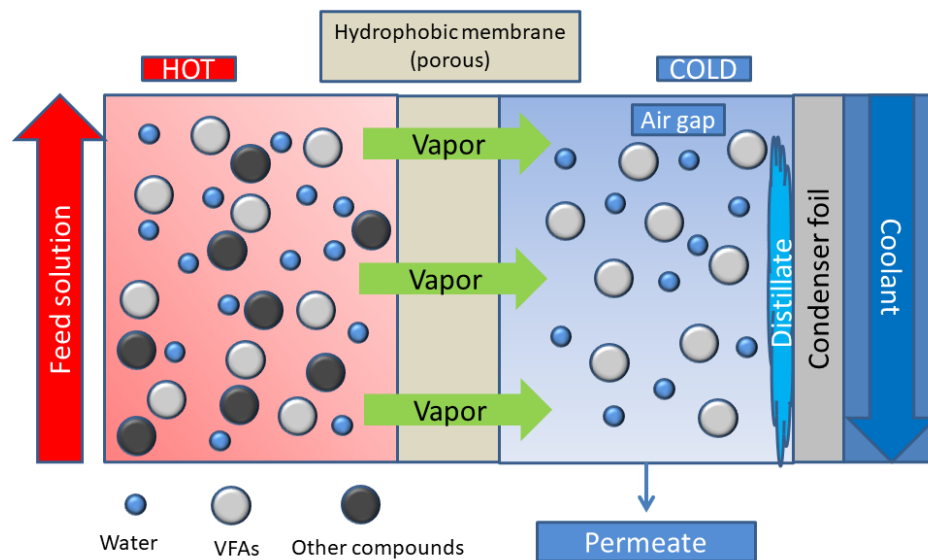


Figure 3.4 Tentative MD process scheme for VFAs recovery (Aghapour Aktij et al., 2020b).

An anaerobic membrane distillation bioreactor with polyvinylidene fluoride (PVDF)-based hydrophobic membrane has been utilized to treat synthetic wastewater that contained acetic acid, propionic acid, butyric acid and isovaleric acid (Yao et al., 2019). The results showed that propionic acid, butyric acid and isovaleric acid were successfully recovered in terms of higher concentrations obtained (1.3,

20.3 and 15.6 mg/L) in the permeate solution than feed solution (1.1, 16.7 and 12.6 mg/L) except for acetic acid, which is associated with higher boiling points than acetic acid that may facilitate transfer rate through the membrane surface during the operation, resulting in a higher recovery rate. Besides, they found that higher temperature showed a negative effect on recovery rate and membrane fouling phenomena. As it is known that the MD process is a thermal membrane separation process, so using low temperature during the operation possibly increased their reliable uses from the point of economic and energy-intensive perspective (Fasahati and Liu, 2014). Another study also used low temperature (35 °C) to separate arsenic from glycerol fermentation broth in the MD process. They utilized polypropylene membranes and exhibited satisfactory resistance to wettability during the processing stages. However, fouling issues are still noticed in their MD process, and surely this is one of the potential challenges for the future progress of MD (Gryta et al., 2013).

3.9 Electrodialysis

The use of electrodialysis (ED) has been widely investigated in the effluent treatment process to recover valuable compounds. The ED process is formed of a separation an ion-exchange membrane where an electric field is supplied for the migration of the anions and cations to the anode and cathode chambers (Figure 3.5) (Ward et al., 2018, Vertova et al., 2009). It is often suggested that the charged form of VFAs are more suitable for recovery processing stages, therefore, a series of charged membranes are placed in between two electrodes to prevent the Donnan repulsion in the ED process (Huang et al., 2007, Wang et al., 2006).

Generally, the conventional electrodialysis (CED) process has been effective for acetic acid recovery than other VFAs compounds (Jones et al., 2015, Pan et al., 2018). Later a study carried out by Tao and co-workers who showed that MF pretreatment could enhance the CED process recovery efficiency with an amount of 92% acetic acid and 85% n-valeric acid. They also found that concentration increased from 11.73 g/L to 19.82 g/L (Tao et al., 2016), which agrees with other studies that also showed that higher concentrated VFAs compounds were achieved after electrodialysis (Bermeo et al., 2003, Scoma et al., 2016). These results attributed to the lower concentrations of VFAs in the initial feed solution, but these concentrations are very low in view of the practical aspects, and it has been proposed to use 200–500 g/L of VFAs concentration as a feedstock in the feed solution (Ramos-Suarez et al., 2021b).

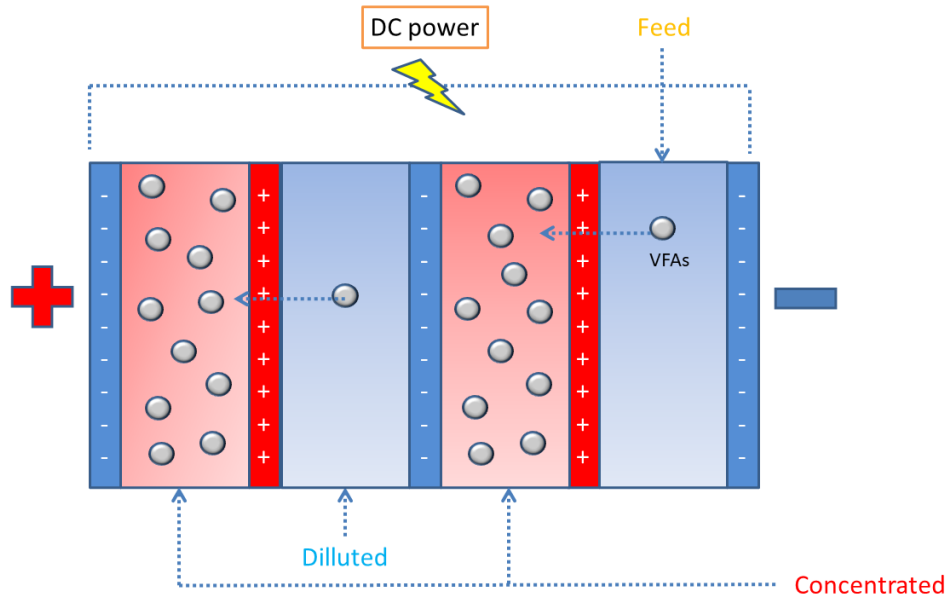


Figure 3.5 Tentative CED process scheme for VFAs recovery (Aghapour Aktij et al., 2020b).

Electrodialysis with bipolar membrane (EDBM) demonstrated as an environment-friendly and energy-efficient technology. Bipolar membranes are typically ion-exchange membranes together with anion and cation exchange through the use of a junction layer in their laminated structures (Pärnamäe et al., 2021, Huang and Xu, 2006b). In some cases, cation exchange membranes are not needed in the direct recovery system using the EDBM process; applying only an anion exchange process, it is possible to recover up to 70% of acetic acid that may save energy consumption and operating costs (Yu et al., 2000). On the other hand, the efficiency of the EDBM process could be increased using a two-stage operation, around 87% of VFAs were recovered from real pig manure hydrolysate (Shi et al., 2018a).

Another important design is the placement of the ED unit in direct contact with the fermentation broth for *in-situ* recovery of VFAs. Dai et al. (Dai et al., 2019) have discussed the feasibility of this alternative integrated system. By coupling the ED unit into fermentation broth, the recovery rate of acetic acid was faster than the alone ED unit due to the use of direct electricity sources. Interestingly, another benefit was observed after combining the unit can simultaneously enhance hydrogen production, potentially influencing the passage of VFAs compounds with 95% and 69% recovery efficiency (Arslan et al., 2017, Zhang and Angelidaki, 2015). However, some drawbacks have been noticed in all ED processes such as membrane operation cost,

non-VFAs anions (such as Cl^-) removal favoured over VFAs anions, requiring additional salts that are not practicable towards further downstream applications (Tao et al., 2016, Zhang and Angelidaki, 2015, Chalmers Brown et al., 2020).

3.10 Pervaporation

Membrane-based pervaporation (PV) is an emerging separation process for the recovery of value-added chemicals from waste streams. In the pervaporation process, liquid mixtures are separated using the solution flow and diffusion of the components through the membrane. The components subjected to separation are absorbed into the membrane and the permeate is collected over the membrane in the vapour-phase (Figure 3.6) (Feng and Huang, 1997).

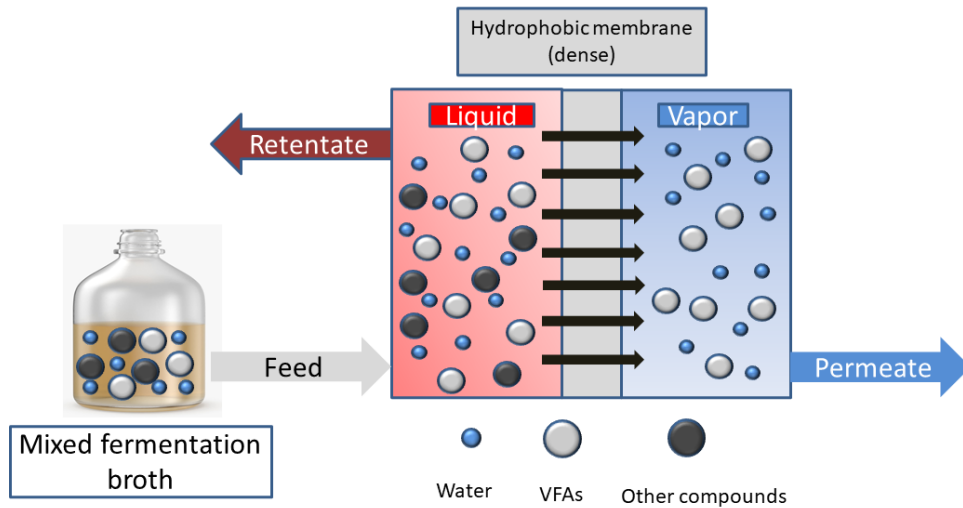


Figure 3.6 Tentative PV process scheme for VFAs recovery (Khalid et al., 2019).

This technique has the potential for VFAs recovery as it is environment-friendly and economical. Pervaporation membranes are highly preferable for acetic acid selection over water. Selectivity performance could be improved by adjusting the membrane pore size (0.2-0.5 nm) and layer mechanism. One study developed a new kind of composite membrane by casting sodium alginate solution onto an N_2 plasma modified polypropylene membrane and further crosslinked by Ca^{2+} and Al^{3+} . They showed that N_2 plasma significantly increased their pore size and hydrophilicity, while the crosslinking mechanism improved the stability and separation factor of acetic acid/water compared to the original membrane (Zhang et al., 2014b), which is

in line with other works that have been discussed the benefits of using a hydrophilic pervaporation membrane prepared by the use of amine-functionalized metal-organic framework (Su et al., 2015), graphene oxide (Dave and Nath, 2016) and molybdenum disulphide (Choudhari et al., 2015). On the contrary, some researchers synthesized hydrophobic pervaporation membranes through the use of common polymers polydimethylsiloxane (Li et al., 2004), zeolite (Bowen et al., 2003) and silicalite (Sano et al., 1997) and exhibited their promises on VFAs recovery because of their high affinity towards organic compounds. Besides, the corresponding permeate fluxes were also double after incorporating such fillers.

Moreover, other than conventional dense hydrophilicity/phobicity membranes, another membrane such as supported liquid membrane has been used for VFAs recovery in the pervaporation technique. A study by Yesil and coauthors utilized the pervaporation method for recovery of mixed VFAs from the fermentation broth using three types of membrane; polytetrafluoroethylene (PTFE), tridodecylamine (TDDA) filled PTFE and composite silicone rubber/PTFE membranes. Results showed that the highest selectivity of VFAs, flux, separation factor and permeance was obtained in the presence of TDDA filled PTFE liquid membrane (Yesil et al., 2020). This is because of lower aqueous–organic interfacial tensions between liquid membranes and VFAs compound, which agrees with a previous report (Qin and Sheth, 2003). However, previous researchers did not focus on product capture from the vapor phase in the commercial method, which is very sensitive in terms of product loss during the pervaporation process, and it should be carefully monitored.

3.11 Forward osmosis

Forward osmosis (FO) is another new approach evaluated for the treatment of the effluents using the semi-permeable membrane panels in which the target solutes from the feed (dilute) solution are transferred to the draw solution (concentrated) over osmotic pressure (Figure 3.7). The FO process does not require any external energy input since it is driven by osmotic potential except a small amount of energy needed to circulate feed and draw solutions (Khan et al., 2021a). This process has a couple of practical advantages such as low membrane fouling, low or no pressure requirements and high retentate efficiency (Cath et al., 2006).

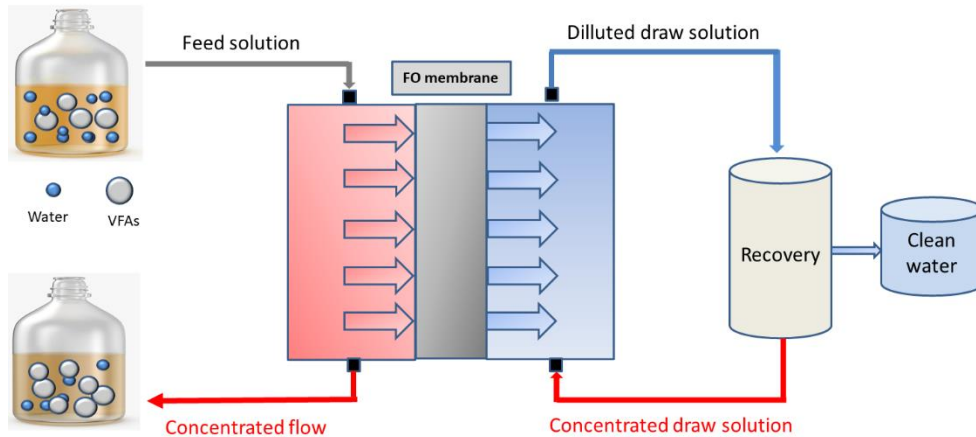


Figure 3.7 Tentative FO process scheme for VFAs recovery (Zhang et al., 2020).

Concentration of VFAs derived from waste streams through FO has been recognized as an emerging technology in recent years (Cagnetta et al., 2017, Garcia-Aguirre et al., 2020). During the FO process, the rejection performances of VFAs compounds appeared to be pH-dependent rather than membrane orientation (Khan et al., 2020). With the increase of pH values, the recovery percentages of individual VFAs components were increased. Around 90% recovery of VFAs was achieved at pH 7.5, while only 30% for pH 4, as investigated by Blandin and his team (Blandin et al., 2019). These results can be described by focusing their ionization constant (pK_a) values, as all VFAs exhibits pK_a around 4.8, thus the rejection rate at pH 7.5 was modulated by charged effects. At higher pH, VFAs compounds and membrane surface charge both became negatively charged, resulting in high retention behaviour due to the formation of electrostatic repulsion (Verliefde et al., 2008). On the other hand, recovery percentages at pH 4 were explained by a size-dependent mechanism, meaning higher molecular weight compounds are better retained than smaller molecular weight compounds (Bellona et al., 2004). Besides, permeate flux is also affected by pH solution, higher flux is obtained when solution pH was higher (Jung et al., 2015). The combination of the FO process with other recovery techniques such as membrane distillation, nanofiltration and reverse osmosis could be more efficient. This can be applied through pre-treatment (NF/RO-FO) and post-treatment (FO-MD) integrated set-up, intending to recover the water and concentrated acid from fermentation broth simultaneously (Zhang et al., 2014a, Cho et al., 2012).

Moreover, some studies proposed a dynamic model for the concentration of VFAs under the FO process. The motivation to develop this dynamic model for controlling the FO operational parameters systematically. By using this model, recovery

efficiency and flux behaviour over time can be optimized. The model was based on the Levenberg-Marquardt algorithm to determine all process variables. After investigating the results, it was found that the concentration percentage of acetic, butyric and valeric acids were enhanced, as complying with the predictions made by the model (Ruprakobkit et al., 2016, Ruprakobkit et al., 2017, Ruprakobkit et al., 2019).

Moreover, the above discussion stated that the FO process has some potential challenges, such as reverse solute diffusion, internal concentration polarization, and membrane fouling. These phenomena should be resolved to obtain a high amount of VFAs from liquid waste streams.

3.12 Pressure-driven membrane filtration

Pressure-driven membrane filtration process is a classical separation method and has significant aspects in purifying mixed waste effluents. These processes can be categorized into four types based on the membrane pore size and driving force (transmembrane pressure) during the operation, including microfiltration (MF), ultrafiltration (UF), nanofiltration (NF), and reverse osmosis (RO) (Figure 3.8). Pressure driven membrane process can be arranged in two ways, such as dead-end and cross-flow membrane filtration. In the dead-end membrane filtration, the feed solution flowed through the vertical direction of the membrane surface with one stream of the membrane module, while the feed solution flowed tangentially toward the membrane surface with two streams (one for retentate and one for permeate) for cross-flow membrane filtration. Moreover, various membrane modules, including tubular, hollow, flat sheets and spiral wounds, are typically utilized for pressure-driven membrane operation (Van der Bruggen et al., 2003c).

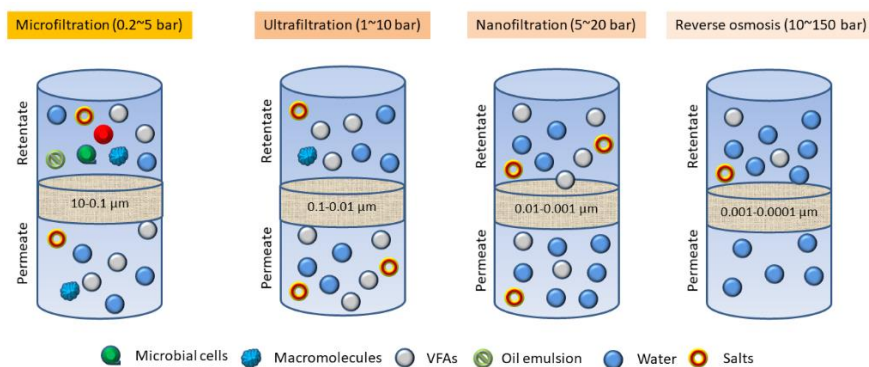


Figure 3.8 Pressure driven membrane filtration process for VFAs recovery (Liao et al., 2018).

In the MF process, the membrane was used with pore sizes ranging from 10 to 0.1 μm and operating hydraulic pressure applied from 0.2 to 5 bar, leading to a higher flux. In general, larger particles such as bacteria/protozoa, suspended particles and emulsified components than pore size can be removed are in the MF process from the feed solution due to the size-exclusion separation mechanism. Phase-inversion, stretching, track etching and sintering techniques are mostly used for the production of hydrophobic MF membranes. Polymeric, ceramic and metallic membranes are frequently applied in the MF operation. On the other hand, the UF process used smaller pore size membranes (varied from 0.1 to 0.01 μm) and higher transmembrane pressure ranges between 1 to 10 bar. Similar to MF, the UF process retained the larger particles such as proteins and sugars by following the size exclusion mechanism. Mainly, the phase inversion technique was selected for the synthesis of polymeric UF membranes. Some polymers are commonly blended during the processing to increase the membranes' hydrophilicity. Notably, both MF/UF membranes are structurally microporous.

In the NF process, membranes can be either porous or dense with a pore size of about 0.01-0.001 μm and molecular cut-off (MWCO) about 300-500 dalton (Da). This makes NF membranes suitable for retaining low molecular weight acids and divalent inorganic ions (Mohammad et al., 2015). The separation mechanism of the NF membrane process is governed by the combination of the Donnan effect, steric and dielectric poles (Ernst et al., 2000). Usually, the NF process operates at applied pressures in the range from 5 to 20 bar. On the other hand, reverse osmosis membranes are generally known as dense non-porous membranes with a pore size between 0.001-0.0001 nm and MWCO about 100 Da. During the RO operation, this filtration process requires relatively high pressure (10–150 bar). Mostly, polymeric/organic membranes have been utilized for NF/RO applications because of their cost-effectiveness and high efficiency.

There is a broad consensus that the pressure-driven membrane processes have better capability in recovering VFAs compounds from different waste streams (Aghapour Aktij et al., 2020b, Zhu et al., 2021a). For instance, Kim et al. (Kim et al., 2005a) investigated the microfiltration performance (ceramic MF membrane) of organic sludge for the recovery of VFAs. Results showed that bacteria were completely removed while more than 80% of VFA could be recovered through the permeate. However, the recovery percentage could be increased to 90% using a modified polyethersulfone microfiltration membrane module (a KrosFlo Research III System) (Tao et al., 2016). In recent years, some studies demonstrated that using MF together

with MBR may open a new possibility for continuous *in-situ* recovery of VFAs from various waste effluent streams such as food waste (Wainaina et al., 2019c), food waste slurry and excess sewage sludge (Parchami et al., 2020b), chicken manure (Yin et al., 2021b) and cow manure (Jomnonkhaow et al., 2021a). The transformation from batch to continuous production and recovery using a newly developed immersed membrane bioreactor eventually led to a sustainable VFAs recovery strategy in the MF process. Similarly, UF has also been applied for VFAs recovery, as the pore size of the membranes is normally less than that could assist in retained low molecular weight VFAs compounds. For example, Longo et al. (Longo et al., 2015a) recovered VFAs from sewage sludge fermentation with the use of an ultrafiltration setup. They successfully recovered a high amount of VFAs, especially acetic acid and propionic acid.

However, MF/UF still possess some limits, such as larger pore size, which are not beneficial for VFAs recovery effectively. In this context, NF/RO membranes with smaller pore sizes have been demonstrated as a potential route for improving the recovery efficiency of VFAs compounds. For instance, Han et al. (Han and Cheryan, 1995) screened several different types of nanofiltration and reverse osmosis membranes for acetic acid recovery from a synthetic solution. At high pH, the recovery percentage of acetic acid increased reaching an average of 40%. In another work, Xie et al. (Xie and Liu, 2015) concentrated 60% of acetic acid from paulownia hot water wood extracts using a nanofiltration module. They suggested that during nanofiltration, multiple parameters such as membrane hydrophobicity affect acetic acid filtration efficiency. Besides, the nanofiltration efficiency was directly influenced by the intermolecular interactions in the biomass, meaning the solution pH plays an important role during the nanofiltration process. For the separation of acetic acid from lignocellulosic substrate, Weng et al. (Weng et al., 2009) reported an acetic acid recovery percentage of 90% in a xylose solution using NF at medium pH of 2.0 and 24.5 bar. Similarly, Malmali et al. (Malmali et al., 2014) could reach a complete separation of acetic acid from biomass hydrolysate using NF. They have clearly noted that the recovery of acetic acid is pH-dependent while using NF. It has been reported that a sequential filtration can enhance the recovery percentage of acetic acid considerably when using NF (Lyu et al., 2015). NF can also be used in combination with RO to increase recovery percentage. Recovery of acetic acid by NF and RO from pulp mill spent sulfite liquor was conducted by Afonso et al. (Afonso, 2012). It was observed that although the NF membrane flux was higher than that of the RO membrane, the retention percentage of acetic was better for RO membrane (89%) compared to the NF membrane (77%).

Considering the fact that pressure-driven membrane filtration process shows a potential scope in recovering a high amount of VFAs compounds compared to the

other techniques. The most reliable feature of this process is membrane properties that have a strong influence on VFAs recovery. In this paper, the pressure-driven membrane filtration process is discussed in detail since it is simple, unique and high efficiency, and various factors play a vital role, hence it is worth investigating.

3.13 Factors affecting pressure driven membrane-assisted recovery of VFAs

In order to guarantee a long-term sustainable membrane filtration for separation of VFAs from different streams a synchrony between different membrane-, medium- and operation-related factors is essential. In pressure driven membrane VFAs separation the main parameters affecting the success level of the process can be listed as; membrane properties (membrane material/composition, pore size, charge, hydrophilicity/phobicity and permeability) and medium characteristics (Feed concentrations, pH, temperature, pressure and ionic strength).

3.13.1 Membrane material

The membrane filtration efficiency is greatly influenced by membrane characteristics such as membrane materials (Choi and Ng, 2008, Sadeghi et al., 2018). Up to present, various qualities of membranes such as metals, ceramics and polymers have been employed for VFAs recovery purposes in pressure-driven membrane filtration. Metallic membranes are used successfully in the MF/UF filtration units. It has been reported that metallic membranes have more strength to high-temperature oxidation and better endurance, which assist with fouling reduction (Zhang et al., 2005b). On the other hand, ceramic membranes have been used widely on a commercial scale for MF/UF systems as they offer high flux, corrosion resistance, low fouling tendency and backwashability (Ersu and Ong, 2008). Moreover, ceramic membranes provide a high flux because of the fewer interactions between the membrane surface and foulants (Baker, 2012). Ceramic membranes have therefore been used for VFA recovery from liquid organic sludge. For example, Kim et al. (Kim et al., 2005a) used a cross-flow microfiltration unit and showed that ceramic membranes could be used to recover more than 80% of VFAs in a solution. Moreover, ceramic membranes (made of α -Al₂O₃) have been successfully applied to remove large particles from the anaerobic digestion streams with low VFAs retention (Zacharof and Lovitt, 2014). However, as both ceramic and metallic membranes have shortcomings when it comes to shaping and modularity, weight and price,

polymeric membranes have been applied on a large scale in the pressure-driven membrane filtration system (Ng et al., 2013, Van der Bruggen et al., 2003c).

As presented elaborately in Table 3.1, variety of polymeric membranes have been used for microfiltration and ultrafiltration in VFA recovery systems. As an example, polyvinylidene fluoride (PVDF)-based membranes have been used in the cross-flow microfiltration for the extraction of VFAs in a solution with concentrations of up to 52 g/L (Trad et al., 2015). In addition, surface modification of polymeric membranes (e.g. modified polyethersulfone) has been reported to result in better recovery percentage of VFAs (around 90%) (Tao et al., 2016). Another commonly used membranes for NF and RO are composite polyamide(PA)-based membranes. Typically composite membranes are anisotropic in nature and composed of two or more highly porous supporting materials. The structure of composite polyamide membranes is characterized by three layers: a top polyamide layer (size around 100 nm), the second layer made of a microporous polysulfone and finally, a non-woven supporting material to provide mechanical durability (Tang et al., 2009). The top layer is considered as the crucial part since it determines the selectivity performance of the membrane. Categorized based on the structural monomer group, fully aromatic PA membranes although fully commercialized, it possesses a rough surface that challenges smooth operation. Alternatively, semi-aromatic poly(piperazinamide)-based PA membranes exhibited a smooth surface and are often used in membrane filtration process. However, fully aromatic based membranes are still considered as a mainstream membrane because of their high recovery efficiency than poly(piperazinamide)-based membrane (Tang et al., 2009, Choi et al., 2008). As summarized in Table 3.2, although fully aromatic based XLE (Polyamide, Dow Filmtec) nanofiltration membrane effectively retained acetic acid (97%), butyric acid (99%) and propionic acid (99%) in a ternary solution, the retention percentages for piperazinamide-based NF-45 (Polyamide, Dow Filmtec) membrane was only 68%, 88% and 72%, respectively (Zhu et al., 2020b). There are several more commercial fully aromatic-based membranes such as NF 90 (Polyamide, Dow Filmtec), NF 97 (Polyamide, Alfa Laval), ES 10 (Aromatic polyamide, Nitto Denko) that have exhibited better VFAs recovery compared to the piperazinamide-based membranes. In addition, fully aromatic membranes performance can be improved by the application of a cross-linker in the parent molecule. In this regard, Zacharof et al. (Zacharof et al., 2016) used polyvinyl alcohol-aromatic cross-linked polyamide membrane LF10 (Polyvinyl alcohol/polyamide, Nitto Denko) in treating agricultural wastewater digestate rich in carboxylic acids. They found that the recovery percentages of acetic and butyric acid were maximal for LF10 (Polyvinyl alcohol/polyamide, Nitto Denko) membrane compared to the piperazine-based polyamide membranes such as NF 270 (Polyamide, Dow Filmtec), HL

(Polyamide/polysulfone, GE Osmonics) DL (Polyamide/polysulfone, GE Osmonics) DK (Polyamide/polysulfone, GE Osmonics). Similar trend was also noticed for reverse osmosis membranes, such as fully aromatic-based SWC5 (Polyamide, Hydranautics) and SWC6 (Polyamide, Hydranautics) RO membranes, capable of recovering more than 80% of acetic acid and 100% of isobutyric acid, while the recovery percentage increased to 95.2% in the presence of coated fully aromatic flat sheet SW 30HR (Polyamide/polysulfone, Dow Filmtec) membrane (Table 3.3). However, the recovery percentage decreased to 60% when the piperazine based polyamide membrane SG (Polyamide, GE Osmonics) used. This indicates that fully aromatic membranes are the most suitable for satisfactory recovery percentages of VFAs.

Moreover, applied membranes for VFAs recovery were mostly flat sheets and spiral wound modules, as presented in Table 3.1-3.3. It was noticed that the recovery percentages of VFAs are quite similar in both type of membranes, but the use of flat sheet membrane is higher than spiral wound membrane because of their easy cleaning operation and steady water flux (Corzo et al., 2017).

3.13.2 Membrane pore size and molecular weight cut-off

The pore size of the membranes has been called as the backbone of the MF, UF and NF and is well-understood that membrane pore size has a fundamental relationship with the retentate and permeate solution characteristics (Dizge et al., 2011). The selectivity of MF membranes are determined by indicating the pore size, while for pore sizes for UF, NF and RO membranes are usually presented in MWCO (expressed as Da or kDa). Generally, the pore sizes of the MF and UF membrane are relatively large (section 2.12) that allows removing larger particles, microorganisms and macromolecules, while small MWCO of NF and RO membranes assist with the retention/removal of low molecular weight compounds/ions.

In addition, membrane permeability is an effect of pore size, which describes the passage rate of a compound through the unit area of the membrane per unit time and pressure applied. Membrane has the most important role in defining permeability as its selectivity acts as a resistance against the flow of all compounds through the membrane. In general, there is a trade-off between membrane permeability and its selectivity as higher permeability tends to lower the selectivity and vice versa (Park et al., 2017). When separation of VFAs from the anaerobic digestion effluent is to be conducted, considering the complex composition of the effluent high selectivity towards VFAs is sought that may challenge membrane permeability and process productivity.

Table 3.1 shows that MF and UF membranes have been actively used for clarification of VFAs containing solutions rather selective retention of VFAs (Trad et al., 2015, Longo et al., 2015a). Although, some studies have reported that a marginal amount of VFAs could be retained while applying MF or UF, surprisingly, there are reports on negative retention percentages for VFAs using MF or UF (Zacharof and Lovitt, 2014, Jänisch et al., 2019). As such, the acetic acid concentration of permeate solution (1.265.85 mg/L) was higher than retentate solution 1.083.30 mg/L in the presence of a Membralox ceramic microfiltration membrane (Pall Corporation). Whereas the same trend was observed for ultrafiltration membrane (UH050, Microdyn-Nadir), having a higher acetic acid concentration in the permeate solution (3.45 g/L) compared to that of the original hydrolysate solution (3.33 g/L). These results are achieved due to the larger pore size of MF/UF membranes. As the pore size range provided by MF and UF does not satisfy selective removal of VFAs, smaller pore sizes in the range of NF and RO are required for this purpose.

Similarly, membrane permeability in MF and UF have a minimal influence on VFAs recovery (Zacharof and Lovitt, 2014). Although ceramic membranes have been reported to show higher permeability than their polymeric counterparts, their VFAs recovery percentage is inferior to that of polymeric membranes (Kim et al., 2005a, Zacharof et al., 2016). For example, MF ceramic membranes were used to recover about 87% of VFAs, while polymeric ones could reach up to 92.8% (Table 3.1). A recent study has suggested the application of high permeability ceramic membranes for the fractionation of higher molecular weight compounds and polymeric membranes with lower permeability for the removal of lower molecular weight substances (Luiz-Santos et al., 2020).

Applying nanofiltration, experimental results indicated that 200 Da MWCO membrane can provide a high recovery percentage for acetic acid (78%) compared to 200-400 Da and 1000 Da membranes that exhibited only 22% and 9% , respectively (Table 2) (Afonso, 2012). There is a general consensus on the direct relation between MWCO and VFAs recovery percentage (Zacharof et al., 2016, Bellona and Drewes, 2005). For example, it has been reported that when the MWCO was increase from 200 to 300 Da, acetic acid recovery percentage of dropped from 85% to 83%. Based on our own unpublished results, the percentage of VFAs recovery dropped to almost half when 150-300 Da (Acetic acid, 22%, Butyric acid, 30%) membrane was used compared to that of <150 Da membrane (Acetic acid, 72.2%, Butyric acid, 69.7%). The highest amount of VFAs recovered (>90%) has been obtained in using NF membranes with about 100 Da MWCO, which is attributed to the average molecular weight of VFAs is around 100 g/mol or larger,

leading to higher retention in the 100 Da membrane (Choi et al., 2008, Zhu et al., 2020b, Ecker et al., 2012, Wainaina et al., 2019a).

For NF membrane, as shown in Table 3.2, direct relation between permeability and selectivity exist as the water permeability reduced VFAs recovery increases. The permeability rate of HL, DL, DK and LF 10 membranes were found to be 118.43, 56.02, 44.60 and 15.95 L/(m²h), respectively, leading to an ascending order recovery percentages of VFAs of 22%, 45%, 57.2% and 72.2%. The LF 10 that provided a higher recovery percentage at low permeability, practically requires higher filtration pressures that may hinder the economic feasibility of the filtration process (Zacharof et al., 2016). NF 90 and NF 270 are among the most popular NF membranes used for VFAs recovery. Among the two, NF90 membrane, although low in permeability, has had better VFAs recovery performance. Similarly, the ES10 flat sheet membrane with permeability of 1.67 L/(m²h) performed better in the recovery of acetic and propionic acids compared to NF 270 with a permeability around 3.88 L/(m²h) (Bellona and Drewes, 2005). Moreover, as reported by Afonso et al. (Afonso, 2012), the recovery percentage of acetic was more than 3 times higher in the case of NP030 (29%) compared to NP010 membrane (9%) as the former possesses lower permeability. This was the common trend for other commercial membranes as the lowest permeability demonstrated the best recovery amount of acetic acid. For example, PA 100 (Polyamide, Permeonics Pvt Ltd) flat sheet membrane had the permeability of 2.8 and exhibited 30% acetic acid recovery, while PA 150 (Polyamide, Permeonics Pvt Ltd), PA 400 (Polyamide, Permeonics Pvt Ltd) and PES 150 (Poly ether sulphonate, NovaSep) membranes had lower recovery percentages between 2-12% (Maiti et al., 2012). Lyu et al. (Lyu et al., 2016) also confirmed that the lower permeability rate of TS40 (Polypiperazine amide, Microdyn-Nadir) flat sheet membrane help 7% acetic acid recovery while for the higher permeability membrane XN45 (Polyamide, Microdyn-Nadir) this was only 3%.

Based on the expected MWCO, reverse osmosis membranes are similar or better in performance compared to nanofiltration membranes in VFAs recovery. The literature available lack presentation of MWCO for the RO membranes used for VFAs recovery. Considering NF and RO membranes researched, it was noticed that when a membrane with MWCO of about 100 Da is used butyric acid recovery of about 78% can be expected while MWCO of higher than 150 Da membrane can drop the recovery to 62-68% (Table 3) (Cho et al., 2012, Ozaki and Li, 2002). Interestingly, Yasin et al. (Yasin et al., 2020) found that two membranes with the same MWCO range (200-400 Da) showed different recovery percentages for acetic acid of 50% and 10%. These types of results confirm that the presence of various

functional groups on the membrane surface can strongly affect the recovery percentages of VFAs in NF and RO processes.

As shown in Table 3.3, the effect of permeability on concentration VFAs using RO membranes has also been investigated. Liu et al. (Liu et al., 2020a) concentrated higher percentage of acetic acid in using a SWC5 membrane (81.92%) than with SWC6 membrane of higher permeability. The flat sheet membrane ES 20 demonstrated twice permeation flux than other commercial membranes and therefore, attributed to lower recovery percentages (Ozaki and Li, 2002). The performance of RO membrane from Alfa Laval also is in agreement with these findings. In this regard, RO 98pHt (membrane permeability of 3.15) recovered around 44.21% of acetic acid present in the feed, while a recovery percentage of 47.51% was achieved using RO 99 membrane (2.60 permeability) (Zhou et al., 2013a). However, in contradiction to the general trend, it reported that XLE membrane (permeability of 100 L/(m²h)) succeeded to retain 78% of butyric acid while the lower permeability membrane LE (70 L/(m²h)) could only provide 62%. On the other hand, a series of membranes such as CPA3 (2.6 L/(m²h), acetic acid 40.1%), CPA2 (3.1 L/(m²h), acetic acid 43.5%), ESPA2 (5.8 L/(m²h), acetic acid 54.5%), SG (2.36 L/(m²h), acetic acid 60%), BW30 (2.92 L/(m²h), acetic acid 68%) BW30FR (3.98 L/(m²h), acetic acid 70%) showed linear outcome (Table 3) (Nguyen et al., 2015, Lyu et al., 2016). These results indicate the importance of building the synchrony between higher selectivity and higher permeability in order to build a robust membrane filtration process satisfying both productivity and purity of the final VFAs rich stream (Werber et al., 2016).

Moreover, the applied pressure is also integrated with membrane pore size and permeability rate, which has played a vital role in the pressure-driven membrane filtration process for the transport of solutes onto the membrane surface and influences the recovery percentage of VFAs compounds. Substantial VFAs recovery percentages are obtained at increased pressure with a higher polarization layer of the membrane at low flow velocity during the filtration process (Table 1-3) (Abidi et al., 2016). It is recommended to control the operating pressure so that there is no very high initial flux that causes the membrane to be performed insufficiently altogether (Choi et al., 2008). As presented in Table 3.2, when pressure is increased from 8 to 24 bar during NF and RO, a minimal increase is obtained for the recovery percentage of acetic acid and butyric acid. The reason can be explained in two ways; firstly, at higher pressures, the water flux through the membrane is higher than that of the solute and ,secondly, charge effects influence concentration polarization behavior of solute transport eventually determining the recovery rate of the solute (Gherasim et al., 2013).

3.13.3 Membrane charge

The membrane surface charge is considered as a crucial parameter towards the effective membrane filtration process (Moritz et al., 2001). Membrane surface charge can be determined by measuring the zeta potential values and it provides a clear understanding of electrostatic interaction between the feed components and the membrane's surface. Suppose the membranes surface charge is positive, and feed components charge are negative. In this case, strong electrostatic attraction forces are observed between the membrane surface and media components leading to reduced retention percentage. On the other hand, electrostatic repulsive forces occur between the negatively charged membrane surface and the negatively charged feed components, consequently, enhancing retention percentages according to the Donnan theory. The Donnan effect is referred to the interaction between charged molecules that are solubilized and charged membrane surface at their equilibrium state, as described by the British chemist Frederick George Donnan (Donnan, 1995, Rho et al., 2020). MF and UF membranes have require chemical surface modification to produced charged on their surface as they are uncharged initially (Bowen et al., 2005). Most thin-film composites membranes of NF and RO are synthesized with a negatively charged surface at alkaline and neutral conditions and positively charged at acidic conditions. Commonly, NF membranes possess a higher negative charge compared to the RO membranes, therefore making them a favorable choice to retain the negatively charged VFAs. In addition, stoke diameters of compounds plays a role in the membrane recovery process (Cho et al., 2012). Membrane surface charge also depends on the solution chemistry (Childress and Elimelech, 1996). It is presented in the literature that NF 90 membrane is more negative at neutral and alkaline conditions than NF-200, resulting in higher retention percentage of acetic acid (85%) by NF 90 than NF 200 (Bellona and Drewes, 2005). Table 3.1-3.3 represents the recovery percentages of VFAs with respect to various membranes, considering that nearly all membranes are negatively charged.

3.13.4 Membrane hydrophilicity/phobicity

Membrane hydrophilicity is one of the key influencing factors in membrane filtration performance. Membrane hydrophilicity or -phobicity is defined by the extent of membrane surface affinity to water molecules (Rana and Matsuura, 2010). The identification of the surface hydrophilicity or hydrophobicity can be determined through contact angle measurements. If the water droplet contact angle with the membrane surface is more than 90 degrees, the membrane can be termed as hydrophobic, while values less than 90 degrees indicate a hydrophilic surface (Law,

2014). Membranes with a hydrophobic surface are more prone to fouling by the deposition and adsorption of microorganisms, proteins and suspended particles. On the other hand, hydrophilic membranes are less affected by the above mentioned medium component, sustaining their retention-permeation performance (Salgin et al., 2013, Kumar and Ismail, 2015). As presented in Table 1, membranes of different hydrophobicity and hydrophilicity have been used for VFAs recovery in MF/UF filtration systems. In this regard, many studies have focused on the enhancement of the hydrophilicity of PVDF membranes through various surface modification techniques in order to boost their filtration performance (Liang et al., 2013, Hashim et al., 2009). The quality of the hydrophilic membrane also plays a great role, e.g. the recovery percentage of VFAs dropped from around 90% to 80% when hydrophilized PES membrane was replaced with a hydrophilic ceramic MF substitute (Tao et al., 2016). The effect of hydrophilicity becomes even more pronounced when it comes to NF and RO (Zhu et al., 2017, Zhao and Ho, 2014). It is a common practice to make the active layer of the NF and RO membranes using polyamide and poly(piperazinamide)-based materials that are hydrophilic in nature due to the presence of extra carboxylic acid groups, and amine and ketone groups (Cho et al., 2012). Therefore, the contact angles of the NF and RO membranes are usually low (hydrophilic surface), which assist them in recovering a higher amount of VFAs during the filtration process. As shown in Table 3.2, the nanofiltration membrane DK flat sheet can retain a high amount of VFAs than a DL flat sheet membrane just due to its higher hydrophilicity (Vieira et al., 2018). Similarly, the contact angle value of NP030 (Polyethersulphone, Microdyn-Nadir) flat sheet membrane is lower than NP010 (Polyethersulphone, Microdyn-Nadir) flat sheet membrane (Vieira et al., 2018); as a result, higher retention percentage of acetic acid has been reported using NP030. However, in general, both membranes (NP010 and NP030) recovery percentages are very low because of their parent raw material, polyethersulfone, which is hydrophobic in nature (Zhao et al., 2013). Recent studies have been shown that upon surface modification of the membrane by adding hydrophilic groups as supporting material in their reaction chain induces. Among them, polyvinyl alcohol (PVA)-based thin-film composite membranes show hydrophilic properties due to the inherent hydrophilic nature of PVA (Zhu et al., 2020a). As shown in Table 2, NTR 729 and LF 10 membranes exhibited premium VFAs recovery percentage as these membranes are made of PVA blended PA membrane.

Among all hydrophilic RO membranes show the best recovery percentage (Table 3.3). For instances, the contact angle of the XLE membrane is lower than LE RO membrane therefore this led to a higher recovery percentage of butyric acid (around 78%) from the fermentation broth using XLE. A study by Hurwitz et al. (Hurwitz and Hoek, 2006) showed that SG membrane have a higher contact angle in the pH

range of 2 to 12 compared to XLE membrane, making a less suitable for the recovery of VFAs. The recovery percentage of acetic acid was around 43.5% for CPA 2 flat sheet membrane and only 40% for CPA 3 flat sheet membrane due to their water contact angle difference (Yin et al., 2017, Dolar et al., 2012). On the other hand, it was noticed that hydrophobic membranes such as RO 90, RO 99, RO 98 could recover only 50% of acetic acid, these differences might have result from their high contact angle ($>90^\circ$) (Malmali et al., 2014). As expected, the recovery percentage was significantly high (above 95% of acetic acid) when using seawater hydrophilic RO membranes (SWC4, SWC5, SW30, SW30 HR) (Baek et al., 2012). Moreover, brackish water hydrophilic RO membrane (BW 30) showed a better recovery percentage of acetic acid (68%) than ESPA 2 flat sheet membrane (54%) as a result of hydrophilicity (Simon and Nghiem Long, 2014).

Table 3.1 Effect of membrane characteristics on VFAs recovery (MF-UF)

Filtration module	Membrane module	Manufacturer	Membrane material	Membrane area (m ²)	Pressure	MWCO/pore size	VFAs recovered	Ref
Cross-flow MF	Tubular, monolith	Nihon Japan	Gaishi, Ceramic	Tubular: 0.035 Monolith: 0.12	TMP 30-200 kPa	Monolith: 0.1, 0.2, 0.5 µm Tubular: 1.0, 2.0, 5.0 µm	87%	(Kim et al., 2005a)
Cross-flow MF	Membralox model, monolith	Pall Corporation, UK	Ceramic	0.22	-	0.2 µm	21.08mM Acetic acid and 15.81 mM Butyric acid	(Zacharof and Lovitt, 2014)
Tangential flow/MF	mPES MiniKros™, hollow fiber	KrosFlo® Research III, USA	Modified polyethersulfone	0.26	2 bar at inlet	2 µm	92.8%	(Tao et al., 2016)
Cross-flow MF	Hollow fiber	GPC, France	Polyvinylidene fluoride	0.155	0.4 bar at permeate side	0.2 µm	Total VFAs concentration 52 g/L	(Trad et al., 2015)
Cross-flow UF	MO P13U 1m, Tubular	Berghof Group, Germany	Polyvinylidene fluoride (PVDF)	0.31	10 kPa	MWCO: 15 kDa	VFAs concentration 7453 mgCOD/L	(Longo et al., 2015a)

Table 3.2 Effect of membrane characteristics on VFAs recovery (NF)

Filtration module	Membrane module	Manufacturer	Membrane material	Membrane area (m ²)	Pressure	MWCO/pore size (µm)	VFA recovered	Ref
Dead-end NF	NTR729, Flat sheet	Nitto-Denko, Japan	Polyvinylalcohol, polyamide	0.00145	250 psig	MWCO: 700 Da	Acetic acid, 40%	(Han and Cheryan, 1995)
Dead-end NF	MX07, Flat sheet	GE Osmonics, USA	Polyamide	0.00145		MWCO: 300-500 Da	Acetic acid, 38%	
Crossflow NF	HL, Flat sheet	GE Osmonics, USA	Polyamide, polysulfone	0.0042	15 bar	MWCO: 100-300 Da	Butyric acid, 8%	(Cho et al., 2012)
Crossflow NF	Duraslick, Flat sheet	GE Osmonics, USA	-	0.0042		MWCO: 100-300 Da	Butyric acid, 6%	
Dead-end NF	Desal DL, Flat sheet	GE Osmonics, USA	Polyamide, polysulfone	0.0138	8 bar	MWCO: 150-300 Da	Acetic acid, Butyric acid, 100%, Propionic acid, 30%	(Xiong et al., 2015)
Dead-end NF	Desal DK, Flat sheet	GE Osmonics, USA	Polyamide, polysulfone	0.0138		MWCO: 150-300 Da	Butyric acid, 100%, Propionic acid, 50%	
Dead-end NF	NF97, Flat sheet	Alfa Laval, Denmark	Polyamide	0.00132		MWCO: 200 Da	Acetic acid, 78%	
Dead-end NF	NF99 HF, Flat sheet	Alfa Laval, Denmark	Polyamide	0.00132		MWCO: 200 Da	Acetic acid, 15%	(Afonso, 2012)
Dead-end NF	NF200, Flat sheet	Dow Filmtec, USA	Polyamide	0.00132	26 bar	MWCO: 200-400 Da	Acetic acid, 22%	
Dead-end NF	NF270, Flat sheet	Dow Filmtec, USA	Polyamide	0.00132		MWCO: 200-400 Da	Acetic acid, 24%	

Dead-end NF	NF200, sheet	Flat	Dow Filmtec, USA	Polyamide	0.00132	26 bar	MWCO: 200-400 Da	Acetic acid, 22%
Dead-end NF	NF270, sheet	Flat	Dow Filmtec, USA	Polyamide	0.00132		MWCO: 200-400 Da	Acetic acid, 24%
Dead-end NF	NP010, sheet	Flat	Microdyn-Nadir, Germany	Polyethersulphone	0.00132		MWCO: 1000 Da	Acetic acid, 9%
Dead-end NF	NP030, sheet	Flat	Microdyn-Nadir, Germany	Polyethersulphone	0.00132		MWCO: 400 Da	Acetic acid, 29%
Dead-end NF	HL, Flat sheet		GE Osmonics, USA	Polyamide, polysulfone	0.00146		MWCO: 150-300 Da	Acetic acid, 22%, Butyric acid, 30%
Dead-end NF	DL, Flat sheet		GE Osmonics, USA	Polyamide, polysulfone	0.00146		MWCO: 150-300 Da	Acetic acid, 45%, Butyric acid, 30%
Dead-end NF	DK, Flat sheet		GE Osmonics, USA	Polyamide, polysulfone	0.00146		MWCO: 150-300 Da	Acetic acid, 57.2%, Butyric acid, 45.2%, (Zacharof et al., 2016)
Dead-end NF	NF270, sheet	Flat	Dow Filmtec, USA	Polyamide	0.00146	1500 kPa	MWCO: 150-200 Da	Acetic acid, 52.6%, Butyric acid, 69.7%
Dead-end NF	LF10, Flat sheet		Nitto Denko, Japan	Polyvinyl alcohol-polyamide	0.00146		MWCO: <150 Da	Acetic acid, 72.2%, Butyric acid, 69.7%
Dead-end NF	HL, Flat sheet		GE Osmonics, USA	Polyamide, polysulfone	0.0127		MWCO: 100-300 Da	Acetic acid, 91.1%
Dead-end NF	DL, Flat sheet		GE Osmonics, USA	Polyamide, polysulfone	0.0127		MWCO: 100-300 Da	Acetic acid, 94.8%, (Ecker et al., 2012)
Dead-end NF	DK, Flat sheet		GE Osmonics, USA	Polyamide, polysulfone	0.0127	25 bar	MWCO: 100-300 Da	Acetic acid, 96.1%

Dead-end NF	HT, Flat sheet	Hydranautics, USA	-	0.0127		MWCO: 720 Da	Acetic acid, 77.7%,	(Jänisch et al., 2019)
Dead-end NF	NF270, Flat sheet	Dow Filmtec, USA	Polyamide	0.0127		MWCO: 270 Da	Acetic acid, 92.7%,	
Dead-end NF	KO, Flat sheet	Koch, USA	-	0.0127		MWCO: 1000 Da	Acetic acid, 71.1%,	
Dead-end NF	XN45, flat sheet	Microdyn-Nadir, Germany	Polyamide	0.0037		MWCO: 500 Da	Acetic acid, 36%	
Dead-end NF	NF 90	Dow Filmtec, USA	Polyamide	0.0037		-	Acetic acid, 28%	
Organophile NF	M3#	PolyAn, Germany	PV composite polymer	0.0037		-	Acetic acid, 74% Propionic acid, 84%	
Dead-end NF	NF-45	Dow Filmtec, USA	Polyamide	0.003		MWCO: 200 Da	Acetic acid, 68% Butyric acid, 88%	(Zhu et al., 2020b)
Dead-end NF	XLE	Dow Filmtec, USA	Polyamide	0.003	20 bar	MWCO: 100 Da	Propionic acid, 72% Acetic acid, 97% Butyric acid, 99%	
Cross-flow NF	NF-90, Flat sheet	Dow Filmtec, USA	Polyamide	0.01387	550 kPa	MWCO: 200 Da	Propionic acid, 85%, Acetic acid, 83%	(Bellona and Drewes, 2005)
Cross-flow NF	NF-200, Flat sheet	Dow Filmtec, USA	Polyamide	0.01387		MWCO: 300 Da	Acetic acid, 83%	
Cross-flow NF	NF90, Flat sheet	Dow Filmtec, USA	Polyamide	0.015	20 bar	MWCO: ~200-400 Da	Acetic acid, 50%	(Yasin et al., 2020)

Cross-flow NF	NF270, Flat sheet	Dow Filmtec, USA	Polyamide	0.015		MWCO: ~200-400 Da	Acetic acid, 10%	
Crossflow NF	ES10, Flat sheet	Nitto Denko, Japan	Aromatic polyamide	0.006	280±3kPa	MWCO: 100 Da	Acetic acid, 98% Propionic acid, 98%	(Choi et al., 2008)
Crossflow NF	NF270, Flat sheet	Dow Filmtec, USA	Piperazine-based polyamide	0.006		MWCO: 200-300 Da	Acetic acid, 78% Propionic acid, 82%	
Crossflow NF	NF90, Flat sheet	Dow Filmtec, USA	Polyamide	0.036		MWCO: 200-400 Da	Acetic acid, 50%	
Crossflow NF	NF270, Flat sheet	Dow Filmtec, USA	Polyamide	0.036	10 bar	MWCO: 200-400 Da	Acetic acid, 4.5%	(Nguyen et al., 2015)
Crossflow NF	NF245, Flat sheet	Dow Filmtec, USA	Polyamide	0.036		MWCO: <300 Da	Acetic acid, 6.7%	
Crossflow NF	DK, Flat sheet	GE Osmonics, USA	Polyamide, polysulfone	0.036		MWCO: 150-300 Da	Acetic acid, 4.9%	
Crossflow NF	Desal-5 Spiral wound	GE Osmonics, USA	Polyamide, polysulfone	0.2	24.5 bar	MWCO: 150-300 Da	Acetic acid, 90%	(Weng et al., 2009)
Crossflow NF	PA 100, Flat sheet	Permeonics Pvt Ltd, India	Polyamide	0.014		MWCO: 100 Da	Acetic acid, 30%	
Crossflow NF	PA 150, Flat sheet	Permeonics Pvt Ltd, India	Polyamide	0.014	8 bar	MWCO: 150 Da	Acetic acid, 5%	(Maiti et al., 2012)
Crossflow NF	PA 400, Flat sheet	Permeonics Pvt Ltd, India	Polyamide	0.014		MWCO: 400 Da	Acetic acid, 10%	
Crossflow NF	PES 150, Spiral wound	NovaSep, France	Poly ether sulphonate	0.278		MWCO: 150 Da	Acetic acid, 12%	

Dead-end NF	NF90, Flat sheet	Dow Filmtec, USA	Aromatic polyamide	0.00146	400 psi	MWCO: 200-400 Da	Acetic acid, 75% Propionic acid, 80% Isobutyric acid, 95% Valeric acid, 84%	(Zhang et al., 2018a)
Crossflow NF	DL, spiral wound	General Electric Co., USA	Polyamide, polysulfone	0.32	10 bar	MWCO: 150 Da	Acetic acid, 30%	(Lyu et al., 2015)
Crossflow NF	DK, spiral wound	General Electric Co., USA	Polyamide, polysulfone	0.32		MWCO: 300 Da	Acetic acid, 38%	
Crossflow NF	DK, Flat sheet	GE Osmonics, USA	Polyamide	0.0042		MWCO: 150-300 Da	Acetic acid, 9%	
Crossflow NF	DL, Flat sheet	GE Osmonics, USA	Polyamide	0.0042		MWCO: 150-300 Da	Acetic acid, 6%	
Crossflow NF	NF270, Flat sheet	Dow Filmtec, USA	Polypiperazine amide	0.0042		MWCO: 200-400 Da	Acetic acid, 9%	(Lyu et al., 2016)
Crossflow NF	NF90, Flat sheet	Dow Filmtec, USA	Polyamide	0.0042	10-20 bar	MWCO: 200-400 Da	Acetic acid, 30%	
Crossflow NF	XN45, Flat sheet	Microdyn-Nadir, Germany	Polyamide	0.0042		MWCO: 300-500 Da	Acetic acid, 3%	
Crossflow NF	TS40, Flat sheet	Microdyn-Nadir, Germany	Polypiperazine amide	0.0042		MWCO: 200-300 Da	Acetic acid, 7%	

Table 3.3 Effect of membrane characteristics on VFAs recovery (RO)

Filtration mode	Membrane module	Manufacturer	Membrane material	Membrane area (m ²)	Pressure	MWCO/pore size (µm)	VFA recovered	Ref
RO	Spiral wound	Sempas Membrantechnik, Germany	Polyamide	0.7	10 bar	-	Acetic acid, 45% Propionic acid, 60% Butyric acid, 80% Valeric acid, 83% Isobutyric acid, 100% Isovaleric acid, 100%	(Hausmanns et al., 1996)
Crossflow RO	SWC5 Wound	Hydramautics, USA	Polyamide	0.003116	4 MPa	-	Acetic acid, 81.92%	(Liu et al., 2020a)
Crossflow RO	SWC6 Wound	Hydramautics, USA	Polyamide	0.003116	-	-	Acetic acid, 81.32%	(Liu et al., 2020a)
Crossflow RO	ES20, Flat sheet	Nitto Denko, Japan	Polyamide	0.006	3 kg/cm ²	MWCO: <200 Da	Acetic acid, 68%	(Ozaki and Li, 2002)
Crossflow RO	RO98pHt	Alfa Laval, Sweden	Polyamide	0.0174	20 bar	-	Acetic acid, 90%	(Zhou et al., 2013b)
Crossflow RO	CPA2, Flat sheet	Hydramautics, USA	Polyamide	0.036	-	-	Acetic acid, 43.5%	
Crossflow RO	CPA3, Flat sheet	Hydramautics, USA	Polyamide	0.036	-	-	Acetic acid, 40.1%	
Crossflow RO	ESPA2, Flat sheet	Hydramautics, USA	Polyamide	0.036	-	-	Acetic acid, 54.5%	(Nguyen et al., 2015)
Crossflow RO	XLE, Flat sheet	Dow Filmtec, USA	Polyamide	0.036	20 bar	MWCO: ~100 Da	Acetic acid, 79.8%	
Crossflow RO	SG, Flat sheet	GE Osmonics, USA	Polyamide	0.036	-	-	Acetic acid, 60.5%	

3.13.5 VFAs concentrations

The concentration of feed solution also influences membrane filtration performance and consequently the VFAs recovery percentage (Table 3.4-3.6). Feed concentrations may vary with respect to the source of VFAs. Generally, microfiltration and ultrafiltration process cannot effectively retain VFAs, and there are no substantial concentration changes observed for initial and filtered VFAs solution. On the other hand, the accomplishment of NF/RO processes revealed a significant VFAs concentration change in the retentate and permeate solution; therefore, the concentration of VFAs in feed solution plays a crucial role in the recovery percentage of NF/RO process (Zhu et al., 2020b).

The initial concentration of VFAs in the feed can affect final recovery results. For example, Han et al. (Han and Cheryan, 1995) used three concentrations of 1%, 5% and 7.5% of acetic acid and showed that 40% of acetic acid was recovered at 1%, while the recovery percentage dropped to 20% when the initial VFAs concentration was increased to 7.5%. This might be due to the ion exchange capacity of the membrane surface (Han and Cheryan, 1995). When the feed concentration is high, the excess ions can pass through the membrane easily and lowering the apparent recovery percentage of the VFAs compounds. Moreover, permeability also decreases at a higher concentration because water and the permeating ions compete for a specific membrane area (Han and Cheryan, 1995). It has also been reported in the literature recovery percentage stays unchanged regardless of the initial concentration of VFAs when a NF 90 membrane fully aromatic active layer is used for filtration (Nguyen et al., 2015).

In contrast, the use of RO membrane supports higher recovery percentage at higher initial concentrations. As presented by Zhou et al. (Zhou et al., 2013b), the recovery percentage of acetic acid gradually increased from 50% to 55% as the initial feed concentration of acetic acid increased from 10 to 50 g/L using RO 98pHt membrane. Following these results, Liu et al. (Liu et al., 2020a) conducted the acetic acid concentrated process through the use of the reverse osmosis membrane and found that there are no considerable changes in the recovery percentage observed at varying concentrations. The similar results are also documented by a previous study (Zhou et al., 2013a).

3.13.6 Medium pH

In the pressure-driven membrane filtration process, solution pH is a key parameter on the percentage of VFAs recovery, controlled by the acidic/basic medium.

Previous literature indicate that the recovery percentages of VFAs is significantly enhanced at higher pH ranges and vice versa (Zhu et al., 2021b). Here, acidity constant (pKa) values of VFAs are considered as crucial in recovery success. The pKa values of VFAs compounds are at about 4.75 (acetic acid), 4.82 (butyric acid), 4.88 (propionic acid), 4.84 (valeric acid), 4.8 (caproic acid), which implies that higher recovery percentages will be observed at beyond pKa values as acids convert to their dissociated forms. For instance, this concept can be verified through the experimental study carried out by Han et al. (Han and Cheryan, 1995), who recovered more than 75% of acetic acid at pH 6.8, but the recovery amount significantly decreased to 10% when the pH was 2.7. This means that at higher pH, the NF membrane becomes negatively charged and solute (acetic acid) transferred to acetate, which is also negatively charged, thus electrostatic repulsion occurred and retained percentages increased eventually. On the other hand, at lower pH solute became positive in charge and is attracted to the negative membrane surface, thereby decreasing the retention percentages. Although all VFAs compounds recovery percentage showed higher at neutral to alkaline pH medium, interestingly, a study by Xiong et al. (Xiong et al., 2015) reported that higher recovery percentage of butyric acid is observed even in highly acidic medium of pH 3 and continues to neutral pH. The relation between the recovery percentage and pH in NF/RO filtration has been presented in references listed in Table 3.5-3.6.

It has been reported that size-exclusion was not the only mechanism dominating the retention percentage. Maiti et al. (Maiti et al., 2012) used 150 Da PA, 400 Da and 150 Da PES membranes for acetic acid recovery and found that increased recovery percentages were achieved at higher pH ranges. It should be pointed out that the Stokes radius of acetic acid is 0.206 nm which is 0.5 times smaller than 100 and 150 Da membranes and 0.33 times smaller than 400 Da membrane. Therefore, the higher recovery of acetic acid in an alkaline medium is influenced by other mechanisms such as Donnan effect. Moreover, Zhang et al. (Zhang et al., 2018a) confirmed that the charge effects primarily governed a higher recovery percentage of acetic acid at pH 8 under the nanofiltration process. While the solution-diffusion mechanism additionally influences the recovery percentages of VFAs in RO filtration. Generally, the structure of the reverse osmosis membrane is composed of a nonporous dense layer that plays a vital role in the recovery percentage of uncharged molecules (Zhou et al., 2013b, Lyu et al., 2016).

3.13.7 Operating temperature

The operating temperature can also affect the recovery percentage of VFAs during pressure-driven membrane filtration. From the literature, it is evident that increasing the temperature causes decrease in recovery percentages of VFAs (Table 3.4-3.6). The lower recovery percentages of VFAs compounds are attributed to the higher solute diffusion at an increased temperature, which assists in the transport of solute over the membrane surface, enhancing the mass transfer rate obtained (Nilsson et al., 2008, Snow et al., 1996). Additionally, the polymer structure in the active layer and pore size of the membrane surface significantly changes at a higher temperature, resulting in a low recovery of VFAs at a higher permeate flux. Regarding nanofiltration, Lyu et al. (Lyu et al., 2016) reported that the recovery percentage of acetic acid was reduced to 20% (at 45 °C) from 40% of the initial recovery rate at 15 °C by NF 90 membrane. Other types of membranes such as DK, DL, NF270, XN45 and TS40 showed low acetic acid recovery percentages (8-4%) at varied temperature (15-45 °C). The same trend was also observed for reverse osmosis membranes, as the recovery percentage of acetic acid was calculated >80% at 20 °C, but reduced to below 70% at 35 °C (Liu et al., 2020a).

3.13.8 Ionic strength

Effluent with high ionic strength, e.g. inorganic salts can alter the trend for the selective separation of VFAs during membrane filtration (Choi et al., 2008, Zhu et al., 2020b). Previous studies have reached different conclusions regarding the recovery percentage of VFAs when a mixed effluent is used as feed (Table 3.4-3.6). For instance, Xiong et al. (Xiong et al., 2015) achieved limited recovery percentage of acetic and butyric acids when salts were added in the actual digestion liquor. Adding salt increases the osmotic pressure in the solution, resulting in a higher retention scheme of VFAs. Zacharof et al. (Zacharof et al., 2016) reported that elevation in ionic strength improved the recovery percentages of acetic acid and butyric acid. They used four types of salts (sodium carbonate, sodium bicarbonate, sodium chloride and calcium chloride) at two different concentrations (50 mM and 100 mM). Synthetic VFAs mixtures containing salt solution showed an increased recovery percentages for both concentrations. Although all salts provided satisfactory results, among them, sodium bicarbonate and sodium chloride were the dominant co-existing ions in terms of VFAs retention percentage. This was also experimented on raw agricultural wastewater effluent containing salts where an enhanced effect on butyric acid retention over acetic acid was observed (Zacharof et al., 2016).

Table 3.4 Effect of medium characteristics on VFAs recovery (MF-UF)

Filtration mode	Feed media	Initial concentrations	VFAs	pH	Temperature	VFAs recovered	Ref
Crossflow MF	Liquid organic sludge	-	-	5-6	35°C	87%	(Kim et al., 2005a)
Crossflow MF	Agricultural wastewater + Synthetic VFAs mixture (acetic and butyric acid)	24.38 mM Acetic acid, 18.91 mM Butyric acid	-	8.25	-	21.08 mM Acetic acid, 15.81 mM Butyric acid	(Zacharof and Lovitt, 2014)
Tangential flow MF	Activated sludge	11.73 g/L Total VFAs	-	6	37°C	92.8% total VFAs	(Tao et al., 2016)
Crossflow MF	Glucose or Agrowaste (Straw)	-	-	6	35°C	Total VFAs 52 g/L	(Trad et al., 2015)
Crossflow UF	Sewage sludge	315.6 mg COD/gTVS	-	5-10.5	35± 1°C	Total VFAs 7453 mgCOD/L	(Longo et al., 2015a)

Table 3.5 Effect of medium characteristics on VFAs recovery (NF)

Filtration mode	Feed media	Initial concentrations	VFAs	pH	Temperature	VFAs recovered	Ref
Dead-end NF	Acetic acid solution	1% Acetic acid		5.6	50°C	Acetic acid, 40%	(Han and Cheryan, 1995)
Cross flow NF	Synthetic fermentation broth	0-5 g/L Butyric acid		3	37°C	Butyric acid, 8%	(Cho et al., 2012)
Dead-end NF	Lignocellulosic willow biomass	Whole 0.7-1.2 g/L Acetic acid 1.6-2.4 g/L Propionic acid 1-2 g/L Butyric acid		7	25±0.5°C	62% Acetic acid 50% Propionic acid 100% Butyric acid	(Xiong et al., 2015)
Dead-end NF	Condensate of eucalyptus spent sulphite liquor	6.8 g/L Acetic acid	Natural	pH 2.4	25°C	77% Acetic acid	(Afonso, 2012)
Dead end NF	Digested wastewater	Acetic acid 21.08 mM, 15.81 mM butyric acid		8.5	50°C	72.2% Acetate and Butyrate	69.7% (Zacharof et al., 2016)
Dead end NF	Silage juice from pilot plant	19 g/L Acetic acid		3.9	25°C	96.1% Acetic acid	(Ecker et al., 2012)
Dead end NF	Sugar beet fermentation broth	3.3 g/L acetic acid				Acetic acid, 74%	(Jamisch et al., 2019)
Dead end NF	Grass cut fermentation broth	6.83 g/L acetic acid				Propionic acid, 84%	

Dead end NF	Grass cut fermentation broth	14.28 g/L acetic acid 2.05 g/L propionic acid 0.35 g/L valeric acid 8.40 g/L acetic acid							
Dead end NF	Corn-triticale fermentation broth	2.81 propionic acid 6.23 g/L butyric acid 2.54 g/L Valeric acid 1.56 Caproic acid							
Dead end NF	Organic and organic salts	100mM Acetic acid 100mM Propionic acid 100mM Butyric acid	8	20±7°C				68% Acetic acid 79% Propionic acid 86% Butyric acid	(Zhu et al., 2020b) (Bellona and Drewes, 2005)
Cross flow NF	Organic acids	10-15 mg/mL Acetic acid	7					85% Acetic acid	(Yasin et al., 2020)
Cross flow NF	Dimethyl terephthalate process wastewaters	14611±565 mg/L Acetic acid	7	25±1°C				100% Acetic acid	(Choi et al., 2008)
Cross flow NF	Domestic waste waters	100-500 mg/L 40 mg VFA/L	6.7-8.7	25-35°C				98% acetic acid 98% Propionic acid	(Nguyen et al., 2015)
Cross flow NF	Lignocellulosic hydrolysate	5 g/L Acetic acid	10-11	20°C				50% Acetic acid	(Weng et al., 2009)
Crossflow NF	Model solution of Xylose and Acetic acid	5 g/L Acetic acid	9.1	25°C				90% Acetic acid	(Mati et al., 2012)
Cross flow NF	Rice straw hydrolysate	2 g/L Acetic acid	9	30°C				60% Acetic acid	

Cross flow NF	Hydrothermal wastewater	liquefaction	2500 mg/L Acetic acid 2000 mg/L propionic acid 350 mg/L Isobutyric acid 300 mg/L Valeric acid	8	25°C	75% Acetic acid, 80% Propionic acid, 95% Isobutyric acid, 84% Valeric acid,	(Zhang et al., 2018a)
Cross flow NF	Hydrothermal rice straw	liquefaction of	1.809 g/L Acetic acid	-	35°C	38% Acetic acid	(Lyu et al., 2015)
Crossflow NF	Hydrothermal hydrolysate	liquefaction	2000 mg/L Acetic acid	2.78	25°C	41.57% Acetic acid	(Lyu et al., 2016)
Crossflow NF	Hydrothermal hydrolysate	liquefaction	2000 mg/L Acetic acid	9.52	25°C	97.73% Acetic acid	

Table 3.6 Effect of medium characteristics on VFAs recovery (RO)

Filtration mode	Feed media	Feed Characteristics /Initial VFAs	pH	Temperature	VFAs recovered	Ref
RO	Model solution of acetic acid	20 mmol/L Acetic acid	2-3.6	18 ± 22°C	Acetic acid, 45% Propionic acid, 60% Butyric acid, 80% Valeric acid, 83% Isobutyric acid, 100% Isovaleric acid, 100%	(Hausmanns et al., 1996)
Crossflow RO	Model solution of acrylic acid and acetic acid	1.5% Acetic acid	-	25°C	Acetic acid, 81.92% Acetic acid, 81.32%	(Liu et al., 2020a)
Crossflow RO	Organic compounds	10 mg/L Acetic acid	9	25 ± 2°C	Acetic acid, 68%	(Ozaki and Li, 2002)
Crossflow RO	Model Solution of monosaccharides and acetic acid	5 g/L Acetic acid	9.88	25°C	Acetic acid, 90%	(Zhou et al., 2013b)
Cross flow RO	Lignocellulosic hydrolysate	5 g/L Acetic acid	10-11	20°C	Acetic acid, 79.8%	(Nguyen et al., 2015)
	Sugar beet fermentation broth	3.3 g/L acetic acid			Acetic acid, 99.2%	(Janisch et al., 2019)

	Grass cut fermentation broth	6.83 g/L acetic acid			
		14.28 g/L acetic acid			
		2.05 g/L propionic acid			
		0.35 g/L valeric acid			
		8.40 g/L acetic acid			
		2.81 propionic acid			
		6.23 g/L butyric acid			
		2.54 g/L Valeric acid			
		1.56 Caproic acid			
Cross flow RO	Hydrothermal hydrolysate	2000 mg/L Acetic acid	2.78	25°C	(Lyu et al., 2016)
Cross flow RO	Cornstover hydrolysate	3.445 g/L Acetic acid	5.75	42°C	(Malmali et al., 2014)
Cross flow RO	Synthetic fermentation broth	1000ppm acetic acid	Butyric 3	37°C	(Cho et al., 2012)
Cross flow RO	Model Solution of monosaccharides and acetic acid	5 g/L Acetic acid	9.91	25°C	(Zhou et al., 2013a)
					Acetic acid, 70%
					Acetic acid, 55%
					Butyric acid, 78%
					Acetic acid, 47.51%

4. DEVELOPMENT OF ELECTROSPUN NANOFIBER MEMBRANES FOR FOOD INDUSTRY WASTEWATER TREATMENT

This chapter explains the details of materials and chemicals, experimental setups and analytical methods that have been used to build this research work. This part has been divided into sections for a better understanding of Study I (application of PES/HPC electrospun nanofibers membranes for food industry wastewater treatment) and Study II (application of PES/PAN electrospun nanofibers membranes for food industry wastewater treatment).

4.1 One-step fabrication of novel polyethersulfone-based composite electrospun nanofibers membrane for food industry wastewater treatment

4.1.1 Introduction

Pollution of the world's water supplies has been noted as a major issue. Contaminants in wastewater may include a wide range of substances such as microbes, colloids and proteins as well as ions of heavy metals and dyestuffs. Among them, dyestuff-contaminated industrial wastewater has significantly negatively impacted water and land quality, human health, and the ecosystem. It is the most challenging compound to remove from the industrial effluent streams because of having a stable and complex structure (Pervez et al., 2020e, Morshed et al., 2020b, Pervez et al., 2019b). Notably, the food industry uses a variety of dyestuffs for their manufacturing purposes, and methylene blue (MB) is one of them. One of the most often utilized dyes in the manufacture of consumer goods like roasters, cutlery and paper sheets is MB (cationic azo dye). It may permanently harm the eyesight of people and animals

alike by causing severe eye burns. Acute palpitations and wheezing may be caused by some substances, which might exacerbate lung difficulties (Pervez et al., 2021c, Jing et al., 2021b, Kaya-Özkipir et al., 2022). The investigation of suitable techniques for eliminating MB from wastewater discharge by the food sector is thus of fundamental relevance.

Adsorptive removal of dyes from industrial effluents has particularly been identified as one of the most workable and effective methods by virtue of its simplicity, high efficiency and availability of pollutants capture sites in their structure (Hossain et al., 2021a, Sharma et al., 2022, Pervez et al., 2020b). As of today, electrospun-based nanofibers membrane materials, usually with smaller diameters (less than 100 nm) and higher surface area, have been used widely to replace traditional adsorbents. Electrospinning process is carried out by applying an electric field (high voltage power supply) in which the working solution contained syringe is connected to the spinneret using a needle, and Taylor cone-formed indicates the development of nanofibers membrane. After that, a stainless steel plate is used to collect the as-synthesized nanofibers membrane. Till now, there are various polymers have been applied to fabricate nanofibers membranes because of their feasibility in the electrospinning process, meaning higher adjustability in diameter, alignment and orientation in a linear form (Pervez et al., 2020f, Pervez and Stylios, 2018c, Pervez and Stylios, 2018a, Xu et al., 2022, Talukder et al., 2021b).

Compared with other polymers, polyethersulfone (PES) rely on their suitable thermal stability, mechanical strength and chemical resistance, making them a suitable material in the realm of wastewater treatment. PES has long been used to fabricate conventional commercial membranes because of their high permeability, affinity and selectivity (Al-Ghafri et al., 2018, Talukder et al., 2022b, Pervez et al., 2022a). Accordingly, electrospun-based PES nanofibers membranes are currently applied on a large scale to remove pollutants from industrial effluents. For example, Koushkbaghi and co-workers (Koushkbaghi et al., 2018) fabricated dual layers chitosan/PVA/PES filled with aminated-Fe₃O₄ nanoparticles for the removal of Cr(VI) and Pb(II) ions. The adsorption capacity was strongly affected by solution pH, as such, pH 6 provides the maximum adsorption capacity for Cr(VI) (while lower pH was found to be suitable for maximum Pb(II) ions. In a similar approach, Zheng et al. (Zheng et al., 2022) prepared ionic liquid grafted polyethersulfone electrospun nanofibrous membrane and demonstrated that developed membranes could be multifunctional material such as exhibited dye, heavy metals and antibacterial efficiency. Nevertheless, PES-based electrospun nanofiber membranes showed some limitations, such as hydrophobicity, low solubility, and stability, which need to be addressed in order to achieve satisfactory performance.

Conversely, the usage of cellulose-based natural materials in electrospinning is on the rise because of their functionality, durability, and uniformity. Among them, hydroxypropyl cellulose (HPC), a non-ionic ether of natural cellulose, is a polymer with temperature-dependent water solubility, excellent mechanical and thermal stability, and good chemical characteristics. It is becoming more popular because of its renewable ability, simplicity of manufacture, non-toxicity, and optical elements (Wang et al., 2016). Besides, surface wettability with an aqueous medium, heat resistance, and molecular transmission phenomena have been seen in HPC-based electrospun nanofiber membranes, making them a desirable for wastewater treatment. For instance, Soraya Hassanpour et al. (Hassanpour et al., 2019) reported that methylene blue (MB) dye was adsorbed from an aqueous solution using a new biocompatible adsorbent based on hydroxypropyl cellulose (HPC) and itaconic acid nanogels. For phenol adsorption, composite hydrogels based on hydroxypropyl cellulose (HPC) and graphene oxide (GO) were developed and employed with a maximum adsorption capacity of 136.5 mg/g (Wang et al., 2018). However, no one has yet reported on the synthesis and production of PES/HPC-based electrospun nanofiber membranes and their use in wastewater treatment, thus further research is needed.

The present study is, therefore, aimed to fabricate a unique PES/HPC composite nanofiber membrane utilizing a one-step electrospinning scheme and then used for the first time to remove the MB from an aqueous solution. Usually, selected operational parameters such as initial solution pH, contact time, initial MB concentration and ionic strength concentration were investigated carefully in order to gain insights into the adsorption process.

4.1.2 Materials and methods

In this study, polyethersulfone (PES, Ultrason E 6020 P) with a molecular weight of 65800 g/mol was purchased from BASF SE (Ludwigshafen, Germany). Hydroxypropyl cellulose (HPC, 99%, CAS no. 9004-64-2) was purchased from Shanghai Honest Chem. Co., Ltd. (Shanghai, China). *N,N*-dimethylacetamide (DMAc) (CAS No.:127-19-5) was obtained from TNJ Chemical Industry Co., Ltd, Hefei, China. Methylene blue (95% pure), was obtained from Sigma Aldrich Co., Ltd. (Darmstadt, Germany). A nonwoven polyethylene terephthalate (PET) paper was acquired from Guocheng Co. (Wuxi, China) and used as a collector for electrospun nanofiber membranes in this experiment. Other materials and reagents were employed without additional modification, and deionized (DI) water was used throughout the whole experiment.

One-step electrospinning

As shown in Figure 4.1, the PES/HPC nanofiber membranes were produced using the one-step electrospinning process. A solution of pristine PES/HPC was prepared by dissolving 10% PES (w/v) and 4% HPC (w/v) into 86 mL DMAc solution under stirring for 4 h at room temperature. After that, the electrospinning process was carried out on a laboratory size electrospinning machine (Foshan Lepton precision measurement and control technology Co., Ltd., M06, Foshan, China) (Figure 4.2). The prepared solutions were transferred to separate 20 mL syringe pumps. Each solution was injected at a feeding rate of 1.0 mL/h under an applied voltage of 7.5 kV at 28°C. The distance between the needle tip and the stainless steel plate was adjusted to 18 cm. The optimum electrospinning process conditions were determined by preliminary experiments. The nanofiber membranes were removed from the PET non-woven sheet and were placed in a vacuum dryer oven (Zhengzhou Keda Machinery And Instrument Equipment Co., Ltd., Henan, China) for 5 hours at 60 °C, to remove the DMAc solvent. The pristine PES nanofiber membranes were also made using the same procedure, for comparison purposes, but without the addition of HPC.

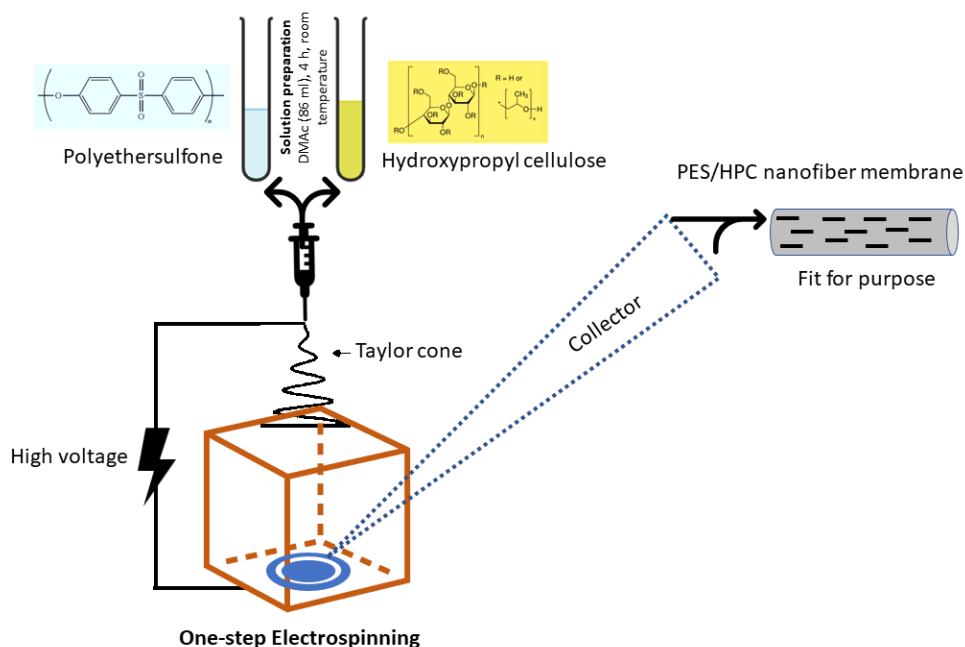


Figure 4.1 Illustration of one-step electrospinning nanofiber membrane fabrication process



Figure 4.2 Image of the electrospinning nanofiber membrane fabrication commercial machine.

Analytical methods

An NDJ-8S digital rotating viscometer was used to measure the solution's viscosity (Movel Scientific Instrument Co., Ltd, Ningbo, China). The pH was determined by a DZS-706A multi-parameter analyzer and the conductivity of the solution using a conductivity meter (INESA Scientific Instrument Co., Ltd., Shanghai, China). A professional DropMeter A-300 was used to measure the water contact angles of the membranes (Kudos Instruments Corp. Newyork, USA). A Phenom desktop scanning electron microscope was used to analyze the nanofiber membrane surface morphologies (SEM, Thermo Fisher Scientific, Tokyo, Japan). Samples were gold-sputtered and the accelerating voltage was 5kV prior to the acquisition of SEM photos . The acquired SEM photos were utilized to analyze the fibre diameter distribution behaviour of the membrane, which was processed using ImageJ software (<https://imagej.nih.gov/ij/download.html>). Fourier transform infrared spectroscopy (IR, Interspectrum, low noise DLATGS, FTIR-920; Estonia) was used to detect the

presence of functional groups in the nanofiber membranes. The spectra were collected within the wavenumber ranged from 400 to 4000 cm^{-1} . Thermal gravimetric analysis (TGA) was carried out in a nitrogen environment with a heating rate of $10^\circ/\text{min}$ using a TG 209 F1 Libra (Netzsch Instruments, Wolverhampton, United Kingdom). The crystal structure of the membranes was determined using an X-ray diffractometer (Empyrean, Malvern PANalytical, Worcestershire, United Kingdom), with scans being taken from $2\theta = 10^\circ$ to 80° . The tensile strength of the membranes was determined by using the tensile strength tester KD-III type BA-100m (Transcell technology, Shenzhen, China).

Batch adsorption studies

Effect of solution pH

The effect of solution pH was investigated by following the experimental procedures: a total of 10 mg weighted adsorbents were put into VWR centrifuge tubes (polypropylene) holding 10 mL of 400 mg/L MB solution and magnetically swirled for 24 hours at a speed of 200 r/min under different pH conditions (3-10), at room temperature. The pH of the solution was adjusted by adding buffer solution that had been previously made in the presence of 0.1 M HCl and NaOH. Following each test, a predetermined quantity of solution was taken at certain intervals and filtered through a 0.45 μm membrane filter. A Perkin-Elmer Lambda 25 UV-Vis spectrophotometer (Massachusetts, USA) was used to measure the concentration of MB after that, at 200 – 800 nm wavelength range. The adsorption capacity of MB at time t (q_t , mg/g) was calculated using the following equation (1) (Pervez et al., 2021b):

$$q_t = \frac{(C_0 - C_t)V}{m} \quad (1)$$

where C_0 (mg/L) and C_t (mg/L) are the initial MB concentration and that at time t , V (L) is the volume of MB solution, and m (g) is the adsorbent amount.

Effect of initial MB concentration

The effect of the initial concentrations of MB on the equilibrium adsorption capacity by pristine PES and PES/HPC nanofiber membranes was examined. In order to create workable solutions for the different batch experiments, the stock solution was diluted in deionized water first. In order to assess the impact of MB concentration on adsorption performance, a series of the identical procedures were carried out under a range of different MB concentrations (200, 400, 600, 800 and 1000 mg/L) at the neutral pH and room temperature.

Effect of ionic strength concentration

In the presence of the produced pristine PES and PES/HPC nanofiber membranes, a standard adsorption approach was used to evaluate the influence of ionic strength on the adsorption capacity of MB. In a similar approach, 10 mg of adsorbents were put into 10 mL of 400 mg/L MB solution at neutral pH by adding varying concentrations of NaCl (0.1 M-0.5 M) and stirred for 24 hours.

Recyclability

The recyclability of the adsorbents was determined by soaking them in a 2 mM HCL solution for 6 hours at room temperature. Five regeneration cycles were carried out under identical experimental conditions, with each tested adsorbent being washed twice with DI water and then prepared for the next adsorption cycle. Following that, the concentration of MB was measured in order to determine the adsorption capacity of the membrane.

4.1.3 Results and Discussion

SEM

SEM images were used to determine the analysis of morphological traits of electrospun nanofiber membranes made of PES and PES/HPC, respectively (see Figures 4.3a and b). Regarding average diameter distribution, the smooth surface of the pristine PES nanofiber membrane is characterized by homogeneous high in diameter fibers with a diameter of 261.5 nm (Figure 4.3c). The surface of the PES/HPC nanofiber membrane, on the other hand, has lower diameter fibres (average diameter approximately 168.5 nm) under the same process conditions and only after anchoring HPC, resulting in a more homogeneous structure with more compact fiber stacking (Figure 4.3d). In addition, the reason behind this phenomenon might be described by decreasing the solution viscosity (PES, 2268 mPa/s and PES/HPC, 1845 mPa/s), which in turn reduces the nanofiber diameter, increasing of solution conductivity (PES, 1.6 mS/cm and PES/HPC, 2.2 mS/cm), also has the same effect of reducing fibre diameter, as reported elsewhere (Tan et al., 2005, Wang et al., 2010). Composite polymer nanofiber membranes with smaller diameters have a high specific surface area at a given volume than those with a higher diameter, and hence more active sites to adsorb more organic pollutants during the adsorption (Metwally et al., 2018, Pervez et al., 2021f).

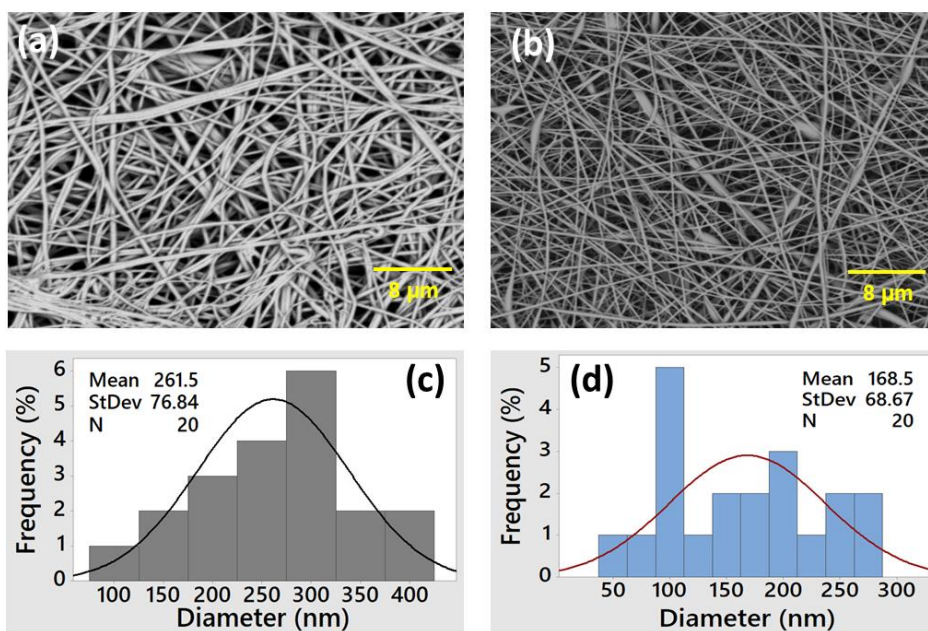


Figure 4.3 SEM images and average diameter distribution of pristine PES (a, c) and PES/HPC (b, d) nanofiber membranes.

FT-IR

FTIR is well-known for its effectiveness in interpreting structural data, by providing the vibrational band's shape, intensity and changes of environmental and conformation characteristics at the molecular level of polymers. Figure 4.4 depicts the FTIR spectra of the pristine PES and the blended PES/HPC electrospun nanofiber membrane. From the spectrum of pristine PES nanofiber membrane, it was noticed that, the absorption peaks appeared at 710 cm^{-1} and 820 cm^{-1} , assigned to CH_2 bond C-H stretching, respectively. The characteristic bands of functional groups at $1106 - 1150\text{ cm}^{-1}$, 1319 cm^{-1} , 1568 cm^{-1} , 1670 cm^{-1} , and 1750 cm^{-1} correspond to $\text{O}=\text{S}=\text{O}$, C-O stretching, C=C stretching, N-C=O carbonyl vibrations and C=O stretching, respectively (Zhang et al., 2013a). The stretching vibration of aromatic C-H groups is also responsible for the two prominent absorption broader peaks observed at 2830 cm^{-1} and 3250 cm^{-1} (Homaieghar et al., 2010a). The absorption peaks of the blended PES/HPC membrane are almost identical to those of the pristine PES nanofiber membrane, except for smaller additional peaks across the blended membrane spectrum, For example, the wide absorption peak at 3583 cm^{-1} is attributed to the OH stretching vibration of free hydroxyl and hydrogen bonds. After that, a shoulder

peak at 1635 cm^{-1} (C=O stretching), 1164 cm^{-1} (C-O asymmetric stretching) and two consecutive sharp narrow peaks were counted at 895 cm^{-1} (C-O deformation and -CH₂ rocking) and 726 cm^{-1} for twisting of O-H, which are typical of the nature of HPC polymer (El-Wakil et al., 2010, Guirguis and Moselhey, 2013). Based on these findings, it can be concluded that the successful interaction between PES and HPC was dominated by physical contact rather than a chemical reaction.

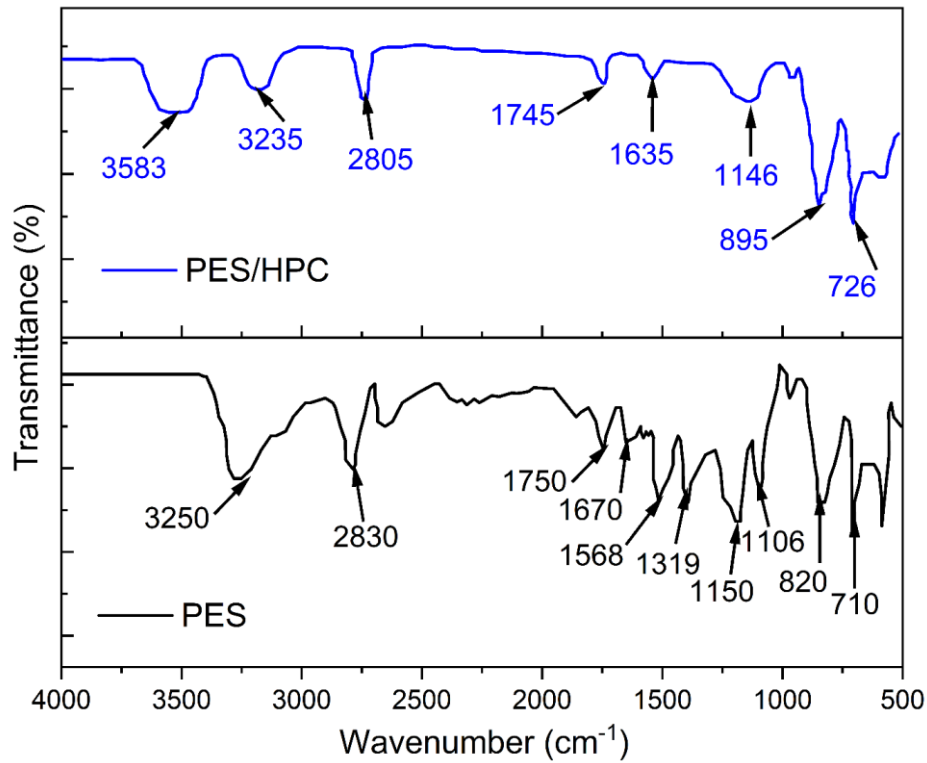


Figure 4.4 FTIR spectra of PES and PES/HPC nanofiber membranes.

XRD

Figure 4.5 shows the XRD patterns for the pristine PES and PES/HPC blended electrospun nanofiber membrane. Due to the amorphous nature of PES polymer, the pure PES nanofiber membrane displayed a strong characteristic peak at $2\theta = 13.54^\circ$. Also, there was another peak that emerged at $2\theta = 43.14^\circ$ because of the second carbon pair existence in the neighbouring chain (Laghaei et al., 2016a). The effect of the addition of HPC on the blended PES/HPC nanofiber membrane did not show any major changes with a broader peak at $2\theta = 12.44^\circ$. It is considered that the

somewhat ordered amorphous phase of the HPC is responsible for the wide peak at $2\theta = 20.1^\circ$, while the crystalline phase of the main chain backbone-backbone *d*-spacing corresponds to the peak at $2\theta = 8.94^\circ$ (Halamus et al., 2008).

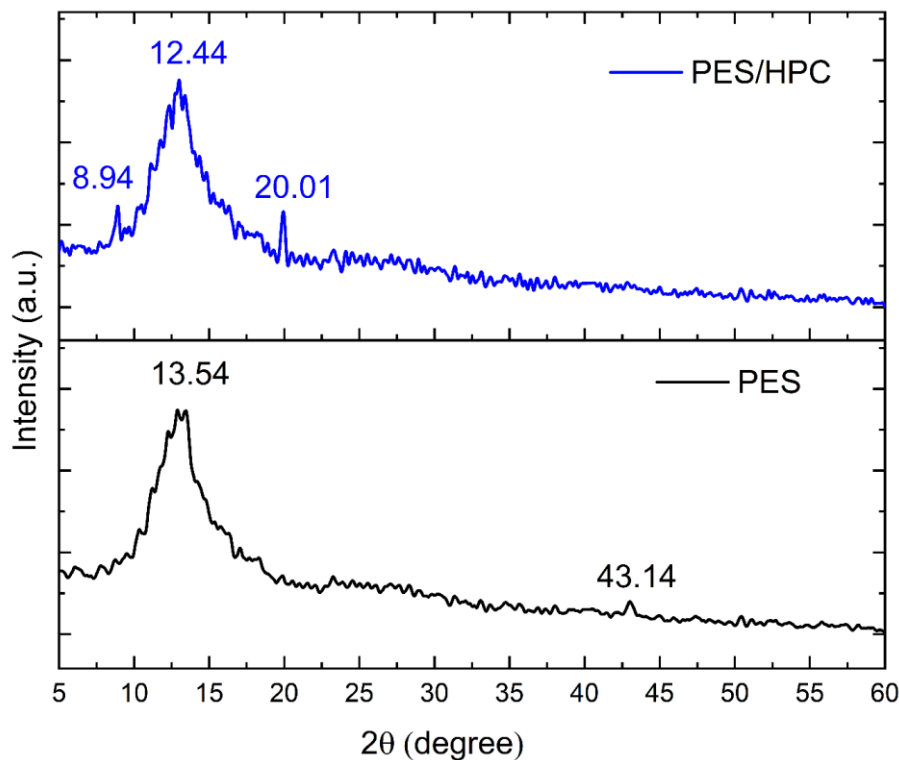


Figure 4.5 XRD pattern of PES and PES/HPC nanofiber membranes.

TGA

Figure 4.6 displays the results of a TGA profile on the thermal stability of the pristine PES and the blended PES/HPC electrospun nanofiber membranes, and now receiving particular attention. The pristine PES nanofiber membrane exhibited three phases of weight loss, whereby the weight loss in the first phase (30-100°C) was less than 5%, because of water molecules evaporation that had been physically attached to the polymer backbone chain. Following that, elimination of the leftover solvent from the pristine nanofiber membrane surface occurred during the second phase degradation, which took place between 140 and 400°C, and resulted in a weight loss of 21%. And when deterioration reached a temperature between 496 and 673°C, where, the ether bond (C-O) fracture of the pristine PES nanofiber membrane caused the greatest weight loss (around 54%) (Ayyaru and Ahn, 2018b). The case of the PES/HPC blended electrospun nanofiber membrane is interesting; it exhibits a two-

phase thermal degradation pattern; a modest weight loss between 1%-5% was detected during the first phase (30-100°C) due to moisture evaporation, and the major weight loss occurred from 285 to 650°C (around 71%), with a maximum degradation peak found at 355°C which was much lower, than the HPC polymer reported in the literature (Huang et al., 2013). Overall it has been observed that the blended PES/HPC nanofiber membrane demonstrated better thermal performance (total weight loss 76%) compared to the pristine PES nanofiber membrane (total weight loss 80%), which is consistent with earlier studies that found blended nanofiber membranes to be acceptable for thermally coupled wastewater applications (Awad et al., 2021b).

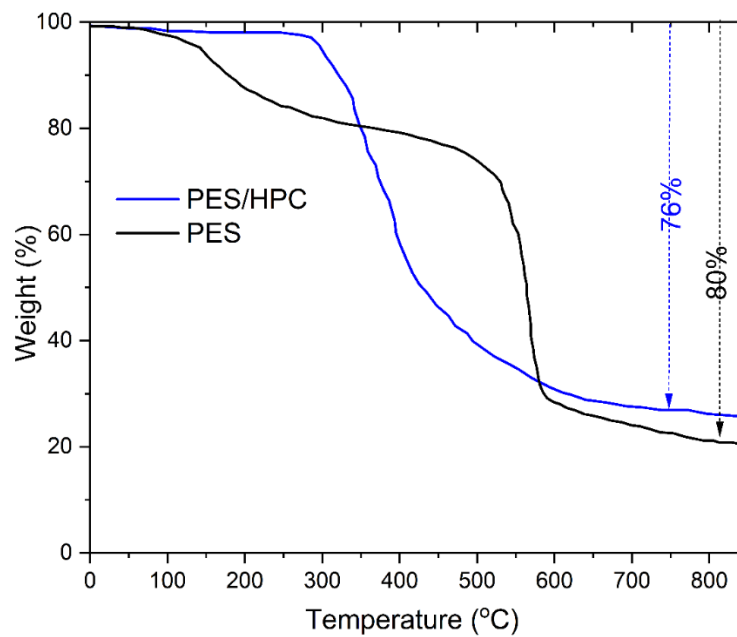


Figure 4.6 TGA curves of PES and PES/HPC nanofiber membranes.

Mechanical property

The mechanical properties of the electrospun NM have been proven to be critical in wastewater treatment (Bae et al., 2016b). The mechanical characteristics between pristine PES and blended PES/HPC nanofiber membranes were examined in this study using tensile studies, and the findings are presented in Figure 4.7. A larger strain percentage (27.12%) was observed in the pristine PES nanofiber membrane, although the tensile strength of the membrane was much reduced (around 3 MPa). A 30.2% increase in tensile strength (3.82 MPa) was seen in the blended PES/HPC

nanofiber membrane, as compared to the pristine PES nanofiber membrane, demonstrating that the intercalation of HPC into the PES matrix significantly improves intermolecular interaction. Additionally, because of the presence of surface hydroxyls, it is possible to increase the number of physical or chemical cross-linking sites, which is favourable to mechanical qualities (Wang et al., 2019d). Also, a larger number of nodes may be found in the fiber pores thanks to a reduction in the overall diameter of the blended PES/HPC nanofiber membrane due to HPC inclusion (increased surface area), resulting in higher tensile strength.

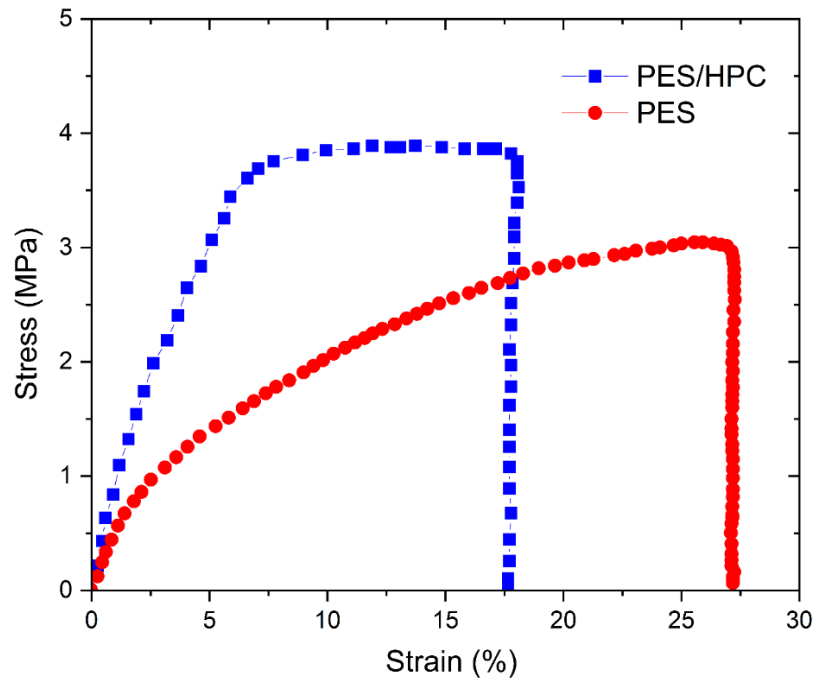


Figure 4.7 Stress-strain curve of PES and PES/HPC nanofiber membranes.

Hydrophilicity

The membrane's surface wettability, particularly hydrophilicity, is thought to be a significant characteristic for improving water purification performance (Bui and McCutcheon, 2013a). In this study, the hydrophilicity of two electrospun nanofiber membranes was assessed by measuring their contact angle. For the pristine PES electrospun nanofiber membrane, the contact angle was $81.10 \pm 1.3^\circ$ (Figure 4.8a), which indicates that the membrane had less hydrophilicity with a rough surface (Figure 4.8c). A lower contact angle of $55.4 \pm 0.9^\circ$, was found for the blended PES/HPC electrospun nanofiber membrane, indicating that the membrane is more hydrophilic and smooth surface (Figure 4.8b and d). The contact angle of the

membranes tend to decrease when HPC polymer is added to the solution, as reported in a previous study by Gradinaru et al. (Gradinaru et al., 2020). Overall, this study implies that because of their hydrophilicity, PES/HPC membranes will adsorb more dye molecules, utilizing high porosity behaviour to generate a stronger affinity between water/dye and membrane surface (Wang et al., 2019b, Wang et al., 2018).

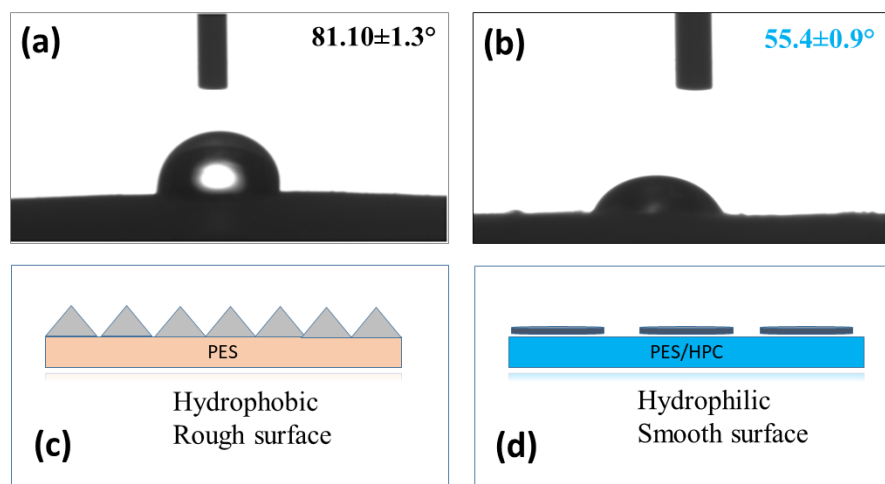


Figure 4.8 Water contact angle of pristine PES (a) and PES/HPC nanofiber membranes with their surface states (c) and (d), respectively.

MB adsorption studies

Effect of initial concentration

The adsorbent's binding sites are influenced by the initial dye concentration, which has an indirect effect on dye adsorption capability. Consequently, the adsorption capacity was tested under optimum condition at various starting concentrations ranging from 50-1000 mg/L. The adsorption capacity of both adsorbents is favorably influenced by the starting concentration, as can be shown in Figure 4.9. The fast adsorption capacity (43.47-186.12 mg/g) of a PES/HPC blended nanofiber membrane was seen with an increase in starting concentration from 50-400 mg/L while further increasing concentration of up to 1000 mg/L, resulted in a slightly increased adsorption capacity of 198.78 mg/g. When the concentration is more than 400 mg/L in both scenarios, a reasonable increase in adsorption capacity indicates that equilibrium has been attained. A similar pattern was seen for the pristine PES nanofiber membrane, although the adsorption capacity was relatively low throughout the entire varied concentrations, with the highest capacity of 41.02 mg/g was achieved at 400 mg/L. This result indicates that an increase in concentration

promotes mass transfer, which in turn raises the driving force for MB adsorption. MB molecules are also transported in significant numbers from the aqueous phase to the nanofiber membrane's solid surface, resulting in an increased adsorption capacity (Li et al., 2020b).

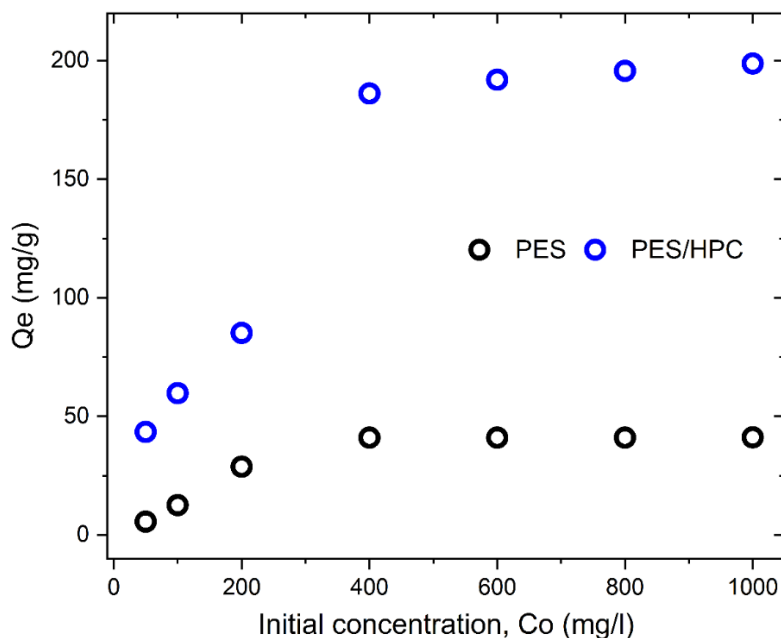


Figure 4.9 Effect of initial concentrations on the MB adsorption capacity of PES and PES/HPC nanofiber membrane.

Adsorption kinetics

The study of adsorption kinetics is crucial for determining the rate constant of the whole adsorption process in relation to contact time. Therefore, the kinetic behaviour of MB adsorption onto PES and PES/HPC membranes was studied, with the findings shown in Figures 4.10a and b, respectively. At the start of the experiment, the adsorption rate was quick, but it steadily slowed as the duration continued, until it reached equilibrium. The equilibrium for MB adsorption is attained in 1080 min and it takes 1440 min with PES, but only 840 min with the PES/HPC, whereby 75% of MB is adsorbed within 360 min. These findings show that the introduction of HPC into PES resulted in a surface area with more MB-capture active sites.

4. Development of electrospun nanofiber membrane for food industry wastewater treatment

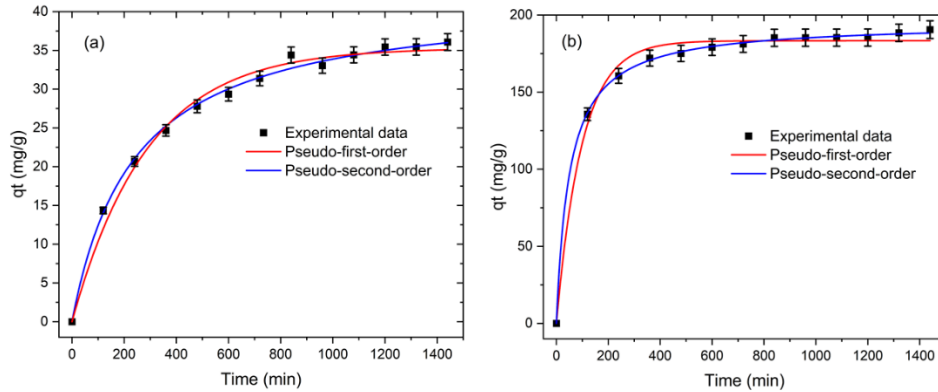


Figure 4.10 Pseudo-first-order kinetic model and pseudo-second-order kinetic model for the MB adsorption on PES (a) and PES/HPC (b).

Moreover, nonlinear pseudo-first-order (PFO) (equation 2) and pseudo-second-order (PSO) (equation 3) models were used to explain adsorption kinetics.

$$Q_t = Q_e(1 - e^{-k_1 t}) \quad (2)$$

$$Q_t = \frac{k_2 Q_e^2 t}{1 + k_2 Q_e t} \quad (3)$$

Where q_t (mg/g) represents the adsorption capacity of MB at any time t ; k_1 (min^{-1}) and k_2 (g/mg/min) are the kinetic rate constants for the Pseudo-first order and Pseudo-second order, respectively.

Figure 4.10a and b, illustrates the fitted curves, with the fitted values reported in Table 4.1. For PES, PSO had a higher correlation co-efficiency PSO ($R^2= 0.9965$) than PFO ($R^2= 0.9893$). When the PES/HPC blended nanofiber membrane was present, the correlation co-efficiency of PFO ($R^2= 0.9995$) was lower than that of PSO ($R^2= 0.9908$) in terms of R^2 . MB adsorption onto PES and PES/HPC nanofiber membranes was found to be well-fitted by the PSO kinetic model, suggesting that the adsorption process of MB is dominated by the chemisorption mechanism, in which electron exchange occurs between the adsorbent and arsenic molecule binding sites, rather than by the electrostatic mechanism. Previous investigations have also shown that the pseudo-second-order kinetic model for MB adsorption may have a good fitting. For example, Luo et al. (Luo et al., 2021) observed that the adsorption of MB follows a second-order kinetic model when they used cellulose nanofiber-based highly flexible compressible super assembled aerogel. Based on our research, it can be concluded that the PES/HPC nanofiber membrane demonstrates outstanding molecular adsorption performance of MB in a short period of time, making it suitable for practical use.

Table 4.1 Kinetics parameters for MB adsorption.

Samples	Pseudo-first order			Pseudo-second order		
	K ₁ (min ⁻¹)	q _e (mg/g)	R ²	K ₂ (g/mg/min)	q _e (mg/g)	R ²
PES	0.0034	35.31	0.9893	0.0001	41.9531	0.9960
PES/HPC	0.0101	183.32	0.9908	0.0004	195.0212	0.9995

Adsorption isotherms

Adsorption isotherms are a key factor in the adsorption process. Using this scheme, the maximum adsorption capacity could be identified by determining the relationship between adsorbent and adsorbate equilibrium concentration. Herein, the adsorption behaviour is investigated using two widely used nonlinear isotherm models, namely the Langmuir model (equation 4) and Freundlich model (equation 5). The Langmuir fitted model indicates that the adsorption process occurs monolayer onto the homogeneous solid adsorbent surface, while the Freundlich fitted isotherm model indicates that the adsorption process occurs multilayer onto the heterogeneous solid adsorbent surface (López-Luna et al., 2019a, Talukder et al., 2021d).

$$Q_e = \frac{q_{\max} K_L C_e}{1 + K_L C_e} \quad (4)$$

$$Q_e = K_F C_e^{1/n} \quad (5)$$

Where q_{\max} denotes the maximum adsorption capacity of MB (mg/g); K_L represents the constant of the Langmuir equation, C_e used for the measurement of solution concentration at equilibrium; $1/n$ highlights the intensity of the adsorption, and K_F indicates the constant of the Freundlich equation.

A set of fitted curves can be shown in Figure 4.11, while a list of derived isotherm parameters can be found in Table 4.2. Based on the correlation co-efficiency values (R^2), the adsorption isotherms for both membranes were consistent with the Langmuir isotherm model, demonstrating monolayer adsorption on the heterogeneous surface of adsorbents (Hossain et al., 2021a). According to, the PES/HPC nanofiber membrane has a maximum MB adsorption capacity of 259.74 mg/g, while the pure PES nanofiber membrane has a capacity of just 48.00 mg/g. This implies that the PES/HPC nanofiber membrane considerably increased the adsorption capacity of MB, which is integrated with the K_L value of the adsorbent, since a higher K_L of the adsorbent results in improved adsorption performance at low concentration (Cao et al., 2012b). Table 4.3 compares our adsorbent to other adsorbents for MB adsorption and shows that PES/HPC has an excellent adsorption capacity and it is much higher than others. The exceptional performance of the PES/HPC nanofiber membrane might be explained by the presence of sulfonic and

4. Development of electrospun nanofiber membrane for food industry wastewater treatment

hydroxyl groups on the membrane's surface, which interact with the cationic site of MB electrostatically. This shows that the PES/HPC nanofiber membrane may be a highly efficient adsorbent for removing pollutants from wastewater.

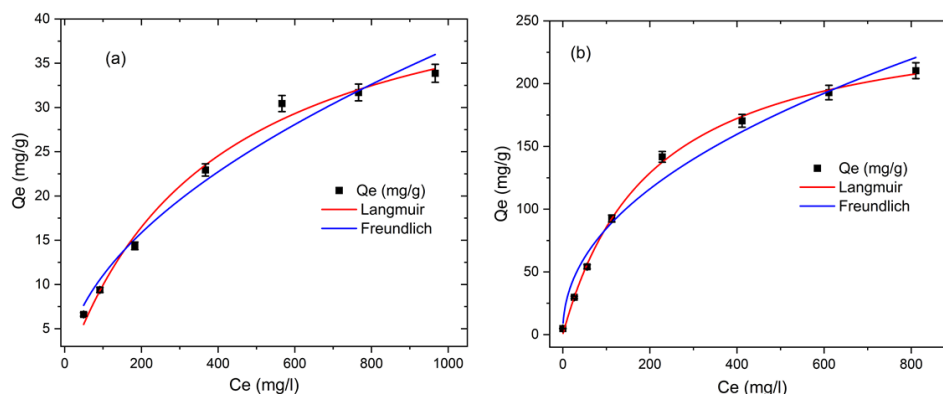


Figure 4.11 The adsorption isotherms of MB by PES (a) and PES/HPC (b) according to Langmuir and Freundlich equations.

Table 4.2 Adsorption isotherms parameters for MB.

Samples	Langmuir			Freundlich		
	q_{\max} (mg/g)	K_L (L/mg)	R^2	K_F (mg/g)	$1/n$	R^2
PES	48.0076	0.0026	0.9913	1.0012	0.5211	0.9747
PES/HPC	259.7402	0.0049	0.9984	10.1847	0.4593	0.9693

Table 4.3 Comparison of the MB adsorption capacity with previously reported literature.

Adsorbent	Optimum MB conc. (mg/L)	Optimum pH	Kinetic order	Isotherm	q_{\max} (mg/g)	Ref.
Cellulose nanofibrils	100	9.0	-	Langmuir	122	(Chan et al., 2015)
Deacetylated cellulose acetate (DA)@polydopamine (PDA) nanofibers	50	6.5	2nd order	Langmuir	88.2	(Cheng et al., 2020)
Graphene/TEMPO-Oxidized Cellulose nanofibrous	100	6.5	2nd order	Langmuir	227.27	(Hussain et al., 2018)
Cellulose citrate	100	3.0	2nd order	Langmuir	96.2	(Olivito et al., 2021)

Hydroxypropyl cellulose (HPC)/graphene oxide hydrogels	-	-	2nd order	Freundlich	118.4	(Liu et al., 2015b)
Cellulose sponge	30	7.0	2nd order	Langmuir	123.46	(Ma et al., 2020a)
Vanadium pentoxide (V ₂ O ₅) nanoparticles/PES	1	10	2nd order	Freundlich	85%	(Homaeighar et al., 2016a)
PES nanofibers	400	7	2nd order	Langmuir	48.0	Present work
PES/HPC nanofibers	400	7	2nd order	Langmuir	259.74	Present work

Adsorption mechanism

The pH of the solution has been thought to be important because the surface charge of adsorbents and the adsorbate are very dependent on pH values determining the adsorption performance. Consequently, the MB adsorption capacity was examined in the presence of PES and PES/HPC nanofiber membranes at different pH values ranging from 3 to 10, and the findings are shown in Figure 4.12. With respect to both membranes, the pH range between 3 and 5 was found to be steady while the pH value rose from 5 to 7 and then progressively attained the greatest MB adsorption capacity between 7 and 10 for both membranes. Particularly, the highest adsorption capacity of MB was 33.68 mg/g and 147.09 mg/g for PES and PES/HPC, respectively, at neutral pH, which is in line with previously published research (Yue et al., 2019). The reason for these results can be explained as follows; (1) the protonation behaviour of existing functional groups causes the nanofiber membrane surface to become positively charged at acidic pH. As a result of electrostatic repulsion between the positively charged membrane surface and the cationic MB molecules, adsorption uptake was decreased, (2) On the contrary, when the pH is changed to neutral or alkaline, the nanofiber membrane surface charge exhibits greater negativity, leading to a higher adsorption capacity. In the case of the blended PES/HPC membrane, sulfonic and hydroxyl groups deprotonate at neutral pH, resulting in the membrane's negative charge (Ding et al., 2016). Overall, it was shown that at higher pH levels, the PES/HPC membrane developed an electrostatic attraction ionic interaction with the positive-charged MB molecules, which resulted in a tendency towards a larger adsorption capacity, especially at neutral pH levels. Furthermore, the zeta potential, as shown in Figure 4.12 (inset), provides additional evidence of these occurrences. For PES and PES/HPC nanofiber membranes, the point of zero charge (pzc) was observed at pH 6.3 and 5.5, respectively. Thus, both

membranes have a positive $<pzc$ and negative $>pzc$ surface charge, with the negatively charged surface favouring adsorption through electrostatic attraction, as is evident in our experimental study.

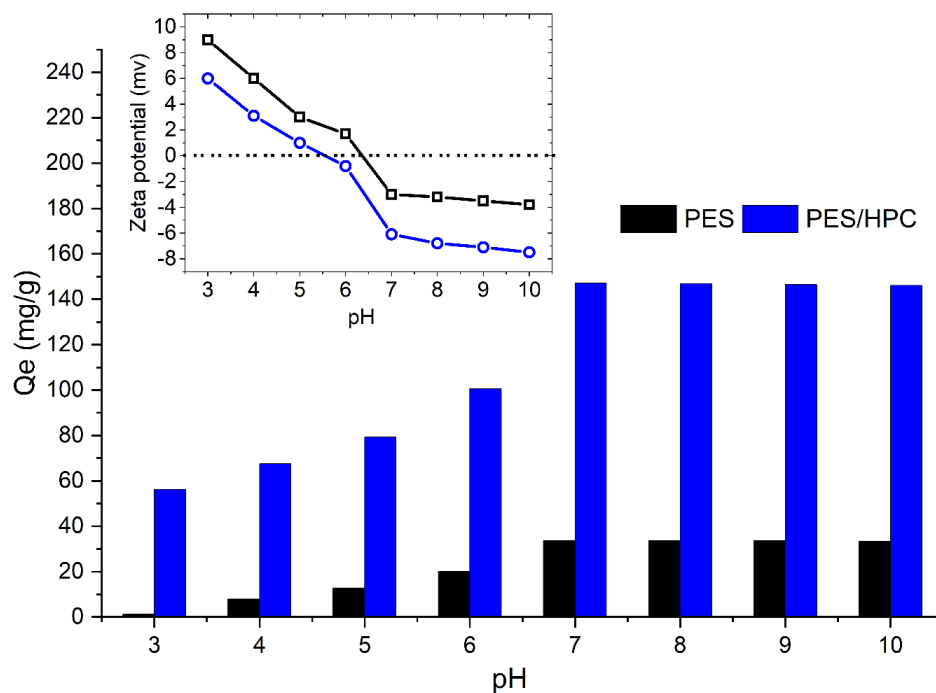


Figure 4.12 Effect of pH on the MB adsorption capacity.

Based on the above discussion, the tentative adsorption mechanism was depicted in Figure 4.13. In adsorption, dye is adsorbed by the nanofiber membrane, and it is essential to establish the mechanism that provides this desired adsorption capacity. Sulfonyl functional groups are enriched in the backbone of the polyethersulfone compound and interact with a cationic MB dye through various forces such as electrostatic interaction, hydrogen bond, Π - Π interaction, and others (Zhou et al., 2022). The presence of sulfone groups, which are more polar than ether groups, results in a more charged exchange between the adsorbent and adsorbate, thus enhancing electrostatic attraction and leading to a noticeable improvement of adsorption capacity for the PES/HPC nanofiber membrane (Baig et al., 2021). It is worth mentioning that the synthesized PES/HPC nanofiber membrane demonstrated improved adsorption capability at neutral pH, which implies that the blended membrane surface includes a significant number of oxygen-containing functional groups, which are deprotonated at higher pH and facilitate electrostatic adsorption.

The addition of HPC also provided hydroxyl groups and facilitated the adsorption process by making both electrostatic interaction and hydrogen bonding and contributed to the adsorption process. Furthermore, the presence of ionic strength decreased the adsorption capacity (Table 4), which is another proof that the electrostatic interaction was dominant for MB adsorption by the blended PES/HPC nanofiber membrane.

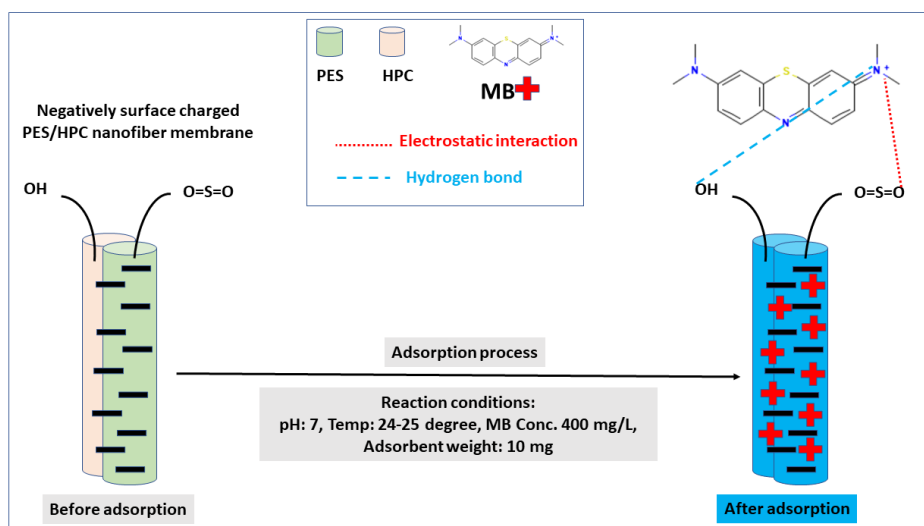


Figure 4.13 Proposed adsorption mechanism of MB in the presence of PES/HPC nanofiber membrane.

Effect of ionic strength

A wide range of contaminants such as suspended and dissolved chemicals, acids or alkalis, salts, metal ions, and other hazardous substances may be found in food manufacturing wastewater. The presence of ions raises the ionic strength of the solution, which might affect the efficacy of the adsorption process. Thus, NaCl was added to the solution in variable concentrations to study the influence of ionic strength on the adsorption capacity of MB in PES, and PES/HPC nanofiber membranes and the obtained results are shown in Table 4.4. It was noticed that when the concentration of NaCl was increased, the MB adsorption capacity was reduced simultaneously. This could be attributed to the evolving of electrostatic repulsion between dye molecules and negatively charged adsorbent surfaces at higher NaCl concentrations, as Na⁺ ions of NaCl compete for binding sites on the membrane surface with cationic MB, less adsorption occurs. A similar phenomenon was also observed for MB adsorption on a cellulose-based bio adsorbent, as reported by Liu et al. (Liu et al., 2015a).

4. Development of electrospun nanofiber membrane for food industry wastewater treatment

Table 4.4 Effect of NaCl concentrations and recyclability tests on MB adsorption capacity by PES and PES/HPC nanofiber membrane, respectively.

Samples	Control, (mg/g)	Qe NaCl Concentrations (M) , Qe (mg/g)				
		0.1	0.2	0.3	0.4	0.5
PES	32.47	29.44	27.34	23.77	21.88	20.44
PES/HPC	185.45	182.32	180.21	179.15	178.05	177.25
Cycles, Qe (mg/g)						
		1	2	3	4	5
PES	32.47	30.17	27.14	24.05	22.13	20.45
PES/HPC	185.45	183.12	181.88	178.18	176.21	174.85

Reusability

Commercially accessible adsorbents can only compete if they can be used repeatedly and can be regenerated. Adsorbents are judged to be effective based on the presence of these characteristics. As a result, a series of experiments were carried out employing PES and PES/HPC membranes for up to five cycles under optimum conditions (Table 4.4). According to the results, the original PES nanofiber membrane lost 32.2% of its adsorption capacity after five cycles, but the PES/HPC nanofiber membrane lost only 4.5%, indicating that the blended PES/HPC membrane is more reusable. For the PES/HPC nanofiber membrane, the smaller fiber diameter (resulting in a greater surface area) and increased hydrophilicity are credited with its exceptional performance. Given its high recyclability, the PES/HPC nanofiber membrane adds another important property in its wastewater treatment adsorption capacity.

4.2 Fabrication of polyethersulfone/polyacrylonitrile electrospun nanofiber membrane for food industry wastewater treatment

4.2.1 Introduction

The wastewaters discharged from the food industries show a broad variety of compositions and strength, since the items produced vary and the raw materials used are different. Typically, food industrial wastewater effluent has a moderate to high biological oxygen demand (BOD) and chemical oxygen demand (COD), high concentrations of dyestuffs, dissolved and suspended particles, oils, greases, as well as, a very high nutritional content, including phosphorus- and nitrogen-containing compounds (Pervez et al., 2021d, Jing et al., 2021c). Dyestuffs are among the most stable compounds with various complex structures that are difficult to remove from effluent. In addition, dye-contaminated effluent shows an adverse impact on the water/Land, human health, and our ecosystem (Pervez et al., 2020d, Morshed et al., 2020a, Pervez et al., 2019a, Pervez et al., 2022b). Thus, it is essential to build an appropriate technique for the effective treatment of dye-contaminated food industry wastewater.

Several technologies have been applied for the removal of dyes from wastewater, such as coagulation (Wei et al., 2015), biological (S Lopes et al., 2020) or catalytic oxidation (Liu et al., 2017) and membranes purification (Pervez et al., 2020a) that have been applied for the treatment of dye in wastewater. Among them, the use of nanofiber membrane has received particular attention from the scientific community because of its easy application, high efficiency and the potential economic feasibility. A typical nanofiber membrane shows a large surface area, small diameter (less than 100 nm) and a high porosity that may provide easily accessible binding sites to tailor its performances, especially in water treatment (Pervez et al., 2020g, Pervez and Stylios, 2018d). Electrospinning is now one of the most appropriate and efficient ways for preparing nanofibrous membranes, as compared to other processes, because it has good repeatability, good scalability, excellent versatility and operation flexibility. In general, a polymer solution is loaded into a syringe which is connected through a tube into the spinneret (needle) and a high voltage

assisted Taylor cone-formed between the grounded collector and the needles, produces nanofiber webs with certain properties. The grounded plate can be made of stainless steel or copper for collecting the nanofiber membrane and prepared for further investigation (Pervez and Stylios, 2018b, Talukder et al., 2021a, Talukder et al., 2021c).

Various polymers have been employed for the fabrication of electrospun nanofiber membranes with high efficiency of sequestration of pollutants from wastewater (T. M et al., 2021b). Polyethersulfone (PES) is a high-performance aromatic polymer in which aromatic groups are joined in *para* positions together by sulfone and ether groups to form the fundamental repeating unit of the polymer backbone (Al-Husaini et al., 2021a). PES-based materials have widely been used to make conventional membranes because of their outstanding film-forming ability, chemical resistance, mechanical and thermal stabilities. Conventional PES membranes are typically not identical on both sides of their surface and their ultimate structure is influenced by operational parameters (Barth et al., 2000, Talukder et al., 2022a). Additionally, PES has been also utilized as a popular raw polymeric material for the production of electrospun nanofiber membranes, benefiting from its good spinnability, good mixing nature and reduced agglomeration propensity. Recently, PES-based electrospun nanofiber membranes have found application for removing pollutants from contaminated water. Bornillo et al. (Bornillo et al., 2020) fabricated PES-poly(2-(dimethylamino)ethyl methacrylate) composite electrospun nanofiber membrane and tested its adsorptive ability of heavy metal from wastewater with a maximum adsorption capacity for copper(II) of 161.30 mg_{Cu}/g at neutral pH. Similarly, Min and co-workers (Min et al., 2012) prepared micro structured PES-based electrospun nanofiber membranes investigating their efficiency for the removal of heavy metals and dyes from water. After conducting a series of adsorption tests, they observed maximum adsorption capacities of 161 mg_{Cu}/g and 1000 mg_{Dye}/g, respectively for copper (II) the Sunset Yellow FCF dye, where the pH resulted as the most critical factor in determining the adsorption capacity. Comparably, Schäfer et al. (Schäfer et al., 2018) developed β -Cyclodextrin-PES composite nanofibers and found that the addition of β -cyclodextrin to PES polymer enhanced hormone adsorption performance significantly, with 3.2 to 3.7 $\times 10^{-5}$ ng/cm² for PES and 11.5 to 29 $\times 10^{-5}$ ng/cm² for PES combined with β -cyclodextrin. The application of PES nanofiber for membrane water purification is often criticized for the lacking of functional groups and thus the reduced hydrophilicity of this polymer (Nasreen et al., 2013). The blending of PES with other functional components preserves the above-mentioned properties of this polymer, disclosing novel materials with even unexpected features. Blending is a key process for

obtaining new qualities in polymeric materials while minimizing the steps of the process and the associated costs. Polyacrylonitrile (PAN) has been long used to prepare traditional membranes for water treatment due to its outstanding mechanical and thermal stability and the relative chemical properties. PAN-based electrospun nanofiber membranes have shown interesting characteristics such as surface wettability with water, heat resistance and molecule transmission phenomena, which make them a suitable membrane in wastewater treatment. Previous reports state that the adsorption capacity of the composite nanofiber membrane is increased after incorporating PAN as a copolymer. For instance, Aijaz et al. (Aijaz et al., 2021) synthesized magnetic/polyetherimide-acrylonitrile composite nanofiber membranes used for nickel ions removal from aqueous solutions. They reported that the developed composite membrane exhibited a higher amount of adsorption capacity ($102 \text{ mg}_{\text{Ni}}/\text{g}$) which maybe achieved because of PAN matrix inclusion. In a comparative study, pure chitosan nanofibrous membrane adsorption capacity was $872 \text{ mg}_{\text{Dye}}/\text{g}$ for acid blue-113 (Li et al., 2018), but after being coated with PAN the maximum adsorption was increased to $1708 \text{ mg}_{\text{Dye}}/\text{g}$. Noteworthy, previous studies found that PES/PAN composite blended membranes showed improved morphological and physicochemical properties, fouling resistance and increased permeation capacity (Ling and Chen, 1995, Amirilargani et al., 2012, Reddy and Patel, 2008). However, the synthesis of PES/PAN based electrospun nanofiber and their application for wastewater treatment is rarely reported in the literature, and deserves further investigations.

Taking into account the above-discussed considerations, we may assume that the customary anchoring of hydrophobic polymer may result in improving the water purification performance of the PES nanofiber membrane. In the present study, a novel PES/PAN composite electrospun nanofiber membrane was prepared using a general nanofiber membrane development protocol and applied to remove methylene blue (MB) from aqueous solutions for the first time. MB was chosen because it is a popular cationic azo-dye used to produce foodstuffs such as roasters, cutlery, paper sheets, food packing, and food additives. However, due to its harmful impact, this type of colour may be regarded as a pollutant. It creates eye burns and can harm the eyes of people and animals irreversibly. People with pulmonary issues may have severe palpitations or wheezing after breathing (Zhu et al., 2018). Hence, it is worth researching the effective clearance of MB from food industrial wastewater effluent. Various characterization techniques such as scanning electron microscopy (SEM), Fourier-transform infrared spectroscopy (FTIR), thermogravimetric analysis (TGA), x-ray diffraction (XRD) and contact angle were used for the determination of the structure-property relationship of the as-prepared composite nanofiber membrane. Adsorption performances were studied in detail, including kinetics and

isotherm investigations, as well as the influence of inorganic anions and reusability. Finally, an adsorption mechanism was proposed in order to fully understand the adsorption process of this material.

4.2.2 Materials and methods

In this study, polyethersulfone (PES, Ultrason E 6020 P) was obtained from BASF SE (Ludwigshafen, Germany) with a molecular weight of 65.8 kDa. Polyacrylonitrile (PAN, 99%) was purchased from Shanghai SSS Reagent Co., Ltd., (Shanghai, China). *N,N*-dimethylacetamide (DMAc) (CAS No.:127-19-5) was obtained from TNJ Chemical Industry Co., Ltd, Hefei, China. Methylene blue ($\geq 95\%$) was bought from Sigma Aldrich Co., Ltd. (Darmstadt, Germany). Non-woven polyethylene terephthalate paper was obtained from Guocheng CO. (Wuxi, China) and employed as an electrospun nanofiber membrane cover of the collector. Deionized (DI) water was used throughout the experimental procedures. Other materials and reagents, unless otherwise stated, were used directly without any further modification.

Fabrication of electrospun nanofiber membrane-based adsorbents

The fabrication of the electrospun nanofiber membrane, depicted in Figure 4.14, requires the preparation of a polymer solution obtained by compounding in DMAc (86 mL), PES (12 wt%) and PAN (2 wt%) by stirring for 4 h at room temperature.

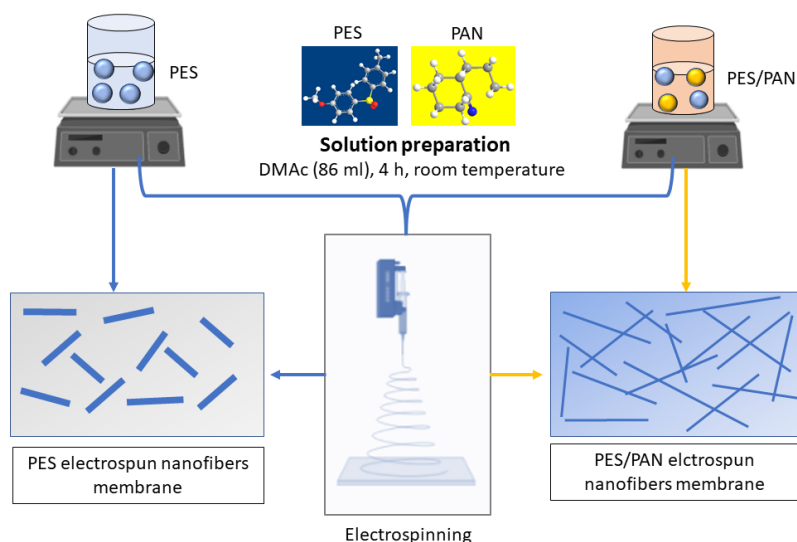


Figure 4.14 Illustration of electrospun nanofiber membrane fabrication process

The prepared solution was transferred into a 20-mL plastic syringe connected to a metallic needle (20 gauge). During the electrospinning, solutions were injected at a flow rate of 0.8 mL/h (maintained by a syringe pump) under an applied voltage of 15.5 kV at 28 °C. When a Taylor cone was observed, the successful preparation of electrospun nanofiber was confirmed and finally, a nanofiber mat was collected onto the non-woven PET fabric which was placed at 18 cm distance from the needle tip. The whole experimental process required 3 h. The formed nanofiber membranes were separated from the PET non-woven sheet. The membranes were dried in vacuum at 60 °C for the removal of the solvent. PES nanofiber membrane was prepared by following the same protocol in the absence of PAN.

Instrumentation and methods

The electrospinning process was performed with a laboratory scale electrospinning machine (Foshan Lepton precision measurement and control technology Co., Ltd., M06, Foshan, China). Solution pH values were measured through a DZS-706A multi-parameter analyzer from INESA Scientific Instrument Co., Ltd., (Shanghai, China). The solution's viscosity and conductivity were measured using an NDJ-8S digital rotating viscometer (Movel Scientific Instrument Co., Ltd, Ningbo, China) and a conductivity meter (INESA Scientific Instrument Co., Ltd., Shanghai, China), respectively. Water contact angles of the as-prepared membranes were determined using a professional DropMeter A-300 from Kudos Instruments Corp. (Newyork, USA). Surface morphologies of the nanofiber membranes were analyzed by a Phenom desktop Scanning Electron Microscope (SEM) from Thermo Fisher Scientific (Tokyo, Japan) at accelerating voltage of 5kV. The samples were gold-sputtered before SEM image collection. Fiber diameter distributions were determined using the ImageJ software (National Institute of Health, USA). Fourier transform infrared (FT-IR) spectra were acquired with a low noise DLATGS FTIR-920 spectrophotometer from Interspectrum (Estonia) in the wavenumber range 400-4000 cm^{-1} . Thermogravimetric analysis (TGA) was carried out under protective nitrogen atmosphere with a TG 209 F1 Libra from Netzsch Instruments (Wolverhampton, United Kingdom) at a heating rate of 10 °C/min. X-ray diffraction patterns were determined by an Empyrean diffractometer from Malvern PANalytical (Worcestershire, United Kingdom) in the 2θ range 10-80°. Tensile testing was performed with a KD-III model BA-100m dynamometer from Transcll Technology (Shenzhen, China).

Adsorption studies

MB concentrations were determined by using the absorbance at wavelength of 664 nm with a Perkin-Elmer Lambda 25 UV-Vis spectrophotometer (Massachusetts, USA). The aliquots of the MB solutions were filtered through a 0.45 μm PTFE membrane before UV-Vis analysis. The instrumental calibration was performed by analyzing MB solutions with known concentrations obtained by progressive dilution of a MB standard solution (1000 mg/L). The adsorption experiments were carried out in batch-mode for MB solutions in the presence of the prepared nanofiber membranes. The investigation on the effect of pH (2, 4, 6, 7, 8 and 10) was carried out as follow. 10 mg of adsorbent were introduced into a polypropylene centrifuge tube containing 10 mL of a pH-buffered solution MB (400 mg/L) and stirred for 24 h at room temperature. The investigations on the influence of MB concentration (200, 400, 600, 800 and 1000 mg/L) on adsorption performance were similarly performed. The effect of inorganic anions (Cl^- , SO_4^{2-} , HCO_3^- and PO_4^{3-}) on the removal efficiency of MB was investigated with a constant concentration of 1 mM under optimized conditions. The recyclability tests of the adsorbents was measured using a 2 mM HCl solution for 6 h at room temperature. It was found that this pH range is lower than the nanofiber membrane surface zeta potential, hence the nanofiber membrane surface charge inverts from negative to positive, allowing MB to be released from the adsorbent surface via electrostatic repulsion (Liu et al., 2020b). Five regeneration cycles were performed under the same experimental conditions and each tested adsorbent was washed with DI water two times and prepared for the subsequent adsorption cycle, and the concentration of MB was again measured to calculate the adsorption capacity of the membrane.

4.2.3 Results and Discussion

Membrane characterization

Fiber surface morphology is a crucial parameter that deals with structural characteristics and plays a key role in any application. Scanning electron microscopy was used for the analysis of the surface morphology and average diameter distribution of PES and PES/PAN electrospun nanofiber membranes (Figures 4.15a-b). The pristine PES nanofiber membrane exhibits a smooth surface with uniform thicker fibers with an average diameter of 261 nm. The fibers of the PES/PAN membrane, in comparison to that of PES fibers, were found thinner with an average diameter around 151 nm and with a more uniform structure with a more compact fibers stacking. This smaller diameter formation can be ascribed to the lower viscosity of the solution after adding PAN into PES solution (PES, 2268 mPa/s and PES/PAN, 1986 mPa/s) and higher conductivity ((PES, 1.6 mS/cm and PES/PAN,

2.4 mS/cm), as reported elsewhere (Tan et al., 2005, Wang et al., 2010). Nanofiber membranes with smaller diameters have a higher specific surface area than those with a larger diameter, this means that this membrane surface could adsorb more organic pollutants during the adsorption study since it has a higher number of active sites (Awad et al., 2021a).

Surface wettability, especially hydrophilicity, is considered a useful indicator for membrane with higher water purification performance (Bui and McCutcheon, 2013b). In this work, hydrophilicity was determined through the measurement of the contact angle for both electrospun nanofiber membranes. As shown in Figure 4.15c, the contact angle was $81.1 \pm 1.3^\circ$ for pristine PES electrospun nanofiber membrane, indicating that pristine PES membrane has low hydrophilicity. On the contrary, blended PES/PAN electrospun nanofiber membrane showed a lower contact angle of $65.9 \pm 1.2^\circ$, meaning that the blended membrane has higher hydrophilicity (Figure 4.15d). This might be achieved due to the addition of hydrophilic polymer such as PAN, which is able to improve the overall substance's hydrophilicity through the formation of hydrophilic carboxylic groups on the blended PES/PAN membrane surface, resulting in a lower contact angle (Meng et al., 2014, Plisko et al., 2020). Previous studies also found that the contact angle of the membranes tends to decrease when PAN polymer is added to the PES solution (Pasaoglu et al., 2016, Kumar et al., 2016a). Overall, this result indicates that PES/PAN membrane would adsorb more dye molecules because of their hydrophilicity and thus higher compatibility with aqueous solutions (Wang et al., 2019c).

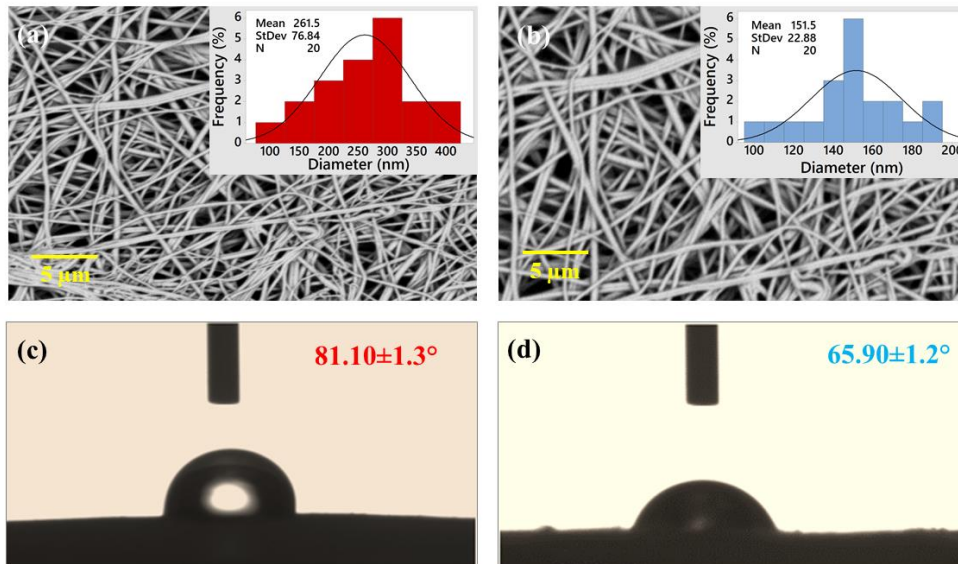


Figure 4.15 SEM images and water contact angle of pristine PES (a, c) and PES/PAN (b, d) nanofiber membranes; insets are the diameter distribution of corresponding nanofiber membranes.

The FTIR spectra of pristine PES and blended PES/PAN electrospun nanofiber membrane are shown in Figure 4.16a. For the pristine PES nanofiber membrane, the absorption peaks are identified at 710 cm^{-1} (CH_2 bond), 820 cm^{-1} (C-H stretching). The functional groups are strongly exhibited at $1106\text{-}1150\text{ cm}^{-1}$ ($\text{O}=\text{S}=\text{O}$), 1319 cm^{-1} (C-O stretching), 1568 cm^{-1} (C=C stretching), 1670 cm^{-1} (N-C=O carbonyl vibrations) and 1750 cm^{-1} (C=O stretching) (Zhang et al., 2013b). In addition, the two characteristics absorption peaks at 2830 cm^{-1} and 3250 cm^{-1} (broader) are assigned to the stretching vibration of aromatic C-H groups (Homaieghar et al., 2010b). Whereas for the blended PES/PAN membrane, the absorption peaks are almost similar to the pristine PES nanofiber membrane absorption peaks, indicating that the anchoring polymer does not alter the structure. Particularly noted is that, the absorption peaks at 2240 cm^{-1} and 1675 cm^{-1} are corresponding the stretching of the symmetrical $\text{C}\equiv\text{N}$ group and C=O group, which are typical bonds of PAN polymer (Lohokare et al., 2008). These results further indicate, in combination with the uniform morphology observed by SEM, the successful interaction between PES and PAN (Yar et al., 2017).

The XRD patterns for the pristine PES and PES/PAN blended electrospun nanofiber membrane are shown in Figure 4.16b. The pristine PES nanofiber membrane had a major characteristics peak at $2\theta = 13.5^\circ$ which is attributed to the typical amorphous nature of the PES polymer. Additionally, the second peak appeared at $2\theta = 43.1^\circ$ because of the second carbon pairs found at the neighbouring chain (Laghaei et al., 2016b). On the other hand, the blended PES/PAN nanofiber exhibited a similar broader shift peak at $2\theta = 13.0^\circ$. which shows the amorphous nature of that blended nanofiber membrane.

The thermal stability of the pristine PES and blended PES/PAN electrospun nanofiber membranes was investigated using a thermogravimetric analysis (TGA), and the results are shown in Figure 4.16c. The thermal behaviour of both membranes involves three phases of weight loss. For the pristine PES nanofiber, the first phase ($30\text{-}100^\circ\text{C}$) of weight loss was observed below 5%, corresponding to the evaporation of physically adsorbed water molecules on the fibers. The second phase occurred between 140 and 400°C and resulted in 21% of weight loss, which is attributed to the slow evaporation of residual DMAc solvent from the nanofiber membrane surface (Al-Husaini et al., 2021b). Finally, the largest weight loss (around 54%) was recorded at the third phase ranging between 496 and 673°C , corresponding to the polymer degradation (Ayyaru and Ahn, 2018a). The blended PES/PAN nanofiber

membrane also shows a similar three-phase thermal degradation pattern, in which a slight amount of weight loss (between 1 and 3%) was observed at the first phase (30-100 °C) because of moisture evaporation. Whereas, 12% weight loss from 225 to 334 °C was noticed in the second phase, ascribed to sufficient chemical reactions within the PAN polymer substance and the nitrile groups cyclization exhibit in their side-chain (Kizildag, 2021, Ji et al., 2008). The addition of PAN into PES resulted in decreasing weight loss (around 48%) from 515 to 671 °C in the third phase, and overall, it has been shown that the blended PES/PAN nanofiber membrane showed better thermal stability (total weight loss 73%) than the pristine PES nanofiber membrane (total weight loss 80%). To some extent, this observation can correlate with previous investigations claiming that the blending of nanofiber membrane is suitable for thermally coupled wastewater application (Awad et al., 2021a).

The mechanical properties of electrospun nanofiber membranes have been found to be crucial in treating wastewater (Bae et al., 2016a). In this work, the mechanical properties through the stress-strain curve of pristine PES nanofiber membrane and blended PES/PAN nanofiber membrane were investigated, and the results are shown in Figure 4.16d. As can be seen, the pristine PES nanofiber membrane exhibited a higher strain percentage (27.1%) with a lower tensile strength (around 3 MPa), while the blended PES/PAN nanofiber membrane has a highest tensile strength (4.4 MPa) and a lower strain (21.7%). These results indicated that adding PAN into PES enhanced its tensile properties. Moreover, the presence of PAN decreased the whole diameter of the blended PES/PAN nanofiber membrane (higher surface area), which means there is a large number of nodes available in the fiber pores, thereby promoting the tensile strength property.

4. Development of electrospun nanofiber membrane for food industry wastewater treatment

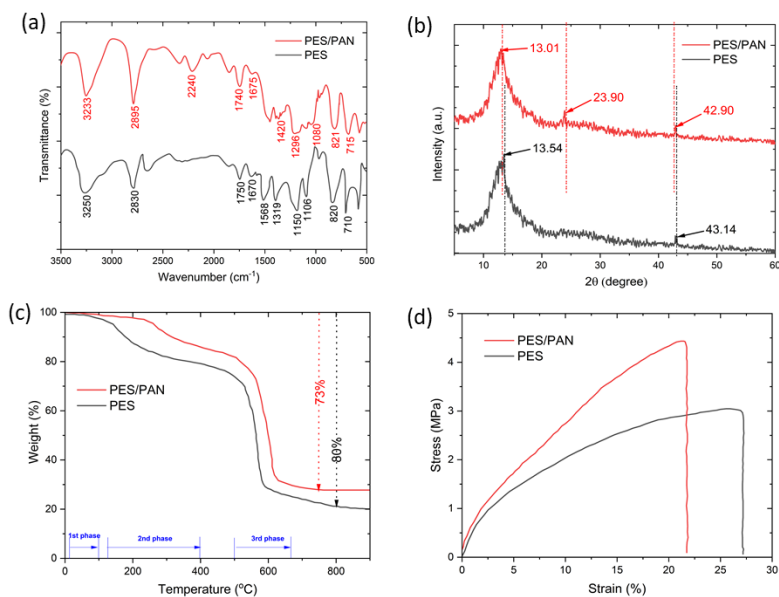


Figure 4.16 FTIR spectra (a), XRD patterns (b), TGA profiles (c) and stress-strain curve (d) of PES and PES/PAN nanofiber membranes.

MB adsorption studies

Various process factors for determination of MB adsorption capacities, such as the influence of pH, initial concentration and contact time of MB were analyzed for the determination of the membrane performance and the optimized work conditions. After that, the impact of inorganic anions on MB adsorption capacity was carefully investigated and also recyclability of the adsorption process was carried out to ensure the durability of as-synthesized adsorbents. The modelling kinetics-isotherms fitting was performed to gain insights into the adsorption process of MB in the presence of electrospun nanofiber membrane-based adsorbents.

Effect of pH

The pH can strongly affect the surface charge of adsorbents and adsorbate and thus the adsorption performance of the membrane. Therefore, the adsorption capacity of MB was investigated at various pH ranging from 3 to 10 in the presence of PES and PES/PAN nanofiber membranes, and the results are presented in Figure 4.17a. A stable MB adsorption capacity was observed within pH range from 3 to 5 for both membranes, while showing an upward trend of adsorption capacity when pH value increased from 5 to 7 and then gradually reached the highest adsorption capacity from 7 to 10. Notably, the adsorption capacity was the maximum yet at neutral pH

provides with an amount of 33.7 mg/g and 364.9 mg/g for PES and PES/PAN, respectively, which is in common agreement with previously published literature (Mohammad and Atassi, 2020a, Yam-Cervantes et al., 2020). At acidic pH, the nanofiber membrane surface is positively charged due to the protonation of functional groups. Hence, electrostatic repulsion occurred between the positively charged membrane surface and cationic MB molecules and ultimately reduced the adsorption uptake. On the contrary, the charged nanofiber membrane surface shows more negative when pH shifts to neutral/alkaline conditions. Importantly, the addition of nitrile groups produced carboxylate groups on the surface of the PES/PAN nanofiber membrane under neutral/alkaline medium by hydrolysis reaction (Pérez-Álvarez et al., 2019). The generation of carboxylate groups yielded more negatively charged on the PES/PAN membrane surface with respect to the pristine PES at higher pH with the resulting generation of an electrostatic attraction with the positively charged MB. In particular, the maximum attraction interaction between membrane and MB appeared at neutral pH, which resulted in an improved adsorption capacity.

Moreover, these phenomena can be further supported by observing zeta potential, as shown in Figure 4.17b. The point of zero charge (pzc) was found at pH 6.3 and 4.8 for PES and PES/PAN nanofiber membrane, respectively. This means that the surface charge of the membranes is positive below pzc and negative above the value of pzc, whereas the negatively charged surface favours the adsorption process through electrostatic attraction, as proven in the experimental analysis. The introduction of hydrolysable PAN with PES, enhanced the overall negative charge of the blended PES/PAN nanofiber membrane (see Figure 4.17b), thus improving the MB adsorption capacity. Interestingly, it was noticed that the adsorption capacity maintained a higher trend even below the pzc, indicating that other driving forces besides electrostatic attraction also influence the adsorption process. This observation further demonstrated that the developed PES/PAN nanofiber membrane is suitable for treating MB containing wastewater in a wide range of pH, this means that no adjustment of pH is necessary during the pre-treatment stages (Lu et al., 2019a).

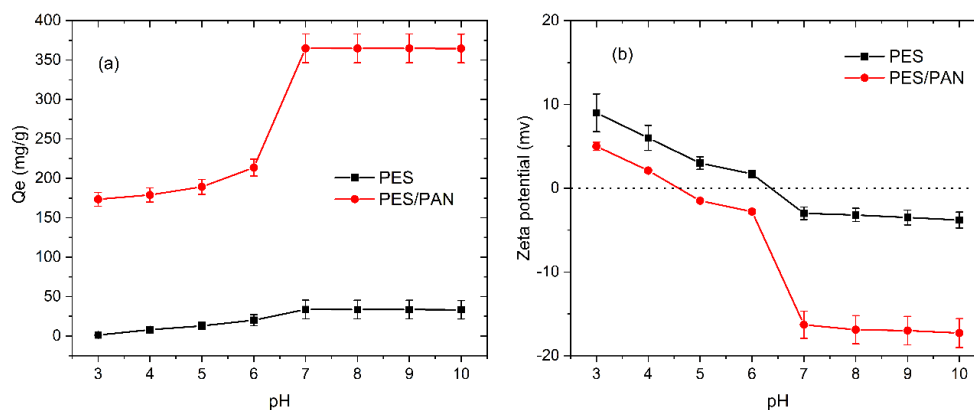


Figure 4.17 Effect of pH on MB adsorption capacity (a) and zeta potential (b) of PES and PES/PAN electrospun nanofiber membranes.

Effect of initial concentration of dye on PES/PAN adsorption capacity

The initial dye concentration indirectly affects dye adsorption capacity by controlling the binding sites of the adsorbent. Therefore, the adsorption capacity was measured at different initial concentration of MB in the ranges 50-1000 $\text{mg}_{\text{MB}}/\text{L}$. As shown in Figure 4.18, it is evident that the initial concentration positively influences the adsorption capacity for both adsorbents. For PES/PAN blended nanofiber membrane, rapid increase of the adsorption capacity was observed (46.0-514.9 mg/g) with an increase in initial concentration from 50 to 400 $\text{mg}_{\text{MB}}/\text{L}$ while further increasing concentration up to 1000 $\text{mg}_{\text{MB}}/\text{L}$, slightly increased the adsorption capacity to 552.5 mg/g . Similarly, the same trend was noticed for the pristine PES nanofiber membrane, but the adsorption capacity was very low in all the MB concentrations, and the maximum capacity of 41.0 mg/g was obtained at 400 $\text{mg}_{\text{MB}}/\text{L}$. In both cases, beyond 400 $\text{mg}_{\text{MB}}/\text{L}$ concentration, a fair adsorption capacity increase means reaching the plateau. This result indicates that adsorption is facilitated by a rise in concentration, which enhances mass transfer and the driving force for MB adsorption. In addition, a large amount of MB molecules are transferred to the solid surface of the nanofiber membrane from the aqueous phase, thereby leading to a higher adsorption capacity (Li et al., 2020a). The higher concentration of MB in solution also affords the swelling of the polymer membrane, facilitating the diffusion of the organic compound in the polymer and thus further uptake of dye by membrane.

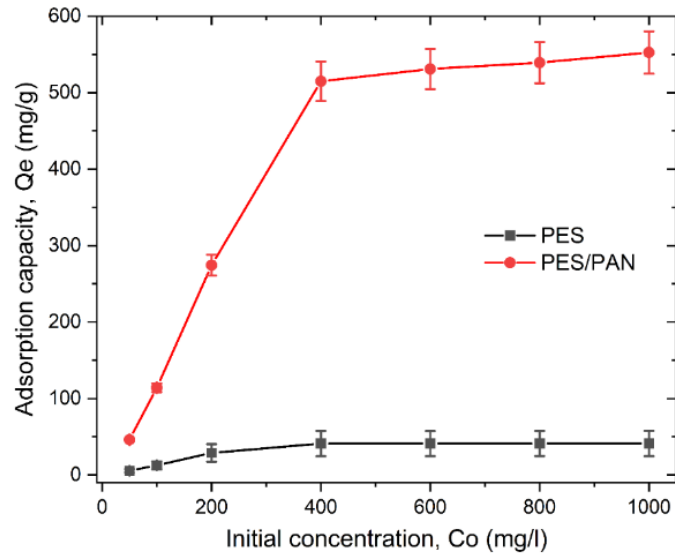


Figure 4.18 Effect of MB concentrations on adsorption capacity of PES and PES/PAN fiber membrane.

Adsorption kinetics

Studies on dye adsorption kinetics provide information on rate constants of the entire adsorption process with respect to the contact time of the dye with the adsorber (Li et al., 2019a). The kinetic behavior of MB adsorption onto the PES and PES/PAN blended nanofiber membranes was investigated and the results presented in Figures 4.19a and b, respectively.

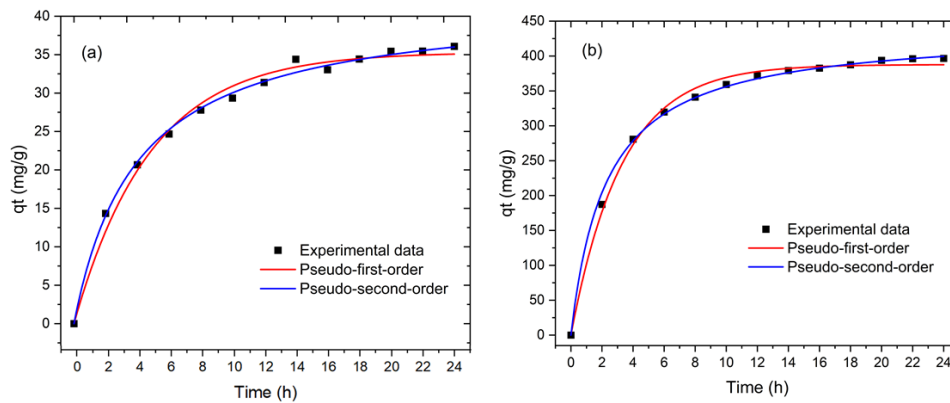


Figure 4.19 Pseudo-first-order kinetic model and pseudo-second-order kinetic model for the MB adsorption on PES (a) and PES/PAN (b).

The rapid adsorption rate was seen at the beginning of the experiment, but it gradually slowed as the period lengthened until it achieved an equilibrium state. The equilibrium for MB adsorption is reached for PES, within 18 h and lasted for 24 h, while 12 h were required for PES/PAN fiber membrane, whereby 75% of MB is adsorbed within 6 h. These results highlight that the incorporation of PAN into PES enhanced the membrane performance with higher adsorption active sites for MB capture.

Moreover, the adsorption kinetics were fitted by nonlinear pseudo-first-order (PFO) and pseudo-second-order (PSO) models (Pervez et al., 2021e). The fitted curves are shown in Figure 4.19 a and b, and the calculated fitted values have been given in Table 4.5. For PES, correlation co-efficiency was somewhat greater for PSO ($R^2=0.9965$) than PFO ($R^2=0.989$). On the contrary, lower correlation co-efficiency was observed for PFO ($R^2=0.9953$) compared to PSO ($R^2=0.997$) in the presence of the PES/PAN blended nanofiber membrane. These results suggest that the PSO kinetic model strongly fit the MB adsorption onto PES and PES/PAN nanofiber membrane, which means that the adsorption process of MB is dominated by the chemisorption mechanism in which charge attraction occurs between adsorbent binding sites and MB molecules (Li et al., 2019c). Previous studies indicated the accurate fitting of MB adsorption with the pseudo-second-order kinetic model. Haider et al. (Haider et al., 2015a) reported the adsorption of MB followed a second-order kinetic model by using ethylenediamine-grafted-polyacrylonitrile electrospun nanofiber membrane. It can readily infer that the current PES/PAN nanofiber membrane exhibits an excellent adsorption performance of MB within a short time, which is favorable for practical implementation.

Table 4.5 Kinetics parameters for MB adsorption by PES and PES/PAN membranes.

Adsorbent	*Pseudo-first order			*Pseudo-second order		
	$Q_t = Q_e(1 - e^{-k_1 t})$			$Q_t = \frac{k_2 Q_e^2 t}{1 + k_2 Q_e t}$		
	K_1 (min^{-1})	q_e (mg/g)	R^2	K_2 (g/mg/min)	q_e (mg/g)	R^2
PES	0.0034	35.3161	0.989	0.0001	41.9531	0.996
PES/PAN	0.3041	387.765	0.995	0.001	487.5860	0.997

* Where q_t (mg/g) represents the adsorption capacity of MB at any time t ; k_1 (min^{-1}) and k_2 (g/mg/min) are the kinetic rate constants

for the pseudo-first order and pseudo-second order models, respectively.

Adsorption isotherms

Adsorption isotherms provide important information on adsorption processes. From this analysis, the relationship between adsorbent/adsorbate equilibrium

concentration is investigated at which maximum adsorption capacity can be identified. Two common non-linear isotherm models, namely the Langmuir and the Freundlich models, were applied to determine the adsorption behaviour. Langmuir fitted model means that the adsorption process was monolayer onto the homogeneous solid adsorbent surface, and there is no evidence that adsorbed MB molecules interact with neighbouring active sites, on the other hand, Freundlich fitted isotherm model followed the multilayer adsorption process onto the heterogeneous solid surface of the adsorbent (López-Luna et al., 2019b). Fitted curves are shown in Figure 4.20, and the isotherms calculated parameters are listed in Table 4.6. Results demonstrate that the adsorption isotherm for both membranes obeyed the Langmuir isotherm model based on the correlation co-efficiency values (R^2), indicating monolayer adsorption associated with the heterogeneous surface of adsorbents (Hossain et al., 2021b, Pervez et al., 2021a). The PES/PAN nanofiber membrane exhibits a maximum adsorption capacity of 1010.10 mg/g, whereas the pristine PES nanofiber membrane showed only the adsorption capacity of 48.00 mg/g. This indicates that the PES/PAN nanofiber membrane significantly enhanced the adsorption capacity of MB, which is integrated with the value of K_L since a higher K_L of the adsorbent determines better adsorption performance at low concentration (Cao et al., 2012a). As shown in Table 4.7, the comparison between our adsorbent and other adsorbents for MB adsorption found that PES/PAN has excellent adsorption capacity noticeably higher than others.

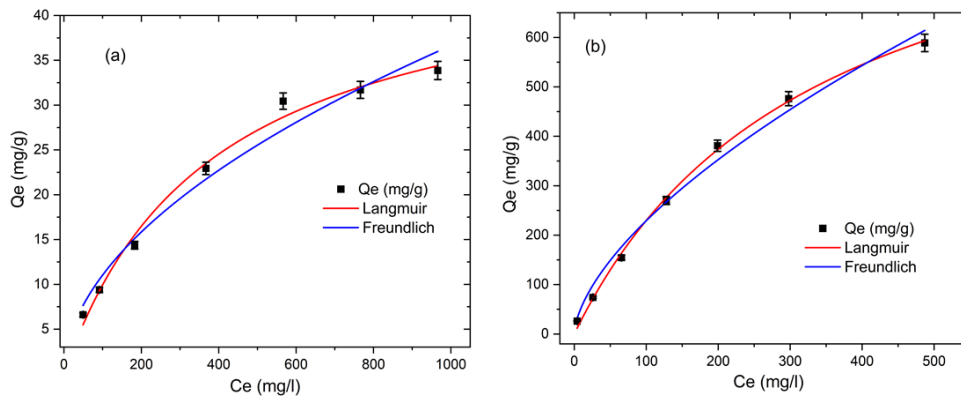


Figure 4.20 The adsorption isotherms of MB by PES (a) and PES/PAN (b) according to Langmuir and Freundlich equations.

Table 4.6 Adsorption isotherms parameters for MB.

Adsorbent	* Langmuir	* Freundlich
	$Q_e = \frac{q_{\max} k_L C_e}{1 + k_L C_e}$	$Q_e = K_F C_e^{1/n}$

4. Development of electrospun nanofiber membrane for food industry wastewater treatment

	q_{\max} (mg/g)	K_L (L/mg)	R^2	K_F (mg/g)	1/n	R^2
PES	48.0076	0.0026	0.9913	1.0012	0.5211	0.9747
PES/PAN	1010.1010	0.0586	0.9983	13.0085	0.6228	0.9881

* Where q_{\max} denotes the maximum adsorption capacity of MB (mg/g); K_L represents the constant of the Langmuir equation, C_e used for the measurement of solution concentration at equilibrium; 1/n highlights the intensity of the adsorption, and K_F indicates the constant of the Freundlich equation.

Table 4.7 Comparison of the MB adsorption capacity with previously reported literature.

Adsorbent	Initial MB conc. (mg/L)	pH	Kinetics	Isotherm	q_{\max} (mg/g)	Ref.
PAN nanofibers	15	8	2nd order	Freundlich	42.0	(Chabalala et al., 2021)
PAN/ β cyclodextrin (β -CD) nanofibers	15	8	2nd order	Freundlich	79.3	(Chabalala et al., 2021)
PAN hard yarn waste/MWCNT-OH nanofibrous	30	10	2nd order	Freundlich	8.0	(Swaminathan et al., 2021)
Functionalized PES nanofibers	500 μ mol/L	6	2nd order	Langmuir	625.0	(Xu et al., 2018c)
Cross-linked PES nanofibers	250 μ mol/L	10	2nd order	Freundlich	478.4	(Chen et al., 2018)
Ethylenediamine (EDA)-grafted polyacrylonitrile (PAN)	400	'	2nd order	Freundlich	94	(Haider et al., 2015a)
Vanadium pentoxide (V_2O_5) nanoparticles/PES	1	10	2nd order	Freundlich	85%	(Homaeigohar et al., 2016b)
Mesoporous carbon nanofibers	40	6	2nd order	Langmuir	119.2	(Li et al., 2016)
PES nanofibers	400	7	2nd order	Langmuir	48.0	Present work
PES/PAN nanofibers	400	7	2nd order	Langmuir	1010.1	Present work

Effect of inorganic anions

Inorganic ions are constantly encountered in industrial wastewater effluents since they have been used as additives in the dye manufacturing process. Consequently, these substances affect the wastewater purification operation, thus it is important to investigate these anions containing MB simulated effluent. Herein, selective anions

such as Cl^- , SO_4^{2-} , HCO_3^- and PO_4^{3-} were used to determine their influence on MB adsorption capacity by the membrane, and the results are presented in Figure 4.21a. As expected, the presence of various inorganic anions inhibited the MB adsorption capacity compared to the case of absence. It was found that Cl^- ion has exhibited a negative effect on MB adsorption behavior by the membrane. This could be explained from the point of competition between MB with foreign ions. Chloride anions compete with the membrane for the coordination to the positive charged dye. On the other hand, SO_4^{2-} and HCO_3^- showed little effect on the MB adsorption capacity by the membrane which may be attributed to a reduced constant of binding of these anions to the MB (Lu et al., 2019b). Interestingly, the addition of PO_4^{3-} enhanced the adsorption capacity because the solution pH value was increased in the presence of hydrogen phosphate ions, which may assist in accelerating the electrostatic interaction between MB and membrane surface, resulting in improved adsorption performance (Ma et al., 2020b).

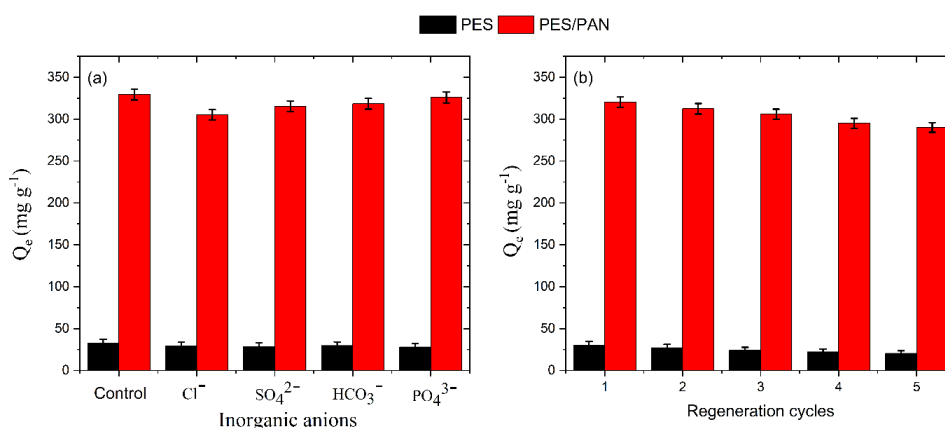


Figure 4.21 (a) Effect of inorganic anions on MB adsorption capacity and (b) recyclability tests by PES and PES/PAN nanofiber membrane, respectively.

Reusability

The produced adsorbent must have shown a strong reusable and regenerable ability to compete with commercially available adsorbents. These features are regarded to be the most important sign of an adsorbent's effectiveness. Therefore, a series of regeneration cycle tests were conducted using PES and PES/PAN nanofiber membrane up to 5 cycles under optimized conditions (Figure 4.21b). It was found that 32% of adsorption capacity was reduced after 5 cycles by PES, while only 0.93% for the PES/PAN nanofiber membrane, this indicates that blended PES/PAN nanofiber has better reusability compared to the original PES nanofiber membrane.

The outstanding performance of the PES/PAN nanofiber membrane is ascribed to the smaller fiber diameter (corresponded to the larger surface area) and higher hydrophilicity. Overall, it can be concluded that the PES/PAN nanofiber membrane developed is an effective adsorbent for real wastewater purification because of their efficacy and great recyclability.

Adsorption mechanism

The adsorption mechanism of MB by the use of the PES/PAN nanofiber membrane was investigated, and its schematic representation diagram is shown in Figure 4.22.

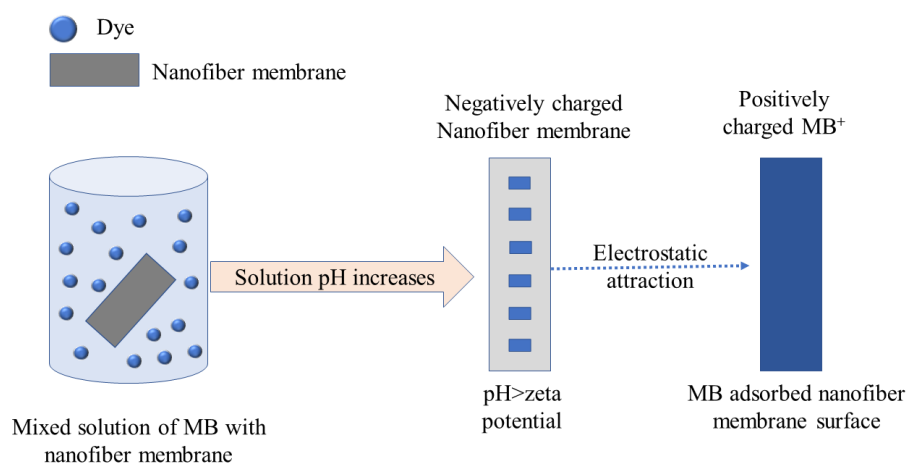


Figure 4.22 Proposed adsorption mechanism of MB in the presence of PES/PAN nanofiber membrane.

It was found that electrostatic attraction was mainly responsible for MB adsorption, which can be clearly stated from the solution pH and membrane surface zeta potential behavior. When solution pH was lower than point of zero charge of the membrane, the surface became positively charged and offered a strong electrostatic repulsion with the cationic dye MB, resulting in a reduced adsorption capacity. On the contrary, when solution pH was higher than point of zero charge, the membrane surface became negatively charged and showed a strong electrostatic interaction with the cation dye MB, thereby leading to an excellent adsorption phenomenon. Importantly, the prepared PES/PAN nanofiber membrane showed superior adsorption capacity at neutral pH, this indicates that the blended membrane surface has a large number of functional groups, which can be deprotonated at higher pH and promote adsorption capacity electrostatically. Besides, hydrogen bonding and π - π interaction may also contribute to the adsorption process to some extent (Sahu

et al., 2020). Moreover, it was found that adsorption capacity was decreased due to inorganic ions presence, which is additional evidence that electrostatic attraction was mainly responsible for MB adsorption by PES/PAN nanofiber membrane.

5. PROCESS INTENSIFICATION OF PRESSURE-DRIVEN MEMBRANE FILTRATION FOR RESOURCE RECOVERY FROM FOOD WASTE

This chapter explains the details of materials and chemicals, experimental setups and analytical methods that have been used to build this research work. This part has been divided into sections for a better understanding of Study I (application of microfiltration and Ultrafiltration for production and recovery of VFAs and Study II (High amount recovery of VFAs using nanofiltration).

5.1 Double-stage membrane-assisted anaerobic digestion process intensification for production and recovery of volatile fatty acids from food waste

5.1.1 Introduction

In recent years, bioconversion of organic waste to a range of value-added products has been identified as one of the best waste management approaches. Food waste (FW) is recognized as a mainstream organic waste candidate for a biorefinery due to its ease of collection, accessibility and enormous generation volume. According to the Food and Agriculture Organization (FAO), about one-third of world food is wasted along the supply chain of food system per year. Specifically, European Union member states are reported to generate around 89 million tons of food waste in 2012 (Braguglia et al., 2018). Moreover, FW is a rich blend of carbohydrates, proteins and lipids that can be used as potential precursors for the production of biochemical and biomaterial through microbial conversion (Lukitawesa et al., 2020, Strazzera et al., 2018).

Traditionally, food waste is managed through landfilling, incineration and composting; however, these processes are either low yielding, not economically feasible or have negative impacts on the environment. Therefore, anaerobic digestion (AD) technology is considered as a feasible medium for converting food waste to valuable resources. It is a cost-effective technology that generates biogas as a renewable energy carrier while treating high moisture and nutrient-rich waste organics (Rajendran et al., 2020). Mainly, four steps are associated with the anaerobic digestion process; hydrolysis, acidogenesis, acetogenesis and methanogenesis, and as a result biogas is generated as the dominant final product. Biogas is utilized for the production of electricity, transport fuel and heat (Holm-Nielsen et al., 2009).

As the market appeal for biogas has been challenged recently, the attention has been shifted towards intermediate products that are more valuable and diverse in terms of application such as volatile fatty acids (VFAs). VFAs are short-chain aliphatic mono-carboxylate compounds that contain two to six carbon chains, such as acetic acid, propionic acid, butyric acid, valeric acid and caproic acid. These acids have a wide range of applications; for example they are considered as chemical precursors for biofuels (Choi et al., 2011) and bioplastic production (Cheah et al., 2019). They are also used extensively in textiles, food, cosmetics and pharmaceutical industry (Lim et al., 2008b). It has been reported that net profit in VFAs production (9.12 USD/m³) is nearly 3-times higher than biogas (3.71 USD/m³) (Khatami et al., 2021, Pervez et al., 2022a). Conventionally, the commercial production of VFAs is mainly obtained from aldehydes and alkenes-based petroleum resources. However, the production of VFAs from bio-based processes, such as anaerobic digestion, is now gaining more attention due to their environmental sustainability benefits.

Nevertheless, anaerobically digested-based VFAs effluent has limited applications in large-scale as the effluent contains various complex substances including unconverted proteins, lipids and outflow microorganisms (Zacharof and Lovitt, 2013a). Extraction of VFAs from these mixed effluents is one of the potentially challenging tasks due to their low concentration. These obstacles can be eliminated either through the increase in the production yield or by the development of a sustainable downstream process that efficiently extract and purify VFAs.

Regarding VFAs production and recovery, AD membrane bioreactors (AD MBR) have gained considerable success in recent years. Although the MBR system has long been employed for wastewater treatment (Pervez et al., 2020b), the potential of using anaerobic digestion technology for VFAs production has not been fully investigated. Among different membrane separation techniques, the submerged or side-stream pressure-driven membrane filtration processes have been recognized as a sustainable and effective method. This effectiveness is due to the possibility of

producing solid-free VFAs solution, low energy demand and small environmental footprint (Aghapour Aktij et al., 2020a). Previous literature has shown that microfiltration (MF) is a suitable method for the recovery of VFAs and nutrients (e.g. $\text{NH}_4^+\text{-N}$ and $\text{PO}_4^{3-}\text{-P}$) from liquid digested effluent. For example, Kim et al. (Kim et al., 2005b) studied the application of a crossflow microfiltration-coupled fermenter system and showed that a significant amount of suspended solids were removed. In that study, over 80% of VFAs were recovered by using MF membranes with different pore sizes. Gerardo et al. (Gerardo et al., 2013) recovered nutrients and metals from anaerobically digested effluent using crossflow microfiltration. Recent studies have also shown that VFAs solutions could be recovered through the *in-situ* immersed microfiltration membranes (Wainaina et al., 2019d). However, it was examined that the MF permeate solution can still contain some foreign substances (microorganisms, particulate matter and macromolecules) that need to be purified prior to further application. Ultrafiltration (UF) is another pressure-driven membrane filtration technique that has been identified as a promising pathway for VFAs purification. Although there are some reports of UF application for VFAs recovery (Longo et al., 2015b, Zacharof et al., 2019), to the authors knowledge, there are no report available in the literature using UF in a sequence with immersed MF membranes for the recovery of VFAs from anaerobically digested effluent of food waste.

In this study, a novel approach was introduced to the process of production, recovery and purification of VFAs from food waste. This approach optimizes AD as it inhibits the production of biogas for VFAs accumulation. It also integrates *in situ* VFAs recovery using immersed MBR coupled with external UF membrane unit. With this goal in mind, at first conditions for maximizing VFAs production through different pH levels were investigated in batch AD. The detected optimum condition was then applied to a semi-continuous immersed MBR system for production and recovery of VFAs effluent on different organic loading rates. The effluent was further put through ultrafiltration to seek the optimum purification approach.

5.1.2 Materials and methods

Substrate and inoculum

The food waste (FW) was used as the substrate and collected from Gryaab AB (wastewater treatment plant) and Renova AB (solid waste treatment plant), and both companies are based in Gothenburg, Sweden. The food waste slurry was prepared from households and retailers based on food waste (diluted with 20% water and screw pressed by a 10mm mesh) obtained from the Gothenburg region municipality

and then refrigerated and stored in a cold room at 4-5 °C before loading into the bioreactors chamber. The detailed characterization data can be found in previous report (Parchami et al., 2020a). The granulated bacteria originated from the full scale up-flow anaerobic sludge blanket reactor of Hammarby Sjöstad, Stockholm, Sweden and used as inoculum for the batch reactors. The setup of fermentation broth was maintained according to the previous study (Wainaina et al., 2020b) and treated as inoculum seed in the semi-continuous membrane bioreactors for VFAs production.

Batch fermentation

Anaerobic batch fermentations assays were set up with the goal of investigating the effect of different initial pH levels on methanogens inhibition and VFAs production and accumulation. In this regard, pH levels of 4, 5, 6, 8, 10 and 12 were experimented. The tests were carried out in 120 mL serum bottles with a working volume of 50 mL. 1 gVS of a substrate and 1 gVS of inoculum were loaded in each bottle and filled up to 50 mL with distilled water. All experiments were conducted in triplicates. Additionally, three reactors were assigned as control, which represented the samples without initial pH adjustment. The pH levels were set accordingly prior to sealing and flushing (3 minutes) the reactors with nitrogen gas to ensure anaerobic conditions. The bottles were incubated in water bath shakers with conditions set to 37°C and 125 rpm. 250 µL gas sample were taken daily in first three days and then every 2 to 3 days of the experiment with a gas-tight syringe (VICI Precision Sampling Inc, USA) to analyze volume and the composition of biogas. On the same sampling days, 1 mL liquid aliquot was taken to be used in VFA analysis. The batch fermentation was carried out for 27 days.

Semi-continuous Immersed Microfiltration Membrane Bioreactor

The immersed membrane bioreactor (iMBR) setup consisted of a 2.5 L bioreactor with a working volume of 2 L, equipped with an immersed flat sheet microfiltration membrane panels. The second-generation Integrated Permeate Channel (IPC) membrane panels were kindly supplied by the Flemish Institute of Technological Research, VITO NV, Belgium, with an effective area of 68.2 cm²/panel and average pore size of 0.3µm. The clean water permeability of the membrane was about 3000–4000 L/h/m²/bar. Hydrophilic polyethersulfone (PES) was the material that constituted the coating of either side of the spacer fabric. Membrane panels were placed inside a spacer box and then submerged inside the reactor (Figure 5.1). To provide mixing, nitrogen sparging was utilized with a nitrogen flow of 1 L/min during fermentation, which was raised to 3 L/min during daily filtration intervals. The flow of the nitrogen was regulated with the help of a gas flowmeter (Dwyer

5. Process Intensification of pressure-driven membrane filtration for resource recovery from
food waste

Instruments, USA). A peristaltic pump was purchased from the Watson Marlow Fluid Technology Group (Wilmington, UK) and connected to the permeate channel. During the experiment, the flow of the permeate was recorded with an Atrato 710-V11-D ultrasonic flowmeter (Titan Enterprises Ltd., United Kingdom) while a pressure transmitter (KELLER, Switzerland) measured the pressure on the permeate line. The reactor was filled with 10 gVS/L of sludge and 1 gVS/L of food waste (FW) and the pH value was set to 6. Following a 10-day batch startup phase, from day 11, a filtration cycle consisting of 4-minute filtration and 1-minute backwash was applied to the reactor. Every day, 200 mL filtrate was withdrawn from the MBR and was replaced with the same volume of FW, followed by pH adjustment to 6. For VFA analysis, samples were taken from the filtrate while TSS and pH samples were taken from the main reactor. Moreover, gas samples were also taken from the system to analyze methane amount. However, these methane amounts were not reported as the values turned out to be lower than the detection limits of the analytical instruments. The starting feeding OLR value was 1 gVS/L, which was then raised to 3 and 6 gVS/L throughout the experiment. When total suspended solid (TSS) value was increased, it resulted in high transmembrane pressure (TMP), therefore chemical cleaning was applied to the system according to Plevri et al. (Plevri et al., 2021). At first, the system was filled with NaOCl (200 ppm) at 45°C for 45 minutes. Afterwards, water was run through the system for 10 minutes, the reactor was filled with H₃PO₄ (1%) and it was cleaned for another 45 minutes. The cleaning ended with the system being run thoroughly with water to get rid of any chemical remains.

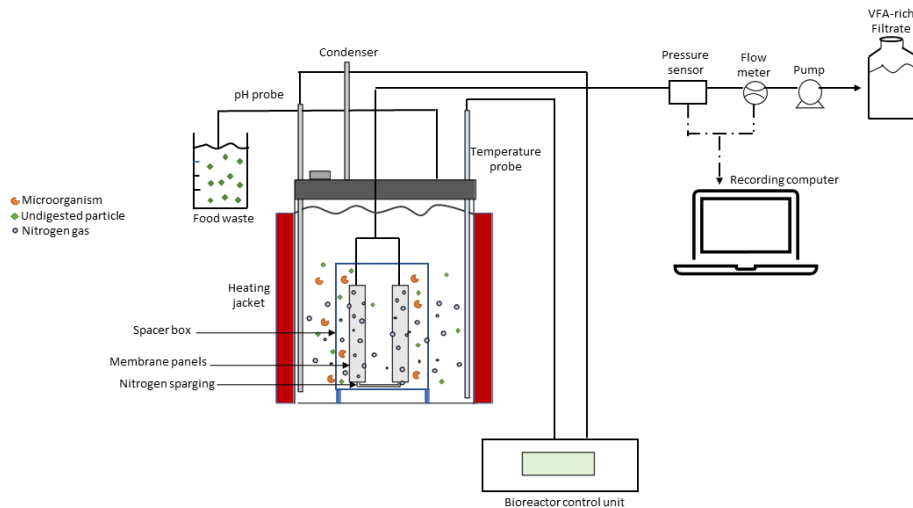


Figure 5.1 Schematic diagram of the semi-continuous immersed microfiltration membrane bioreactor.

Ultrafiltration process

The ultrafiltration experiments were carried out on laboratory scale using LABCELL CF-1 membrane filtration unit (Koch Membrane System, United Kingdom) (Figure 5.2). The filtration system was used in tangential flow filtration mode with an effective membrane surface area of 28 cm², which provided feed-side pressures of up to 6 bar. Two commercial flat sheet ultrafiltration membranes (Microdyn Nadir, Germany) with two different molecular weight cut-offs (MWCO), 50 kDa and 10 kDa, were used for ultrafiltration. The detailed properties of the membranes are presented in Table 5.1.

Table 5.1 Characteristics of used ultrafiltration membranes.

Name	UH050 P	UP010 P
Producer	Microdyn Nadir	Microdyn Nadir
MWCO (kDa)	50	10
Type	flat sheet	flat sheet
Membrane material	hydrophilic	hydrophilic
Membrane chemistry	Polyethersulfone (PES)	Polyethersulfone (PES)
Pure water permeability (LMH/bar)	≥ 85.0 (≥ 3.4)	≥ 50.0 (≥ 2.0)
Thickness (μm)	210 – 250	210 – 250
pH Range	0.0 – 14.0	0.0 – 14.0
Chlorine Tolerance	200 ppm (sanitization) at pH ≥ 10.5	200 ppm (sanitization) at pH ≥ 10.5

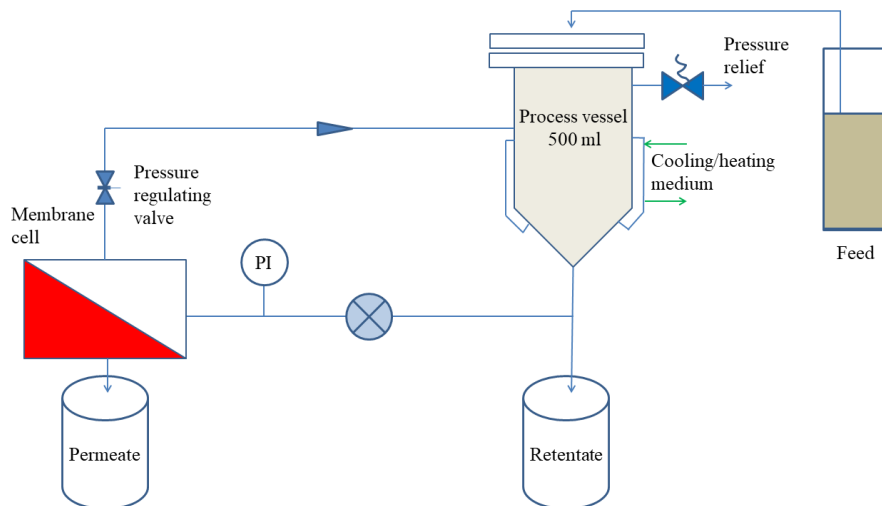


Figure 5.2 Schematic diagram of the ultrafiltration unit.

The UF unit's feed solution was composed of a mixture of FW AD effluent from different permeate recovery intervals. Before starting the experiment, flat sheet membranes were cut into the required shape and were placed in warm tap water for 30 minutes. This was done to remove the glycerol from the membrane surface and pores as recommended by the supplier. The filtration machine unit was cleaned twice by Milli-Q water and NaOH (pH 10) subsequently prior to each experiment, before and after membrane installation. A thermostatic water-recirculating water bath was used to control the filtration temperature ranges between 20-21°C and 37°C through a water jacket connection. About 300 mL feed solution was loaded to the feed container for each experiment. A constant feed-side pressure of 5 bar was provided by the pump installed on the filtration unit throughout filtration. Two pH levels, 4 (pre-set) and 5.4 (as received), were used during ultrafiltration. In each test, 250 mL of the initial feed was collected as permeate and 50 mL ended up as retentate on the feed-side. The permeate flux was estimated by recording the permeate weight in 2-minute intervals.

Analytical methods

For gas (CH₄, CO₂ and H₂) analysis, gas chromatograph (Clarus 550 Perkin Elmer, Norwalk, CT, USA) with a packed column (CarboxenTM 1000, 6'×1.8" OD, 60/80 Mesh, Supelco, Shelton, CT, USA) and a thermal conductivity detector (Perkin-Elmer, Norwalk, CT, USA) was used. The injection temperature was set at 200°C. The carrier gas was N₂ with a flow rate of 40 mL/min (75°C). For analysis of VFAs, liquid samples of 1 mL were mixed with 200 µL of an acid mix (mixture of orthophosphoric and formic acids with volume ratio of 3:1). The samples were then centrifuged for 5 minutes at 12500×g, and the supernatant was syringe filtered. From the filtered part, 250 µL was transferred into glass vials and topped with butanol (internal standard) and 500 µL of distilled water. VFAs analysis was then performed with GC.

Total solids (TS), total suspended solids (TSS), volatile solids (VS), volatile suspended solids (VSS) and dissolved solids (DS) content were evaluated in accordance with the APHA 2005 Standard Methods (Federation and Association, 2005). Test kits were used to measure total chemical oxygen demand (tCOD), soluble chemical oxygen demand (sCOD) (CSB 15000 test kit), ammonium nitrogen (NH₄⁺-N, Ammonium 100 test kit), orthophosphate (PO₄³⁻-P, Phosphate 45 ortho) and total Kjeldahl nitrogen (TKN 16). These kits were purchased from MACHEREY-NAGEL GmbH & Co. KG (Germany) and the analytical data were processed through the use of Nanocolor 500D photometer. The color change percentages of feed, permeate, and retentate samples were measured by a UV-Vis

spectrophotometer under the range of wavelength between 200-600 nm. The membrane permeates flux was obtained according to Eq.1.

$$J_{permeate} = \left(\frac{Q_f}{A_m} \right) = \left(\frac{dv}{dt} \right) \quad (1)$$

where v represent the volume, t is time (h), membrane area (A_m) and Q_f is the volumetric flow rate (L/h).

5.1.3 Results and Discussion

Evaluation of VFAs production from food waste

In order to find optimum process conditions for the anaerobic digestion of food waste for maximum production and accumulation of VFAs, batch AD assays with different initial pH were performed. As pH is one of the main factors affecting acidogenic fermentation of VFAs (Wainaina et al., 2019b), AD was conducted at different initial pH. The results of changes in the VFAs concentration and distribution were observed. Overall, the VFA production peaked on day eight in most of the experimented pH values. The highest VFA production value (13.81 g/L) was recorded for the treatment with initial pH 6 on day 8, with pH 8 and pH 10 (12.75 g/L) in the next place. After the peak value on day 8, VFA production started to decrease in the following days. None of the pH extremes (pH 4 and 12) resulted in a high VFAs production performance; the production in said pHs remained between 2 to 8 g/L. In confirmation with other literature, this can be explained by the inhibitory effect of highly alkaline or acidic condition on acidogenic bacteria (Wainaina et al., 2020b). In terms of VFA profiles, acetic acid was the dominant VFA in most of the pH values; on higher pH such as 10 and 12, the highest percentages of acetic acid were observed (70-80% and 60-65%, respectively), while on lower pH the percentages ranged around 20-60% (pH 4), 30-45% (pH 5), 25-50% (pH 6) and 10-55% (pH 8). These results are in line with the work of (Cheah et al., 2019, Zhang et al., 2005a), both in which pH of 9 and 10 was reported to have the highest percentage for acetic acid. The exceptions were the pH 5 and 6, in which butyric acid was dominant in the VFAs distribution.

This domination of butyric acid domination in pH 5-6 can also be observed in the work of Ren et al. (2007) and Wang et al. (2014a). Furthermore, in the work of Lukitawesa et al. (2020), this dominance was explained with the pathways related to acidogenesis process; as a result of Embden-Meyerhoff and pentose phosphate pathways, butyrate is the main product in both of the pH values. It can also be observed that in increased pH, the percentages of butyric acid decreases.

As the accumulation of VFAs in a batch AD system is in direct relation with methane production inhibition, besides VFA analysis, daily gas samples were also taken from the batch reactors and analyzed to determine H₂, CH₄ and CO₂ production. According to the literature, production of VFAs is observed during the acidogenesis stage along with hydrogen, therefore, H₂ production in significant amounts can indicate increased VFAs production (Wainaina et al., 2019d). As it can be seen in the results presented in Figure 5.3, the increase in H₂ production is accompanied by higher VFAs generation.

As seen in Figure 5.3, the highest point of H₂ production was reached on around day 3 for pH 5 (150 NmL) and 6 (100 NmL), which correlates with the highest VFA production levels at mentioned pH values. While relatively low (50 NmL) H₂ production was observed for pH 4, when the initial pH value is increased to 10 or 12, the lowest values were reported (below 25 NmL). This can be explained by higher pH values being suboptimal for bacteria that produce hydrogen, thus resulting in decreased production (Zhao et al., 2017). Regarding CH₄ production, low production levels are observed until day 8. Inhibiting methanogens to promote VFAs production was one of the goals of this study and this was ensured by making alternations in the initial treatment pH. For methanogens, the optimum pH varies from 6.5 to 7.2 (Yin et al., 2021a), therefore, as expected, the reactors with pH values lower or higher than this range produced low to no methane: for pH 5, CH₄ production stayed below 50 NmL over the course of 20 days while for pH 12, it did not even reach 25 NmL. The pH levels were only adjusted at the beginning of the experiment and were not controlled throughout the process. Because of this initial control, as VFAs production occurred, the pH went through alternations. This led to more suitable conditions for methanogenesis after day 8; reaching 270 NmL at day 27 for pH 8, followed by 200 NmL for pH 10. CO₂ production among different pHs generally followed a similar pattern and stayed below 200 NmL, pH 8 being the level where the most CO₂ was produced. Similarly to H₂ and CH₄, CO₂ production was also the lowest pH 12, stating that this pH is not suitable for none of the producing microorganisms. The pH of the AD medium was also measured at the end of the fermentation period (day 27). Overall, in all treatments, other than pH 12, the final pH level was around pH 6. The drastic change in the pH values of treatments starting at 8 and 10 can be explained as the result of an increase in the acidity of the medium due to VFA generation.

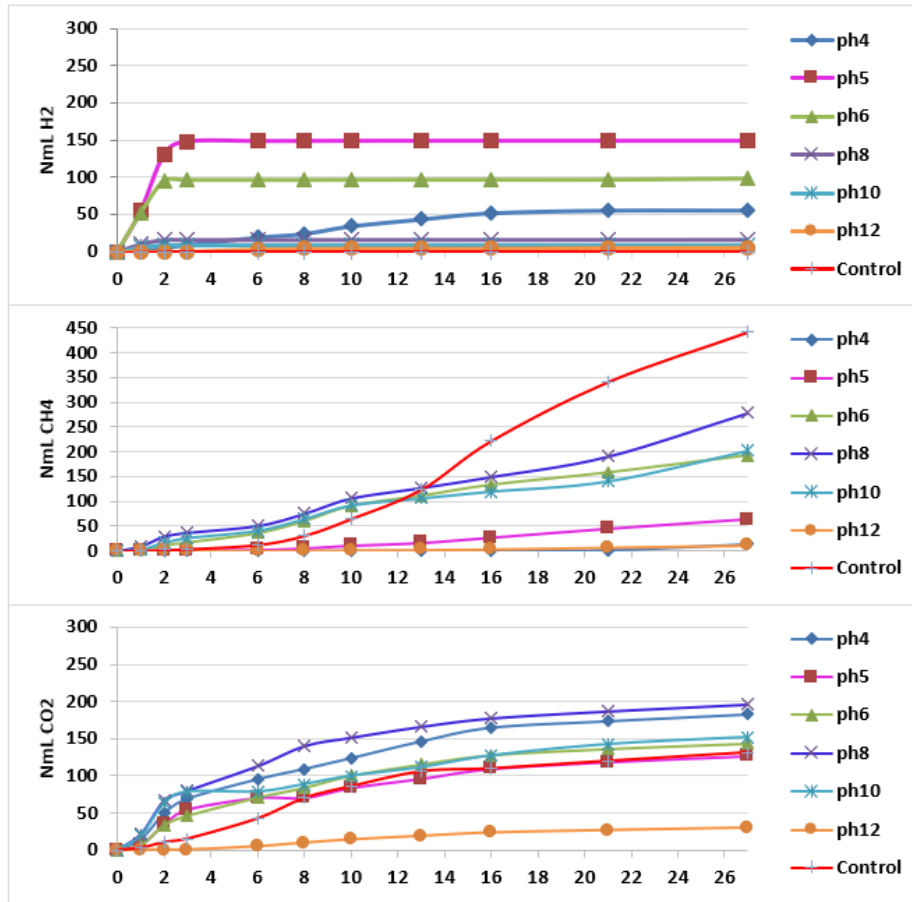


Figure 5.3 Changes in the total volume of H₂, CH₄ and CO₂ during anaerobic digestion of food waste at different pH values.

MBR-assisted VFAs production and recovery

Based on the batch results, the optimal AD condition for the production of VFAs from food waste was selected. This condition was applied in a semi-continuous fermentation process in an iMBR for the production and *in situ* recovery of VFAs. In this regard, the pH of the iMBR medium was adjusted to 6 once a day, while AD and filtration were conducted for 98 days at three different OLRs. The profile of changes in VFAs production and distribution, and alternations in daily pH are presented in Figure 5.4.

Conditions of the iMBR were determined based on previous screening tests (Mahboubi et al., 2020). The bioreactor was initially loaded with a food waste

medium containing 10 gVS/L. The MBR was running in batch mode for the first ten days of the experiment to assist acclimatization (in this period, no feeding was conducted). By the end of this period (day 10), the total VFAs concentration in the bioreactor reached 1.8 g/L. Starting from day 11, the membrane bioreactor was transitioned into semi-continuous mode at an initial OLR of 1 gVS/L.d. From day 11 to 32, total VFAs production ranged between 1.2 to 1.8 g/L. As OLR 1 proved inefficient to give rise to VFAs production, after two HRTs, from day 32 the OLR was raised three-times to 3 gVS/L.d. Based on the fluctuations observed in the pH of the medium throughout a 24 h cycle, on day 43, 4 g of 2-bromoethanesulfonic acid (BES) was added to the medium to ensure methane inhibition. This was followed by a rapid increase in VFA production, peaking at 8.2 g/L on day 56 (overall average around 6.4 g/L), which is 3.5-times the highest value reached before the addition of BES. After observing a stabilization and then decrease over the course of ten days, the OLR was raised to 6 gVS/L.d, on day 68, which boosted VFAs accumulation (up to 14 g/L), peaking at 16 g/L on day 90.

VFAs yields were also determined for every OLR in the period of system stability. The yield values ranged between 0.1 gVFA/gVS_{added} and 0.2 gVFA/gVS_{added}, through different OLRs, with the highest value achieved by day 51 under OLR 3 gVS/L.d. In a similar work conducted by Parchami et al. (2020a) with the OLR of 0.2 gVS/L.day, as a consequence of good mixing (mass transfer), low loading high substrate degradability, the yields averaged 0.38 gVFA/gVS_{added}. Another similar work was performed by Wainaina et al. (2019d) with the same pH and an alike setup but with OLRs of 2 and 4 gVS/L.d obtained VFA yield of 0.54 gVFA/gVS_{added}. Comparatively the achieved yield values in this study can be considered low, which can be the results of poor mixing and mass transfer related issues in a submerged membrane bioreactor where the medium is only being agitated through gas sparging through membrane panel inbuilt diffusers. These mixing imperfections were more pronounced at higher OLRs. Besides mixing problems, a high concentration of undigested organics leads to an increase in TSS and viscosity levels (Figure 5.4). Especially after raising the OLR to 6 gVS/L.d, the TSS levels ranged from 30 to 45 g/L, which is considered extremely high for an immersed membrane bioreactor. Besides, the expectation of an increasing trend of yields following the increase of OLR was not observed. Resembling situation was also reported by Jomnonkhaow et al. (2021b), which was described as a result of highly viscous fermentation broth (Lim et al., 2008a) and high solid rates having a negative effect on mass transfer between the organic substrates and microbes (Wainaina et al., 2020d).

VFAs distributions varied through the course of the experiment. Overall, in the experiment, butyric acid was the dominant VFA (20-70%, with concentrations

varying from 0.1 to 7.6 gVFA/gVS_{added}). The second notable dominance was by acetic acid with 15-55% (0.1–4 gVFA/gVS_{added}). These were followed up by propionic acid (5-40%, 0.1 to 0.8 gVFA/gVS_{added}) and caproic acid (5-25%, 0.05 to 3.2 gVFA/gVS_{added}). When investigated based on the stages of the experiment, acetic acid was the dominant acid (50-100%) in the startup phase. Butyric (30-35%) and propionic acids (5-10%) appeared in the composition from day 4. A similar profile, where acetic acid formed 50% of the total VFA produced, was observed till day 14, which was the point isovaleric, caproic and valeric acids were also detected in the system. However, the addition of BES to the media induced a metabolic shift in VFAs profile; propionic acid, which was one of the dominant VFAs, gradually decreased from forming 40% in day 43, to below 5% by day 68. A similar result was observed in the work of Murali et al. (2021) where as a result of BES addition, propionic acid production went down. This occurrence was justified as a consequence of using chemical inhibitors of methanogenesis leading [H] (metabolic hydrogen) into different [H] sinks like propionate production, meaning that this addition caused prioritization of other processes. Acetic acid was also mostly dominant after the addition of BES. This is directly related to methane inhibition with BES; when methanogenesis is inhibited, acetate is not utilized (Zinder et al., 1984), therefore its concentration in the reactor increases.

Changes in the COD and ammonium content of the MBR at different OLRs is presented in Table 5.2. According to Liu et al. (2008), the variations in the C/N ratio can be a sign of the dominance of certain group of microorganisms; for example, a high C/N ratio is linked with carbohydrate-rich substrates, which are reported to be advantageous environments for butyric acid producing bacteria. This information is in line with the results obtained in the process; for ratios above 40%, butyric acid is the dominant acid in the composition (with the exception of day 51 with a ratio of 74.13). In this regard, Liu et al. (2008) present that the fraction of butyric acid increased to 32% with the C/N ratio going up to 30 from 5. Similarly, in the AD MBR, the percentage of butyric acid doubled when the C/N ratio increased from 30 to 59.

Table 5.2 C/N ratios of days from different OLR values.

Day	C/N Ratio
35	30.06
51	74.13
61	40.47
72	81.25
85	66.66
96	59.04

5. Process Intensification of pressure-driven membrane filtration for resource recovery from food waste

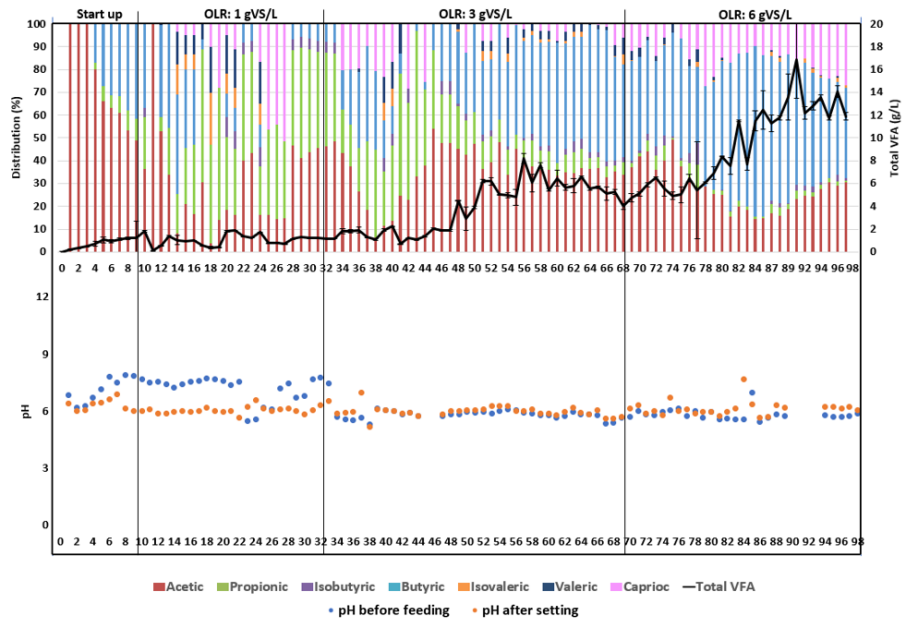


Figure 5.4 The profile of VFAs concentration and distribution and changes in the medium pH throughout the AD MBR experiment.

3.3 MBR filtration performance

One of the purposes of this study was to obtain a setup where *in situ* recovery of VFAs was possible with high efficiency for longer periods of time. This was achieved as VFAs were recovered semi-continuously with the aid of the iMBR with a HRT of 10 days. The experiment continued for a matter of 97 days with a starting flux of 10.5 liter per m²/h (LHM). Overall, it can be claimed that the membrane performed decently until day 58, at that point it was handling 16.6 g TSS/L (Figure 5.5). The TSS of the system till this point can be considered high as in literature values of 8 to 15 g/L are observed as the TSS operation range for water treatment systems with iMBR (Iorhemen et al., 2016). Furthermore, from the start of the experiment till day 20, stable and very low TMP values of 6-10 mbar were observed. Filtration issues surfaced from day 30 as the effects of fouling and changes in the membrane surface condition became more apparent (TMP of 20 mbar). In order to alleviate fouling, chemical cleaning was applied on day 32. However, due to the characteristics of the media (over 10 g/L TSS), TMP increase resumed from day 35. A similar situation of short-lived TMP drop was observed in the work of Veral et al. (Veral et al., 2020) as well; this was due to only “offline physical cleaning” being applied to the system which lead to the foulants still remaining in the reactor. By day 84, as the TSS content reached 45 g/L, the membrane was excessively fouled, and TMP reached 500 mbar. This complies with the findings of Sambusiti et al. (Sambusiti et al., 2020) and Jomnonkhaow et al. (Jomnonkhaow et al., 2021b). It is discussed that increased TMP values are the fault of high TSS. This high value is due to difficulties in removal of other developments like biofilm or biopolymer deposition only with backwashing and gas sparging.

This dramatic rise in TMP levels might be due to not only the deposition of particulate matter on the membrane surface but also the compaction of the cake layer. This layer hindered easy convection through membrane pores and caused extensive pressure drop through the cake layer. Fouling increases membrane hydraulic resistance and eventually the TMP (Mahboubi et al., 2020). One of the biggest goals of the experiment was to challenge the iMBR system to its filtration potential limit at high TSS and OLRs. Overall, this goal was achieved as the system functioned over the course of 3 months. The problems only arose when OLR was pushed to limits where bioconversion requirements were not favored by filtration performance.

5. Process Intensification of pressure-driven membrane filtration for resource recovery from food waste

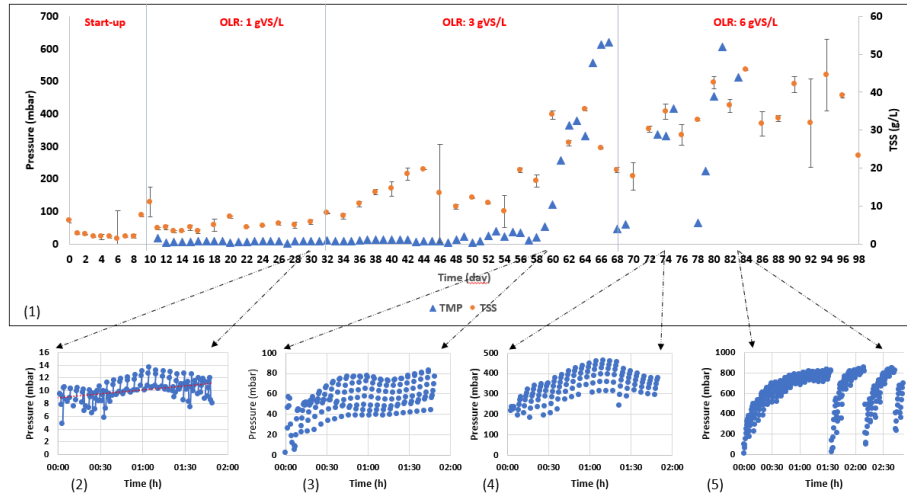


Figure 5.5 1) The changes in the TMP and TSS values throughout the experiment with highlights of 2) day 30 3) day 59 4) day 73 5) day 83 representing different stages of fermentation and filtration.

Ultrafiltration of AD VFA effluent

Changes in the physicochemical characteristics of VFAs effluent by ultrafiltration

In Table 5.3 and 5.4, the obtained physicochemical parameters after ultrafiltration are listed. As expected, the removal percentages of solids/particle were significantly higher in each UF filtration run. It was noticed that at mesophilic temperatures, the data corresponding to pH 5.4 exhibited better performance than pH 4 for both membranes (Table 5.3). However, the removal percentage was higher for 50 kDa with 86.12% (3.03 to 0.42 g/L) of TS, DS of 82.8% (2.33 to 0.4 g/L) than 10 kDa, with the removal rate for TS of 65.6% (3.03 to 1.04 g/L) and DS of 57.9% (2.33 to 0.98 g/L). These outcomes are in agreement with previous reports where the higher pH is more suitable for solids removal in ultrafiltration (Fouzia et al., 2015). On the other hand, at room temperature, the removal rate was higher for pH 4 compared to pH 5.4 for both membranes (Table 5.4). It was observed that the removal percentage was higher for 10 kDa with 80.2% of TS, DS of 80.2% than 50 kDa, with the removal rate for TS of 61.9% and DS of 61.8%. The phenomena could be ascribed to the particles and metabolites from anaerobic digestion being generally negatively charged and membrane becoming positively charged at low pH. Therefore, an electrostatic attraction occurs. This attraction allows particles to pass through the pores, resulting in higher removal rate at pH 4 in comparison to 5.4. Even with membranes of smaller molecular cut-off size, this occurrence is possible (Mahmoud et al., 2003b).

Regarding COD concentrations, the removal percentages were increased at higher pH; for example, at pH 4, 3.7% of TCOD and 6.1% of SCOD were removed while at pH 5.4, this removal rate was 3-times and 2-times higher, respectively (Table 5.3). Previous studies reported that hydroxide ion concentration increases at higher pH and this results in a higher generation of hydroxyl free radicals besides contributing to greater COD removal percentages (Aziz and Kasongo, 2021b). However, in some cases, pH 4 shows a greater COD removal than pH 5.4. As shown in Table 3, the removal percentage of SCOD by the 10 kDa membrane at pH 5.4 was 16.0%, while the value increased to 20.9% for pH 4. Besides, at room temperature, the removal percentage of TCOD by the 50 kDa membrane was higher at pH 4 (Table 5.4). This could be due to the positive surface charge at low pH and influences on COD removal rate (Chan et al., 2007).

Regarding the removal of $\text{NH}_4^+\text{-N}$ from the effluent, the removal percentage increased more than 6-times when the pH was increased from 4 to 5.4. (Table 5.3). The same trend was also recorded when the filtration was conducted at room temperature using both membranes (Table 4). This increment could be attributed to the conversion of ammonium ions to ammonia gas at higher pH (Mohammed-Nour et al., 2019a). It can be seen that pH adjustment accelerates ammonia removal performance, which is related to the deprotonation of carboxylic groups on the tight membranes in the ultrafiltration process (Chu et al., 2017a). The removal of ammonium from VFAs effluents is a great opportunity for VFAs solutions generated from organic waste as potential carbon sources for the denitrification of wastewater. During UF experiments, high concentration of phosphate retained in the concentrate while the permeate was poor in phosphate (Table 5.3 and 5.4). This presents a high recovery percentage for phosphorus. At mesophilic temperature, the P removal efficiency was around 16.8% for 10 kDa (pH 5.4), while 10.0% removal was reached when the 50 kDa membrane was used at the same pH value. This could be a result of the generation of electrostatic attraction between positively surface charged membrane and negatively charged phosphate ions at lower pH, which leads to a high recovery efficiency of P. However, a slightly higher removal efficiency was achieved with the membrane with the bigger MWCO at pH 4 in comparison to pH 5.4 at room temperature. This may be due to the solubilization of phosphorous.

As expected, during treatments, the nitrogen content (in form of TKN) retained by the UF membrane has increased as the pH decreased (Table 5.3 and 5.4). This could be due to the fact that pH 4, which is a value that is close to the isoelectric point of proteins and causes protein precipitation which enhances the removal efficiency. In this regard, the removal percentages are higher at room temperature as a result of the alternations in mass transfer through the membrane pores by temperature. Moreover, the UV-vis absorbance spectra clearly shows that the retentate solutions is intensified in color compared to the feed stock solution while the permeate is rather fully transparent (Figure 5.6 A and B).

Table 5.3 Physicochemical properties of microfiltered and ultrafiltered streams (Temperature 37°C, Pressure=5 bar).

Parameters	Feed	50 kDa						10 kDa											
		pH 5.4			pH 4			pH 5.4			pH 4								
		Retentate	Permeate	Retentate	Permeate	Retentate	Permeate	Retentate	Permeate	Retentate	Permeate	Retentate	Permeate						
TS (g/L)	3.03 ± 0.57	2.54 ± 0.22	0.42 ± 0.05	3.28 ± 0.08	1.50 ± 0.16	3.07 ± 0.15	1.04 ± 0.19	5.37 ± 1.28	1.84 ± 0.08	0.70 ± 0.36	0.14 ± 0.08	0.02 ± 0.00	0.31 ± 0.04	0.06 ± 0.02	0.24 ± 0.14	0.06 ± 0.05	0.23 ± 0.09	0.10 ± 0.02	
TSS (g/L)	2.33 ± 0.21	2.40 ± 0.31	0.4 ± 0.02	2.97 ± 0.04	1.44 ± 0.19	2.83 ± 0.29	0.98 ± 0.25	5.14 ± 1.38	1.74 ± 0.11	2.57 ± 1.51	1.05 ± 0.32	0.63 ± 0.80	1.45 ± 0.24	0.67 ± 0.43	1.79 ± 0.07	0.76 ± 0.31	1.88 ± 0.14	1.14 ± 0.59	
VS (g/L)	1.35 ± 0.38	0.61 ± 0.01	0.52 ± 0.28	0.70 ± 0.05	0.63 ± 0.04	0.69 ± 0.21	0.63 ± 0.04	0.79 ± 0.12	0.66 ± 0.19	4.0 ± 0.00	4.45 ± 0.07	3.55 ± 0.07	4.45 ± 0.07	3.85 ± 0.07	5.10 ± 0.14	3.45 ± 0.07	4.35 ± 0.07	3.95 ± 0.07	
TCOD (g/L)	4.05 ± 0.07	4.45 ± 0.07	3.55 ± 0.07	4.20 ± 0.14	3.80 ± 0.14	5.00 ± 0.28	3.40 ± 0.00	4.60 ± 0.28	3.20 ± 0.84	1.75 ± 0.70	185 ± 0.70	170 ± 1.41	85 ± 0.70	75 ± 0.70	180 ± 0.00	150 ± 0.00	280 ± 1.41	165 ± 2.12	
NH ⁴⁺ -N (mg/L)	77 ± 0.70	80.25 ± 0.35	69.25 ± 0.49	89.25 ± 0.21	75.25 ± 0.07	93 ± 0.70	64 ± 0.00	116.5 ± 2.26	75.5 ± 0.14	16.8 ± 0.42	4.35 ± 0.35	12.45 ± 0.07	6.6 ± 0.14	10.2 ± 0.28	4.5 ± 0.98	12.3 ± 0.56	5.85 ± 0.77	10.95 ± 0.35	
PO ₄ ³⁻ -P (mg/L)																			
TKN (mg/L)																			

5. Process intensification of pressure-driven membrane filtration for resource recovery from
food waste

Table 5.4 Physicochemical properties of microfiltered and ultrafiltered streams (Room temperature, Pressure=5 bar).

Parameters	50 kDa						10 kDa					
	pH (5.4)			pH (4)			pH (5.4)			pH (4)		
	Retentate	Permeate	Retentate	Permeate	Retentate	Permeate	Retentate	Permeate	Retentate	Permeate	Retentate	Permeate
TS (g/L)	6.72 ± 1.07	6.07 ± 0.12	3.31 ± 0.83	6.30 ± 0.33	2.56 ± 0.05	6.73 ± 0.24	2.81 ± 1.03	6.95 ± 0.94	1.33 ± 0.60	0.02 ± 0.00	1.57 ± 1.93	0.75 ± 0.15
TSS (g/L)	0.08 ± 0.02	0.17 ± 0.01	0.04 ± 0.02	0.31 ± 0.24	0.03 ± 0.01	5.16 ± 1.69	0.05 ± 0.01	6.20 ± 0.79	1.31 ± 0.60	0.02 ± 0.00	5.16 ± 1.69	0.75 ± 0.15
DS (g/L)	6.64 ± 1.04	5.90 ± 0.11	3.27 ± 0.80	5.99 ± 0.09	2.53 ± 0.04	4.00 ± 0.08	2.76 ± 1.01	2.97 ± 0.72	0.84 ± 0.62	0.02 ± 0.00	4.00 ± 0.08	0.85 ± 0.97
VS (g/L)	4.26 ± 1.10	3.56 ± 0.08	1.16 ± 0.84	2.35 ± 0.29	0.39 ± 0.38	0.63 ± 0.43	0.85 ± 0.97	0.56 ± 0.08	0.50 ± 0.50	0.02 ± 0.00	0.63 ± 0.43	0.56 ± 0.08
VSS (g/L)	0.57 ± 0.04	0.65 ± 0.04	0.54 ± 0.08	0.62 ± 0.08	0.42 ± 0.02	14 ± 0.28	0.56 ± 0.50	9.95 ± 0.63	9.15 ± 1.34	0.02 ± 0.00	14 ± 0.28	11.65 ± 0.35
TCOD (g/L)	12.65 ± 0.21	13.05 ± 0.21	11.4 ± 0.56	12.30 ± 0.70	11.15 ± 0.49	14.05 ± 0.63	11.65 ± 0.35	9.70 ± 1.27	10 ± 0.42	0.02 ± 0.00	14.05 ± 0.63	11.15 ± 0.07
SCOD (g/L)	12.4 ± 0.14	12.7 ± 0.28	11.05 ± 0.63	12.4 ± 0.70	11.05 ± 0.07	330 ± 1.41	235 ± 0.70	290 ± 1.41	255 ± 0.70	0.02 ± 0.00	330 ± 1.41	235 ± 0.70
NH ⁴⁺ -N (mg/L)	315 ± 0.07	280 ± 0.00	240 ± 2.82	280 ± 0.70	230 ± 1.41	85.50 ± 0.28	65 ± 1.27	91.75 ± 1.06	69.5 ± 2.40	0.02 ± 0.00	85.50 ± 0.28	65 ± 1.27
PO ₄ ³⁻ -P (mg/L)	80.75 ± 1.48	81.75 ± 0.63	70.50 ± 0.42	91.75 ± 1.06	74 ± 0.84	5.55 ± 0.91	12.6 ± 0.70	10.05 ± 0.07	8.1 ± 0.14	0.02 ± 0.00	5.55 ± 0.91	12.6 ± 0.70
TKN (mg/L)	18.15 ± 0.21	4.65 ± 0.35	13.5 ± 0.56	7.5 ± 0.14	10.65 ± 0.35					0.02 ± 0.00		

5. Process intensification of pressure-driven membrane filtration for resource recovery
from food waste

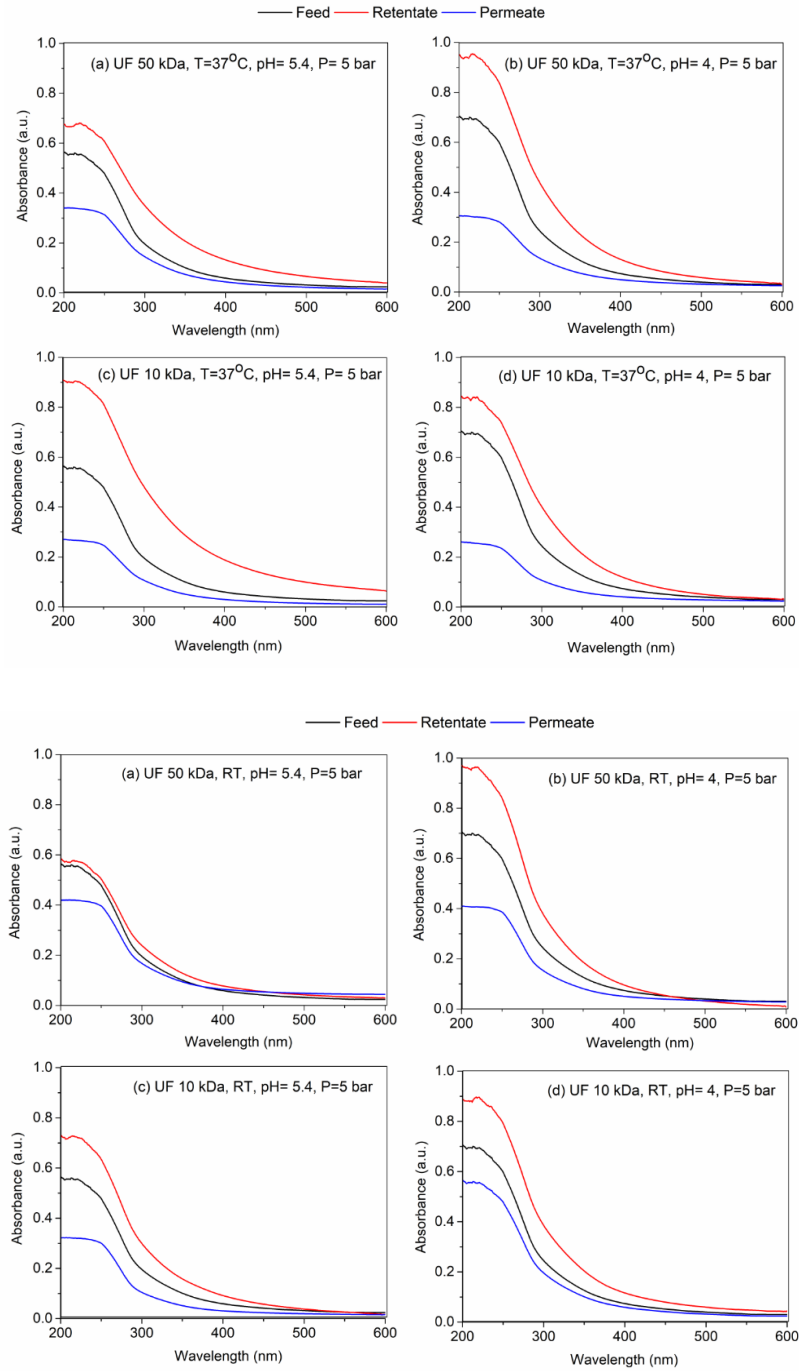


Figure 5.6 UV-Vis spectra of feed (F), permeate (P) and retentate (R) upon ultrafiltration (Temperature 37°C, Pressure=5 bar) (A) and (Room temperature, Pressure=5 bar) (B).

Regarding the effect of UF on VFAs composition and concentration, it can be seen in Figure 5.7 A and B that the employed membranes are permeable to VFAs. However, marginal decrease in the VFAs content of the permeate compared to the feed influent was observed. The changes in the pH and the reduction of the MWCO to 10 kDa is assumed as the cause of this occurrence. The minimal interaction between the favorable compounds such as VFAs and the UF membrane is favorable as it reduces the loss of value-added products in the effluent during purification.

On the other hand, the pH of the solution has an important role in accumulating VFAs in pressure-driven membrane filtration as it affects retention performances (Zhu et al., 2021c). As noticed, the concentration of VFAs in feed, retentate, and permeate solutions were slightly changed with changes in the pH. Higher retentate VFAs concentrations were recorded in pH 4 (in both conditions presented in Figure 5.7 A and B); 2.42 g/L and 5.82 g/L of total VFAs using 50 kDa membrane. However, as 10 kDa membrane was used at pH 5.4, the total VFAs concentration in the retentate was recorded as 3.44 g/L and 6.58 g/L. The achieved retention concentrations could be explained by the size and charge effect. At pH 4, the retention behavior was circulated by the size effect: VFAs molecules were uncharged (or negative) at low pH and these can easily passed through the surface of a positively charged membrane. Alternatively, at pH 5.4, the VFAs compounds and membrane surface are charged, whose effect dominates the retention phenomenon (Bruni et al., 2021). At higher pH (5 and above), VFAs molecules are in a dissociated state that is negatively charged. Therefore, the negatively charged membrane tends to reject negatively charged compounds because of the electrostatic repulsion effect, resulting in a higher retention amount. These results are in agreement with published literature (Da Ros et al., 2020a). In addition, differences in the retention were observed at room and mesophilic temperatures. The obtained results could be explained with the pore sizes of the membrane becoming wider, slightly losing selectivity and having an increase in permeability at higher temperatures.

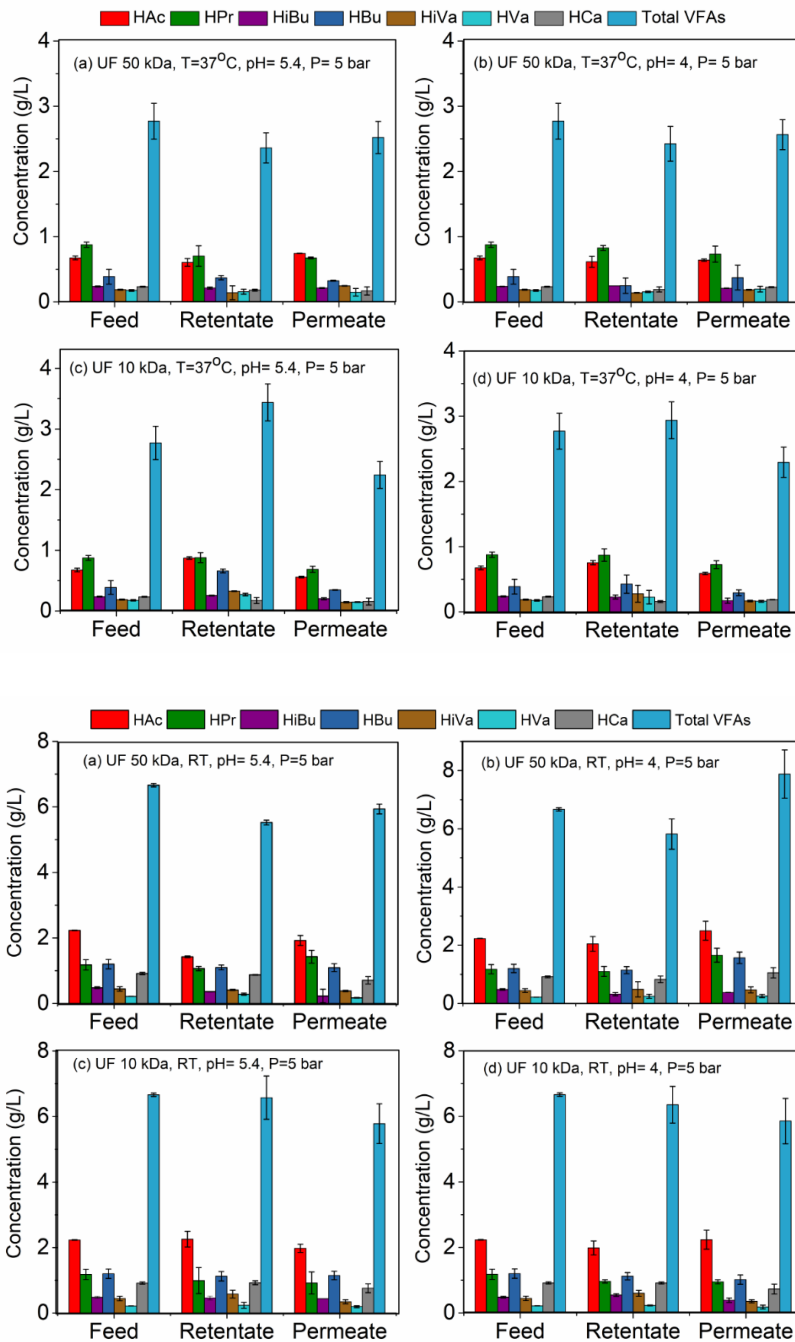


Figure 5.7 Changes in the concentrations of VFAs before and after ultrafiltration (Temperature 37°C, Pressure=5 bar) (A) and Room temperature, Pressure=5 bar (B).

Membrane performance during ultrafiltration

Changes in the membrane performance defines feasibility of the filtration process and the output flux is the main indicator in said definition. The membrane permeate flux-time profile is shown in Figure 5.8 A and B. Due to the very high initial flux selected for the UF experiments in the current study, an initial drop in permeate flux was observed and flux leveling out followed this as filtration time proceeded. The initial plunge in permeate flux can be explained with membrane pore narrowing and blockage, surface gel layer formation due to concentration polarization. Most importantly, particulate matter deposition also occurs on the membrane surface along with cake layer formation and its compaction (Lee et al., 2021). At mesophilic temperature, the percentage of flux decline was 58% (439.2-182.1 LMH for 50 kDa) at pH 5.4 within an interval of 21 min. This drop in flux was similar to the situation that occurred when effluent with an initial pH of 4 was applied. As expected, the permeability of the 10 kDa membrane was observed to be less than that of 50 kDa. After 35 min of filtration (durations were set based on same permeate volume collection), the highest flux decline (289.2-64.2 L MH) was observed for 10 kDa at pH 5.4 (77%). At pH 4, the initial flux (96.2 LMH) through the 10 kDa membrane was the lowest value observed in all of the treatments. This presents the tradeoff between selectivity and permeate flux, which should be evaluated based on the productivity needed versus purity of the final product of filtration. A possible explanation to the trends observed is that the larger pore sized membranes are more susceptible to pore blockage by foulants and. Also, as they have a higher convective throughput, there is a greater driving force for particle deposition on the membrane surface compared to membranes with smaller pore sizes (Liu et al., 2021). Moreover, as mentioned in the previous section, temperature plays a role in changing membrane selectivity and permeability. In this regard, the results clearly indicate that UF filtration at room temperature resulted in a reduction in the permeate flux drop when compared to that of mesophilic temperature. This can be both due to the lack of flexibility of membrane pores in expansion and higher viscosity of the permeate solution as a result of low temperature.

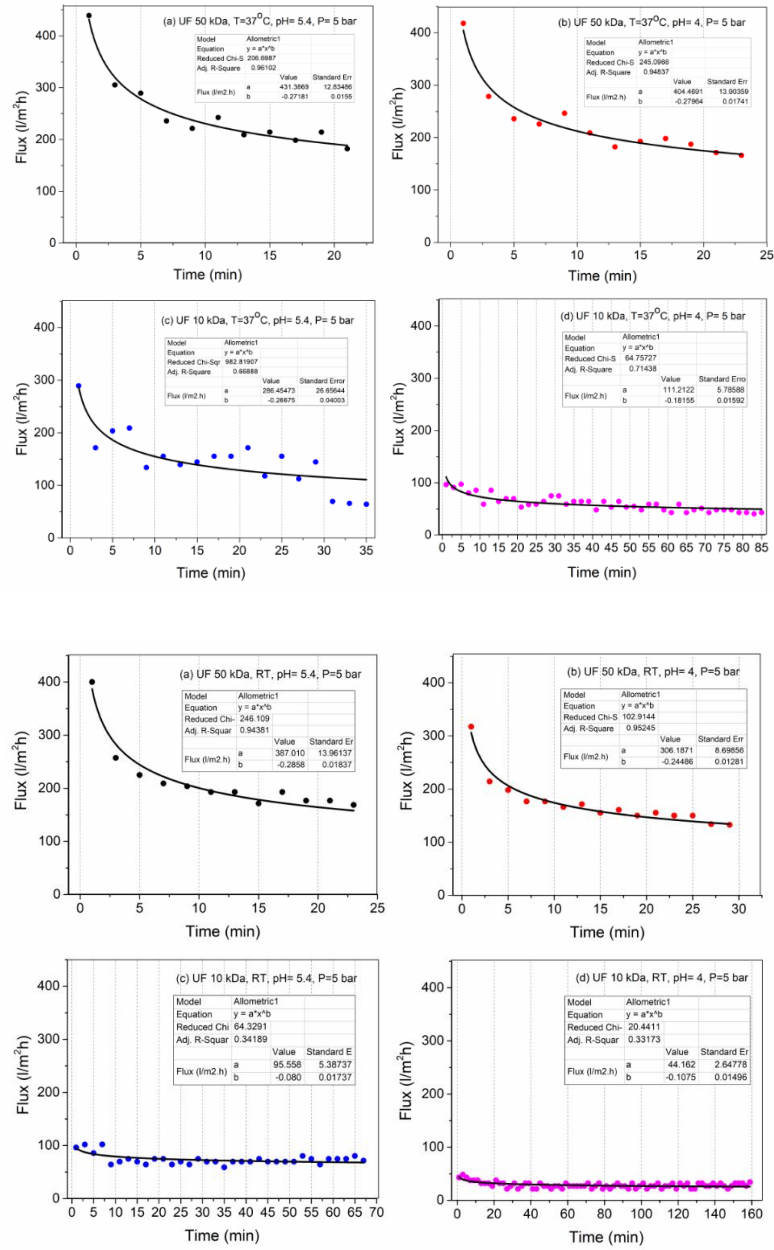


Figure 5.8 Changes in the permeate flux during ultrafiltration of VFA-containing effluent (Temperature 37° C, Pressure=5 bar (A) and Room temperature, Pressure=5 bar (B).

5.2 Feasibility of nanofiltration process for high efficient recovery and concentrations of food waste-derived volatile fatty acids

5.2.1 Introduction

Waste biorefinery models are one of the emerging concepts complying to fundamentals circular economy while compassing the Sustainable Development Goals (SDGs) adopted by The United Nations (Venkata Mohan et al., 2016, Leong et al., 2021, Naddeo and Taherzadeh, 2021). Among the organic waste streams of interest to be used in a waste-based biorefinery, food waste (FW) is considered as one of the most available (regardless of location), rich in a mixture of carbohydrates, proteins, lipids and other nutrients, and therefore a good candidate as a feedstock to a biorefinery (Bigdeloo et al., 2021). Annually around 1.3 billion tons of food waste is generated worldwide, as estimated by the Food and Agriculture Organization (FAO) (Papargyropoulou et al., 2014). FW, if not properly handled, can cause negative environmental impacts such as greenhouse gas emissions, and land, air and water pollution. Conventionally, food waste management was carried out through composting, incineration, and landfilling, which are not the most praised strategies when it comes to resource efficiency, nutrient recovery environmental benefits (Schanes et al., 2018). Additionally, these management processes are facing technological and compliance feasibility issues (Salemdeeb et al., 2017, Thi et al., 2015). Thus, selecting an environment-friendly and economic oriented management approach within the framework of turning food waste into value-added products is highly demanded (Ma and Liu, 2019).

Anaerobic digestion (AD) has been acknowledged as a sustainable and feasible organic waste valorization technique due to its high conversion efficiency, cost-effectiveness and technical viability (Ren et al., 2018, Xu et al., 2018b). In the AD process, food waste is loaded in an anaerobic digester that where is four main successive stages of hydrolysis, acidogenesis, acetogenesis, and methanogenesis organic matter is converted to biogas (methane (53–70%), carbon dioxide (30–50%), other gaseous compounds) and digestate. However, intermediate products of AD such as VFAs are of more market appeal and unit value compared to biogas (Wainaina et al., 2020a, Kleerebezem et al., 2015, Lü et al., 2021). VFAs are

carboxylic acids (acetic acid, propionic acid, butyric acid, valeric acid and caproic acid) containing six or fewer carbon atoms in their chain. AD-assisted waste-derived VFAs production is considered as a sustainable platform compared to the currently achieved synthetic route, i.e., fossil-based sources (Huq et al., 2021, Aydin et al., 2018). VFAs have many industrial applications from bioplastics and biofuels to cosmetics and pharmaceuticals (Agnihotri et al., 2022). However, in order to market VFAs acquired from AD, VFAs should be effectively recovered/separated (collected in pure form) from microorganism particle-riched mixed effluent and concentrated to favorable levels (Atasoy et al., 2018, Chen et al., 2021).

Various technologies such as adsorption, electrodialysis, ion exchange and solvent extraction have been used to improve the VFAs purity in AD fermentation liquid (Pervez et al., 2022b). Above all, membrane technology has proved to be a promising sustainable and energy efficient solely physical approach towards VFAs recovery (Ramos-Suarez et al., 2021b, Bhatt et al., 2020). Due to mechanisms involved in permeate selectivity, nanofiltration has attracted widespread attention in recent years. The pore sizes of the nanofiltration membranes lie between 1-10 nanometers that are beneficial for rejecting low molecular weight VFAs. The retention mechanism of the NF process is dominated by charged and size exclusion. Several literature have shown the ability of NF in VFAs recovery. Han et al. (Han and Cheryan, 1995) screened several NF membranes for acetic acid recovery from model solutions. In addition, Zacharof et al. (Zacharof et al., 2016) used the NF process to treat agricultural wastewater, and 75% of VFAs compounds, including acetic and butyric acid, were recovered. Regardless of the great interest in the application of FW in a waste-biorefinery and the complexity involved in waste generated VFAs separation, purification and concentration from FW digestate, there is lack of available information in the application of pressure-driven membrane processes in this regard.

Therefore, in this study, actual ultrafiltered VFAs effluent was provided from a semi-continuous microfiltration immersed membrane bioreactor set up for anaerobic digestion of food waste. The obtained VFAs effluent was then subjected to NF with alternation in defining parameters. The effect of changes in the pH of the media and NF membrane pore size during the experimental work on VFAs recovery percentage was investigated. Furthermore, a two-stage recyclability system was carried out for the improvement in the VFAs recovery performance. The results acquired in this research work will present a new insight on the essential role of pressure-driven membranes in the development of new generations of waste-based biorefinery.

5.2.2 Materials and methods

Materials and reagents

For the nanofiltration feed solution, a certain amount of ultrafiltered permeate solution was collected from the resultant effluent of an immersed microfiltration acidogenic fermentation MBR using food waste as feedstock (Parchami et al., 2020b). As the MBR was working parallel to the ultrafiltration and nanofiltration, all collected samples were stored in the lab refrigerators at 4°C for 24 hours prior to use. The solution's pH values were adjusted with the addition of 1 mol L⁻¹ sulphuric acid and sodium hydroxide. Two different commercial flat sheet nanofiltration membranes, TS 40 and XN 45 (Microdyn Nadir, Germany), were used in the current study, and their characteristics are presented in Table 5.5.

Table 5.5 Characteristics of used nanofiltration membranes.

Name	TS 40	XN 45
Producer	Microdyn Nadir	Microdyn Nadir
MWCO (Da)	200-300	300-500
Type	flat sheet	flat sheet
Membrane backing material	Non-Woven Polyester	Non-Woven Polyester
Membrane chemistry	Thin-Film Polypiperazine	Thin-Film Polypiperazine
Flux Range (1 m ² h ⁻¹) (GFD)	40.8 -61.2 (24.0 -36.0)	47.6 -73.1 (28.0 -43.0)
Thickness (µm)	130-170	130-170
pH Range	1.0 12.0	1.0 12.0
Chlorine Tolerance	< 0.1 ppm	< 0.1 ppm

Nanofiltration procedure

A commercial laboratory-scale cross-flow filtration cell of the Koch membrane system (KMS LABCELL CF-1, United Kingdom) was used for the nanofiltration experiments. The schematic diagram of the filtration unit is presented in Figure 5.9. The membrane effective area was 28 cm². The operating mode was batch-wise with constant temperature (20-21°C) and applied pressure of 15 bar through the application of high-pressure nitrogen. A new membrane was used for every experimental run which was flushed for 45 minutes with MiliQ water before loading the feed solution. Before starting each filtration batch, the liquor was decanted at room temperature for 2-3 hours. A 200 mL feed solution was typically used for every NF batch, aiming at 50 mL retentate collection. In time intervals of 2 min, the permeate solution weight was recorded using for the measurement of permeate flux. The pH of the VFAs effluent obtained from the MBR was adjusted before NF to 4,

5.4, 7 and pH 9 for both membranes. After each experimental run, the filtration unit was cleaned twice with NaOH solution (pH 10) and finally rinsed MiliQ water.

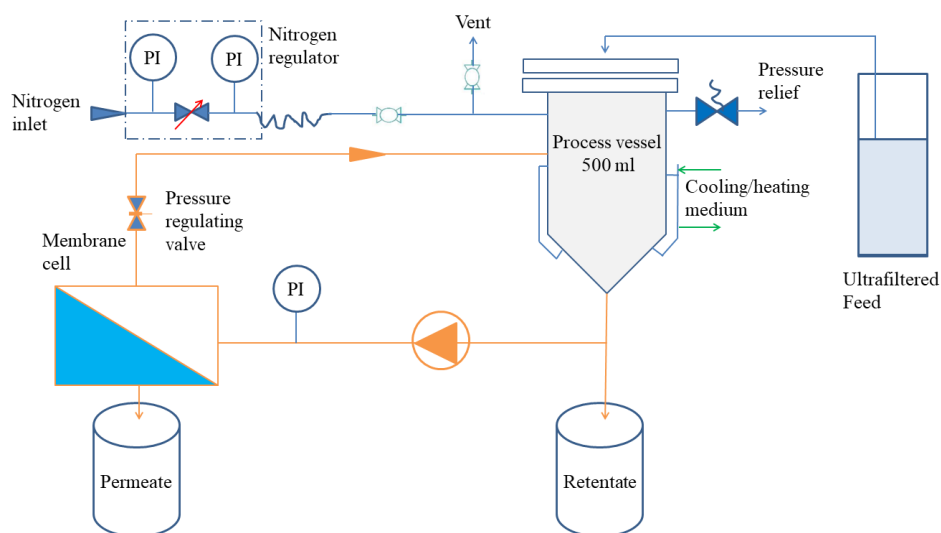


Figure 5.9 Schematic diagram of the nanofiltration system.

Analytical methods

Solution pH was measured using a FiveEasy F20 pH meter (Mettler Toledo, OH, USA). Total suspended solids (TSS), total solids (TS), dissolved solids (DS), volatile suspended solids (VSS), and volatile solids (VS) were continuously measured by following the standard methods of the American Public Health Association (Federation and Association, 2005). CSB 15000 test kit was used for the measurement of soluble chemical oxygen demand (SCOD) and total chemical oxygen demand (TCOD), Ammonium 100 test kit for ammonium nitrogen concentration ($\text{NH}_4^{+}\text{-N}$) and Phosphate 45 for orthophosphate concentration ($\text{PO}_4^{3-}\text{-P}$), respectively, (MACHEREY-NAGEL GmbH & Co. KG, Germany) using a portable Nanocolor 500D Photometer. The concentrations of VFAs (Acetic acid, HAC; Propionic acid, HPr; Isobutyric acid, HiBu; Butyric acid, HBU; Isovaleric acid, Hiva; Valeric acid, HVa; Caproic acid, HCa) were determined using high-performance liquid chromatography (HPLC, Waters Corporation, Milford, CT, USA) equipped with an H_2 -based column. The detailed operating procedures can be found in our previous study (Wainaina et al., 2019c). A Biochrom Libra S50-based UV-Vis spectrophotometer (Biochrom Ltd., Cambridge, UK) was used for the measurement of the color change of different liquid streams of feed, permeate, and

retentate using wavelengths between 200–600 nm. The recovery or retention percentages of VFAs compounds and membrane permeate flux was calculated according to Eq. 1 and Eq. 2, respectively.

$$R_{ret(\%)} = \left(1 - \frac{C_p}{C_f}\right) \times 100 \quad (1)$$

Where C_p represent the concentration of permeate and C_f denotes the feed concentration, respectively.

$$J_{permeate} = \left(\frac{Q_f}{A_m}\right) = \left(\frac{dv}{dt}\right) \quad (2)$$

Where V represent the amount of volume, t is time (h), membrane area (A_m), and Q_f is the volumetric flow rate ($L h^{-1}$).

Repeated filtration

A two-stage repeated NF filtration was proposed in this study according to the flow diagram presented in Figure 5.10. Sequencing (SQ), as the first approach, was conducted with a feed solution volume of 200 mL aiming at the collection of 50 mL retentate and 150 mL permeate. After each SQ stage, 10 mL solution was withdrawn from the retentate for further characterization and a fresh 160 mL feed solution was added in the 2nd. This procedure was further applied in cycle 3. For recirculation (RC) experiments the same initial feed volume of 200 mL was used in 3 consecutive filtration cycles, however, in this case after every filtration cycle the 150 mL permeate was returned back to the filtration tank joining the retentate for another round of filtration.

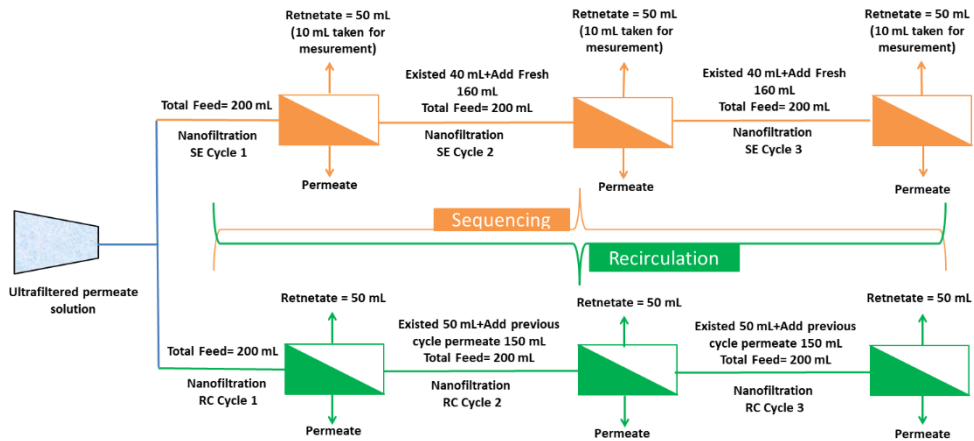


Figure 5.10 Two-stage recyclability system of nanofiltration.

5.2.3 Results and Discussion

The effect of pH in changes in physicochemical parameters of the media during NF

Physicochemical parameters are regarded as one of the most important factors defining the aquatic environment quality. The pre-treated ultrafiltered solutions were subjected to nanofiltration (Table 5.6 and 5.7). As can be seen, NF reduced the solids content (TS, TSS, DS, VS, VSS) significantly. For 200-300 Da membrane (Table 5.6), the removal percentage of total solids was 63% (3.17 to 1.17 g L⁻¹) at the as received pH 5.4, but it increased to 85% (3.17 to 0.46 g L⁻¹) as the pH was reduced to 4. On the contrary, when pH was increased to 7 and 9, the removal percentage reduced marginally to 83-78%. The same trend was also noticed for 300-500 Da membrane (Table 5.7). The results prove that at lower pH (pH 4) better solid removal is obtained in the aforementioned NF membranes, attributed to the generation of electrostatic attraction at low pH between negatively charged particles and positively charged membrane surface. When electrostatic attraction occurs, the membrane surface allowed passing the particles from their pores and showed a higher removal rate (Mahmoud et al., 2003a). Furthermore, as seen, the larger amount of solids contents removal produces transparent permeate solutions and reduced absorbance values (Figure 5.11 A and B).

The COD contents are linearly decreased in the permeate solutions for both membranes at different pH. As can be seen in Table 5.6, the feed TCOD concentration was 6.85 g L⁻¹, whereas the permeate TCOD concentration decreased to 4.7 g L⁻¹ (pH 4), 3 g L⁻¹ (pH 5.4), 1.15 g L⁻¹ (pH 7) and 0.5 g L⁻¹ (pH 9). As a result, the removal efficiency of 31.38% increased to 92.70% when the pH value reached 9. On the other hand, the corresponding TCOD removal efficiency increased from 21.16% (pH 4) to 76.64% (pH 9) by 300-500 Da membrane (Table 3), expectedly lower than that of the 200-300 Da membrane. Moreover, in both cases, the removal percentage trend of SCOD was higher than TCOD removal efficiency (Table 5.6 and 5.7). The obtained results can be supported by the previous studies stating that the concentration of hydroxide ions is increased at higher pH, thereby promoting the production of hydroxyl free radicals on a large scale contributing to a higher removal efficiency of TCOD and SCOD in the permeate solution (Aziz and Kasongo, 2021a, Capar et al., 2006).

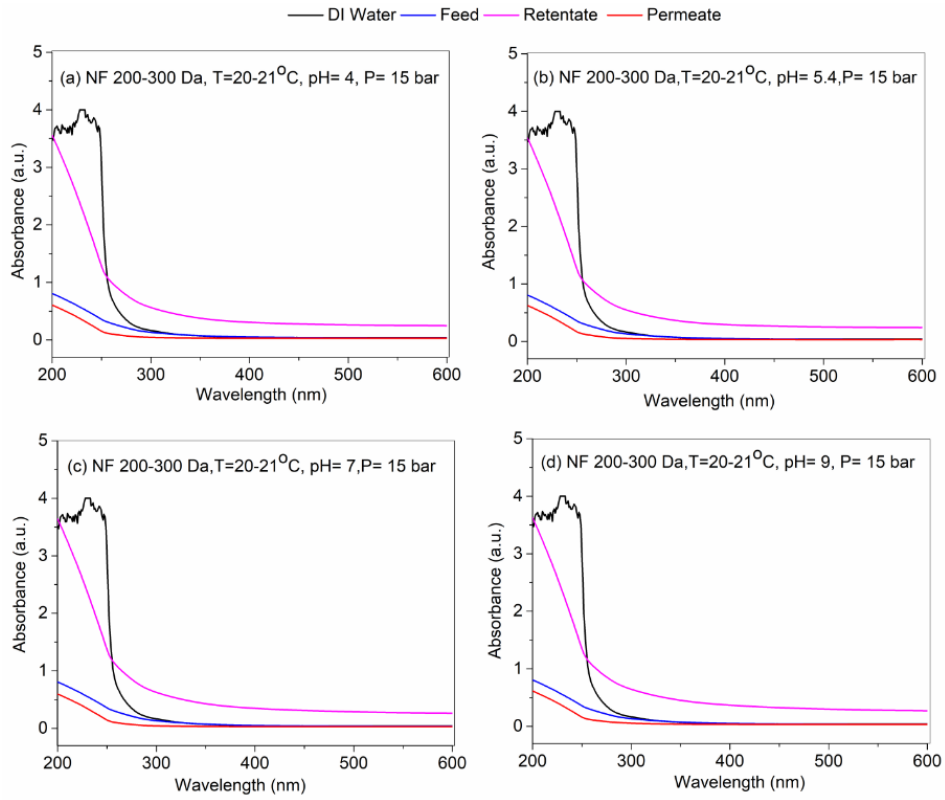
5. Process intensification of pressure-driven membrane filtration for resource recovery from
 food waste

Table 5.6 Physicochemical parameters of nanofiltered solution (Pore size: 200-300Da, Temperature 20-21°C, Pressure=15 bar); (F= Feed, R= Retentate, P= Permeate).

Parameters	200-300Da			pH(4)			pH(5.4)			pH(7)			pH(9)		
	F	R	P	F	R	P	F	R	P	F	R	P	F	R	P
TS (g L ⁻¹)	3.17 ± 0.18	9 ± 0.90	0.46 ± 0.14	12.25 ± 3.60	1.17 ± 0.04	18.38 ± 3.40	0.51 ± 0.19	18.15 ± 2.39	0.68 ± 0.07						
TSS (g L ⁻¹)	0.1 ± 0.02	0.43 ± 0.26	0.04 ± 0.00	0.14 ± 0.14	0.04 ± 0.00	0.92 ± 0.90	0.05 ± 0.01	0.71 ± 0.32	0.08 ± 0.12						
DS (g L ⁻¹)	3.07 ± 0.15	8.57 ± 1.17	0.42 ± 0.14	12.11 ± 3.46	1.13 ± 0.04	17.46 ± 4.49	0.34 ± 0.21	17.44 ± 2.06	0.63 ± 0.05						
VS (g L ⁻¹)	1.14 ± 0.05	2.72 ± 0.28	0.56 ± 0.14	3.56 ± 0.08	0.46 ± 0.36	8.60 ± 2.57	0.53 ± 0.07	8.01 ± 0.01	0.59 ± 0.01						
VSS (g L ⁻¹)	0.52 ± 0.05	0.39 ± 0.24	0.06 ± 0.05	0.62 ± 0.11	0.38 ± 0.00	0.95 ± 0.43	0.41 ± 0.02	0.83 ± 0.09	0.49 ± 0.15						
TCOD (g L ⁻¹)	6.85 ± 0.49	10.5 ± 0.70	4.7 ± 0.42	11.02 ± 3.53	3 ± 1.41	12.65 ± 7.07	1.15 ± 0.07	13.29 ± 2.12	0.5 ± 0.07						
SCOD (g L ⁻¹)	8 ± 0.98	10.25 ± 0.77	5 ± 0.56	12 ± 0.70	2.8 ± 0.28	14 ± 0.28	1.25 ± 0.07	15.75 ± 0.63	0.45 ± 0.07						
NH ⁴⁺ -N (mg L ⁻¹)	145 ± 0.70	415 ± 3.53	65 ± 0.70	355 ± 9.19	85 ± 0.70	365 ± 9.19	45 ± 0.14	445 ± 9.19	41 ± 0.70						
PO ₄ ³⁻ -P (mg L ⁻¹)	62.75 ± 0.21	171 ± 5.51	7.90 ± 2.40	173.25 ± 11.24	3.85 ± 1.48	178.75 ± 6.71	1.6 ± 0.28	33.75 ± 3.88	1.95 ± 0.49						

Table 5.7 Physicochemical parameters of nanofiltered solution (Pore size: 300-500Da, Temperature 20-21°C, Pressure=15 bar).

Parameters	F	300-500Da			pH(4)			pH(7)			pH(9)		
		R	P	K	R	P	K	R	P	K	R	P	K
TS (g L ⁻¹)	3.17 ± 0.18	6.52 ± 2.46	0.81 ± 0.18	7.2 ± 0.02	1.72 ± 1.55	10.1 ± 1.78	12.88 ± 0.33	1.41 ± 0.04					
TSS (g L ⁻¹)	0.1 ± 0.02	0.48 ± 0.14	0.04 ± 0.02	0.26 ± 0.22	0.05 ± 0.01	0.6 ± 0.16	0.05 ± 0.01	0.04 ± 0.00					
DS (g L ⁻¹)	3.07 ± 0.15	6.04 ± 2.31	0.77 ± 0.15	6.94 ± 0.19	1.67 ± 0.01	9.5 ± 1.95	11.55 ± 0.04	1.37 ± 0.04					
VS (g L ⁻¹)	1.14 ± 0.05	2.47 ± 1.51	0.57 ± 0.12	3.02 ± 0.00	1 ± 0.02	4.35 ± 0.86	0.26 ± 0.02	0.62 ± 1.57					
VSS (g L ⁻¹)	0.52 ± 0.05	0.6 ± 0.08	0.33 ± 0.01	0.66 ± 0.11	0.37 ± 0.38	0.74 ± 0.22	0.43 ± 0.05	0.47 ± 0.50					
TCOD (g L ⁻¹)	6.85 ± 0.49	10.5 ± 0.70	5.4 ± 1.27	11 ± 1.41	3.2 ± 0.14	12 ± 1.41	1.85 ± 0.21	1.6 ± 0.14					
SCOD (g L ⁻¹)	8 ± 0.98	7.3 ± 3.67	5.85 ± 1.20	9.35 ± 0.07	3.45 ± 0.07	12.4 ± 3.11	1.9 ± 0.14	1.65 ± 0.21					
NH ⁴ -N (mg L ⁻¹)	145 ± 0.70	325 ± 6.36	75 ± 2.12	215 ± 2.12	85 ± 0.70	260 ± 2.82	50 ± 1.41	70 ± 0.70					
PO ₄ ³⁻ -P (mg L ⁻¹)	62.75 ± 0.21	128 ± 4.66	8.8 ± 0.42	112 ± 0.14	8.8 ± 0.42	117.75 ± 3.88	4.35 ± 0.07	1.85 ± 0.21					



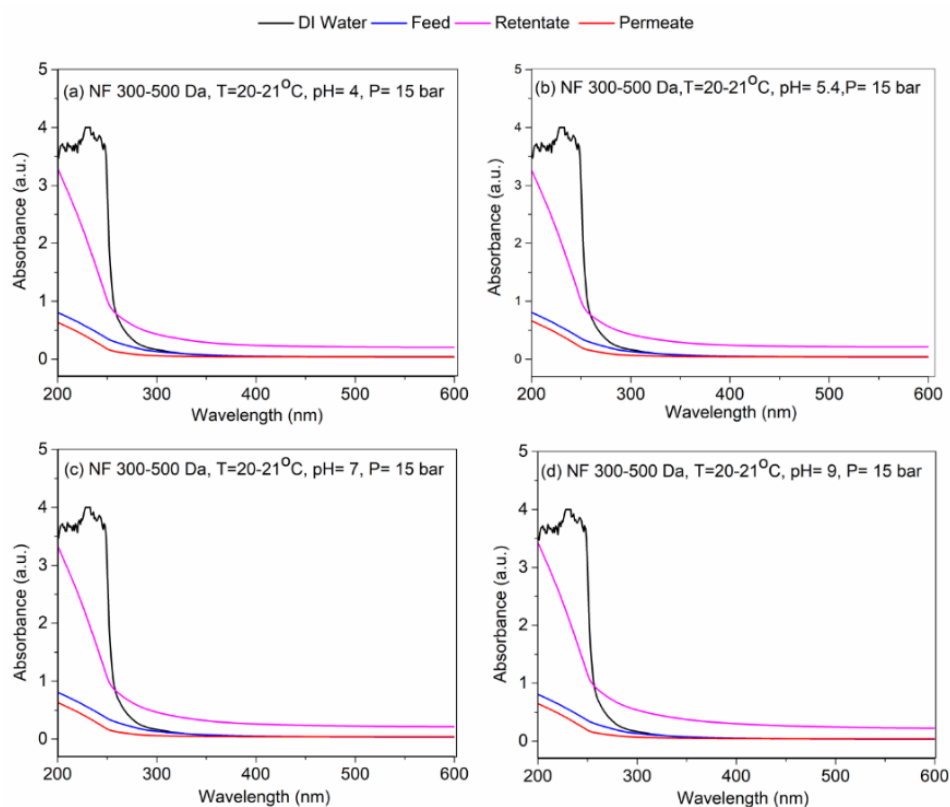


Figure 5.11 UV-Vis spectra of DI water, feed, retentate and permeate upon nanofiltration membrane (200-300 Da) (A), and upon nanofiltration membrane (300-500 Da) (B).

Given the characteristics of the nanofiltration process, it has proven to be promising for nutrients such as $\text{NH}_4^+\text{-N}$ and $\text{PO}_4^{3-}\text{-P}$ recovery from fermentation broth (Rongwong et al., 2018b, Gerardo et al., 2015). As can be seen for $\text{NH}_4^+\text{-N}$, the feed concentration was 145 mg L^{-1} , while after filtration, the retentate concentration reached 445 mg L^{-1} and 330 mg L^{-1} at pH 9 for 200-300 Da membrane and 300-500 Da membranes, respectively (Tables 5.6 and 5.7). The reason could be that ammonium ions are converted to ammonia at higher pH resulting in such increment in $\text{NH}_4^+\text{-N}$ concentration in the retentate solution (Mohammed-Nour et al., 2019b). For all assessed membranes, it can be noticed that when pH was adjusted to 4, the retention concentration of $\text{NH}_4^+\text{-N}$ was increased to 415 mg L^{-1} (Table 5.6) and 325 mg L^{-1} (Table 5.7), respectively, which can be due to the carboxylic group's deprotonation behavior with the dense membrane in the nanofiltration process (Chu et al., 2017b).

For $\text{PO}_4^{3-}\text{-P}$, the pH has an apparent influence on the removal/recovery percentage in nanofiltration process. The feed concentration of $\text{PO}_4^{3-}\text{-P}$ was 62.75 mg L^{-1} , and after nano filtered with 200-300 Da membrane, the retentate solution concentrations were found to be around 178 and 173.25 mg L^{-1} for pH 4 and 5.4, respectively (Table 5.6), and for 300-500 Da it appeared 126 and 112 mg L^{-1} (Table 5.7). Whereas as the pH increased to 7 and 9, the retention solution concentrations decreased to 171.75 mg L^{-1} and 33.75 mg L^{-1} as for 200-300 Da (Table 5.6); however, in the presence of 300-500 Da, the retention concentrations also reduced to 117.75 mg L^{-1} and 12.25 mg L^{-1} (Table 5.7). This means that lower pH increased recovery efficiency while higher pH improved removal percentage of $\text{PO}_4^{3-}\text{-P}$. It could be explained by electrostatic attraction between negatively charged phosphate ions and positively charged nanofiltration membrane surface at lower pH, thereby increasing the recovery efficiency and for higher pH, vice versa (Camarillo et al., 2009). Further, this result is in agreement with previous studies dealing with $\text{PO}_4^{3-}\text{-P}$ riched effluents treatment by nanofiltration (Nir et al., 2018, Niewersch et al., 2014).

The effect of pH on VFAs recovery during NF

The nanofiltration process is an attractive choice for the recovery of chemical compounds such as VFAs. However, it is observed that various operational parameters play a role in NF performance. Solution pH has been identified as one of the most influential parameters in compounds retention during NF. Hence, the concentrations and recovery percentages of individual VFAs as a function of pH was investigated (Table 5.8 and 5.9). As shown in Table 5.8, for HAc, the recovery percentage increases from 65% to 98% as solution pH increased from 4 to 9. The same trends are noticed for HPr (55%-93%), HiBu (31%-98%), HBu (53%-96%), HiVa (32%-83%), HVa (21%-60%), HCa (48%-96%) and TVFAs (50%-91%) when the solution pH increased from 4 to 9. It can be observed that concentrations and recovery percentages for all VFAs increase when the solution pH increases, except for HPr, HiBu, HBu, HVa and HCa, which at pH 7 show higher recovery percentages than HAc. This phenomenon has been achieved due to the variations of molecular weight, meaning that higher molecular weight represents a better recovery percentage. Similarly, Xiong et al. and his colleagues (Xiong et al., 2015), evaluated that at pH 7 acetic acid has a lower recovery percentage than butyric acid because of its lower molecular weight

Moreover, the retention mechanism of the nanofiltration process can be described by the size and charged effect. At pH 4, it can be found that a smaller amount of VFAs compounds are recovered because of the size effect. Since VFAs compounds are generally uncharged at pH 4, and they have lower molecular weights (Table 5.10)

than the pore size (MWCO) of the membrane, thus leading to a low recovery percentage. On the other hand, when pH values of 5.4, 7 and 9 are selected, the recovery percentages are significantly increased. This is mainly attributed to the charge effect. VFAs (see pKa values in Table 5.10) and nanofiltration membranes are negatively charged at higher pH (above isoelectric point). Therefore, electrostatic repulsion occurs, preventing VFAs to pass through the membrane resulting in a higher recovery percentage. Similar results have been reported in several previous works regarding higher VFAs recovery at higher pH in the nanofiltration process (Zhu et al., 2020b, Zhang et al., 2018b, Zacharof and Lovitt, 2013c, Bellona and Drewes, 2005).

NF membrane with a larger pore size (300-500 Da) was also applied for the recovery of VFAs at different pH. As shown in Table 5.9, a similar increasing trend was observed for concentration and recovery percentages of VFA, but the performance was distinctively poorer than that of the membrane with a lower MWCO. For HAc, the recovery percentage achieved at pH 9 was 90% reaching a concentration of 4.52 g L⁻¹, while the recovery percentages were higher for HBU (93%) and HCa (94%). Also, for pH 7, the recovery percentages of HBU (84%) and HCa (82%) were higher than HAc (76%). However, when the pH was adjusted to 4 and 5.4, the recovery percentage of HPr was dominant with 53% and 54%, respectively. It can be seen that the retention performance of HBU and HPr is favoured over HAc, which may be achieved due to the higher molecular weight of the former compounds (Van der Bruggen et al., 2002, Van der Bruggen and Vandecasteele, 2003).

Overall, to summarize the influence of pH on VFAs concentration and recovery percentage, it seems that lower pore size membrane TS 40 has shown better performance than higher pore size membrane XN 45. However, pH 9 was found to be the best for both membranes. Therefore, it can be concluded that TS 40 membrane at pH 9 for VFAs recovery would be a feasible choice for NF of food waste-based anaerobically digested liquid.

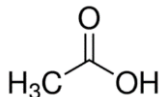
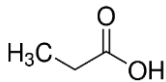
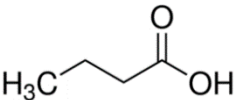
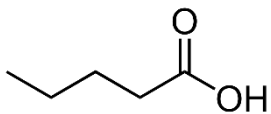
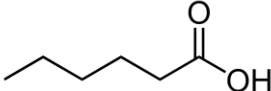
Table 5.8 VFAs concentration via nanofiltration (Pore size: 200-300Da, Temperature 20-21°C, Pressure=15 bar)
(F= Feed, R= Retentate, P= Permeate, R%= Recovery percentage).

Solute _s (g L ⁻¹)	200-300Da			pH(4)			pH(5.4)			pH(7)			pH(9)		
	F	R	P	R%	K	R	R%	K	R	R%	K	R%	K	R	R%
HAc	1.25±0.01	3.25±0.28	0.43±0.14	65	3.69±0.04	0.32±0.04	74	4.24±0.50	0.18±0.05	85	4.92±0.03	0.02±0.03	98		
HPy	0.72±0.02	1.50±0.02	0.32±0.00	55	1.73±0.15	0.26±0.00	63	2.55±0.53	0.06±0.01	92	2.57±0.36	0.05±0.01	93		
HiBu	0.15±0.11	0.18±0.08	0.1±0.01	31	0.26±0.04	0.08±0.00	44	0.55±0.11	0.01±0.00	92	0.59±0.11	0.01±0.00	93		
HBu	1.09±0.02	2.33±0.11	0.51±0.06	53	3.07±0.25	0.32±0.08	70	4.14±4.06	0.07±0.12	93	4.18±0.04	0.04±0.00	96		
HIVa	0.38±0.04	0.49±0.08	0.26±0.27	32	0.84±0.13	0.17±0.00	55	1.10±0.28	0.11±0.00	71	1.28±0.13	0.06±0.00	83		
HVa	0.52±0.18	0.46±0.24	0.41±0.12	21	0.82±0.09	0.33±0.01	37	1.28±0.22	0.22±0.01	58	1.31±0.11	0.2±0.04	60		
HCa	0.53±0.00	1.03±0.09	0.28±0.03	48	1.41±0.15	0.17±0.06	66	2.04±0.09	0.03±0.00	95	2.06±0.10	0.02±0.02	96		
Total VFAs	4.64±0.38	9.27±1.12	2.31±0.35	50	11.85±1.25	1.65±0.43	64	15.86±1.44	0.68±0.11	85	16.94±1.60	0.4±0.07	91		

Table 5.9 VFAs concentration via nanofiltration (Pore size: 300-500Da, Temperature 20-21°C, Pressure=15 bar).

Solute (g L ⁻¹)	300-500Da			pH (4)			pH (5.4)			pH (7)			pH (9)		
	R	P	R%	R	P	R%	R	P	R%	R	P	R%	R	P	R%
HAc	1.25±0.01	2.38±0.02	0.64±0.00	48	2.57±0.45	0.61±0.45	51	3.80±0.09	0.3±0.02	76	4.52±2.56	0.12±0.03	90		
HPr	0.72±0.02	1.46±0.08	0.34±0.00	53	1.50±0.22	0.33±0.17	54	1.88±0.07	0.23±0.04	68	2.01±0.01	0.19±0.03	73		
HIBu	0.15±0.11	0.27±0.00	0.08±0.04	44	0.33±0.09	0.06±0.01	55	0.41±0.03	0.05±0.00	66	0.43±0.01	0.04±0.02	72		
HBu	1.09±0.02	1.68±0.75	0.66±0.34	39	2.21±0.04	0.53±0.00	51	3.67±0.01	0.17±0.00	84	4.10±0.07	0.07±0.00	93		
HIVa	0.38±0.04	0.68±0.25	0.21±0.018	44	0.76±0.00	0.19±0.00	50	0.99±0.01	0.13±0.00	64	1.04±0.12	0.12±0.00	68		
HVa	0.52±0.18	0.71±0.09	0.35±0.13	33	0.82±0.13	0.33±0.04	37	1.23±0.06	0.23±0.11	56	1.26±0.02	0.22±0.00	57		
HCa	0.53±0.00	0.84±0.30	0.32±0.04	39	1.15±0.01	0.24±0.06	54	1.74±0.01	0.09±0.02	82	2.01±0.01	0.03±0.00	94		
Total VFAs	4.64±0.38	8.05±0.72	2.60±0.38	44	9.38±0.81	2.29±0.54	51	13.77±1.30	1.21±0.20	74	15.40±1.54	0.79±0.17	83		

Table 5.10 Characteristics of VFAs compounds.

Name	Chemical formula	Structure	Molecular weight (g L ⁻¹)	Dissociation constant (pKa) at 25 °C
Acetic acid	C ₂ H ₄ O ₂		60.05	4.76
Propionic acid	C ₃ H ₆ O ₂		74.08	4.88
Butyric acid	C ₄ H ₈ O ₂		88.11	4.82
Valeric acid	C ₅ H ₁₀ O ₂		102.13	4.84
Caproic acid	C ₆ H ₁₂ O ₂		116.15	4.88

Membrane performance during NF

The membrane performance was evaluated through recording the changes in in the permeate flux during nanofiltration. Figure 5.12 and 5.13 show the flux time profile for 200-300 Da and 300-500 Da MWCO membranes, respectively for filtration conducted at different values of pH. As can be seen, that flux rate decreased with time that could be attributed to different fouling mechanisms in a semi-dead-end filtration systems such as concentration polarization and gel layer formation on the membrane surface leading to a declining flux trend (van den Berg and Smolders, 1990).

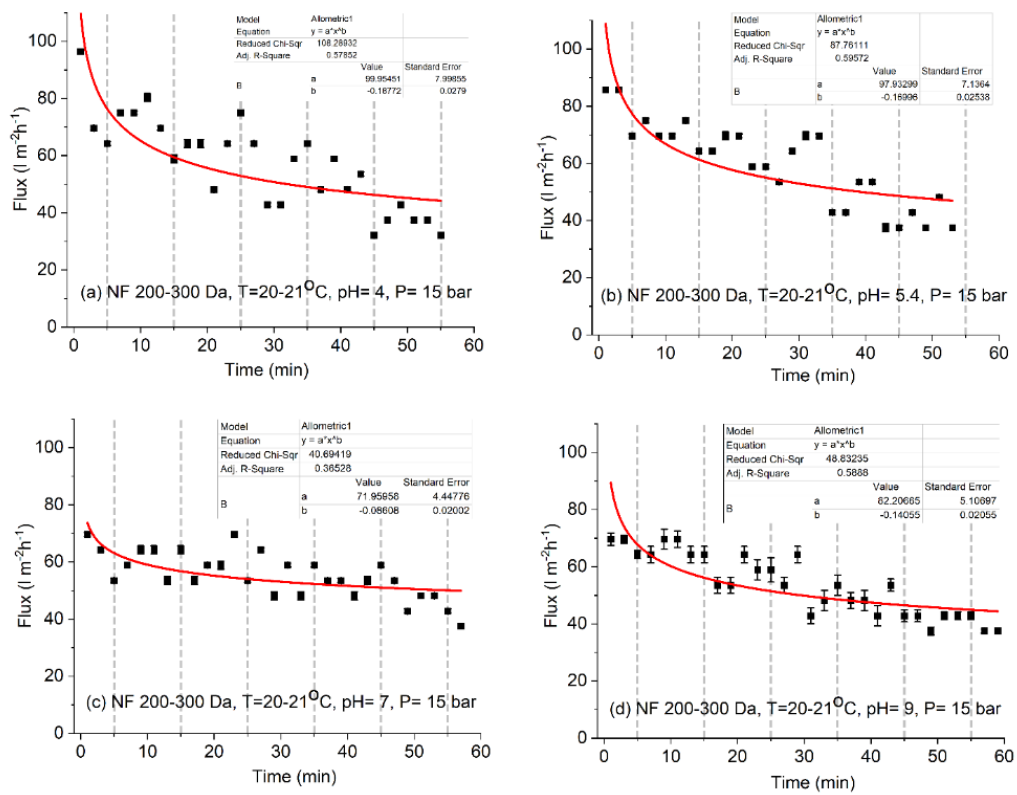


Figure 5.12. Flux-time profile at various pH for 200-300 Da nanofiltration membrane (Temperature 20-21°C, Pressure=15 bar).

. 5. Process intensification of pressure-driven membrane filtration for resource recovery
from food waste

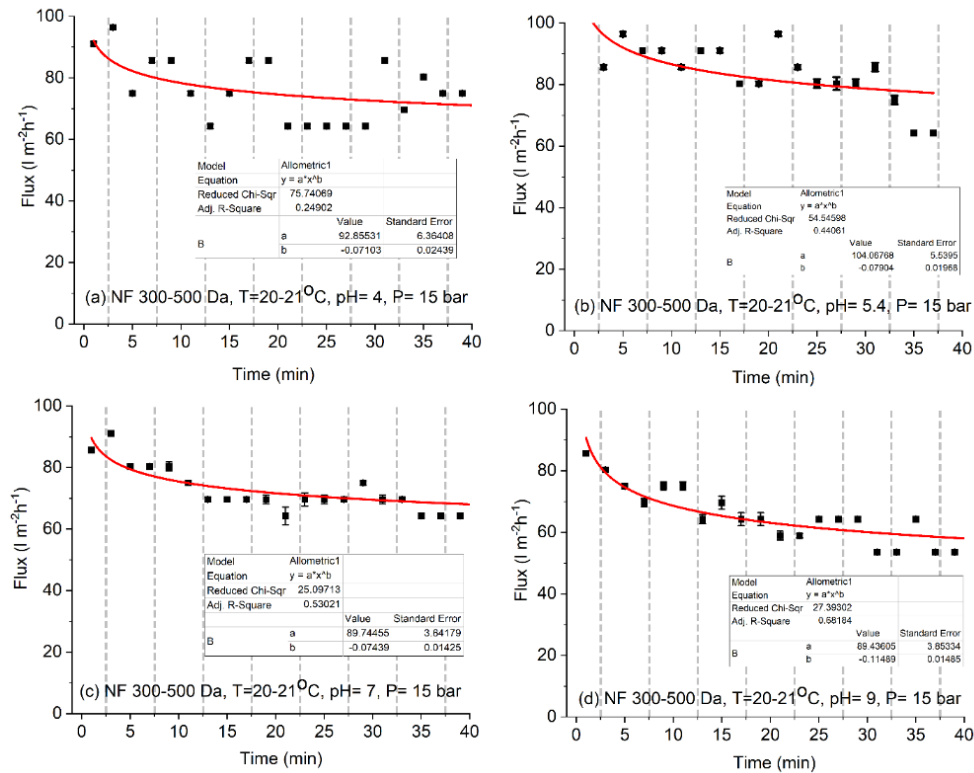


Figure 5.13 Flux-time profile at various pH for 300-500 Da nanofiltration membrane (Temperature 20-21°C, Pressure=15 bar)

The average permeates flux is calculated and presented in Table 5.11. It was noticed that the highest flux occurred at pH 4 for both membranes used, with XN 45 offering the highest rate of about 84.79 l m⁻²h⁻¹ (Table 5.11). On the contrary, at pH 9, the permeate flux was considerably lower for all treatments, with the smallest flux obtained for TS 40 at 52.91 l m⁻²h⁻¹ (Table 5.11). This can be potentially correlated with the maximum recovery percentage of VFAs at pH 9 as a common phenomenon in a dead-end nanofiltration systems (Zhang et al., 2018b, Werber et al., 2016, Lyu et al., 2016).

It is observed that acidic conditions favored permeate flux through membranes, which can be described by the neutralizing behaviour of membranes, as pH decreases, the membrane's surface charge moves near the isoelectric point, resulting in an increase in flux across the membranes (Al-Amoudi and Lovitt, 2007, Al-Amoudi et al., 2008).

On the other hand, alkali conditions reduce the flux through the membranes. Generally, polyamide-based nanofiltration membranes are strongly affected by solution pH. The membrane morphology changes under alkali conditions as the surface layer swells as a function of hydration, thereby decreasing liquid passage through the membrane pores, consequently lowering the flux. Overall, previous research fully support the results acquired in this study regarding changes in permeate flux by pH (Freger et al., 2000, Xiong et al., 2015).

Table 5.11 Permeate flux rate at various pH using two nanofiltration membrane.

Solution pH	Permeate flux ($l\ m^{-2}h^{-1}$)	
	200-300 Da	300-500 Da
4.0	58.75	84.79
5.4	56.95	73.94
7	55.71	70.68
9	52.91	62.40

Permeate recirculation and sequential filtration

In this stage of study the aim was to investigate the influence of recirculation and refiltration of permeate on VFAs recovery rate and also the effect of stage-wise batch reloading on VFAs retention and accumulation. For this purpose, a two-stage recycling process was designed, including sequencing (SQ) or recirculation (RC) of up to 3 cycles as presented in Figure 5.10. As the results present, when sequencing NF cycles were introduced (Figure 5.14a), the concentration and recovery percentages of individual acids and total VFAs (inset) was enhanced by the number of cycles.

For each cycle, fresh feed solution was added to the existing retentate solution. Among all VFAs, HAc was dominant with an increased concentration from 1.25 to 9.36 g L⁻¹ up to the 2nd cycle, while at the 3rd cycle, HBU turned to be the main recovered product with a concentration of 13.26 g L⁻¹. Interestingly, total recovery of HBU, HiBu, HiVa, HVa and HCa was achieved by the end of the 3rd cycle. These results confirm that the higher molecular weight favored achieving better recovery percentages (Van der Bruggen et al., 2002). Therefore, the composition of the effluent obtained from the microfiltered anaerobic MBR plays an important role in defining the dinal distribution of VFAs after NF (Wainaina et al., 2019c, Parchami et al., 2020b, Wainaina et al., 2020a). Moreover, the concentration of total VFAs has shown significant jump from 4.65 to 41.42 g L⁻¹ (around 96% recovery at the 3rd cycle) introducing NF as a promising approach for VFAs recovery and concentration (Young et al., 2013, Ramos-Suarez et al., 2021a).

The recirculation method was applied to the same effluent in order to investigate VFAs build up behavior through recirculation of permeate. The results of this stage are presented in Figure 5.14b. The experiments were repeated up to 3rd cycle using the previous cycles permeate as a feed solution into the existing retentate. It was observed that the concentration and recovery percentages of individual acids experience a slight decrease by cycle addition. For HAc, the concentration increased a marginally (5.75 to 5.79 g L⁻¹ for the 1st and 2nd cycle, respectively), however, it reduced to 4.98 g L⁻¹ by the 3rd cycle. This trend was also observed for the rest VFAs compounds. In addition, the recovery percentage dropped to 40-50% in each cycle for individual VFAs. This observation implied that the acids have not been in the liquid retentate but adsorbed in small amounts on the surface of membrane because of limited adsorption sites available during the recirculation method (Jiang et al., 2018, Yang et al., 2013b, Ahsan et al., 2014).

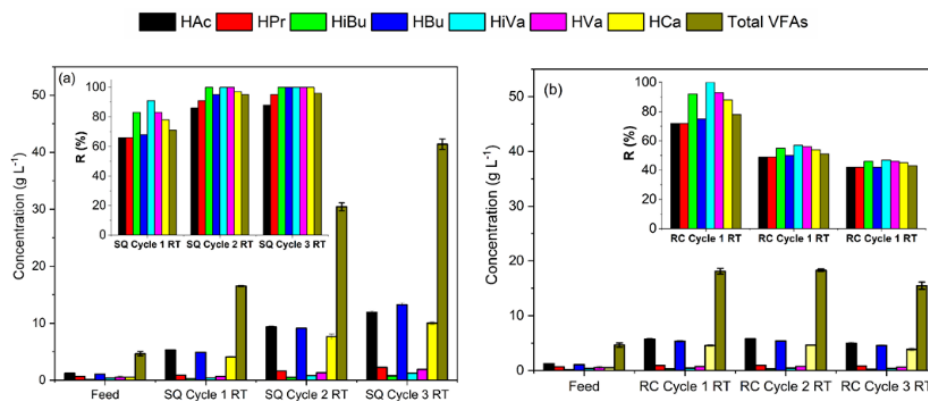


Figure 5.14 VFAs concentration and recovery percentages for NF (a) sequencing and (b) recirculation experiments

6. CONCLUSIONS AND FUTURE PERSPECTIVE

The findings in this thesis demonstrated that the electrospun nanofiber membranes and pressure-driven membrane filtration technologies application potential of wastewater treatment (methylene blue removal) and resource recovery (VFAs purification and concentration), respectively. The following conclusions can be listed as follows:

- As an additive, HPC is claimed to have potential use in treating industrial wastewater. HPC was successfully used to develop a new PES-based electrospun nanofiber membrane in the current study. According to morphological evidence, the synthesized PES/HPC blended nanofiber membrane was devoid of beads and had an ultrathin diameter (261.5 nm) compared to the original PES nanofiber membrane (168.5 nm). Furthermore, it displayed increased hydrophilicity, thermal stability, and mechanical stability, all of which are important properties in the adsorption process. Aside from that, it demonstrated increased hydrophilicity as well as thermal and mechanical stability, all of which are critical in the adsorption process. PES/HPC nanofiber membrane took only 840 minutes (where 75% of MB adsorbed within 360 min) to achieve equilibrium, while 1080 minutes was required for pure PES nanofiber membrane, and kinetics data revealed that the pseudo-second-order (PSO) model has performed much better than the pseudo-first-order (PFO) model. The findings of the adsorption isotherms revealed that the PES/HPC blended nanofiber membrane has an excellent MB adsorption capacity of 259.74 mg/g at neutral pH at room temperature, which is much superior to the pure PES nanofiber membrane (48.00 mg/g) obeying the Langmuir model. With regard to ionic strength, the adsorption capacity of the PES/HPC was decreased with increased ionic strength concentrations but the recyclability was maintained for up to 5 cycles with good adsorption results.

- In addition to the previous observation, another novel PES-based electrospun nanofiber membrane was obtained by incorporating PAN as an additive reported to have a potential application for treating industrial wastewater. Subsequently, investigating the morphological data suggested that the synthesized PES/PAN blended nanofiber membrane was beads free with an ultrathin diameter (151.5 nm) with good hydrophilicity, thermal and mechanical stability that are essential in the adsorption process. In this case, MB adsorption equilibrium reached within 12 h for PES/PAN and 18 h for PES, and adsorption capacity of MB reached to 1010 mg_{MB}/g at neutral pH under room temperature by maintaining pseudo-second-order model (PSO) and the Langmuir model. Adsorption capacity was reduced in the presence of some inorganic anions and recyclability continued up to 5 cycles.
- In this work, long-term (98 days) production and *in-situ* recovery of volatile fatty acids from food waste was obtained using a microfiltration-assisted anaerobic membrane bioreactor. The higher concentrations of VFAs above 16 g/L (0.2 gVFA/gVS_{added}) was achieved thanks to the inhibition of methanogenesis. MBR filtration capabilities were challenged at high TSS content of above 45 g/L in this study. The purification and concentration of VFAs were boosted after the combination of a downstream ultrafiltration after the microfiltration of the VFAs effluent. A permeate that is rich in VFAs could be successfully recovered through ultrafiltration using 10 and 50 kDa MWCO membranes. The recovered final solution is free of particles and microorganisms, low in COD (other than that contributed by VFAs), ammonium and phosphorous content. However, it was observed that the purified concentration of VFAs after MF-UF was not ready to use directly for the final application because of having other substances. Therefore, another downstream purification process is required, such as adsorption, distillation, nanofiltration/reverse osmosis in order to get high purity VFAs solution.
- Thus, the present study has been employed NF as an effective downstream process for the removal and/or recovery of VFAs and other medium nutrients from the effluent of food waste AD. Two commercially available nanofiltration membranes of 200-300 Da and 300-500 Da MWCO were used at varying solution pH (4 to 9). The nanofiltered permeate was almost particle-free solution (more than 80% of solids substances eliminated), plus more than 90% of COD was removed at pH 9. Alongside, the recovered concentration of ammonia and NH⁴⁺-N and PO₄³⁻-P recovery was increased at higher working pH (9). It was proven that at higher pH VFAs recovery

was enhanced, with acetic acid exhibiting high recovery rates of up to 98% at a pH of 9. However, in contradiction to lower pH ranges (pH 4) increase in the pH came at the expense of reduction in permeates flux ($52.91 \text{ l m}^{-2}\text{h}^{-1}$ for 200-300 Da). The electrostatic state of the membrane, forms of acids and membrane pore size played defining roles during NF at different pH. Furthermore, two approaches of NF sequencing and recirculation were applied to the feed solution, where through sequencing complete recovery for butyric, valeric and caproic acids were obtained by the 3rd cycle. Overall, the results presented provide clear evidence for the suitability of pressure-driven membrane filtration for VFAs recovery in a waste-based biorefinery.

FUTURE PERSPECTIVE

Research undertaken in this thesis contributes to a better understanding of the possible use of electrospun nanofiber membrane in the purification of food industries wastewater and pressure-driven membrane filtration in recovering resources from food waste-based feedstock. Although the results obtained suggested the feasibility of both membrane types, future research and development efforts might focus on the following areas:

- Electrospun nanofiber membrane cited their less mechanical properties and stability that are unreliable for long-term operation, preparation of hybrid electrospun nanofibers-based membranes by incorporating various high-performance polymers and nanomaterials should be carried out in order to tailor their functional properties (creating more pollutants capture sites on their surface) towards effective treatment of industrial wastewater.
- The application of electrospun nanofibers membranes should be extended by treating other kinds of food dyes, COD, BOD, phosphorous, ammonia, and real food industry wastewater effluent contained various substrates for enhancing their technical and economic feasibility.
- The integration of electrospun nanofibers membranes into the pressure-driven membrane filtration in replacing the conventional membranes should be performed in order to set up next-generation electrospun nanofibers membranes filtration based technology for resource recovery as well.
- Driven by the promising performance of the pressure-driven membrane filtration for VFAs recovery, it is also interesting to utilize machine learning insights for further process intensification.

REFERENCES

- Abels, C., Carstensen, F. & Wessling, M. (2013) 'Membrane processes in biorefinery applications', *J. Membr. Sci.*, 444, pp. 285-317. <https://doi.org/10.1016/j.memsci.2013.05.030>
- Abidi, A., Gherraf, N., Ladjel, S., et al. (2016) 'Effect of operating parameters on the selectivity of nanofiltration phosphates transfer through a Nanomax-50 membrane', *Arab. J. Chem.*, 9, pp. S334-S341. <https://doi.org/10.1016/j.arabjc.2011.04.014>
- Acharya, C., Nakhla, G. & Bassi, A. (2006a) 'Operational Optimization and Mass Balances in a Two-Stage MBR Treating High Strength Pet Food Wastewater', *Journal of Environmental Engineering*, 132, pp. 810-817. [https://doi.org/10.1061/\(asce\)0733-9372\(2006\)132:7\(810\)](https://doi.org/10.1061/(asce)0733-9372(2006)132:7(810))
- Acharya, C., Nakhla, G., Bassi, A., et al. (2006b) 'Treatment of High-Strength Pet Food Wastewater Using Two-Stage Membrane Bioreactors', *Water Environment Research*, 78, pp. 661-670. <https://doi.org/10.2175/106143006X99812>
- Aderibigbe, D. O., Giwa, A.-R. A. & Bello, I. A. (2017) 'Characterization and treatment of wastewater from food processing industry: A review', *Imam Journal of Applied Sciences*, 2, pp. 27.
- Afonso, M. D. (2012) 'Assessment of NF and RO for the potential concentration of acetic acid and furfural from the condensate of eucalyptus spent sulphite liquor', *Sep. Purif. Technol.*, 99, pp. 86-90. <https://doi.org/10.1016/j.seppur.2012.08.027>
- Aghapour Aktij, S., Zirehpour, A., Mollahosseini, A., et al. (2020a) 'Feasibility of membrane processes for the recovery and purification of bio-based volatile fatty acids: A comprehensive review', *Journal of Industrial and Engineering Chemistry*, 81, pp. 24-40. <https://doi.org/10.1016/j.jiec.2019.09.009>
- Aghapour Aktij, S., Zirehpour, A., Mollahosseini, A., et al. (2020b) 'Feasibility of membrane processes for the recovery and purification of bio-based volatile fatty acids: A comprehensive review', *J. Ind. Eng. Chem.*, 81, pp. 24-40. <https://doi.org/10.1016/j.jiec.2019.09.009>
- Agnihotri, S., Yin, D.-M., Mahboubi, A., et al. (2022) 'A glimpse of the world of volatile fatty acids production and application: A review', *Bioengineered.*, 13, pp. 1249-1275. 10.1080/21655979.2021.1996044

- Ahmad, N. N. R., Ang, W. L., Leo, C. P., et al. (2021) 'Current advances in membrane technologies for saline wastewater treatment: A comprehensive review', *Desalination*, 517, pp. 115170. <https://doi.org/10.1016/j.desal.2021.115170>
- Ahsan, L., Jahan, M. S. & Ni, Y. (2013) 'Recovery of acetic acid from the prehydrolysis liquor of kraft based dissolving pulp production process: Sodium hydroxide back extraction from the trioctylamine/octanol system', *Ind. Eng. Chem. Res.*, 52, pp. 9270-9275. <https://doi.org/10.1021/ie401285v>
- Ahsan, L., Jahan, M. S. & Ni, Y. (2014) 'Recovering/concentrating of hemicellulosic sugars and acetic acid by nanofiltration and reverse osmosis from prehydrolysis liquor of kraft based hardwood dissolving pulp process', *Bioresour. Technol.*, 155, pp. 111-115. <https://doi.org/10.1016/j.biortech.2013.12.096>
- Aijaz, M. O., Karim, M. R., Alharbi, H. F., et al. (2021) 'Magnetic/polyetherimide-acrylonitrile composite nanofibers for nickel ion removal from aqueous solution', *Membranes*, 11, pp. 50. <https://doi.org/10.3390/membranes11010050>
- Al-Amoudi, A. & Lovitt, R. W. (2007) 'Fouling strategies and the cleaning system of NF membranes and factors affecting cleaning efficiency', *J. Membr. Sci.*, 303, pp. 4-28. <https://doi.org/10.1016/j.memsci.2007.06.002>
- Al-Amoudi, A., Williams, P., Al-Hobaib, A. S., et al. (2008) 'Cleaning results of new and fouled nanofiltration membrane characterized by contact angle, updated DSPM, flux and salts rejection', *Appl. Surf. Sci.*, 254, pp. 3983-3992. <https://doi.org/10.1016/j.apsusc.2007.12.052>
- Al-Amshawe, S., Yunus, M. Y. B. M., Azoddein, A. A. M., et al. (2020) 'Electrodialysis desalination for water and wastewater: A review', *Chemical Engineering Journal*, 380, pp. 122231. <https://doi.org/10.1016/j.cej.2019.122231>
- Al-Asheh, S., Bagheri, M. & Aidan, A. (2021) 'Membrane bioreactor for wastewater treatment: A review', *Case Studies in Chemical and Environmental Engineering*, 4, pp. 100109. <https://doi.org/10.1016/j.cscee.2021.100109>
- Al-Ghafri, B., Bora, T., Sathe, P., et al. (2018) 'Photocatalytic microbial removal and degradation of organic contaminants of water using PES fibers', *Applied Catalysis B: Environmental*, 233, pp. 136-142. <https://doi.org/10.1016/j.apcatb.2018.03.095>
- Al-Husaini, I. S., Lau, W.-J., Yusoff, A. R. M., et al. (2021a) 'Synthesis of functional hydrophilic polyethersulfone-based electrospun nanofibrous membranes for water treatment', *J. Environ. Chem. Eng.*, 9, pp. 104728. <https://doi.org/10.1016/j.jece.2020.104728>
- Al-Husaini, I. S., Lau, W.-J., Yusoff, A. R. M., et al. (2021b) 'Synthesis of functional hydrophilic polyethersulfone-based electrospun nanofibrous membranes for water treatment', *Journal of Environmental Chemical Engineering*, 9, pp. 104728. <https://doi.org/10.1016/j.jece.2020.104728>

- Ali, A. S. M., El-Aassar, M. R., Hashem, F. S., et al. (2019) 'Surface Modified of Cellulose Acetate Electrospun Nanofibers by Polyaniline/ β -cyclodextrin Composite for Removal of Cationic Dye from Aqueous Medium', *Fibers and Polymers*, 20, pp. 2057-2069. [10.1007/s12221-019-9162-y](https://doi.org/10.1007/s12221-019-9162-y)
- Alkhudhiri, A., Darwish, N. & Hilal, N. (2012) 'Membrane distillation: A comprehensive review', *Desalination*, 287, pp. 2-18. <https://doi.org/10.1016/j.desal.2011.08.027>
- Alsebaei, M. K. & Ahmad, A. L. (2020) 'Membrane distillation: Progress in the improvement of dedicated membranes for enhanced hydrophobicity and desalination performance', *Journal of Industrial and Engineering Chemistry*, 86, pp. 13-34.
- Amirilargani, M., Sabetghadam, A. & Mohammadi, T. (2012) 'Polyethersulfone/polyacrylonitrile blend ultrafiltration membranes with different molecular weight of polyethylene glycol: preparation, morphology and antifouling properties', *Polym. Adv. Technol.*, 23, pp. 398-407. <https://doi.org/10.1002/pat.1888>
- Anasthas, H. M. & Gaikar, V. G. (2001) 'Adsorption of acetic acid on ion-exchange resins in non-aqueous conditions', *React. Funct. Polym.*, 47, pp. 23-35. [https://doi.org/10.1016/S1381-5148\(00\)00066-3](https://doi.org/10.1016/S1381-5148(00)00066-3)
- Anderson, R. B., Hamielec, A. E. & Stifel, G. R. (1968) 'Diffusion-controlled adsorption processes', *Can. J. Chem. Eng.*, 46, pp. 419-423. <https://doi.org/10.1002/cjce.5450460607>
- Anvari, A., Azimi Yancheshme, A., Kekre, K. M., et al. (2020) 'State-of-the-art methods for overcoming temperature polarization in membrane distillation process: A review', *Journal of Membrane Science*, 616, pp. 118413. <https://doi.org/10.1016/j.memsci.2020.118413>
- Arantes, M. K., Alves, H. J., Sequinel, R., et al. (2017) 'Treatment of brewery wastewater and its use for biological production of methane and hydrogen', *International Journal of Hydrogen Energy*, 42, pp. 26243-26256. <https://doi.org/10.1016/j.ijhydene.2017.08.206>
- Arslan, D., Zhang, Y., Steinbusch, K. J. J., et al. (2017) 'In-situ carboxylate recovery and simultaneous pH control with tailor-configured bipolar membrane electro dialysis during continuous mixed culture fermentation', *Sep. Purif. Technol.*, 175, pp. 27-35. <https://doi.org/10.1016/j.seppur.2016.11.032>
- Asfand, F. & Bourouis, M. (2015) 'A review of membrane contactors applied in absorption refrigeration systems', *Renew. Sust. Energ. Rev.*, 45, pp. 173-191. <https://doi.org/10.1016/j.rser.2015.01.054>
- Asgharnejad, H., Khorshidi Nazloo, E., Madani Larijani, M., et al. (2021) 'Comprehensive review of water management and wastewater treatment in food processing industries in the framework of water-food-environment nexus', *Comprehensive Reviews in Food Science and Food Safety*, pp. <https://doi.org/10.1111/1541-4337.12782>
- Ashraf, A., Ramamurthy, R. & Rene, E. R. (2021) 'Wastewater treatment and resource recovery technologies in the brewery industry: Current trends and

- emerging practices', *Sustainable Energy Technologies and Assessments*, 47, pp. 101432. <https://doi.org/10.1016/j.seta.2021.101432>
- Atasoy, M., Owusu-Agyeman, I., Plaza, E., et al. (2018) 'Bio-based volatile fatty acid production and recovery from waste streams: Current status and future challenges', *Bioresour. Technol.*, 268, pp. 773-786. <https://doi.org/10.1016/j.biortech.2018.07.042>
- Awad, R., Haghghat Mamaghani, A., Boluk, Y., et al. (2021a) 'Synthesis and characterization of electrospun PAN-based activated carbon nanofibers reinforced with cellulose nanocrystals for adsorption of VOCs', *Chem. Eng. J.*, 410, pp. 128412. <https://doi.org/10.1016/j.cej.2021.128412>
- Awad, R., Haghghat Mamaghani, A., Boluk, Y., et al. (2021b) 'Synthesis and characterization of electrospun PAN-based activated carbon nanofibers reinforced with cellulose nanocrystals for adsorption of VOCs', *Chemical Engineering Journal*, 410, pp. 128412. <https://doi.org/10.1016/j.cej.2021.128412>
- Awange, J. 2021. *Lake Victoria monitored from space*, Gewerbestr, Springer, Cham.
- Aydin, S., Yesil, H. & Tugtas, A. E. (2018) 'Recovery of mixed volatile fatty acids from anaerobically fermented organic wastes by vapor permeation membrane contactors', *Bioresour. Technol.*, 250, pp. 548-555. <https://doi.org/10.1016/j.biortech.2017.11.061>
- Ayyaru, S. & Ahn, Y.-H. (2018a) 'Fabrication and separation performance of polyethersulfone/sulfonated TiO₂ (PES-STiO₂) ultrafiltration membranes for fouling mitigation', *J. Ind. Eng. Chem.*, 67, pp. 199-209. <https://doi.org/10.1016/j.jiec.2018.06.030>
- Ayyaru, S. & Ahn, Y.-H. (2018b) 'Fabrication and separation performance of polyethersulfone/sulfonated TiO₂ (PES-STiO₂) ultrafiltration membranes for fouling mitigation', *Journal of Industrial and Engineering Chemistry*, 67, pp. 199-209. <https://doi.org/10.1016/j.jiec.2018.06.030>
- Aziz, M. & Kasongo, G. (2021a) 'The removal of selected inorganics from municipal membrane bioreactor wastewater using UF/NF/RO membranes for water reuse application: A pilot-scale study', *Membranes.*, 11, pp. 117. <https://doi.org/10.3390/membranes11020117>
- Aziz, M. & Kasongo, G. (2021b) 'The removal of selected inorganics from municipal membrane bioreactor wastewater using UF/NF/RO membranes for water reuse application: A pilot-scale study', *Membranes*, 11, pp. 117. <https://doi.org/10.3390/membranes11020117>
- Bae, J., Baek, I. & Choi, H. (2016a) 'Mechanically enhanced PES electrospun nanofiber membranes (ENMs) for microfiltration: The effects of ENM properties on membrane performance', *Water. Res.*, 105, pp. 406-412. <https://doi.org/10.1016/j.watres.2016.09.020>
- Bae, J., Baek, I. & Choi, H. (2016b) 'Mechanically enhanced PES electrospun nanofiber membranes (ENMs) for microfiltration: The effects of ENM properties on membrane performance', *Water Research*, 105, pp. 406-412. <https://doi.org/10.1016/j.watres.2016.09.020>

- Baek, Y., Kang, J., Theato, P., et al. (2012) 'Measuring hydrophilicity of RO membranes by contact angles via sessile drop and captive bubble method: A comparative study', *Desalination.*, 303, pp. 23-28. <https://doi.org/10.1016/j.desal.2012.07.006>
- Bai, L., Jia, L., Yan, Z., et al. (2018) 'Plasma-etched electrospun nanofiber membrane as adsorbent for dye removal', *Chemical Engineering Research and Design*, 132, pp. 445-451. <https://doi.org/10.1016/j.cherd.2018.01.046>
- Baig, N., Shetty, S., Moustafa, M. S., et al. (2021) 'Selective removal of toxic organic dyes using Tröger base-containing sulfone copolymers made from a metal-free thiol-yne click reaction followed by oxidation', *RSC Advances*, 11, pp. 21170-21178. 10.1039/D1RA03783H
- Baker, R. W. 2012. *Membrane technology and applications*, New Jersey, United States, John Wiley & Sons.
- Barbera, M. & Gurnari, G. 2018. *Wastewater treatment and reuse in the food industry*, Gewerbestr, Springer, Cham.
- Barrera-Díaz, C., Roa-Morales, G., Ávila-Córdoba, L., et al. (2006) 'Electrochemical Treatment Applied to Food-Processing Industrial Wastewater', *Industrial & Engineering Chemistry Research*, 45, pp. 34-38. 10.1021/ie050594k
- Barth, C., Gonçalves, M. C., Pires, A. T. N., et al. (2000) 'Asymmetric polysulfone and polyethersulfone membranes: effects of thermodynamic conditions during formation on their performance', *J. Membr. Sci.*, 169, pp. 287-299. [https://doi.org/10.1016/S0376-7388\(99\)00344-0](https://doi.org/10.1016/S0376-7388(99)00344-0)
- Battista, F., Remelli, G., Zanzoni, S., et al. (2020) 'Valorization of residual orange peels: Limonene recovery, volatile fatty acids, and biogas production', *ACS Sustainable Chem. Eng.*, 8, pp. 6834-6843. <https://doi.org/10.1021/acssuschemeng.0c01735>
- Bélafi-Bakó, K., Nemestóthy, N. & Gubicza, L. (2004) 'A study on applications of membrane techniques in bioconversion of fumaric acid to L-malic acid', *Desalination.*, 162, pp. 301-306. [https://doi.org/10.1016/S0011-9164\(04\)00063-3](https://doi.org/10.1016/S0011-9164(04)00063-3)
- Bellona, C. & Drewes, J. E. (2005) 'The role of membrane surface charge and solute physico-chemical properties in the rejection of organic acids by NF membranes', *J. Membr. Sci.*, 249, pp. 227-234. <https://doi.org/10.1016/j.memsci.2004.09.041>
- Bellona, C., Drewes, J. E., Xu, P., et al. (2004) 'Factors affecting the rejection of organic solutes during NF/RO treatment—a literature review', *Water. Res.*, 38, pp. 2795-2809. <https://doi.org/10.1016/j.watres.2004.03.034>
- Beltrán-Heredia, J., Torregrosa, J., García, J., et al. (2001) 'Degradation of olive mill wastewater by the combination of Fenton's reagent and ozonation processes with an aerobic biological treatment', *Water Science and Technology*, 44, pp. 103-108. <https://doi.org/10.2166/wst.2001.0262>
- Benamar, A., Mahjoubi, F. Z., Barka, N., et al. (2020) 'Olive mill wastewater treatment using infiltration percolation in column followed by aerobic

- biological treatment', *SN Applied Sciences*, 2, pp. 655. 10.1007/s42452-020-2481-1
- Berglund, K. A., Yedur, S. & Dunuwila, D. D. 1999. Succinic acid production and purification. Michigan: Google Patents.
- Bermeo, M. A., Maturana, A., Estévez, S. L., et al. (2003) 'Use of electrodialysis as a vfa recovery process From acidogenic of msw synthetic leachates', *Rev. de Ing.*, pp. 97-102. <http://dx.doi.org/10.16924%2Fria.v0i17.504>
- Bhatia, S. K. & Yang, Y.-H. (2017) 'Microbial production of volatile fatty acids: current status and future perspectives', *Rev. Environ. Sci. Biotechnol.*, 16, pp. 327-345. <https://doi.org/10.1007/s11157-017-9431-4>
- Bhatt, A. H., Ren, Z. & Tao, L. (2020) 'Value proposition of untapped wet wastes: Carboxylic acid production through anaerobic digestion', *iScience.*, 23, pp. 101221. <https://doi.org/10.1016/j.isci.2020.101221>
- Bianchi, C. L., Ragaini, V., Pirola, C., et al. (2003) 'A new method to clean industrial water from acetic acid via esterification', *Appl. Catal. B. Environ.*, 40, pp. 93-99. [https://doi.org/10.1016/S0926-3373\(02\)00144-3](https://doi.org/10.1016/S0926-3373(02)00144-3)
- Bigdeloo, M., Teymourian, T., Kowsari, E., et al. (2021) 'Sustainability and circular economy of food wastes: waste reduction strategies, higher recycling methods, and improved valorization', *Mater. Circ. Econ.*, 3, pp. 3. <https://doi.org/10.1007/s42824-021-00017-3>
- Bjorge, D., Daels, N., De Vrieze, S., et al. (2009) 'Performance assessment of electrospun nanofibers for filter applications', *Desalination*, 249, pp. 942-948. <https://doi.org/10.1016/j.desal.2009.06.064>
- Blahušiak, M., Schlosser, Š. & Cvengroš, J. (2012) 'Simulation of a new regeneration process of solvents with ionic liquid by short-path distillation', *Sep. Purif. Technol.*, 97, pp. 186-194. <https://doi.org/10.1016/j.seppur.2012.03.010>
- Blandin, G., Rosselló, B., Monsalvo, V. M., et al. (2019) 'Volatile fatty acids concentration in real wastewater by forward osmosis', *J. Membr. Sci.*, 575, pp. 60-70. <https://doi.org/10.1016/j.memsci.2019.01.006>
- Bornillo, K. A. S., Kim, S. & Choi, H. (2020) 'Cu (II) removal using electrospun dual-responsive polyethersulfone-poly (dimethyl amino) ethyl methacrylate (PES-PDMAEMA) blend nanofibers', *Chemosphere.*, 242, pp. 125287. <https://doi.org/10.1016/j.chemosphere.2019.125287>
- Bouchareb, R., Bilici, Z. & Dizge, N. (2021) 'Potato Processing Wastewater Treatment Using a Combined Process of Chemical Coagulation and Membrane Filtration', *CLEAN – Soil, Air, Water*, 49, pp. 2100017. <https://doi.org/10.1002/clen.202100017>
- Bowen, T. C., Li, S., Noble, R. D., et al. (2003) 'Driving force for pervaporation through zeolite membranes', *J. Membr. Sci.*, 225, pp. 165-176. <https://doi.org/10.1016/j.memsci.2003.07.016>
- Bowen, W. R., Cheng, S. Y., Doneva, T. A., et al. (2005) 'Manufacture and characterisation of polyetherimide/sulfonated poly(ether ether ketone) blend membranes', *J. Membr. Sci.*, 250, pp. 1-10. <https://doi.org/10.1016/j.memsci.2004.07.004>

- Braguglia, C. M., Gallipoli, A., Gianico, A., et al. (2018) 'Anaerobic bioconversion of food waste into energy: A critical review', *Bioresource Technology*, 248, pp. 37-56. <https://doi.org/10.1016/j.biortech.2017.06.145>
- Bruni, C., Foglia, A., Eusebi, A. L., et al. (2021) 'Targeted Bio-Based Volatile Fatty Acid Production from Waste Streams through Anaerobic Fermentation: Link between Process Parameters and Operating Scale', *ACS Sustainable Chemistry & Engineering*, 9, pp. 9970-9987. 10.1021/acssuschemeng.1c02195
- Bui, N.-N. & McCutcheon, J. R. (2013a) 'Hydrophilic Nanofibers as New Supports for Thin Film Composite Membranes for Engineered Osmosis', *Environmental Science & Technology*, 47, pp. 1761-1769. 10.1021/es304215g
- Bui, N.-N. & McCutcheon, J. R. (2013b) 'Hydrophilic nanofibers as new supports for thin film composite membranes for engineered osmosis', *Environ. Sci. Technol.*, 47, pp. 1761-1769. <https://doi.org/10.1021/es304215g>
- Bustillo-Lecompte, C., Mehrvar, M. & Quiñones-Bolaños, E. (2016) 'Slaughterhouse wastewater characterization and treatment: an economic and public health necessity of the meat processing industry in Ontario, Canada', *Journal of Geoscience and Environment Protection*, 4, pp. 175-186.
- Cagnetta, C., D'Haese, A., Coma, M., et al. (2017) 'Increased carboxylate production in high-rate activated A-sludge by forward osmosis thickening', *Chem. Eng. J.*, 312, pp. 68-78. <https://doi.org/10.1016/j.cej.2016.11.119>
- Camarillo, R., Asencio, I. & Rincón, J. (2009) 'Micellar enhanced ultrafiltration for phosphorus removal in domestic wastewater', *Desalin. Water. Treat.*, 6, pp. 211-216. <https://doi.org/10.5004/dwt.2009.640>
- Cao, Q., Huang, F., Zhuang, Z., et al. (2012a) 'A study of the potential application of nano-Mg(OH)₂ in adsorbing low concentrations of uranyl tricarbonate from water', *Nanoscale.*, 4, pp. 2423-2430. 10.1039/C2NR11993E
- Cao, Q., Huang, F., Zhuang, Z., et al. (2012b) 'A study of the potential application of nano-Mg(OH)₂ in adsorbing low concentrations of uranyl tricarbonate from water', *Nanoscale*, 4, pp. 2423-2430. 10.1039/C2NR11993E
- Capar, G., Yilmaz, L. & Yetis, U. (2006) 'Reclamation of acid dye bath wastewater: Effect of pH on nanofiltration performance', *J. Membr. Sci.*, 281, pp. 560-569. <https://doi.org/10.1016/j.memsci.2006.04.025>
- Cath, T. Y., Childress, A. E. & Elimelech, M. (2006) 'Forward osmosis: principles, applications, and recent developments', *J. Membr. Sci.*, 281, pp. 70-87. <https://doi.org/10.1016/j.memsci.2006.05.048>
- Cebreiros, F., Guigou, M. D. & Cabrera, M. N. (2017) 'Integrated forest biorefineries: Recovery of acetic acid as a by-product from eucalyptus wood hemicellulosic hydrolysates by solvent extraction', *Ind. Crops. Prod.*, 109, pp. 101-108. <https://doi.org/10.1016/j.indcrop.2017.08.012>
- Cecconet, D., Molognoni, D., Callegari, A., et al. (2018) 'Agro-food industry wastewater treatment with microbial fuel cells: Energetic recovery issues',

- International Journal of Hydrogen Energy*, 43, pp. 500-511.
<https://doi.org/10.1016/j.ijhydene.2017.07.231>
- Cevasco, G. & Chiappe, C. (2014) 'Are ionic liquids a proper solution to current environmental challenges?', *Green. Chem.*, 16, pp. 2375-2385.
<https://doi.org/10.1039/C3GC42096E>
- Chabalala, M. B., Al-Abri, M. Z., Mamba, B. B., et al. (2021) 'Mechanistic aspects for the enhanced adsorption of bromophenol blue and atrazine over cyclodextrin modified polyacrylonitrile nanofiber membranes', *Chem. Eng. Res. Des.*, 169, pp. 19-32. <https://doi.org/10.1016/j.cherd.2021.02.010>
- Chalmers Brown, R., Tuffou, R., Massanet Nicolau, J., et al. (2020) 'Overcoming nutrient loss during volatile fatty acid recovery from fermentation media by addition of electro dialysis to a polytetrafluoroethylene membrane stack', *Bioresour. Technol.*, 301, pp. 122543.
<https://doi.org/10.1016/j.biortech.2019.122543>
- Chan, C. H., Chia, C. H., Zakaria, S., et al. (2015) 'Cellulose nanofibrils: a rapid adsorbent for the removal of methylene blue', *RSC Advances*, 5, pp. 18204-18212. 10.1039/C4RA15754K
- Chan, G. Y. S., Chang, J., Kurniawan, T. A., et al. (2007) 'Removal of non-biodegradable compounds from stabilized leachate using VSEPRO membrane filtration', *Desalination*, 202, pp. 310-317.
<https://doi.org/10.1016/j.desal.2005.12.069>
- Chatzipaschali, A. A. & Stamatis, A. G. (2012) 'Biotechnological utilization with a focus on anaerobic treatment of cheese whey: Current status and prospects', *Energies*, 5, pp. 3492-3525. <https://doi.org/10.3390/en5093492>
- Cheah, Y.-K., Vidal-Antich, C., Dosta, J., et al. (2019) 'Volatile fatty acid production from mesophilic acidogenic fermentation of organic fraction of municipal solid waste and food waste under acidic and alkaline pH', *Environmental Science and Pollution Research*, 26, pp. 35509-35522. 10.1007/s11356-019-05394-6
- Chen, F., Wang, X., Liu, W., et al. (2016) 'Selective extraction of nitric and acetic acids from etching waste acid using N235 and MIBK mixtures', *Sep. Purif. Technol.*, 169, pp. 50-58. <https://doi.org/10.1016/j.seppur.2016.06.008>
- Chen, H., Meng, H., Nie, Z., et al. (2013) 'Polyhydroxyalkanoate production from fermented volatile fatty acids: effect of pH and feeding regimes', *Bioresour. Technol.*, 128, pp. 533-538. <https://doi.org/10.1016/j.biortech.2012.10.121>
- Chen, H., Shen, H., Su, H., et al. (2017) 'High-efficiency bioconversion of kitchen garbage to biobutanol using an enzymatic cocktail procedure', *Bioresource Technology*, 245, pp. 1110-1121.
<https://doi.org/10.1016/j.biortech.2017.09.056>
- Chen, K., Nikam, S. P., Zander, Z. K., et al. (2020) 'Continuous Fabrication of Antimicrobial Nanofiber Mats Using Post-Electrospinning Functionalization for Roll-to-Roll Scale-Up', *ACS Applied Polymer Materials*, 2, pp. 304-316. 10.1021/acsapm.9b00798

- Chen, S., Du, Y., Zhang, X., et al. (2018) 'One-step electrospinning of negatively-charged polyethersulfone nanofibrous membranes for selective removal of cationic dyes', *J. Taiwan. Inst. Chem. Eng.*, 82, pp. 179-188. <https://doi.org/10.1016/j.jtice.2017.11.018>
- Chen, Y., Ruhyadi, R., Huang, J., et al. (2021) 'A novel strategy for improving volatile fatty acid purity, phosphorus removal efficiency, and fermented sludge dewaterability during waste activated sludge fermentation', *Waste Manage.*, 119, pp. 195-201. <https://doi.org/10.1016/j.wasman.2020.09.044>
- Cheng, J., Zhan, C., Wu, J., et al. (2020) 'Highly Efficient Removal of Methylene Blue Dye from an Aqueous Solution Using Cellulose Acetate Nanofibrous Membranes Modified by Polydopamine', *ACS Omega*, 5, pp. 5389-5400. 10.1021/acsomega.9b04425
- Chiacchierini, E., Restuccia, D. & Vinci, G. (2004) 'Bioremediation of Food Industry Effluents: Recent Applications of Free and Immobilised Polyphenoloxidases', *Food Science and Technology International*, 10, pp. 373-382. 10.1177/1082013204049388
- Childress, A. E. & Elimelech, M. (1996) 'Effect of solution chemistry on the surface charge of polymeric reverse osmosis and nanofiltration membranes', *J. Membr. Sci.*, 119, pp. 253-268. [https://doi.org/10.1016/0376-7388\(96\)00127-5](https://doi.org/10.1016/0376-7388(96)00127-5)
- Cho, Y. H., Lee, H. D. & Park, H. B. (2012) 'Integrated membrane processes for separation and purification of organic acid from a biomass fermentation process', *Ind. Eng. Chem. Res.*, 51, pp. 10207-10219. <https://doi.org/10.1021/ie301023r>
- Choi, J.-d.-r., Chang, H. N. & Han, J.-I. (2011) 'Performance of microbial fuel cell with volatile fatty acids from food wastes', *Biotechnology Letters*, 33, pp. 705-714. 10.1007/s10529-010-0507-2
- Choi, J.-H., Fukushi, K. & Yamamoto, K. (2008) 'A study on the removal of organic acids from wastewaters using nanofiltration membranes', *Sep. Purif. Technol.*, 59, pp. 17-25. <https://doi.org/10.1016/j.seppur.2007.05.021>
- Choi, J.-H. & Ng, H. Y. (2008) 'Effect of membrane type and material on performance of a submerged membrane bioreactor', *Chemosphere.*, 71, pp. 853-859. <https://doi.org/10.1016/j.chemosphere.2007.11.029>
- Choudhari, S. K., Cerrone, F., Woods, T., et al. (2015) 'Pervaporation separation of butyric acid from aqueous and anaerobic digestion (AD) solutions using PEBA based composite membranes', *J. Ind. Eng. Chem.*, 23, pp. 163-170. <https://doi.org/10.1016/j.jiec.2014.08.010>
- Chowdhury, T., Chowdhury, H., Miskat, M. I., et al. 2021. Chapter 19 - Membrane-based technologies for industrial wastewater treatment and resource recovery. In: SHAH, M. P. & RODRIGUEZ-COUTO, S. (eds.) *Membrane-Based Hybrid Processes for Wastewater Treatment*. Elsevier.
- Chu, C.-Y., Tung, L. & Lin, C.-Y. (2013) 'Effect of substrate concentration and pH on biohydrogen production kinetics from food industry wastewater by

- mixed culture', *International Journal of Hydrogen Energy*, 38, pp. 15849-15855. <https://doi.org/10.1016/j.ijhydene.2013.07.088>
- Chu, K. H., Fathizadeh, M., Yu, M., et al. (2017a) 'Evaluation of removal mechanisms in a graphene oxide-coated ceramic ultrafiltration membrane for retention of natural organic matter, pharmaceuticals, and inorganic salts', *ACS Applied Materials & Interfaces*, 9, pp. 40369-40377. <https://doi.org/10.1021/acsami.7b14217>
- Chu, K. H., Fathizadeh, M., Yu, M., et al. (2017b) 'Evaluation of removal mechanisms in a graphene oxide-coated ceramic ultrafiltration membrane for retention of natural organic matter, pharmaceuticals, and inorganic salts', *ACS Appl. Mater. Interfaces.*, 9, pp. 40369-40377. <https://doi.org/10.1021/acsami.7b14217>
- Chung, T.-S., Li, X., Ong, R. C., et al. (2012) 'Emerging forward osmosis (FO) technologies and challenges ahead for clean water and clean energy applications', *Current Opinion in Chemical Engineering*, 1, pp. 246-257. <https://doi.org/10.1016/j.coche.2012.07.004>
- Compton, M., Willis, S., Rezaie, B., et al. (2018) 'Food processing industry energy and water consumption in the Pacific northwest', *Innovative Food Science & Emerging Technologies*, 47, pp. 371-383. <https://doi.org/10.1016/j.ifset.2018.04.001>
- Corzo, B., de la Torre, T., Sans, C., et al. (2017) 'Evaluation of draw solutions and commercially available forward osmosis membrane modules for wastewater reclamation at pilot scale', *Chem. Eng. J.*, 326, pp. 1-8. <https://doi.org/10.1016/j.cej.2017.05.108>
- Coskun, T., Debik, E. & Demir, N. M. (2010) 'Treatment of olive mill wastewaters by nanofiltration and reverse osmosis membranes', *Desalination*, 259, pp. 65-70. <https://doi.org/10.1016/j.desal.2010.04.034>
- Cui, Z. F., Jiang, Y. & Field, R. W. 2010. Fundamentals of pressure-driven membrane separation processes. In: CUI, Z. F. & MURALIDHARA, H. S. (eds.) *Membrane technology*. Elsevier.
- Da Ros, C., Conca, V., Eusebi, A. L., et al. (2020a) 'Sieving of municipal wastewater and recovery of bio-based volatile fatty acids at pilot scale', *Water research*, 174, pp. 115633.
- Da Ros, C., Conca, V., Eusebi, A. L., et al. (2020b) 'Sieving of municipal wastewater and recovery of bio-based volatile fatty acids at pilot scale', *Water. Res.*, 174, pp. 115633. <https://doi.org/10.1016/j.watres.2020.115633>
- Da Silva, A. H. & Miranda, E. A. (2013) 'Adsorption/desorption of organic acids onto different adsorbents for their recovery from fermentation broths', *J. Chem. Eng. Data.*, 58, pp. 1454-1463. <https://doi.org/10.1021/je3008759>
- Dai, K., Wen, J.-L., Wang, Y.-L., et al. (2019) 'Impacts of medium composition and applied current on recovery of volatile fatty acids during coupling of electrodialysis with an anaerobic digester', *J. Clean. Prod.*, 207, pp. 483-489. <https://doi.org/10.1016/j.jclepro.2018.10.019>

- Dave, H. K. & Nath, K. (2016) 'Graphene oxide incorporated novel polyvinyl alcohol composite membrane for pervaporative recovery of acetic acid from vinegar wastewater', *J. Water. Process. Eng.*, 14, pp. 124-134. <https://doi.org/10.1016/j.jwpe.2016.11.002>
- de Carvalho, J. C., Borghetti, I. A., Cartas, L. C., et al. (2018) 'Biorefinery integration of microalgae production into cassava processing industry: Potential and perspectives', *Bioresource Technology*, 247, pp. 1165-1172. <https://doi.org/10.1016/j.biortech.2017.09.213>
- de Nardi, I. R., Del Nery, V., Amorim, A. K. B., et al. (2011) 'Performances of SBR, chemical-DAF and UV disinfection for poultry slaughterhouse wastewater reclamation', *Desalination*, 269, pp. 184-189. <https://doi.org/10.1016/j.desal.2010.10.060>
- Değermenci, N., Cengiz, İ., Yildiz, E., et al. (2016) 'Performance investigation of a jet loop membrane bioreactor for the treatment of an actual olive mill wastewater', *Journal of Environmental Management*, 184, pp. 441-447. <https://doi.org/10.1016/j.jenvman.2016.10.014>
- Deka, B. J., Lee, E.-J., Guo, J., et al. (2019) 'Electrospun Nanofiber Membranes Incorporating PDMS-Aerogel Superhydrophobic Coating with Enhanced Flux and Improved Antiwettability in Membrane Distillation', *Environmental Science & Technology*, 53, pp. 4948-4958. <https://doi.org/10.1021/acs.est.8b07254>
- Demiral, H. & Ercengiz Yildirim, M. (2003) 'Recovery of acetic acid from waste streams by extractive distillation', *Water. Sci. Technol.*, 47, pp. 183-188. <https://doi.org/10.2166/wst.2003.0570>
- Ding, Z., Zhong, L., Wang, X., et al. (2016) 'Effect of lignin-cellulose nanofibrils on the hydrophilicity and mechanical properties of polyethersulfone ultrafiltration membranes', *High Performance Polymers*, 28, pp. 1192-1200. [10.1177/0954008315621611](https://doi.org/10.1177/0954008315621611)
- Dizge, N., Soydemir, G., Karagunduz, A., et al. (2011) 'Influence of type and pore size of membranes on cross flow microfiltration of biological suspension', *J. Membr. Sci.*, 366, pp. 278-285. <https://doi.org/10.1016/j.memsci.2010.10.010>
- Dobosz, K. M., Kuo-Leblanc, C. A., Martin, T. J., et al. (2017) 'Ultrafiltration membranes enhanced with electrospun nanofibers exhibit improved flux and fouling resistance', *Industrial & Engineering Chemistry Research*, 56, pp. 5724-5733. <https://doi.org/10.1021/acs.iecr.7b00631>
- Dogan, Y. E., Satilmis, B. & Uyar, T. (2019) 'Crosslinked PolyCyclodextrin/PolyBenzoxazine electrospun microfibers for selective removal of methylene blue from an aqueous system', *European Polymer Journal*, 119, pp. 311-321. <https://doi.org/10.1016/j.eurpolymj.2019.08.005>
- Dolar, D., Košutić, K. & Ašperger, D. (2012) 'Influence of adsorption of pharmaceuticals onto RO/NF membranes on their removal from water', *Water. Air. Soil. Pollut.*, 224, pp. 1377. <https://doi.org/10.1007/s11270-012-1377-0>

- Donnan, F. G. (1995) 'Theory of membrane equilibria and membrane potentials in the presence of non-dialysing electrolytes. A contribution to physical-chemical physiology', *J. Membr. Sci.*, 100, pp. 45-55. [https://doi.org/10.1016/0376-7388\(94\)00297-C](https://doi.org/10.1016/0376-7388(94)00297-C)
- Drioli, E., Ali, A. & Macedonio, F. (2015) 'Membrane distillation: Recent developments and perspectives', *Desalination*, 356, pp. 56-84. <https://doi.org/10.1016/j.desal.2014.10.028>
- Drioli, E., Curcio, E. & Di Profio, G. (2005) 'State of the art and recent progresses in membrane contactors', *Chem. Eng. Res. Des.*, 83, pp. 223-233. <https://doi.org/10.1205/cherd.04203>
- Ecker, J., Raab, T. & Harasek, M. (2012) 'Nanofiltration as key technology for the separation of LA and AA', *J. Membr. Sci.*, 389, pp. 389-398. <https://doi.org/10.1016/j.memsci.2011.11.004>
- Eda, S., Kumari, A., Thella, P. K., et al. (2017) 'Recovery of volatile fatty acids by reactive extraction using tri-n-octylamine and tri-butyl phosphate in different solvents: Equilibrium studies, pH and temperature effect, and optimization using multivariate taguchi approach', *Can. J. Chem. Eng.*, 95, pp. 1373-1387. <https://doi.org/10.1002/cjce.22803>
- El-Abbassi, A., Hafidi, A., Khayet, M., et al. (2013a) 'Integrated direct contact membrane distillation for olive mill wastewater treatment', *Desalination*, 323, pp. 31-38. <https://doi.org/10.1016/j.desal.2012.06.014>
- El-Abbassi, A., Khayet, M., Kiai, H., et al. (2013b) 'Treatment of crude olive mill wastewaters by osmotic distillation and osmotic membrane distillation', *Separation and Purification Technology*, 104, pp. 327-332. <https://doi.org/10.1016/j.seppur.2012.12.006>
- El-Abbassi, A., Kiai, H., Hafidi, A., et al. (2012) 'Treatment of olive mill wastewater by membrane distillation using polytetrafluoroethylene membranes', *Separation and Purification Technology*, 98, pp. 55-61. <https://doi.org/10.1016/j.seppur.2012.06.026>
- El-Sayed, Y. & Bandosz, T. J. (2004) 'Adsorption of valeric acid from aqueous solution onto activated carbons: role of surface basic sites', *J. Colloid. Interface. Sci.*, 273, pp. 64-72. <https://doi.org/10.1016/j.jcis.2003.10.006>
- El-Wakil, N. A.-E. A., Fahmy, Y., Abou-Zeid, R. E. M., et al. (2010) 'Liquid crystalline behavior of hydroxypropyl cellulose esterified with 4-alkoxybenzoic acid', *Bioresources*, 5, pp. 1834-1845.
- Eregowda, T., Rene, E. R., Rintala, J., et al. (2020) 'Volatile fatty acid adsorption on anion exchange resins: kinetics and selective recovery of acetic acid', *Sep. Sci. Technol.*, 55, pp. 1449-1461. <https://doi.org/10.1080/01496395.2019.1600553>
- Ernst, M., Bismarck, A., Springer, J., et al. (2000) 'Zeta-potential and rejection rates of a polyethersulfone nanofiltration membrane in single salt solutions', *J. Membr. Sci.*, 165, pp. 251-259. [https://doi.org/10.1016/S0376-7388\(99\)00238-0](https://doi.org/10.1016/S0376-7388(99)00238-0)

- Ersu, C. B. & Ong, S. K. (2008) 'Treatment of wastewater containing phenol using a tubular ceramic membrane bioreactor', *Environ. Technol.*, 29, pp. 225-234. <https://doi.org/10.1080/09593330802029012>
- Fargues, C., Lewandowski, R. & Lameloise, M.-L. (2010) 'Evaluation of ion-exchange and adsorbent resins for the detoxification of beet distillery effluents', *Ind. Eng. Chem. Res.*, 49, pp. 9248-9257. <https://doi.org/10.1021/ie100330y>
- Fasahati, P. & Liu, J. 2014. Techno-economic analysis of production and recovery of volatile fatty acids from brown algae using membrane distillation. In: EDEN, M. R., SIIROLA, J. D. & TOWLER, G. P. (eds.) *Comput. Aided. Chem. Eng.*: Elsevier.
- Federation, W. E. & Association, A. (2005) 'Standard methods for the examination of water and wastewater', *American Public Health Association (APHA): Washington, DC, USA*, pp.
- Feng, X. & Huang, R. Y. M. (1997) 'Liquid separation by membrane pervaporation: a review', *Ind. Eng. Chem. Res.*, 36, pp. 1048-1066. <https://doi.org/10.1021/ie960189g>
- Flörke, M., Kynast, E., Bärlund, I., et al. (2013) 'Domestic and industrial water uses of the past 60 years as a mirror of socio-economic development: A global simulation study', *Global Environmental Change*, 23, pp. 144-156. <https://doi.org/10.1016/j.gloenvcha.2012.10.018>
- Fouzia, Y., Abdelouahab, N., Amal, K., et al. (2015) 'Whey ultrafiltration: effect of pH on permeate flux and proteins retention', *World Applied Sciences Journal*, 33, pp. 744-751. 10.5829/idosi.wasj.2015.33.05.149
- Francis, L., Ogunbiyi, O., Saththasivam, J., et al. (2020) 'A comprehensive review of forward osmosis and niche applications', *Environmental Science: Water Research & Technology*, 6, pp. 1986-2015. 10.1039/D0EW00181C
- Freger, V., Arnot, T. C. & Howell, J. A. (2000) 'Separation of concentrated organic/inorganic salt mixtures by nanofiltration', *J. Membr. Sci.*, 178, pp. 185-193. [https://doi.org/10.1016/S0376-7388\(00\)00516-0](https://doi.org/10.1016/S0376-7388(00)00516-0)
- Frenkel, V. S., Cummings, G. A., Maillacheruvu, K. Y., et al. (2017) 'Food-Processing Wastes', *Water Environment Research*, 89, pp. 1360-1383. <https://doi.org/10.2175/106143017X15023776270368>
- Fufachev, E. V., Weckhuysen, B. M. & Bruijninx, P. C. A. (2020) 'Towards catalytic ketonization of volatile fatty acids extracted from fermented wastewater by adsorption', *ACS. Sustainable. Chem. Eng.*, pp. <https://doi.org/10.1021/acssuschemeng.0c03220>
- Galib, M., Elbeshbishy, E., Reid, R., et al. (2016) 'Energy-positive food wastewater treatment using an anaerobic membrane bioreactor (AnMBR)', *Journal of Environmental Management*, 182, pp. 477-485. <https://doi.org/10.1016/j.jenvman.2016.07.098>
- Gangadwala, J., Radulescu, G., Kienle, A., et al. (2008) 'New processes for recovery of acetic acid from waste water', *Clean. Technol. Environ. Policy.*, 10, pp. 245-254. <https://doi.org/10.1007/s10098-007-0101-z>

- Garcia-Aguirre, J., Alvarado-Morales, M., Fotidis, I. A., et al. (2020) 'Up-concentration of succinic acid, lactic acid, and ethanol fermentations broths by forward osmosis', *Biochem. Eng. J.*, 155, pp. 107482. <https://doi.org/10.1016/j.bej.2019.107482>
- Garcia-Castello, E., Cassano, A., Criscuoli, A., et al. (2010) 'Recovery and concentration of polyphenols from olive mill wastewaters by integrated membrane system', *Water Research*, 44, pp. 3883-3892. <https://doi.org/10.1016/j.watres.2010.05.005>
- Garcia, A. A. & King, C. J. (1989) 'The use of basic polymer sorbents for the recovery of acetic acid from dilute aqueous solution', *Ind. Eng. Chem. Res.*, 28, pp. 204-212. <https://doi.org/10.1021/ie00086a013>
- Gebreyohannes, A. Y., Curcio, E., Poerio, T., et al. (2015) 'Treatment of Olive Mill Wastewater by Forward Osmosis', *Separation and Purification Technology*, 147, pp. 292-302. <https://doi.org/10.1016/j.seppur.2015.04.021>
- Gerardo, M. L., Aljohani, N. H. M., Oatley-Radcliffe, D. L., et al. (2015) 'Moving towards sustainable resources: Recovery and fractionation of nutrients from dairy manure digestate using membranes', *Water. Res.*, 80, pp. 80-89. <https://doi.org/10.1016/j.watres.2015.05.016>
- Gerardo, M. L., Zacharof, M. P. & Lovitt, R. W. (2013) 'Strategies for the recovery of nutrients and metals from anaerobically digested dairy farm sludge using cross-flow microfiltration', *Water Research*, 47, pp. 4833-4842. <https://doi.org/10.1016/j.watres.2013.04.019>
- Gherasim, C.-V., Cuhorka, J. & Mikulášek, P. (2013) 'Analysis of lead(II) retention from single salt and binary aqueous solutions by a polyamide nanofiltration membrane: Experimental results and modelling', *J. Membr. Sci.*, 436, pp. 132-144. <https://doi.org/10.1016/j.memsci.2013.02.033>
- Giacobbo, A., Meneguzzi, A., Bernardes, A. M., et al. (2017) 'Pressure-driven membrane processes for the recovery of antioxidant compounds from winery effluents', *Journal of Cleaner Production*, 155, pp. 172-178. <https://doi.org/10.1016/j.jclepro.2016.07.033>
- Goh, E. & Jie, F. (2019) 'To waste or not to waste: Exploring motivational factors of Generation Z hospitality employees towards food wastage in the hospitality industry', *International Journal of Hospitality Management*, 80, pp. 126-135. <https://doi.org/10.1016/j.ijhm.2019.02.005>
- Golob, J., Grilc, V. & Zadnik, B. (1981) 'Extraction of acetic acid from dilute aqueous solutions with trioctylphosphine oxide', *Ind. Eng. Chem. Process. Des. Dev.*, 20, pp. 433-435. <https://doi.org/10.1021/i200014a004>
- Goswami, L., Vinoth Kumar, R., Borah, S. N., et al. (2018) 'Membrane bioreactor and integrated membrane bioreactor systems for micropollutant removal from wastewater: A review', *Journal of Water Process Engineering*, 26, pp. 314-328. <https://doi.org/10.1016/j.jwpe.2018.10.024>
- Gradinaru, L. M., Barbalata-Mandru, M., Drobotu, M., et al. (2020) 'Preparation and Evaluation of Nanofibrous Hydroxypropyl Cellulose and β -Cyclodextrin Polyurethane Composite Mats', *Nanomaterials*, 10, pp. 754.

- Gryta, M. (2008) 'Fouling in direct contact membrane distillation process', *J. Membr. Sci.*, 325, pp. 383-394. <https://doi.org/10.1016/j.memsci.2008.08.001>
- Gryta, M., Markowska-Szczupak, A., Bastrzyk, J., et al. (2013) 'The study of membrane distillation used for separation of fermenting glycerol solutions', *J. Membr. Sci.*, 431, pp. 1-8. <https://doi.org/10.1016/j.memsci.2012.12.032>
- Guillen-Burrieza, E., Ruiz-Aguirre, A., Zaragoza, G., et al. (2014) 'Membrane fouling and cleaning in long term plant-scale membrane distillation operations', *J. Membr. Sci.*, 468, pp. 360-372. <https://doi.org/10.1016/j.memsci.2014.05.064>
- Guirguis, O. W. & Moselhey, M. T. (2013) 'Optical properties of poly (vinyl alcohol)/hydroxypropyl cellulose blends', *Mater Sci: An Indian J*, 9, pp. 8-23.
- Guo, W., Ngo, H.-H. & Li, J. (2012) 'A mini-review on membrane fouling', *Bioresource Technology*, 122, pp. 27-34. <https://doi.org/10.1016/j.biortech.2012.04.089>
- Haider, S., Binagag, F. F., Haider, A., et al. (2014) 'Electrospun oxime-grafted-polyacrylonitrile nanofiber membrane and its application to the adsorption of dyes', *Journal of Polymer Research*, 21, pp. 371. 10.1007/s10965-014-0371-1
- Haider, S., Binagag, F. F., Haider, A., et al. (2015a) 'Adsorption kinetic and isotherm of methylene blue, safranin T and rhodamine B onto electrospun ethylenediamine-grafted-polyacrylonitrile nanofibers membrane', *Desalin. Water. Treat.*, 55, pp. 1609-1619. <https://doi.org/10.1080/19443994.2014.926840>
- Haider, S., Binagag, F. F., Haider, A., et al. (2015b) 'Adsorption kinetic and isotherm of methylene blue, safranin T and rhodamine B onto electrospun ethylenediamine-grafted-polyacrylonitrile nanofibers membrane', *Desalination and Water Treatment*, 55, pp. 1609-1619. 10.1080/19443994.2014.926840
- Halamus, T., Wojciechowski, P. & Bobowska, I. (2008) 'Synthesis and characterization of (hydroxypropyl)cellulose/TiO₂ nanocomposite films', *Polymers for Advanced Technologies*, 19, pp. 807-811. <https://doi.org/10.1002/pat.1038>
- Han, I. S. & Cheryan, M. (1995) 'Nanofiltration of model acetate solutions', *J. Membr. Sci.*, 107, pp. 107-113. [https://doi.org/10.1016/0376-7388\(95\)00107-N](https://doi.org/10.1016/0376-7388(95)00107-N)
- Hang, Y. D. (2004) 'Management and Utilization of Food Processing Wastes', *Journal of Food Science*, 69, pp. CRH104-CRH107. <https://doi.org/10.1111/j.1365-2621.2004.tb13341.x>
- Hart, M. R., Huxsoll, C. C., Tsai, I.-S., et al. (1988) 'Preliminary Studies of Microfiltration for Food Processing Water Reuse', *Journal of Food Protection*, 51, pp. 269-276. <https://doi.org/10.4315/0362-028X-51.4.269>
- Hashim, N. A., Liu, F. & Li, K. (2009) 'A simplified method for preparation of hydrophilic PVDF membranes from an amphiphilic graft copolymer', *J.*

- Membr. Sci.*, 345, pp. 134-141.
<https://doi.org/10.1016/j.memsci.2009.08.032>
- Hassanpour, S., Azhar, F. F. & Bagheri, M. (2019) 'Novel nanogels based on hydroxypropyl cellulose–poly (itaconic acid) for adsorption of methylene blue from aqueous solution: process modeling and optimization using response surface methodology', *Polymer Bulletin*, 76, pp. 933-952.
- Haupt, A. & Lerch, A. (2018) 'Forward osmosis treatment of effluents from dairy and automobile industry – results from short-term experiments to show general applicability', *Water Science and Technology*, 78, pp. 467-475.
10.2166/wst.2018.278
- Hausmanns, S., Laufenberg, G. & Kunz, B. (1996) 'Rejection of acetic acid and its improvement by combination with organic acids in dilute solutions using reverse osmosis', *Desalination.*, 104, pp. 95-98.
[https://doi.org/10.1016/0011-9164\(96\)00030-6](https://doi.org/10.1016/0011-9164(96)00030-6)
- He, Y., Bagley, D. M., Leung, K. T., et al. (2012) 'Recent advances in membrane technologies for biorefining and bioenergy production', *Biotechnol. Adv.*, 30, pp. 817-858. <https://doi.org/10.1016/j.biotechadv.2012.01.015>
- He, Y., Xu, P., Li, C., et al. (2005) 'High-concentration food wastewater treatment by an anaerobic membrane bioreactor', *Water Research*, 39, pp. 4110-4118.
<https://doi.org/10.1016/j.watres.2005.07.030>
- Hestekin, J., Ho, T. & Potts, T. (2010) 'Electrodialysis in the food industry', *Membrane Technology: Volume 3: Membranes for Food Applications*, 3, pp. 75-104.
- Holm-Nielsen, J. B., Al Seadi, T. & Oleskowicz-Popiel, P. (2009) 'The future of anaerobic digestion and biogas utilization', *Bioresource technology*, 100, pp. 5478-5484.
- Homaieghar, S., Zillohu, A. U., Abdelaziz, R., et al. (2016a) 'A Novel Nanohybrid Nanofibrous Adsorbent for Water Purification from Dye Pollutants', *Materials*, 9, pp. 848.
- Homaieghar, S., Zillohu, A. U., Abdelaziz, R., et al. (2016b) 'A novel nanohybrid nanofibrous adsorbent for water purification from dye pollutants', *Materials.*, 9, pp. 848. <https://doi.org/10.3390/ma9100848>
- Homaieghar, S. S., Buhr, K. & Ebert, K. (2010a) 'Polyethersulfone electrospun nanofibrous composite membrane for liquid filtration', *Journal of Membrane Science*, 365, pp. 68-77.
<https://doi.org/10.1016/j.memsci.2010.08.041>
- Homaieghar, S. S., Buhr, K. & Ebert, K. (2010b) 'Polyethersulfone electrospun nanofibrous composite membrane for liquid filtration', *J. Membr. Sci.*, 365, pp. 68-77. <https://doi.org/10.1016/j.memsci.2010.08.041>
- Horiuchi, J. I., Shimizu, T., Tada, K., et al. (2002) 'Selective production of organic acids in anaerobic acid reactor by pH control', *Bioresour. Technol.*, 82, pp. 209-213. [https://doi.org/10.1016/S0960-8524\(01\)00195-X](https://doi.org/10.1016/S0960-8524(01)00195-X)
- Hossain, M. Y., Zhu, W., Pervez, M. N., et al. (2021a) 'Adsorption, kinetics, and thermodynamic studies of cacao husk extracts in waterless sustainable

- dyeing of cotton fabric', *Cellulose*, 28, pp. 2521-2536. 10.1007/s10570-020-03662-0
- Hossain, M. Y., Zhu, W., Pervez, M. N., et al. (2021b) 'Adsorption, kinetics, and thermodynamic studies of cacao husk extracts in waterless sustainable dyeing of cotton fabric', *Cellulose.*, 28, pp. 2521-2536. <https://doi.org/10.1007/s10570-020-03662-0>
- Hua, F. L., Tsang, Y. F., Wang, Y. J., et al. (2007) 'Performance study of ceramic microfiltration membrane for oily wastewater treatment', *Chemical Engineering Journal*, 128, pp. 169-175. <https://doi.org/10.1016/j.cej.2006.10.017>
- Huang, C. & Xu, T. (2006a) 'Electrodialysis with bipolar membranes for sustainable development', *Environmental science & technology*, 40, pp. 5233-5243.
- Huang, C. & Xu, T. (2006b) 'Electrodialysis with bipolar membranes for sustainable development', *Environ. Sci. Technol.*, 40, pp. 5233-5243. <https://doi.org/10.1021/es060039p>
- Huang, C., Xu, T., Zhang, Y., et al. (2007) 'Application of electrodialysis to the production of organic acids: State-of-the-art and recent developments', *J. Membr. Sci.*, 288, pp. 1-12. <https://doi.org/10.1016/j.memsci.2006.11.026>
- Huang, H.-J., Ramaswamy, S., Tschirner, U. W., et al. (2008) 'A review of separation technologies in current and future biorefineries', *Sep. Purif. Technol.*, 62, pp. 1-21. <https://doi.org/10.1016/j.seppur.2007.12.011>
- Huang, W., Huang, W., Yuan, T., et al. (2016) 'Volatile fatty acids (VFAs) production from swine manure through short-term dry anaerobic digestion and its separation from nitrogen and phosphorus resources in the digestate', *Water. Res.*, 90, pp. 344-353. <https://doi.org/10.1016/j.watres.2015.12.044>
- Huang, Y., Kang, H., Li, G., et al. (2013) 'Synthesis and photosensitivity of azobenzene functionalized hydroxypropylcellulose', *RSC Advances*, 3, pp. 15909-15916. 10.1039/C3RA43031F
- Hube, S., Eskafi, M., Hrafnkelsdóttir, K. F., et al. (2020a) 'Direct membrane filtration for wastewater treatment and resource recovery: A review', *Science of The Total Environment*, 710, pp. 136375. <https://doi.org/10.1016/j.scitotenv.2019.136375>
- Hube, S., Eskafi, M., Hrafnkelsdóttir, K. F., et al. (2020b) 'Direct membrane filtration for wastewater treatment and resource recovery: A review', *Sci. Total. Environ.*, 710, pp. 136375. <https://doi.org/10.1016/j.scitotenv.2019.136375>
- Huq, N. A., Hafenstine, G. R., Huo, X., et al. (2021) 'Toward net-zero sustainable aviation fuel with wet waste-derived volatile fatty acids', *Proc. Natl. Acad. Sci.*, 118, pp. e2023008118. <https://doi.org/10.1073/pnas.2023008118>
- Hurwitz, G. & Hoek, E. M. V. Year. Published. Characterizing membrane surface charge by contact angle titration. The 2006 Annual Meeting, 2006 San Francisco, USA.
- Hussain, A., Li, J., Wang, J., et al. (2018) 'Hybrid Monolith of Graphene/TEMPO-Oxidized Cellulose Nanofiber as Mechanically Robust, Highly Functional,

- and Recyclable Adsorbent of Methylene Blue Dye', *Journal of Nanomaterials*, 2018, pp. 5963982. 10.1155/2018/5963982
- Ibupoto, A. S., Qureshi, U. A., Ahmed, F., et al. (2018) 'Reusable carbon nanofibers for efficient removal of methylene blue from aqueous solution', *Chemical Engineering Research and Design*, 136, pp. 744-752. <https://doi.org/10.1016/j.cherd.2018.06.035>
- Igarashi, T., Yagyū, D., Naito, T., et al. (2012) 'Dehydrative esterification of carboxylic acids with alcohols catalyzed by diarylammonium p-dodecylbenzenesulfonates in water', *Appl. Catal. B. Environ.*, 119-120, pp. 304-307. <https://doi.org/10.1016/j.apcatb.2012.03.001>
- Iorhemen, O. T., Hamza, R. A. & Tay, J. H. (2016) 'Membrane bioreactor (MBR) technology for wastewater treatment and reclamation: Membrane fouling', *Membranes*, 6, pp. 33. <https://doi.org/10.3390/membranes6020033>
- Ishihara, K. (2009) 'Dehydrative condensation catalyses', *Tetrahedron.*, 65, pp. 1085-1109. <https://doi.org/10.1016/j.tet.2008.11.004>
- Jänisch, T., Reinhardt, S., Pöhsner, U., et al. (2019) 'Separation of volatile fatty acids from biogas plant hydrolysates', *Sep. Purif. Technol.*, 223, pp. 264-273. <https://doi.org/10.1016/j.seppur.2019.04.066>
- Ji, L., Saquing, C., Khan, S. A., et al. (2008) 'Preparation and characterization of silica nanoparticulate-polyacrylonitrile composite and porous nanofibers', *Nanotechnology.*, 19, pp. 085605. <https://doi.org/10.1088/0957-4484/19/8/085605>
- Jiang, K., Kuang, H., Qin, T., et al. (2018) 'Recovery of monosaccharides from dilute acid corn cob hydrolysate by nanofiltration: modeling and optimization', *RSC Adv.*, 8, pp. 12672-12683. 10.1039/C8RA00236C
- Jing, J., Cao, C., Ma, S., et al. (2021a) 'Enhanced defect oxygen of LaFeO₃/GO hybrids in promoting persulfate activation for selective and efficient elimination of bisphenol A in food wastewater', *Chemical Engineering Journal*, 407, pp. 126890. <https://doi.org/10.1016/j.cej.2020.126890>
- Jing, J., Pervez, M. N., Sun, P., et al. (2021b) 'Highly efficient removal of bisphenol A by a novel Co-doped LaFeO₃ perovskite/PMS system in salinity water', *Science of The Total Environment*, 801, pp. 149490. <https://doi.org/10.1016/j.scitotenv.2021.149490>
- Jing, J., Pervez, M. N., Sun, P., et al. (2021c) 'Highly efficient removal of bisphenol A by a novel Co-doped LaFeO₃ perovskite/PMS system in salinity water', *Sci. Total. Environ.*, 801, pp. 149490. <https://doi.org/10.1016/j.scitotenv.2021.149490>
- Jomnonkhaow, U., Uwineza, C., Mahboubi, A., et al. (2021a) 'Membrane bioreactor-assisted volatile fatty acids production and in situ recovery from cow manure', *Bioresour. Technol.*, 321, pp. 124456. <https://doi.org/10.1016/j.biortech.2020.124456>
- Jomnonkhaow, U., Uwineza, C., Mahboubi, A., et al. (2021b) 'Membrane bioreactor-assisted volatile fatty acids production and in situ recovery from cow

- manure', *Bioresource Technology*, 321, pp. 124456. <https://doi.org/10.1016/j.biortech.2020.124456>
- Jones, R. J., Massanet-Nicolau, J., Guwy, A., et al. (2015) 'Removal and recovery of inhibitory volatile fatty acids from mixed acid fermentations by conventional electrodialysis', *Bioresour. Technol.*, 189, pp. 279-284. <https://doi.org/10.1016/j.biortech.2015.04.001>
- Jung, K., Choi, J.-d.-r., Lee, D., et al. (2015) 'Permeation characteristics of volatile fatty acids solution by forward osmosis', *Process. Biochem.*, 50, pp. 669-677. <https://doi.org/10.1016/j.procbio.2015.01.016>
- Karadag, D., K orođlu, O. E., Ozkaya, B., et al. (2015) 'A review on anaerobic biofilm reactors for the treatment of dairy industry wastewater', *Process Biochemistry*, 50, pp. 262-271. <https://doi.org/10.1016/j.procbio.2014.11.005>
- Katayon, S., Megat Mohd Noor, M. J., Ahmad, J., et al. (2004) 'Effects of mixed liquor suspended solid concentrations on membrane bioreactor efficiency for treatment of food industry wastewater', *Desalination*, 167, pp. 153-158. <https://doi.org/10.1016/j.desal.2004.06.124>
- Katikaneni, S. P. R. & Cheryan, M. (2002) 'Purification of fermentation-derived acetic acid by liquid– liquid extraction and esterification', *Ind. Eng. Chem. Res.*, 41, pp. 2745-2752. <https://doi.org/10.1021/ie010825x>
- Kawabata, N., Yoshida, J.-i. & Tanigawa, Y. (1981) 'Removal and recovery of organic pollutants from aquatic environment. 4. Separation of carboxylic acids from aqueous solution using crosslinked poly (4-vinylpyridine)', *Ind. Eng. Chem. Prod. Res. Dev.*, 20, pp. 386-390. <https://doi.org/10.1021/i300002a030>
- Kaya- zkipper, K., Uzun, A. & Soyer-Uzun, S. (2022) 'A novel alkali activated magnesium silicate as an effective and mechanically strong adsorbent for methylene blue removal', *Journal of Hazardous Materials*, 424, pp. 127256. <https://doi.org/10.1016/j.jhazmat.2021.127256>
- Kertes, A. S., King, C. J. & Blanch, H. W. (2009a) 'Extraction chemistry of fermentation product carboxylic acids', *Biotechnol. Bioeng.*, 103, pp. 431-445. <https://doi.org/10.1002/bit.22375>
- Kertes, A. S., King, C. J. & Harvey W. Blanch, I. b. (2009b) 'Extraction chemistry of fermentation product carboxylic acids', *Biotechnol. Bioeng.*, 103, pp. 431-445. <https://doi.org/10.1002/bit.22375>
- Khalid, A., Aslam, M., Qyyum, M. A., et al. (2019) 'Membrane separation processes for dehydration of bioethanol from fermentation broths: Recent developments, challenges, and prospects', *Renew. Sust. Energ. Rev.*, 105, pp. 427-443. <https://doi.org/10.1016/j.rser.2019.02.002>
- Khan, J. A., Nguyen, L. N., Duong, H. C., et al. (2020) 'Acetic acid extraction from rumen fluid by forward osmosis', *Environ. Technol. Innov.*, 20, pp. 101083. <https://doi.org/10.1016/j.eti.2020.101083>
- Khan, J. A., Vu, M. T. & Nghiem, L. D. (2021a) 'A preliminary assessment of forward osmosis to extract water from rumen fluid for artificial saliva', *Case*.

- Stud. Chem. Environ. Eng.*, 3, pp. 100095.
<https://doi.org/10.1016/j.cscee.2021.100095>
- Khan, S. A., Mubarik, M. S., Kusi-Sarpong, S., et al. (2021b) 'Social sustainable supply chains in the food industry: A perspective of an emerging economy', *Corporate Social Responsibility and Environmental Management*, 28, pp. 404-418. <https://doi.org/10.1002/csr.2057>
- Khatami, K., Atasoy, M., Ludtke, M., et al. (2021) 'Bioconversion of food waste to volatile fatty acids: Impact of microbial community, pH and retention time', *Chemosphere*, 275, pp. 129981.
<https://doi.org/10.1016/j.chemosphere.2021.129981>
- Kim, G.-H., Park, S.-J. & Um, B.-H. (2016) 'Response surface methodology for optimization of solvent extraction to recovery of acetic acid from black liquor derived from *Typha latifolia* pulping process', *Ind. Crops. Prod.*, 89, pp. 34-44. <https://doi.org/10.1016/j.indcrop.2016.04.056>
- Kim, J.-O., Kim, S.-K. & Kim, R.-H. (2005a) 'Filtration performance of ceramic membrane for the recovery of volatile fatty acids from liquid organic sludge', *Desalination*, 172, pp. 119-127.
<https://doi.org/10.1016/j.desal.2004.06.199>
- Kim, J.-O., Kim, S.-K. & Kim, R.-H. (2005b) 'Filtration performance of ceramic membrane for the recovery of volatile fatty acids from liquid organic sludge', *Desalination*, 172, pp. 119-127. <https://doi.org/10.1016/j.desal.2004.06.199>
- Kim, S., Heath, D. E. & Kentish, S. E. (2022) 'Improved carbon dioxide stripping by membrane contactors using hydrophobic electrospun poly(vinylidene fluoride-co-hexafluoro propylene) (PVDF-HFP) membranes', *Chemical Engineering Journal*, 428, pp. 131247.
<https://doi.org/10.1016/j.cej.2021.131247>
- King, C. J. & Starr, J. 1992. Recovery of carboxylic acids from water by precipitation from organic solutions. Google Patents.
- Kizildag, N. (2021) 'Smart composite nanofiber mats with thermal management functionality', *Sci. Rep.*, 11, pp. 4256. <https://doi.org/10.1038/s41598-021-83799-5>
- Kleerebezem, R., Joosse, B., Rozendal, R., et al. (2015) 'Anaerobic digestion without biogas?', *Rev. Environ. Sci. Biotechnol.*, 14, pp. 787-801.
<https://doi.org/10.1007/s11157-015-9374-6>
- Komesu, A., Martinez, P. F. M., Lunelli, B. H., et al. (2015) 'Lactic acid purification by reactive distillation system using design of experiments', *Chem. Eng. Process.: Process. Intensif.*, 95, pp. 26-30.
<https://doi.org/10.1016/j.cep.2015.05.005>
- Koushkbaghi, S., Zakialamdari, A., Pishnamazi, M., et al. (2018) 'Aminated-Fe₃O₄ nanoparticles filled chitosan/PVA/PES dual layers nanofibrous membrane for the removal of Cr(VI) and Pb(II) ions from aqueous solutions in adsorption and membrane processes', *Chemical Engineering Journal*, 337, pp. 169-182. <https://doi.org/10.1016/j.cej.2017.12.075>

- Kumar, M., Shevate, R., Hilke, R., et al. (2016a) 'Novel adsorptive ultrafiltration membranes derived from polyvinyltetrazole-co-polyacrylonitrile for Cu(II) ions removal', *Chemical Engineering Journal*, 301, pp. 306-314. <https://doi.org/10.1016/j.cej.2016.05.006>
- Kumar, R. & Ismail, A. F. (2015) 'Fouling control on microfiltration/ultrafiltration membranes: Effects of morphology, hydrophilicity, and charge', *J. Appl. Polym. Sci.*, 132, pp. <https://doi.org/10.1002/app.42042>
- Kumar, R. V., Goswami, L., Pakshirajan, K., et al. (2016b) 'Dairy wastewater treatment using a novel low cost tubular ceramic membrane and membrane fouling mechanism using pore blocking models', *Journal of Water Process Engineering*, 13, pp. 168-175. <https://doi.org/10.1016/j.jwpe.2016.08.012>
- Laghaei, M., Sadeghi, M., Ghalei, B., et al. (2016a) 'The role of compatibility between polymeric matrix and silane coupling agents on the performance of mixed matrix membranes: Polyethersulfone/MCM-41', *Journal of Membrane Science*, 513, pp. 20-32. <https://doi.org/10.1016/j.memsci.2016.04.039>
- Laghaei, M., Sadeghi, M., Ghalei, B., et al. (2016b) 'The role of compatibility between polymeric matrix and silane coupling agents on the performance of mixed matrix membranes: Polyethersulfone/MCM-41', *J. Membr. Sci.*, 513, pp. 20-32. <https://doi.org/10.1016/j.memsci.2016.04.039>
- Law, K.-Y. (2014) 'Definitions for hydrophilicity, hydrophobicity, and superhydrophobicity: Getting the basics right', *J. Phys. Chem. Lett.*, 5, pp. 686-688. <https://doi.org/10.1021/jz402762h>
- Lee, J., Na, J. & Baek, Y. (2021) 'Effects of impurities from sugar excipient on filtrate flux during ultrafiltration and diafiltration process', *Membranes*, 11, pp. 775. <https://doi.org/10.3390/membranes11100775>
- Lei, Z., Li, C. & Chen, B. (2003) 'Extractive distillation: a review', *Sep. Purif. Rev.*, 32, pp. 121-213. <https://doi.org/10.1081/SPM-120026627>
- Leifeld, V., Dos Santos, T. P. M., Zelinski, D. W., et al. (2018) 'Ferrous ions reused as catalysts in Fenton-like reactions for remediation of agro-food industrial wastewater', *Journal of Environmental Management*, 222, pp. 284-292.
- Leong, H. Y., Chang, C.-K., Khoo, K. S., et al. (2021) 'Waste biorefinery towards a sustainable circular bioeconomy: a solution to global issues', *Biotechnol. Biofuels.*, 14, pp. 1-15. <https://doi.org/10.1186/s13068-021-01939-5>
- Li, C., Lou, T., Yan, X., et al. (2018) 'Fabrication of pure chitosan nanofibrous membranes as effective absorbent for dye removal', *Int. J. Biol. Macromol.*, 106, pp. 768-774. <https://doi.org/10.1016/j.ijbiomac.2017.08.072>
- Li, H., Liu, L., Cui, J., et al. (2020a) 'High-efficiency adsorption and regeneration of methylene blue and aniline onto activated carbon from waste edible fungus residue and its possible mechanism', *RSC Adv.*, 10, pp. 14262-14273. <https://doi.org/10.1039/D0RA01245A>
- Li, H., Liu, L., Cui, J., et al. (2020b) 'High-efficiency adsorption and regeneration of methylene blue and aniline onto activated carbon from waste edible fungus

- residue and its possible mechanism', *RSC Advances*, 10, pp. 14262-14273. 10.1039/D0RA01245A
- Li, K., Zhou, M., Liang, L., et al. (2019a) 'Ultrahigh-surface-area activated carbon aerogels derived from glucose for high-performance organic pollutants adsorption', *J. Colloid. Interface. Sci.*, 546, pp. 333-343. <https://doi.org/10.1016/j.jcis.2019.03.076>
- Li, L., Xiao, Z., Zhang, Z., et al. (2004) 'Pervaporation of acetic acid/water mixtures through carbon molecular sieve-filled PDMS membranes', *Chem. Eng. J.*, 97, pp. 83-86. [https://doi.org/10.1016/S1385-8947\(03\)00102-5](https://doi.org/10.1016/S1385-8947(03)00102-5)
- Li, Q., Xing, J., Li, W., et al. (2009) 'Separation of succinic acid from fermentation broth using weak alkaline anion exchange adsorbents', *Ind. Eng. Chem. Res.*, 48, pp. 3595-3599. <https://doi.org/10.1021/ie801304k>
- Li, S., Jia, Z., Li, Z., et al. (2016) 'Synthesis and characterization of mesoporous carbon nanofibers and its adsorption for dye in wastewater', *Adv. Powder. Technol.*, 27, pp. 591-598. <https://doi.org/10.1016/j.apt.2016.01.024>
- Li, S., Li, Y., Wei, C., et al. (2021) 'One step co-sintering of silicon carbide ceramic membrane with the aid of boron carbide', *Journal of the European Ceramic Society*, 41, pp. 1181-1188. <https://doi.org/10.1016/j.jeurceramsoc.2020.09.065>
- Li, S., Zhao, S., Yan, S., et al. (2019b) 'Food processing wastewater purification by microalgae cultivation associated with high value-added compounds production — A review', *Chinese Journal of Chemical Engineering*, 27, pp. 2845-2856. <https://doi.org/10.1016/j.cjche.2019.03.028>
- Li, X., Swan, J. E., Nair, G. R., et al. (2015) 'Preparation of volatile fatty acid (VFA) calcium salts by anaerobic digestion of glucose', *Biotechnol. Appl. Biochem.*, 62, pp. 476-482. <https://doi.org/10.1002/bab.1301>
- Li, Z., Liu, X., Jin, W., et al. (2019c) 'Adsorption behavior of arsenicals on MIL-101(Fe): The role of arsenic chemical structures', *J. Colloid. Interface. Sci.*, 554, pp. 692-704. <https://doi.org/10.1016/j.jcis.2019.07.046>
- Liang, S., Kang, Y., Tiraferri, A., et al. (2013) 'Highly hydrophilic polyvinylidene fluoride (pvdf) ultrafiltration membranes via postfabrication grafting of surface-tailored silica nanoparticles', *ACS. Appl. Mater. Interfaces.*, 5, pp. 6694-6703. <https://doi.org/10.1021/am401462e>
- Liao, Y., Loh, C.-H., Tian, M., et al. (2018) 'Progress in electrospun polymeric nanofibrous membranes for water treatment: Fabrication, modification and applications', *Prog. Polym. Sci.*, 77, pp. 69-94. <https://doi.org/10.1016/j.progpolymsci.2017.10.003>
- Lim, S.-J., Kim, B. J., Jeong, C.-M., et al. (2008a) 'Anaerobic organic acid production of food waste in once-a-day feeding and drawing-off bioreactor', *Bioresource Technology*, 99, pp. 7866-7874. <https://doi.org/10.1016/j.biortech.2007.06.028>
- Lim, S.-J., Kim, E.-Y., Ahn, Y.-H., et al. (2008b) 'Biological nutrient removal with volatile fatty acids from food wastes in sequencing batch reactor', *Korean*

- Journal of Chemical Engineering*, 25, pp. 129-133. 10.1007/s11814-008-0023-4
- Ling, A.-I. & Chen, Q. (1995) 'Polyacrylonitrile/polysulfone (PAN/PS) blend ultrafiltration (UF) membranes', *Desalination.*, 101, pp. 51-56. [https://doi.org/10.1016/0011-9164\(95\)00008-P](https://doi.org/10.1016/0011-9164(95)00008-P)
- Liu, H., Han, P., Liu, H., et al. (2018) 'Full-scale production of VFAs from sewage sludge by anaerobic alkaline fermentation to improve biological nutrients removal in domestic wastewater', *Bioresour. Technol.*, 260, pp. 105-114. <https://doi.org/10.1016/j.biortech.2018.03.105>
- Liu, J., Chen, K., Zou, K., et al. (2021) 'Insights into the roles of membrane pore size and feed foulant concentration in ultrafiltration membrane fouling based on collision-attachment theory', *Water Environment Research*, 93, pp. 516-523. <https://doi.org/10.1002/wer.1453>
- Liu, L., Gao, Z. Y., Su, X. P., et al. (2015a) 'Adsorption Removal of Dyes from Single and Binary Solutions Using a Cellulose-based Bioadsorbent', *ACS Sustainable Chemistry & Engineering*, 3, pp. 432-442. 10.1021/sc500848m
- Liu, Q., Xie, L., Du, H., et al. (2020a) 'Study on the concentration of acrylic acid and acetic acid by reverse osmosis', *Membranes.*, 10, pp. 142. <https://doi.org/10.3390/membranes10070142>
- Liu, X., Liu, H., Chen, Y., et al. (2008) 'Effects of organic matter and initial carbon–nitrogen ratio on the bioconversion of volatile fatty acids from sewage sludge', *Journal of Chemical Technology & Biotechnology*, 83, pp. 1049-1055. <https://doi.org/10.1002/jctb.1913>
- Liu, X., Zhou, Y., Nie, W., et al. (2015b) 'Fabrication of hydrogel of hydroxypropyl cellulose (HPC) composited with graphene oxide and its application for methylene blue removal', *Journal of Materials Science*, 50, pp. 6113-6123. 10.1007/s10853-015-9166-y
- Liu, Y., Jin, W., Zhao, Y., et al. (2017) 'Enhanced catalytic degradation of methylene blue by α -Fe₂O₃/graphene oxide via heterogeneous photo-Fenton reactions', *Appl. Catal. B-Environ.*, 206, pp. 642-652. <https://doi.org/10.1016/j.apcatb.2017.01.075>
- Liu, Y., Zhao, Y., Cheng, W., et al. (2020b) 'Targeted reclaiming cationic dyes from dyeing wastewater with a dithiocarbamate-functionalized material through selective adsorption and efficient desorption', *Journal of Colloid and Interface Science*, 579, pp. 766-777. <https://doi.org/10.1016/j.jcis.2020.06.083>
- Lohokare, H. R., Muthu, M. R., Agarwal, G. P., et al. (2008) 'Effective arsenic removal using polyacrylonitrile-based ultrafiltration (UF) membrane', *J. Membr. Sci.*, 320, pp. 159-166. <https://doi.org/10.1016/j.memsci.2008.03.068>
- Longo, S., Katsou, E., Malamis, S., et al. (2015a) 'Recovery of volatile fatty acids from fermentation of sewage sludge in municipal wastewater treatment plants', *Bioresour. Technol.*, 175, pp. 436-444. <https://doi.org/10.1016/j.biortech.2014.09.107>

- Longo, S., Katsou, E., Malamis, S., et al. (2015b) 'Recovery of volatile fatty acids from fermentation of sewage sludge in municipal wastewater treatment plants', *Bioresource Technology*, 175, pp. 436-444. <https://doi.org/10.1016/j.biortech.2014.09.107>
- López-Garzón, C. S. & Straathof, A. J. J. (2014) 'Recovery of carboxylic acids produced by fermentation', *Biotechnol. Adv.*, 32, pp. 873-904. <https://doi.org/10.1016/j.biotechadv.2014.04.002>
- López-Luna, J., Ramírez-Montes, L. E., Martínez-Vargas, S., et al. (2019a) 'Linear and nonlinear kinetic and isotherm adsorption models for arsenic removal by manganese ferrite nanoparticles', *SN Applied Sciences*, 1, pp. 950. 10.1007/s42452-019-0977-3
- López-Luna, J., Ramírez-Montes, L. E., Martínez-Vargas, S., et al. (2019b) 'Linear and nonlinear kinetic and isotherm adsorption models for arsenic removal by manganese ferrite nanoparticles', *SN Appl. Sci.*, 1, pp. 950. <https://doi.org/10.1007/s42452-019-0977-3>
- López-Porfiri, P., Gorgojo, P. & Gonzalez-Miquel, M. (2020) 'Green solvents selection guide for bio-based organic acids recovery', *ACS. Sustainable Chem. Eng.*, pp. <https://doi.org/10.1021/acssuschemeng.0c01456>
- Lotfikatouli, S., Hadi, P., Yang, M., et al. (2021) 'Enhanced anti-fouling performance in Membrane Bioreactors using a novel cellulose nanofiber-coated membrane', *Separation and Purification Technology*, 275, pp. 119145. <https://doi.org/10.1016/j.seppur.2021.119145>
- Lü, F., Wang, Z., Zhang, H., et al. (2021) 'Anaerobic digestion of organic waste: Recovery of value-added and inhibitory compounds from liquid fraction of digestate', *Bioresour. Technol.*, 333, pp. 125196. <https://doi.org/10.1016/j.biortech.2021.125196>
- Lu, K., Wang, T., Zhai, L., et al. (2019a) 'Adsorption behavior and mechanism of Fe-Mn binary oxide nanoparticles: Adsorption of methylene blue', *Journal of Colloid and Interface Science*, 539, pp. 553-562. <https://doi.org/10.1016/j.jcis.2018.12.094>
- Lu, K., Wang, T., Zhai, L., et al. (2019b) 'Adsorption behavior and mechanism of Fe-Mn binary oxide nanoparticles: Adsorption of methylene blue', *J. Colloid. Interface. Sci.*, 539, pp. 553-562. <https://doi.org/10.1016/j.jcis.2018.12.094>
- Luiz-Santos, N., Prado-Ramírez, R., Arriola-Guevara, E., et al. (2020) 'Performance evaluation of tight ultrafiltration membrane systems at pilot scale for agave fructans fractionation and purification', *Membranes.*, 10, pp. 261. <https://doi.org/10.3390/membranes10100261>
- Luiz, A., McClure, D. D., Lim, K., et al. (2017) 'Potential upgrading of bio-refinery streams by electrodialysis', *Desalination*, 415, pp. 20-28. <https://doi.org/10.1016/j.desal.2017.02.023>
- Lukitawesa, Patinvoh, R. J., Millati, R., et al. (2020) 'Factors influencing volatile fatty acids production from food wastes via anaerobic digestion', *Bioengineered*, 11, pp. 39-52. 10.1080/21655979.2019.1703544

- Luo, K., Pang, Y., Yang, Q., et al. (2019) 'A critical review of volatile fatty acids produced from waste activated sludge: enhanced strategies and its applications', *Environ. Sci. Pollut. Res.*, 26, pp. 13984-13998. <https://doi.org/10.1007/s11356-019-04798-8>
- Luo, M., Wang, M., Pang, H., et al. (2021) 'Super-assembled highly compressible and flexible cellulose aerogels for methylene blue removal from water', *Chinese Chemical Letters*, 32, pp. 2091-2096. <https://doi.org/10.1016/j.ccllet.2021.03.024>
- Lyu, H., Chen, K., Yang, X., et al. (2015) 'Two-stage nanofiltration process for high-value chemical production from hydrolysates of lignocellulosic biomass through hydrothermal liquefaction', *Sep. Purif. Technol.*, 147, pp. 276-283. <https://doi.org/10.1016/j.seppur.2015.04.032>
- Lyu, H., Fang, Y., Ren, S., et al. (2016) 'Monophenols separation from monosaccharides and acids by two-stage nanofiltration and reverse osmosis in hydrothermal liquefaction hydrolysates', *J. Membr. Sci.*, 504, pp. 141-152. <https://doi.org/10.1016/j.memsci.2015.12.048>
- Ma, M., Chen, Y., Zhao, X., et al. (2020a) 'Effective removal of cation dyes from aqueous solution using robust cellulose sponge', *Journal of Saudi Chemical Society*, 24, pp. 915-924. <https://doi.org/10.1016/j.jscs.2020.09.008>
- Ma, M., Chen, Y., Zhao, X., et al. (2020b) 'Effective removal of cation dyes from aqueous solution using robust cellulose sponge', *J. Saudi. Chem. Soc.*, 24, pp. 915-924. <https://doi.org/10.1016/j.jscs.2020.09.008>
- Ma, Y. & Liu, Y. (2019) 'Turning food waste to energy and resources towards a great environmental and economic sustainability: An innovative integrated biological approach', *Biotechnol. Adv.*, 37, pp. 107414. <https://doi.org/10.1016/j.biotechadv.2019.06.013>
- Mahat, S. B., Omar, R., Che Man, H., et al. (2021) 'Performance of dynamic anaerobic membrane bioreactor (DAnMBR) with phase separation in treating high strength food processing wastewater', *Journal of Environmental Chemical Engineering*, 9, pp. 105245. <https://doi.org/10.1016/j.jece.2021.105245>
- Mahboubi, A., Uwineza, C., Doyen, W., et al. (2020) 'Intensification of lignocellulosic bioethanol production process using continuous double-staged immersed membrane bioreactors', *Bioresource Technology*, 296, pp. 122314. <https://doi.org/10.1016/j.biortech.2019.122314>
- Mahboubi, A., Ylittervo, P., Doyen, W., et al. (2016) 'Reverse membrane bioreactor: Introduction to a new technology for biofuel production', *Biotechnol. Adv.*, 34, pp. 954-975. <https://doi.org/10.1016/j.biotechadv.2016.05.009>
- Mahfud, F. H., Van Geel, F. P., Venderbosch, R. H., et al. (2008) 'Acetic acid recovery from fast pyrolysis oil. An exploratory study on liquid-liquid reactive extraction using aliphatic tertiary amines', *Sep. Sci. Technol.*, 43, pp. 3056-3074. <https://doi.org/10.1080/01496390802222509>

- Mahmoud, N., Zeeman, G., Gijzen, H., et al. (2003a) 'Solids removal in upflow anaerobic reactors, a review', *Bioresour. Technol.*, 90, pp. 1-9. [https://doi.org/10.1016/S0960-8524\(03\)00095-6](https://doi.org/10.1016/S0960-8524(03)00095-6)
- Mahmoud, N., Zeeman, G., Gijzen, H., et al. (2003b) 'Solids removal in upflow anaerobic reactors, a review', *Bioresource Technology*, 90, pp. 1-9. [https://doi.org/10.1016/S0960-8524\(03\)00095-6](https://doi.org/10.1016/S0960-8524(03)00095-6)
- Maiti, S. K., Lukka Thuyavan, Y., Singh, S., et al. (2012) 'Modeling of the separation of inhibitory components from pretreated rice straw hydrolysate by nanofiltration membranes', *Bioresour. Technol.*, 114, pp. 419-427. <https://doi.org/10.1016/j.biortech.2012.03.029>
- Malmali, M., Stickel, J. J. & Wickramasinghe, S. R. (2014) 'Sugar concentration and detoxification of clarified biomass hydrolysate by nanofiltration', *Sep. Purif. Technol.*, 132, pp. 655-665. <https://doi.org/10.1016/j.seppur.2014.06.014>
- Masse, L., Massé, D. I. & Pellerin, Y. (2008) 'The effect of pH on the separation of manure nutrients with reverse osmosis membranes', *J. Membr. Sci.*, 325, pp. 914-919. <https://doi.org/10.1016/j.memsci.2008.09.017>
- Masse, L., Massé, D. I., Pellerin, Y., et al. (2010) 'Osmotic pressure and substrate resistance during the concentration of manure nutrients by reverse osmosis membranes', *J. Membr. Sci.*, 348, pp. 28-33. <https://doi.org/10.1016/j.memsci.2009.10.038>
- Melin, T., Jefferson, B., Bixio, D., et al. (2006) 'Membrane bioreactor technology for wastewater treatment and reuse', *Desalination*, 187, pp. 271-282. <https://doi.org/10.1016/j.desal.2005.04.086>
- Meng, H., Cheng, Q. & Li, C. (2014) 'Polyacrylonitrile-based zwitterionic ultrafiltration membrane with improved anti-protein-fouling capacity', *Applied Surface Science*, 303, pp. 399-405. <https://doi.org/10.1016/j.apsusc.2014.03.015>
- Mengmeng, C., Hong, C., Qingliang, Z., et al. (2009) 'Optimal production of polyhydroxyalkanoates (PHA) in activated sludge fed by volatile fatty acids (VFAs) generated from alkaline excess sludge fermentation', *Bioresour. Technol.*, 100, pp. 1399-1405. <https://doi.org/10.1016/j.biortech.2008.09.014>
- Metwally, B. S., El-Sayed, A. A., Radwan, E. K., et al. (2018) 'Fabrication, characterization, and dye adsorption capability of recycled modified polyamide nanofibers', *Egyptian Journal of Chemistry*, 61, pp. 867-882.
- Millanar-Marfa, J. M. J., Borea, L., Castrogiovanni, F., et al. (2021) 'Self-forming Dynamic Membranes for Wastewater Treatment', *Separation & Purification Reviews*, pp. 1-17.
- Min, D.-J., Choi, K. H., Chang, Y. K., et al. (2011) 'Effect of operating parameters on precipitation for recovery of lactic acid from calcium lactate fermentation broth', *Korean. J. Chem. Eng.*, 28, pp. 1969. <https://doi.org/10.1007/s11814-011-0082-9>
- Min, M., Shen, L., Hong, G., et al. (2012) 'Micro-nano structure poly(ether sulfones)/poly(ethyleneimine) nanofibrous affinity membranes for

- adsorption of anionic dyes and heavy metal ions in aqueous solution', *Chem. Eng. J.*, 197, pp. 88-100. <https://doi.org/10.1016/j.cej.2012.05.021>
- Mohammad, A. W., Teow, Y. H., Ang, W. L., et al. (2015) 'Nanofiltration membranes review: Recent advances and future prospects', *Desalination.*, 356, pp. 226-254. <https://doi.org/10.1016/j.desal.2014.10.043>
- Mohammad, N. & Atassi, Y. (2020a) 'Adsorption of methylene blue onto electrospun nanofibrous membranes of polylactic acid and polyacrylonitrile coated with chloride doped polyaniline', *Sci. Rep.*, 10, pp. 13412. <https://doi.org/10.1038/s41598-020-69825-y>
- Mohammad, N. & Atassi, Y. (2020b) 'Adsorption of methylene blue onto electrospun nanofibrous membranes of polylactic acid and polyacrylonitrile coated with chloride doped polyaniline', *Scientific Reports*, 10, pp. 13412. 10.1038/s41598-020-69825-y
- Mohammed-Nour, A., Al-Sewailem, M. & El-Naggar, A. H. (2019a) 'The influence of alkalization and temperature on ammonia recovery from cow manure and the chemical properties of the effluents', *Sustainability*, 11, pp. 2441. <https://doi.org/10.3390/su11082441>
- Mohammed-Nour, A., Al-Sewailem, M. & El-Naggar, A. H. (2019b) 'The influence of alkalization and temperature on ammonia recovery from cow manure and the chemical properties of the effluents', *Sustainability.*, 11, pp. 2441. <https://doi.org/10.3390/su11082441>
- Molodkina, L. M., Kolosova, D. D., Leonova, E. I., et al. (2012) 'Track membranes in post-treatment of domestic wastewater', *Petroleum Chemistry*, 52, pp. 487-493. 10.1134/S0965544112070092
- Moradi, E., Ebrahimzadeh, H., Mehrani, Z., et al. (2019) 'The efficient removal of methylene blue from water samples using three-dimensional poly (vinyl alcohol)/starch nanofiber membrane as a green nanosorbent', *Environmental Science and Pollution Research*, 26, pp. 35071-35081. 10.1007/s11356-019-06400-7
- Moritz, T., Benfer, S., Arki, P., et al. (2001) 'Influence of the surface charge on the permeate flux in the dead-end filtration with ceramic membranes', *Sep. Purif. Technol.*, 25, pp. 501-508. [https://doi.org/10.1016/S1383-5866\(01\)00080-6](https://doi.org/10.1016/S1383-5866(01)00080-6)
- Morshed, M. N., Pervez, M. N., Behary, N., et al. (2020a) 'Statistical modeling and optimization of heterogeneous Fenton-like removal of organic pollutant using fibrous catalysts: a full factorial design', *Sci. Rep.*, 10, pp. 16133. <https://doi.org/10.1038/s41598-020-72401-z>
- Morshed, M. N., Pervez, M. N., Behary, N., et al. (2020b) 'Statistical modeling and optimization of heterogeneous Fenton-like removal of organic pollutant using fibrous catalysts: a full factorial design', *Scientific Reports*, 10, pp. 16133. 10.1038/s41598-020-72401-z
- Mostafa, N. A. (1999) 'Production and recovery of volatile fatty acids from fermentation broth', *Energy. Convers. Manag.*, 40, pp. 1543-1553. [https://doi.org/10.1016/S0196-8904\(99\)00043-6](https://doi.org/10.1016/S0196-8904(99)00043-6)

- Mukherjee, S. & Munshi, B. (2020) 'Experimental and theoretical analysis of reactive extraction of caproic acid by using TBP in green diluents', *Chem. Eng. Process.: Process. Intensif.*, 153, pp. 107926. <https://doi.org/10.1016/j.cep.2020.107926>
- Murali, N., Srinivas, K. & Ahring, B. K. (2021) 'Increasing the production of volatile fatty acids from corn stover using bioaugmentation of a mixed rumen culture with homoacetogenic bacteria', *Microorganisms*, 9, pp. 337. <https://doi.org/10.3390/microorganisms9020337>
- Muro, C., Riera, F. & del Carmen Díaz, M. 2012. Membrane separation process in wastewater treatment of food industry. *Food industrial processes—methods and equipment*. InTech, Rijeka.
- Naddeo, V. (2021) 'One planet, one health, one future: The environmental perspective', *Water Environment Research*, 93, pp. 1472-1475. <https://doi.org/10.1002/wer.1624>
- Naddeo, V. & Korshin, G. (2021) 'Water, energy and waste: The great European deal for the environment', *Science of The Total Environment*, 764, pp. 142911. <https://doi.org/10.1016/j.scitotenv.2020.142911>
- Naddeo, V. & Liu, H. (2020) 'Editorial Perspectives: 2019 novel coronavirus (SARS-CoV-2): what is its fate in urban water cycle and how can the water research community respond?', *Environmental science-water research & technology*, 6, pp. 1939-1939.
- Naddeo, V. & Taherzadeh, M. J. (2021) 'Biomass valorization and bioenergy in the blue circular economy', *Biomass. Bioenerg.*, 149, pp. 106069. <https://doi.org/10.1016/j.biombioe.2021.106069>
- Nasreen, S. A. A. N., Sundarrajan, S., Nizar, S. A. S., et al. (2013) 'Advancement in electrospun nanofibrous membranes modification and their application in water treatment', *Membranes.*, 3, pp. 266-284. <https://doi.org/10.3390/membranes3040266>
- Neoh, C. H., Noor, Z. Z., Mutamim, N. S. A., et al. (2016) 'Green technology in wastewater treatment technologies: Integration of membrane bioreactor with various wastewater treatment systems', *Chemical Engineering Journal*, 283, pp. 582-594. <https://doi.org/10.1016/j.cej.2015.07.060>
- Neumann, R. & Sasson, Y. (1984) 'Recovery of dilute acetic acid by esterification in a packed chemorectification column', *Ind. Eng. Chem. Process. Des. Dev.*, 23, pp. 654-659. <https://doi.org/10.1021/i200027a005>
- Ng, C. Y., Khoo, L. H., Ng, L. Y., et al. (2020) 'Novel polyethersulfone-cellulose composite thin film using sustainable empty fruit bunches from *Elaeis guineensis* for methylene blue removal', *Polymer Testing*, 86, pp. 106494. <https://doi.org/10.1016/j.polymertesting.2020.106494>
- Ng, L. Y., Chua, H. S. & Ng, C. Y. (2021) 'Incorporation of graphene oxide-based nanocomposite in the polymeric membrane for water and wastewater treatment: A review on recent development', *Journal of Environmental Chemical Engineering*, 9, pp. 105994. <https://doi.org/10.1016/j.jece.2021.105994>

- Ng, L. Y., Mohammad, A. W., Leo, C. P., et al. (2013) 'Polymeric membranes incorporated with metal/metal oxide nanoparticles: A comprehensive review', *Desalination.*, 308, pp. 15-33. <https://doi.org/10.1016/j.desal.2010.11.033>
- Nguyen, N., Fargues, C., Guiga, W., et al. (2015) 'Assessing nanofiltration and reverse osmosis for the detoxification of lignocellulosic hydrolysates', *J. Membr. Sci.*, 487, pp. 40-50. <https://doi.org/10.1016/j.memsci.2015.03.072>
- Nielsen, D. R., Amarasiriwardena, G. S. & Prather, K. L. J. (2010) 'Predicting the adsorption of second generation biofuels by polymeric resins with applications for in situ product recovery (ISPR)', *Bioresour. Technol.*, 101, pp. 2762-2769. <https://doi.org/10.1016/j.biortech.2009.12.003>
- Niewersch, C., Battaglia Bloch, A. L., Yüce, S., et al. (2014) 'Nanofiltration for the recovery of phosphorus — Development of a mass transport model', *Desalination.*, 346, pp. 70-78. <https://doi.org/10.1016/j.desal.2014.05.011>
- Nilsson, M., Trägårdh, G. & Östergren, K. (2008) 'Influence of temperature and cleaning on aromatic and semi-aromatic polyamide thin-film composite NF and RO membranes', *Sep. Purif. Technol.*, 62, pp. 717-726. <https://doi.org/10.1016/j.seppur.2008.03.014>
- Nir, O., Sengpiel, R. & Wessling, M. (2018) 'Closing the cycle: Phosphorus removal and recovery from diluted effluents using acid resistive membranes', *Chem. Eng. J.*, 346, pp. 640-648. <https://doi.org/10.1016/j.cej.2018.03.181>
- Nizami, A. S., Rehan, M., Waqas, M., et al. (2017) 'Waste biorefineries: enabling circular economies in developing countries', *Bioresour. Technol.*, 241, pp. 1101-1117. <https://doi.org/10.1016/j.biortech.2017.05.097>
- Norton, T. & Misiewicz, P. 2012. Ozone for water treatment and its potential for process water reuse in the food industry. In: COLM, O. D., B. K., T., P. J. CULLEN & RICE, R. G. (eds.) *Ozone in Food Processing*. New Jersey, United States: Wiley-Blackwell.
- Obaid, M., Abdelkareem, M. A., Kook, S., et al. (2020) 'Breakthroughs in the fabrication of electrospun-nanofiber-supported thin film composite/nanocomposite membranes for the forward osmosis process: A review', *Critical Reviews in Environmental Science and Technology*, 50, pp. 1727-1795. <https://doi.org/10.1080/10643389.2019.1672510>
- Ochando-Pulido, J. M. & Martinez-Ferez, A. (2012) 'A focus on pressure-driven membrane technology in olive mill wastewater reclamation: state of the art', *Water Science and Technology*, 66, pp. 2505-2516. <https://doi.org/10.2166/wst.2012.506>
- Ochando-Pulido, J. M., Rodriguez-Vives, S., Hodaifa, G., et al. (2012) 'Impacts of operating conditions on reverse osmosis performance of pretreated olive mill wastewater', *Water Research*, 46, pp. 4621-4632. <https://doi.org/10.1016/j.watres.2012.06.026>
- Odey, E. A., Wang, K., Li, Z., et al. (2019) 'Feasibility of wastewater resource recovery using pilot-scale membrane reactor with long-term operation',

- Energy. Environ.*, 30, pp. 662-671.
<https://doi.org/10.1177/0958305X18802782>
- Oliveira, F. S., Araújo, J. M. M., Ferreira, R., et al. (2012) 'Extraction of l-lactic, l-malic, and succinic acids using phosphonium-based ionic liquids', *Sep. Purif. Technol.*, 85, pp. 137-146.
<https://doi.org/10.1016/j.seppur.2011.10.002>
- Olivito, F., Algieri, V., Jiritano, A., et al. (2021) 'Cellulose citrate: a convenient and reusable bio-adsorbent for effective removal of methylene blue dye from artificially contaminated water', *RSC Advances*, 11, pp. 34309-34318. 10.1039/D1RA05464C
- Ozaki, H. & Li, H. (2002) 'Rejection of organic compounds by ultra-low pressure reverse osmosis membrane', *Water. Res.*, 36, pp. 123-130.
[https://doi.org/10.1016/S0043-1354\(01\)00197-X](https://doi.org/10.1016/S0043-1354(01)00197-X)
- Painer, D., Lux, S. & Siebenhofer, M. (2015) 'Recovery of formic acid and acetic acid from waste water using reactive distillation', *Sep. Sci. Technol.*, 50, pp. 2930-2936. <https://doi.org/10.1080/01496395.2015.1085407>
- Pan, X.-R., Li, W.-W., Huang, L., et al. (2018) 'Recovery of high-concentration volatile fatty acids from wastewater using an acidogenesis-electrodialysis integrated system', *Bioresour. Technol.*, 260, pp. 61-67.
<https://doi.org/10.1016/j.biortech.2018.03.083>
- Papargyropoulou, E., Lozano, R., K. Steinberger, J., et al. (2014) 'The food waste hierarchy as a framework for the management of food surplus and food waste', *J. Clean. Prod.*, 76, pp. 106-115.
<https://doi.org/10.1016/j.jclepro.2014.04.020>
- Parchami, M., Wainaina, S., Mahboubi, A., et al. (2020a) 'MBR-assisted VFAs production from excess sewage sludge and food waste slurry for sustainable wastewater treatment', *Applied Sciences*, 10, pp. 2921.
<https://doi.org/10.3390/app10082921>
- Parchami, M., Wainaina, S., Mahboubi, A., et al. (2020b) 'MBR-assisted VFAs production from excess sewage sludge and food waste slurry for sustainable wastewater treatment', *Appl. Sci.*, 10, pp. 2921.
<https://doi.org/10.3390/app10082921>
- Park, H. B., Kamcev, J., Robeson, L. M., et al. (2017) 'Maximizing the right stuff: The trade-off between membrane permeability and selectivity', *Science.*, 356, pp. <https://doi.org/10.1126/science.aab0530>
- Pärnamäe, R., Mareev, S., Nikonenko, V., et al. (2021) 'Bipolar membranes: A review on principles, latest developments, and applications', *J. Membr. Sci.*, 617, pp. 118538. <https://doi.org/10.1016/j.memsci.2020.118538>
- Pasaoglu, M. E., Guclu, S. & Koyuncu, I. (2016) 'Polyethersulfone/polyacrylonitrile blended ultrafiltration membranes: preparation, morphology and filtration properties', *Water. Sci. Technol.*, 74, pp. 738-748.
<https://doi.org/10.2166/wst.2016.252>
- Patange, A., Boehm, D., Giltrap, M., et al. (2018) 'Assessment of the disinfection capacity and eco-toxicological impact of atmospheric cold plasma for

- treatment of food industry effluents', *Science of The Total Environment*, 631-632, pp. 298-307. <https://doi.org/10.1016/j.scitotenv.2018.02.269>
- Pérez-Álvarez, L., Ruiz-Rubio, L., Moreno, I., et al. (2019) 'Characterization and optimization of the alkaline hydrolysis of polyacrylonitrile membranes', *Polymers.*, 11, pp. 1843. <https://doi.org/10.3390/polym11111843>
- Persano, L., Camposeo, A., Tekmen, C., et al. (2013) 'Industrial Upscaling of Electrospinning and Applications of Polymer Nanofibers: A Review', *Macromolecular Materials and Engineering*, 298, pp. 504-520. <https://doi.org/10.1002/mame.201200290>
- Pervez, M. N., Balakrishnan, M., Hasan, S. W., et al. (2020a) 'A critical review on nanomaterials membrane bioreactor (NMs-MBR) for wastewater treatment', *npj Clean. Water.*, 3, pp. 43. <https://doi.org/10.1038/s41545-020-00090-2>
- Pervez, M. N., Balakrishnan, M., Hasan, S. W., et al. (2020b) 'A critical review on nanomaterials membrane bioreactor (NMs-MBR) for wastewater treatment', *npj Clean Water*, 3, pp. 43. [10.1038/s41545-020-00090-2](https://doi.org/10.1038/s41545-020-00090-2)
- Pervez, M. N., Balakrishnan, M., Hasan, S. W., et al. (2020c) 'A critical review on nanomaterials membrane bioreactor (NMs-MBR) for wastewater treatment', *npj. Clean. Water.*, 3, pp. 43. <https://doi.org/10.1038/s41545-020-00090-2>
- Pervez, M. N., Fu, D., Wang, X., et al. (2021a) 'A bifunctional α -FeOOH@GCA nanocomposite for enhanced adsorption of arsenic and photo Fenton-like catalytic conversion of As(III)', *Environ. Technol. Innov.*, 22, pp. 101437. <https://doi.org/10.1016/j.eti.2021.101437>
- Pervez, M. N., Fu, D., Wang, X., et al. (2021b) 'A bifunctional α -FeOOH@GCA nanocomposite for enhanced adsorption of arsenic and photo Fenton-like catalytic conversion of As(III)', *Environmental Technology & Innovation*, 22, pp. 101437. <https://doi.org/10.1016/j.eti.2021.101437>
- Pervez, M. N., He, W., Zarra, T., et al. (2020d) 'New sustainable approach for the production of Fe₃O₄/graphene oxide-activated persulfate system for dye removal in real wastewater', *Water.*, 12, pp. 733. <https://doi.org/10.3390/w12030733>
- Pervez, M. N., He, W., Zarra, T., et al. (2020e) 'New Sustainable Approach for the Production of Fe₃O₄/Graphene Oxide-Activated Persulfate System for Dye Removal in Real Wastewater', *Water*, 12, pp. 733.
- Pervez, M. N., Mahboubi, A., Uwineza, C., et al. (2022a) 'Factors influencing pressure-driven membrane-assisted volatile fatty acids recovery and purification-A review', *Science of The Total Environment*, 817, pp. 152993. <https://doi.org/10.1016/j.scitotenv.2022.152993>
- Pervez, M. N., Mahboubi, A., Uwineza, C., et al. (2022b) 'Factors influencing pressure-driven membrane-assisted volatile fatty acids recovery and purification-A review', *Sci. Total. Environ.*, 817, pp. 152993. <https://doi.org/10.1016/j.scitotenv.2022.152993>
- Pervez, M. N., Mishu, M. R., Stylios, G. K., et al. (2021c) 'Sustainable Treatment of Food Industry Wastewater Using Membrane Technology: A Short Review', *Water*, 13, pp. 3450.

- Pervez, M. N., Mishu, M. R., Stylios, G. K., et al. (2021d) 'Sustainable treatment of food industry wastewater using membrane technology: A short review', *Water.*, 13, pp. 3450. <https://doi.org/10.3390/w13233450>
- Pervez, M. N. & Stylios, G. K. (2018a) 'An Experimental Approach to the Synthesis and Optimisation of a 'Green' Nanofibre', *Nanomaterials*, 8, pp. 383.
- Pervez, M. N. & Stylios, G. K. (2018b) 'An experimental approach to the synthesis and optimisation of a 'green' nanofibre', *Nanomaterials.*, 8, pp. 383. <https://doi.org/10.3390/nano8060383>
- Pervez, M. N. & Stylios, G. K. (2018c) 'Investigating the Synthesis and Characterization of a Novel "Green" H₂O₂-Assisted, Water-Soluble Chitosan/Polyvinyl Alcohol Nanofiber for Environmental End Uses', *Nanomaterials*, 8, pp. 395.
- Pervez, M. N. & Stylios, G. K. (2018d) 'Investigating the synthesis and characterization of a novel "green" H₂O₂-assisted, water-soluble chitosan/polyvinyl alcohol nanofiber for environmental end uses', *Nanomaterials.*, 8, pp. 395. <https://doi.org/10.3390/nano8060395>
- Pervez, M. N., Stylios, G. K., Liang, Y., et al. (2020f) 'Low-temperature synthesis of novel polyvinylalcohol (PVA) nanofibrous membranes for catalytic dye degradation', *Journal of Cleaner Production*, 262, pp. 121301. <https://doi.org/10.1016/j.jclepro.2020.121301>
- Pervez, M. N., Stylios, G. K., Liang, Y., et al. (2020g) 'Low-temperature synthesis of novel polyvinylalcohol (PVA) nanofibrous membranes for catalytic dye degradation', *J. Clean. Prod.*, 262, pp. 121301. <https://doi.org/10.1016/j.jclepro.2020.121301>
- Pervez, M. N., Telegin, F. Y., Cai, Y., et al. (2019a) 'Efficient degradation of Mordant Blue 9 using the fenton-activated persulfate system', *Water.*, 11, pp. 2532. <https://doi.org/10.3390/w11122532>
- Pervez, M. N., Telegin, F. Y., Cai, Y., et al. (2019b) 'Efficient Degradation of Mordant Blue 9 Using the Fenton-Activated Persulfate System', *Water*, 11, pp. 2532.
- Pervez, M. N., Wei, Y., Sun, P., et al. (2021e) ' α -FeOOH quantum dots impregnated graphene oxide hybrids enhanced arsenic adsorption: The mediation role of environmental organic ligands', *Sci. Total. Environ.*, 781, pp. 146726. <https://doi.org/10.1016/j.scitotenv.2021.146726>
- Pervez, M. N., Wei, Y., Sun, P., et al. (2021f) ' α -FeOOH quantum dots impregnated graphene oxide hybrids enhanced arsenic adsorption: The mediation role of environmental organic ligands', *Science of The Total Environment*, 781, pp. 146726. <https://doi.org/10.1016/j.scitotenv.2021.146726>
- Petersen, A. M., Franco, T. & Görgens, J. F. (2018) 'Comparison of recovery of volatile fatty acids and mixed ketones as alternative downstream processes for acetogenesis fermentation', *Biofuel. Bioprod. Biorefin.*, 12, pp. 882-898. <https://doi.org/10.1002/bbb.1938>
- Plácido, J. & Zhang, Y. (2018) 'Evaluation of esterification and membrane based solvent extraction as methods for the recovery of short chain volatile fatty

- acids from slaughterhouse blood anaerobic mixed fermentation', *Waste, Biomass. Valor.*, 9, pp. 1767-1777. <https://doi.org/10.1007/s12649-017-9952-7>
- Plevri, A., Mamais, D. & Noutsopoulos, C. (2021) 'Anaerobic MBR technology for treating municipal wastewater at ambient temperatures', *Chemosphere*, 275, pp. 129961. <https://doi.org/10.1016/j.chemosphere.2021.129961>
- Plisko, T. V., Bildyukevich, A. V., Burts, K. S., et al. (2020) 'Modification of Polysulfone Ultrafiltration Membranes via Addition of Anionic Polyelectrolyte Based on Acrylamide and Sodium Acrylate to the Coagulation Bath to Improve Antifouling Performance in Water Treatment', *Membranes*, 10, pp. 264.
- Puchlik, M. & Struk-Sokołowska, J. Year. Published. Comparison of the composition of wastewater from fruit and vegetables as well as dairy industry. E3S Web of Conferences, 2017. EDP Sciences, 00077.
- Qasim, W. & Mane, A. V. (2013) 'Characterization and treatment of selected food industrial effluents by coagulation and adsorption techniques', *Water Resources and Industry*, 4, pp. 1-12. <https://doi.org/10.1016/j.wri.2013.09.005>
- Qi, J., Tang, J., Zhang, Q., et al. (2019) 'Heat-integrated azeotropic distillation and extractive distillation for the separation of heterogeneous ternary azeotropes of diisopropyl ether/isopropyl alcohol/water', *Ind. Eng. Chem. Res.*, 58, pp. 20734-20745. <https://doi.org/10.1021/acs.iecr.9b03846>
- Qin, Y. & Sheth, J. P. (2003) 'Pervaporation membranes that are highly selective for acetic acid over water', *Ind. Eng. Chem. Res.*, 42, pp. 582-595. <https://doi.org/10.1021/ie020414w>
- Qiu, Y., Zu, Y., Song, C., et al. (2019) 'Soybean processing wastewater purification via Chlorella L166 and L38 with potential value-added ingredients production', *Bioresource Technology Reports*, 7, pp. 100195. <https://doi.org/10.1016/j.biteb.2019.100195>
- Qureshi, N. & Blaschek, H. P. (2001) 'Recovery of butanol from fermentation broth by gas stripping', *Renew. Energ.*, 22, pp. 557-564. [https://doi.org/10.1016/S0960-1481\(00\)00108-7](https://doi.org/10.1016/S0960-1481(00)00108-7)
- Qureshi, N., Hodge, D. B. & Vertes, A. 2014. *Biorefineries: Integrated biochemical processes for liquid biofuels*, Amsterdam, Netherlands, Elsevier.
- Rajabzadeh, A. R., Ruzich, N., Zendejboudi, S., et al. (2012) 'Biomass leachate treatment and nutrient recovery using reverse osmosis: experimental study and hybrid artificial neural network modeling', *Energy. Fuels.*, 26, pp. 7155-7163. <https://doi.org/10.1021/ef301452s>
- Rajendran, K., Mahapatra, D., Venkatraman, A. V., et al. (2020) 'Advancing anaerobic digestion through two-stage processes: Current developments and future trends', *Renewable and Sustainable Energy Reviews*, 123, pp. 109746.
- Ramos-Suarez, M., Zhang, Y. & Outram, V. (2021a) 'Current perspectives on acidogenic fermentation to produce volatile fatty acids from waste', *Reviews*

- in Environmental Science and Bio/Technology*, pp. 10.1007/s11157-021-09566-0
- Ramos-Suarez, M., Zhang, Y. & Outram, V. (2021b) 'Current perspectives on acidogenic fermentation to produce volatile fatty acids from waste', *Rev. Environ. Sci. Biotechnol.*, 20, pp. 439-478. <https://doi.org/10.1007/s11157-021-09566-0>
- Rana, D. & Matsuura, T. (2010) 'Surface modifications for antifouling membranes', *Chem. Rev.*, 110, pp. 2448-2471. <https://doi.org/10.1021/cr800208y>
- Rasrendra, C. B., Girisuta, B., van de Bovenkamp, H. H., et al. (2011) 'Recovery of acetic acid from an aqueous pyrolysis oil phase by reactive extraction using tri-n-octylamine', *Chem. Eng. J.*, 176-177, pp. 244-252. <https://doi.org/10.1016/j.cej.2011.08.082>
- Rebecchi, S., Pinelli, D., Bertin, L., et al. (2016) 'Volatile fatty acids recovery from the effluent of an acidogenic digestion process fed with grape pomace by adsorption on ion exchange resins', *Chem. Eng. J.*, 306, pp. 629-639. <https://doi.org/10.1016/j.cej.2016.07.101>
- Reddy, A. V. R. & Patel, H. R. (2008) 'Chemically treated polyethersulfone/polyacrylonitrile blend ultrafiltration membranes for better fouling resistance', *Desalination.*, 221, pp. 318-323. <https://doi.org/10.1016/j.desal.2007.01.089>
- Ren, N. Q., Chua, H., Chan, S. Y., et al. (2007) 'Assessing optimal fermentation type for bio-hydrogen production in continuous-flow acidogenic reactors', *Bioresour. Technol.*, 98, pp. 1774-1780. <https://doi.org/10.1016/j.biortech.2006.07.026>
- Ren, Y., Yu, M., Wu, C., et al. (2018) 'A comprehensive review on food waste anaerobic digestion: Research updates and tendencies', *Bioresour. Technol.*, 247, pp. 1069-1076. <https://doi.org/10.1016/j.biortech.2017.09.109>
- Reyhanitash, E., Fufachev, E., Van Munster, K. D., et al. (2019) 'Recovery and conversion of acetic acid from a phosphonium phosphinate ionic liquid to enable valorization of fermented wastewater', *Green. Chem.*, 21, pp. 2023-2034. <https://doi.org/10.1039/C9GC00725C>
- Reyhanitash, E., Kersten, S. R. A. & Schuur, B. (2017) 'Recovery of volatile fatty acids from fermented wastewater by adsorption', *ACS. Sustainable. Chem. Eng.*, 5, pp. 9176-9184. <https://doi.org/10.1021/acssuschemeng.7b02095>
- Reyhanitash, E., Zaalberg, B., Ijmker, H. M., et al. (2015) 'CO₂-enhanced extraction of acetic acid from fermented wastewater', *Green. Chem.*, 17, pp. 4393-4400. <https://doi.org/10.1039/C5GC01061F>
- Reyhanitash, E., Zaalberg, B., Kersten, S. R. A., et al. (2016) 'Extraction of volatile fatty acids from fermented wastewater', *Sep. Purif. Technol.*, 161, pp. 61-68. <https://doi.org/10.1016/j.seppur.2016.01.037>
- Rho, H., Cho, J., Westerhoff, P., et al. (2020) 'Intrinsic pKa of nanofiltration membrane surfaces to assess fouling and cleaning behaviors induced by foulant-membrane electrostatic interactions', *Environ. Sci. Technol.*, 54, pp. 7706-7714. <https://doi.org/10.1021/acs.est.0c01846>

- Rodríguez-Llorente, D., Bengoa, A., Pascual-Muñoz, G., et al. (2019) 'Sustainable recovery of volatile fatty acids from aqueous solutions using terpenoids and eutectic solvents', *ACS. Sustainable. Chem. Eng.*, 7, pp. 16786-16794. <https://doi.org/10.1021/acssuschemeng.9b04290>
- Rongwong, W. & Goh, K. (2020) 'Resource recovery from industrial wastewaters by hydrophobic membrane contactors: A review', *J. Environ. Chem. Eng.*, 8, pp. 104242. <https://doi.org/10.1016/j.jece.2020.104242>
- Rongwong, W., Lee, J., Goh, K., et al. (2018a) 'Membrane-based technologies for post-treatment of anaerobic effluents', *npj. Clean. Water.*, 1, pp. 1-11. <https://doi.org/10.1038/s41545-018-0021-y>
- Rongwong, W., Lee, J., Goh, K., et al. (2018b) 'Membrane-based technologies for post-treatment of anaerobic effluents', *npj Clean. Water.*, 1, pp. 21. <https://doi.org/10.1038/s41545-018-0021-y>
- Ruprakobkit, T., Ruprakobkit, L. & Ratanatamskul, C. (2016) 'Carboxylic acid concentration by forward osmosis processes: Dynamic modeling, experimental validation and simulation', *Chem. Eng. J.*, 306, pp. 538-549. <https://doi.org/10.1016/j.cej.2016.07.091>
- Ruprakobkit, T., Ruprakobkit, L. & Ratanatamskul, C. (2017) 'Dynamic modelling of carboxylic acid filtration in forward osmosis process: The role of membrane CO₂ permeability', *Comput. Chem. Eng.*, 98, pp. 100-112. <https://doi.org/10.1016/j.compchemeng.2016.10.017>
- Ruprakobkit, T., Ruprakobkit, L. & Ratanatamskul, C. (2019) 'Sensitivity analysis techniques for the optimal system design of forward osmosis in organic acid recovery', *Comput. Chem. Eng.*, 123, pp. 34-48. <https://doi.org/10.1016/j.compchemeng.2018.12.024>
- S Lopes, L., Vieira, N., R da Luz, J. M., et al. (2020) 'Production of fungal enzymes in Macaúba coconut and enzymatic degradation of textile dye', *Biocatal. Agric. Biotechnol.*, 26, pp. 101651. <https://doi.org/10.1016/j.bcab.2020.101651>
- Saadi, R., Saadi, Z., Fazaeli, R., et al. (2015) 'Monolayer and multilayer adsorption isotherm models for sorption from aqueous media', *Korean. J. Chem. Eng.*, 32, pp. 787-799. <https://doi.org/10.1007/s11814-015-0053-7>
- Sadeghi, I., Kaner, P. & Asatekin, A. (2018) 'Controlling and expanding the selectivity of filtration membranes', *Chem. Mater.*, 30, pp. 7328-7354. <https://doi.org/10.1021/acs.chemmater.8b03334>
- Saha, B., Chopade, S. P. & Mahajani, S. M. (2000) 'Recovery of dilute acetic acid through esterification in a reactive distillation column', *Catal. Today.*, 60, pp. 147-157. [https://doi.org/10.1016/S0920-5861\(00\)00326-6](https://doi.org/10.1016/S0920-5861(00)00326-6)
- Şahin, S. & Kurtulbaş, E. (2020) 'An advanced approach for the recovery of acetic acid from its aqueous media: deep eutectic liquids versus ionic liquids', *Biomass. Conv. Bioref.*, pp. 1-9. <https://doi.org/10.1007/s13399-019-00599-8>
- Sahu, S., Pahi, S., Tripathy, S., et al. (2020) 'Adsorption of methylene blue on chemically modified lychee seed biochar: Dynamic, equilibrium, and

- thermodynamic study', *Journal of Molecular Liquids*, 315, pp. 113743. <https://doi.org/10.1016/j.molliq.2020.113743>
- Sakcharoen, T., Ratanatamskul, C. & Chandrachai, A. (2021) 'Factors affecting technology selection, techno-economic and environmental sustainability assessment of a novel zero-waste system for food waste and wastewater management', *Journal of Cleaner Production*, 314, pp. 128103. <https://doi.org/10.1016/j.jclepro.2021.128103>
- Salemdeeb, R., zu Ermgassen, E. K. H. J., Kim, M. H., et al. (2017) 'Environmental and health impacts of using food waste as animal feed: a comparative analysis of food waste management options', *J. Clean. Prod.*, 140, pp. 871-880. <https://doi.org/10.1016/j.jclepro.2016.05.049>
- Salgin, S., Salgin, U. & Soyer, N. (2013) 'Streaming potential measurements of polyethersulfone ultrafiltration membranes to determine salt effects on membrane zeta potential', *Int. J. Electrochem. Sci.*, 8, pp. 4073-4084.
- Sambusiti, C., Saadouni, M., Gauchou, V., et al. (2020) 'Influence of HRT reduction on pilot scale flat sheet submerged membrane bioreactor (sMBR) performances for Oil&Gas wastewater treatment', *Journal of Membrane Science*, 594, pp. 117459. <https://doi.org/10.1016/j.memsci.2019.117459>
- Sandhu, H. K., Sehrawat, R., Kumar, A., et al. 2020. Overview of Food Industry and Role of Innovation in Food Industry. In: THAKUR, M. & MODI, V. K. (eds.) *Emerging Technologies in Food Science: Focus on the Developing World*. Singapore: Springer Singapore.
- Sano, T., Ejiri, S., Yamada, K., et al. (1997) 'Separation of acetic acid-water mixtures by pervaporation through silicalite membrane', *J. Membr. Sci.*, 123, pp. 225-233. [https://doi.org/10.1016/S0376-7388\(96\)00224-4](https://doi.org/10.1016/S0376-7388(96)00224-4)
- Schäfer, A. I., Stelzl, K., Faghih, M., et al. (2018) 'Poly(ether sulfone) nanofibers impregnated with β -cyclodextrin for increased micropollutant removal from water', *ACS Sustainable. Chem. Eng.*, 6, pp. 2942-2953. <https://doi.org/10.1021/acssuschemeng.7b02214>
- Schanes, K., Dobernig, K. & Gözet, B. (2018) 'Food waste matters - A systematic review of household food waste practices and their policy implications', *J. Clean. Prod.*, 182, pp. 978-991. <https://doi.org/10.1016/j.jclepro.2018.02.030>
- Scoma, A., Varela-Corredor, F., Bertin, L., et al. (2016) 'Recovery of VFAs from anaerobic digestion of dephenolized Olive Mill Wastewaters by Electrodialysis', *Sep. Purif. Technol.*, 159, pp. 81-91. <https://doi.org/10.1016/j.seppur.2015.12.029>
- Sehar, S. (2020) 'Wastewater treatment of food industries through constructed wetland: a review', *International Journal of Environmental Science and Technology*, 17, pp. 4667-4668. <https://doi.org/10.1007/s13762-020-02932-5>
- Sellaoui, L., Dhaouadi, F., Li, Z., et al. (2021) 'Implementation of a multilayer statistical physics model to interpret the adsorption of food dyes on a

- chitosan film', *Journal of Environmental Chemical Engineering*, 9, pp. 105516.
- Shalan, A. E., Afifi, M., El-Desoky, M. M., et al. (2021) 'Electrospun nanofibrous membranes of cellulose acetate containing hydroxyapatite co-doped with Ag/Fe: morphological features, antibacterial activity and degradation of methylene blue in aqueous solution', *New Journal of Chemistry*, 45, pp. 9212-9220. [10.1039/D1NJ00569C](https://doi.org/10.1039/D1NJ00569C)
- Sharma, S., Sharma, G., Kumar, A., et al. (2022) 'Adsorption of cationic dyes onto carrageenan and itaconic acid-based superabsorbent hydrogel: Synthesis, characterization and isotherm analysis', *Journal of Hazardous Materials*, 421, pp. 126729. <https://doi.org/10.1016/j.jhazmat.2021.126729>
- Shen, K., Cheng, C., Zhang, T., et al. (2019) 'High performance polyamide composite nanofiltration membranes via reverse interfacial polymerization with the synergistic interaction of gelatin interlayer and trimesoyl chloride', *Journal of Membrane Science*, 588, pp. 117192. <https://doi.org/10.1016/j.memsci.2019.117192>
- Shi, L., Hu, Y., Xie, S., et al. (2018a) 'Recovery of nutrients and volatile fatty acids from pig manure hydrolysate using two-stage bipolar membrane electrodialysis', *Chem. Eng. J.*, 334, pp. 134-142. <https://doi.org/10.1016/j.cej.2017.10.010>
- Shi, L., Simplicio, W. S., Wu, G., et al. (2018b) 'Nutrient recovery from digestate of anaerobic digestion of livestock manure: a review', *Curr. Pollut. Rep.*, 4, pp. 74-83. <https://doi.org/10.1007/s40726-018-0082-z>
- Shin, C.-H., Kim, J.-Y., Kim, J.-Y., et al. (2009) 'A solvent extraction approach to recover acetic acid from mixed waste acids produced during semiconductor wafer process', *J. Hazard. Mater.*, 162, pp. 1278-1284. <https://doi.org/10.1016/j.jhazmat.2008.06.029>
- Shirazi, S., Lin, C.-J. & Chen, D. (2010) 'Inorganic fouling of pressure-driven membrane processes — A critical review', *Desalination*, 250, pp. 236-248. <https://doi.org/10.1016/j.desal.2009.02.056>
- Shrivastava, V., Ali, I., Marjub, M. M., et al. (2022) 'Wastewater in the food industry: Treatment technologies and reuse potential', *Chemosphere*, 293, pp. 133553. <https://doi.org/10.1016/j.chemosphere.2022.133553>
- Simon, A. & Nghiem Long, D. (2014) 'Effects of hypochlorite exposure on morphology and trace organic contaminant rejection by NF/RO membranes', *Membr. Water. Treat.*, 5, pp. 235-250. <http://dx.doi.org/10.12989/mwt.2014.5.4.235>
- Singh, A., Tiwari, A., Bansal, V., et al. (2007) 'Recovery of acetic acid by reactive distillation: Parametric study and nonlinear dynamic effects', *Ind. Eng. Chem. Res.*, 46, pp. 9196-9204. <https://doi.org/10.1021/ie071070i>
- Singh, A., Tiwari, A., Mahajani, S. M., et al. (2006) 'Recovery of acetic acid from aqueous solutions by reactive distillation', *Ind. Eng. Chem. Res.*, 45, pp. 2017-2025. <https://doi.org/10.1021/ie0505514>

- Singh, N., Petrinic, I., Hélix-Nielsen, C., et al. (2019) 'Influence of Forward Osmosis (FO) membrane properties on dewatering of molasses distillery wastewater', *Journal of Water Process Engineering*, 32, pp. 100921. <https://doi.org/10.1016/j.jwpe.2019.100921>
- Skaggs, R. L., Coleman, A. M., Seiple, T. E., et al. (2018) 'Waste-to-Energy biofuel production potential for selected feedstocks in the conterminous United States', *Renew. Sust. Energ. Rev.*, 82, pp. 2640-2651. <https://doi.org/10.1016/j.rser.2017.09.107>
- Smithells, C. J., Ransley, C. E. & Fowler, R. H. (1936) 'The diffusion of gases through metals-IV—The diffusion of oxygen and of hydrogen through nickel at very high pressures', *Proc. R. Soc. Lond. A. Math. Phys. Sci.*, 157, pp. 292-302. <https://doi.org/10.1098/rspa.1936.0195>
- Snow, M. J. H., de Winter, D., Buckingham, R., et al. (1996) 'New techniques for extreme conditions: high temperature reverse osmosis and nanofiltration', *Desalination.*, 105, pp. 57-61. [https://doi.org/10.1016/0011-9164\(96\)00058-6](https://doi.org/10.1016/0011-9164(96)00058-6)
- Song, L., Li, B., Sirkar, K. K., et al. (2007) 'Direct contact membrane distillation-based desalination: Novel membranes, devices, larger-scale studies, and a model', *Ind. Eng. Chem. Res.*, 46, pp. 2307-2323. <https://doi.org/10.1021/ie0609968>
- Song, X., Luo, W., Hai, F. I., et al. (2018) 'Resource recovery from wastewater by anaerobic membrane bioreactors: Opportunities and challenges', *Bioresour. Technol.*, 270, pp. 669-677. <https://doi.org/10.1016/j.biortech.2018.09.001>
- Sprakel, L. M. J. & Schuur, B. (2019) 'Solvent developments for liquid-liquid extraction of carboxylic acids in perspective', *Sep. Purif. Technol.*, 211, pp. 935-957. <https://doi.org/10.1016/j.seppur.2018.10.023>
- Sroka, E., Kamiński, W. & Bohdziewicz, J. (2004) 'Biological treatment of meat industry wastewater', *Desalination*, 162, pp. 85-91. [https://doi.org/10.1016/S0011-9164\(04\)00030-X](https://doi.org/10.1016/S0011-9164(04)00030-X)
- Strathmann, H. (2010) 'Electrodialysis, a mature technology with a multitude of new applications', *Desalination.*, 264, pp. 268-288. <https://doi.org/10.1016/j.desal.2010.04.069>
- Strazzera, G., Battista, F., Garcia, N. H., et al. (2018) 'Volatile fatty acids production from food wastes for biorefinery platforms: A review', *Journal of Environmental Management*, 226, pp. 278-288. <https://doi.org/10.1016/j.jenvman.2018.08.039>
- Su, Z., Chen, J. H., Sun, X., et al. (2015) 'Amine-functionalized metal organic framework (NH₂-MIL-125(Ti)) incorporated sodium alginate mixed matrix membranes for dehydration of acetic acid by pervaporation', *RSC. Adv.*, 5, pp. 99008-99017. <https://doi.org/10.1039/C5RA21073A>
- Swaminathan, S., Imayathamizhan, N. & Muthumanickam, A. (2021) 'Kinetic and isotherm studies on adsorption of methylene blue using polyacrylonitrile/hydroxyl group functionalized multiwall carbon nanotube

- multilayered nanofibrous composite', *J. Elastomers. Plast.*, 53, pp. 48-67.
<https://doi.org/10.1177/0095244319897284>
- T. M. S., Arshad, A. B., Lin, P. T., et al. (2021a) 'A review of recent progress in polymeric electrospun nanofiber membranes in addressing safe water global issues', *RSC Advances*, 11, pp. 9638-9663. 10.1039/D1RA00060H
- T. M. S., Arshad, A. B., Lin, P. T., et al. (2021b) 'A review of recent progress in polymeric electrospun nanofiber membranes in addressing safe water global issues', *RSC Adv.*, 11, pp. 9638-9663. 10.1039/D1RA00060H
- Talebi, A., Razali, Y. S., Ismail, N., et al. (2020) 'Selective adsorption and recovery of volatile fatty acids from fermented landfill leachate by activated carbon process', *Sci. Total. Environ.*, 707, pp. 134533.
<https://doi.org/10.1016/j.scitotenv.2019.134533>
- Talukder, M. E., Alam, F., Pervez, M. N., et al. (2022a) 'New generation washable PES membrane face mask for virus filtration', *Nanocomposites.*, 8, pp. 13-23. <https://doi.org/10.1080/20550324.2021.2008209>
- Talukder, M. E., Alam, F., Pervez, M. N., et al. (2022b) 'New generation washable PES membrane face mask for virus filtration', *Nanocomposites*, 8, pp. 13-23. 10.1080/20550324.2021.2008209
- Talukder, M. E., Hasan, K. M. F., Wang, J., et al. (2021a) 'Novel fibrin functionalized multilayered electrospun nanofiber membrane for burn wound treatment', *J. Mater. Sci.*, 56, pp. 12814-12834.
<https://doi.org/10.1007/s10853-021-06123-6>
- Talukder, M. E., Hasan, K. M. F., Wang, J., et al. (2021b) 'Novel fibrin functionalized multilayered electrospun nanofiber membrane for burn wound treatment', *Journal of Materials Science*, 56, pp. 12814-12834. 10.1007/s10853-021-06123-6
- Talukder, M. E., Pervez, M. N., Jianming, W., et al. (2021c) 'Chitosan-functionalized sodium alginate-based electrospun nanofiber membrane for As (III) removal from aqueous solution', *J. Environ. Chem. Eng.*, 9, pp. 106693.
<https://doi.org/10.1016/j.jece.2021.106693>
- Talukder, M. E., Pervez, M. N., Jianming, W., et al. (2021d) 'Chitosan-functionalized sodium alginate-based electrospun nanofiber membrane for As (III) removal from aqueous solution', *Journal of Environmental Chemical Engineering*, 9, pp. 106693.
<https://doi.org/10.1016/j.jece.2021.106693>
- Tan, S. H., Inai, R., Kotaki, M., et al. (2005) 'Systematic parameter study for ultra-fine fiber fabrication via electrospinning process', *Polymer*, 46, pp. 6128-6134. <https://doi.org/10.1016/j.polymer.2005.05.068>
- Tang, C. Y., Kwon, Y.-N. & Leckie, J. O. (2009) 'Effect of membrane chemistry and coating layer on physiochemical properties of thin film composite polyamide RO and NF membranes: II. Membrane physiochemical properties and their dependence on polyamide and coating layers', *Desalination.*, 242, pp. 168-182.
<https://doi.org/10.1016/j.desal.2008.04.004>

- Tao, B., Passanha, P., Kumi, P., et al. (2016) 'Recovery and concentration of thermally hydrolysed waste activated sludge derived volatile fatty acids and nutrients by microfiltration, electrodialysis and struvite precipitation for polyhydroxyalkanoates production', *Chem. Eng. J.*, 295, pp. 11-19. <https://doi.org/10.1016/j.cej.2016.03.036>
- Tapera, M. (2019) 'Towards greener preservation of edible oils: A mini-review', *Asian Journal of Applied Chemistry Research*, 4, pp. 1-8. <https://doi.org/10.9734/ajacr/2019/v4i1-230105>
- Thamer, B. M., El-Hamshary, H., Al-Deyab, S. S., et al. (2019) 'Functionalized electrospun carbon nanofibers for removal of cationic dye', *Arabian Journal of Chemistry*, 12, pp. 747-759. <https://doi.org/10.1016/j.arabj.2018.07.020>
- Thi, N. B. D., Kumar, G. & Lin, C.-Y. (2015) 'An overview of food waste management in developing countries: Current status and future perspective', *J. Environ. Manage.*, 157, pp. 220-229. <https://doi.org/10.1016/j.jenvman.2015.04.022>
- Tonucci, M. C., Adarme, O. F. H., Aquino, S. F. d., et al. (2020) 'Synthesis of hybrid magnetic molecularly imprinted polymers for the selective adsorption of volatile fatty acids from anaerobic effluents', *Polym. Int.*, 69, pp. 847-857. <https://doi.org/10.1002/pi.6026>
- Trad, Z., Akimbomi, J., Vial, C., et al. (2015) 'Development of a submerged anaerobic membrane bioreactor for concurrent extraction of volatile fatty acids and biohydrogen production', *Bioresour. Technol.*, 196, pp. 290-300. <https://doi.org/10.1016/j.biortech.2015.07.095>
- Tugtas, A. E. (2014) 'Recovery of volatile fatty acids via membrane contactor using flat membranes: Experimental and theoretical analysis', *Waste. Manag.*, 34, pp. 1171-1178. <https://doi.org/10.1016/j.wasman.2014.01.020>
- Tung, L. A. & King, C. J. (1994) 'Sorption and extraction of lactic and succinic acids at pH > pKa1. I. Factors governing equilibria', *Ind. Eng. Chem. Res.*, 33, pp. 3217-3223. <https://doi.org/10.1021/ie00036a041>
- Uslu, H., İnci, I. s. & Bayazit, S. S. (2010) 'Adsorption equilibrium data for acetic acid and glycolic acid onto Amberlite IRA-67', *J. Chem. Eng. Data.*, 55, pp. 1295-1299. <https://doi.org/10.1021/je900635z>
- Uyar, B., Eroglu, I., Yücel, M., et al. (2009) 'Photofermentative hydrogen production from volatile fatty acids present in dark fermentation effluents', *Int. J. Hydrog. Energy.*, 34, pp. 4517-4523. <https://doi.org/10.1016/j.ijhydene.2008.07.057>
- Valero, D., García-García, V., Expósito, E., et al. (2015) 'Application of electrodialysis for the treatment of almond industry wastewater', *Journal of Membrane Science*, 476, pp. 580-589. <https://doi.org/10.1016/j.memsci.2014.11.007>
- Valta, K., Kosanovic, T., Malamis, D., et al. (2015) 'Overview of water usage and wastewater management in the food and beverage industry', *Desalination and Water Treatment*, 53, pp. 3335-3347. <https://doi.org/10.1080/19443994.2014.934100>

- van den Berg, G. B. & Smolders, C. A. (1990) 'Flux decline in ultrafiltration processes', *Desalination.*, 77, pp. 101-133. [https://doi.org/10.1016/0011-9164\(90\)85023-4](https://doi.org/10.1016/0011-9164(90)85023-4)
- Van der Bruggen, B., Braeken, L. & Vandecasteele, C. (2002) 'Evaluation of parameters describing flux decline in nanofiltration of aqueous solutions containing organic compounds', *Desalination.*, 147, pp. 281-288. [https://doi.org/10.1016/S0011-9164\(02\)00553-2](https://doi.org/10.1016/S0011-9164(02)00553-2)
- Van der Bruggen, B., Lejon, L. & Vandecasteele, C. (2003a) 'Reuse, treatment, and discharge of the concentrate of pressure-driven membrane processes', *Environ. Sci. Technol.*, 37, pp. 3733-3738. <https://doi.org/10.1021/es0201754>
- Van der Bruggen, B. & Vandecasteele, C. (2003) 'Removal of pollutants from surface water and groundwater by nanofiltration: overview of possible applications in the drinking water industry', *Environ. Pollut.*, 122, pp. 435-445. [https://doi.org/10.1016/S0269-7491\(02\)00308-1](https://doi.org/10.1016/S0269-7491(02)00308-1)
- Van Der Bruggen, B., Vandecasteele, C., Van Gestel, T., et al. (2003b) 'A review of pressure-driven membrane processes in wastewater treatment and drinking water production', *Environmental Progress*, 22, pp. 46-56. <https://doi.org/10.1002/ep.670220116>
- Van der Bruggen, B., Vandecasteele, C., Van Gestel, T., et al. (2003c) 'A review of pressure-driven membrane processes in wastewater treatment and drinking water production', *Environ. Prog.*, 22, pp. 46-56. <https://doi.org/10.1002/ep.670220116>
- Venkata Mohan, S., Nikhil, G. N., Chiranjeevi, P., et al. (2016) 'Waste biorefinery models towards sustainable circular bioeconomy: Critical review and future perspectives', *Bioresour. Technol.*, 215, pp. 2-12. <https://doi.org/10.1016/j.biortech.2016.03.130>
- Veral, M. A., Çinar, Ö. & Kizilet, A. (2020) 'Membrane bioreactor and dynamic membrane bioreactor performance comparison under the same conditions', *Avrupa Bilim ve Teknoloji Dergisi*, pp. 30-41. <https://doi.org/10.31590/ejosat.619539>
- Verliefde, A. R. D., Cornelissen, E. R., Heijman, S. G. J., et al. (2008) 'The role of electrostatic interactions on the rejection of organic solutes in aqueous solutions with nanofiltration', *J. Membr. Sci.*, 322, pp. 52-66. <https://doi.org/10.1016/j.memsci.2008.05.022>
- Vertova, A., Aricci, G., Rondinini, S., et al. (2009) 'Electrodialytic recovery of light carboxylic acids from industrial aqueous wastes', *J. Appl. Electrochem.*, 39, pp. 2051. <https://doi.org/10.1007/s10800-009-9871-9>
- Vieira, G. S., Moreira, F. K. V., Matsumoto, R. L. S., et al. (2018) 'Influence of nanofiltration membrane features on enrichment of jussara ethanolic extract (*Euterpe edulis*) in anthocyanins', *J. Food. Eng.*, 226, pp. 31-41. <https://doi.org/10.1016/j.jfoodeng.2018.01.013>

- Vourch, M., Balannec, B., Chaufer, B., et al. (2008) 'Treatment of dairy industry wastewater by reverse osmosis for water reuse', *Desalination*, 219, pp. 190-202. <https://doi.org/10.1016/j.desal.2007.05.013>
- Wainaina, S., Awasthi, M. K., Horváth, I. S., et al. (2020a) 'Anaerobic digestion of food waste to volatile fatty acids and hydrogen at high organic loading rates in immersed membrane bioreactors', *Renew. Energy.*, 152, pp. 1140-1148. <https://doi.org/10.1016/j.renene.2020.01.138>
- Wainaina, S., Awasthi, M. K., Horváth, I. S., et al. (2020b) 'Anaerobic digestion of food waste to volatile fatty acids and hydrogen at high organic loading rates in immersed membrane bioreactors', *Renewable Energy*, 152, pp. 1140-1148. <https://doi.org/10.1016/j.renene.2020.01.138>
- Wainaina, S., Awasthi, M. K., Sarsaiya, S., et al. (2020c) 'Resource recovery and circular economy from organic solid waste using aerobic and anaerobic digestion technologies', *Bioresour. Technol.*, 301, pp. 122778. <https://doi.org/10.1016/j.biortech.2020.122778>
- Wainaina, S., Kisworini, A. D., Fanani, M., et al. (2020d) 'Utilization of food waste-derived volatile fatty acids for production of edible *Rhizopus oligosporus* fungal biomass', *Bioresource Technology*, 310, pp. 123444. <https://doi.org/10.1016/j.biortech.2020.123444>
- Wainaina, S., Lukitawesa, Kumar Awasthi, M., et al. (2019a) 'Bioengineering of anaerobic digestion for volatile fatty acids, hydrogen or methane production: A critical review', *Bioengineered.*, 10, pp. 437-458. <https://doi.org/10.1080/21655979.2019.1673937>
- Wainaina, S., Lukitawesa, Kumar Awasthi, M., et al. (2019b) 'Bioengineering of anaerobic digestion for volatile fatty acids, hydrogen or methane production: A critical review', *Bioengineered.*, 10, pp. 437-458. [10.1080/21655979.2019.1673937](https://doi.org/10.1080/21655979.2019.1673937)
- Wainaina, S., Parchami, M., Mahboubi, A., et al. (2019c) 'Food waste-derived volatile fatty acids platform using an immersed membrane bioreactor', *Bioresour. Technol.*, 274, pp. 329-334. <https://doi.org/10.1016/j.biortech.2018.11.104>
- Wainaina, S., Parchami, M., Mahboubi, A., et al. (2019d) 'Food waste-derived volatile fatty acids platform using an immersed membrane bioreactor', *Bioresource Technology*, 274, pp. 329-334. <https://doi.org/10.1016/j.biortech.2018.11.104>
- Walsh, B. P., Cusack, D. O. & O'Sullivan, D. T. J. (2016) 'An industrial water management value system framework development', *Sustainable Production and Consumption*, 5, pp. 82-93. <https://doi.org/10.1016/j.spc.2015.11.004>
- Wang, J., Zhang, N., Jiang, C., et al. (2018) 'Adsorptive removal of phenol by single and double network composite hydrogels based on hydroxypropyl cellulose and graphene oxide', *Journal of Materials Research*, 33, pp. 3898-3905.
- Wang, K., Yin, J., Shen, D., et al. (2014a) 'Anaerobic digestion of food waste for volatile fatty acids (VFAs) production with different types of inoculum:

- Effect of pH', *Bioresource Technology*, 161, pp. 395-401.
<https://doi.org/10.1016/j.biortech.2014.03.088>
- Wang, L., Li, J., Zhang, S., et al. (2016) 'Preparation and Characterization of All-Biomass Soy Protein Isolate-Based Films Enhanced by Epoxy Castor Oil Acid Sodium and Hydroxypropyl Cellulose', *Materials*, 9, pp. 193.
- Wang, Q., Ju, J., Tan, Y., et al. (2019a) 'Controlled synthesis of sodium alginate electrospun nanofiber membranes for multi-occasion adsorption and separation of methylene blue', *Carbohydrate Polymers*, 205, pp. 125-134.
<https://doi.org/10.1016/j.carbpol.2018.10.023>
- Wang, R., Liu, Y., Li, B., et al. (2012) 'Electrospun nanofibrous membranes for high flux microfiltration', *Journal of Membrane Science*, 392-393, pp. 167-174.
<https://doi.org/10.1016/j.memsci.2011.12.019>
- Wang, S., Liu, J., Hembre, R., et al. (2017) 'Liquid-liquid equilibria of ionic liquids-water-acetic acid mixtures', *J. Chem. Eng. Data.*, 62, pp. 653-664.
<https://doi.org/10.1021/acs.jced.6b00692>
- Wang, Y., Górecki, R. P., Stamate, E., et al. (2019b) 'Preparation of super-hydrophilic polyphenylsulfone nanofiber membranes for water treatment', *RSC Advances*, 9, pp. 278-286. 10.1039/C8RA06493H
- Wang, Y., Górecki, R. P., Stamate, E., et al. (2019c) 'Preparation of super-hydrophilic polyphenylsulfone nanofiber membranes for water treatment', *RSC Adv.*, 9, pp. 278-286. 10.1039/C8RA06493H
- Wang, Y., Huang, X. & Yuan, Q. (2005) 'Nitrogen and carbon removals from food processing wastewater by an anoxic/aerobic membrane bioreactor', *Process Biochemistry*, 40, pp. 1733-1739.
<https://doi.org/10.1016/j.procbio.2004.06.039>
- Wang, Y., Shi, L., Wu, H., et al. (2019d) 'Graphene Oxide-IPDI-Ag/ZnO@Hydroxypropyl Cellulose Nanocomposite Films for Biological Wound-Dressing Applications', *ACS Omega*, 4, pp. 15373-15381. 10.1021/acsomega.9b01291
- Wang, Z., Li, Z., Liu, L., et al. (2010) 'A Novel Alcohol Detector Based on ZrO₂-Doped SnO₂ Electrospun Nanofibers', *Journal of the American Ceramic Society*, 93, pp. 634-637. <https://doi.org/10.1111/j.1551-2916.2009.03480.x>
- Wang, Z., Luo, Y. & Yu, P. (2006) 'Recovery of organic acids from waste salt solutions derived from the manufacture of cyclohexanone by electrodialysis', *J. Membr. Sci.*, 280, pp. 134-137.
<https://doi.org/10.1016/j.memsci.2006.01.015>
- Wang, Z., Ma, J., Tang, C. Y., et al. (2014b) 'Membrane cleaning in membrane bioreactors: A review', *Journal of Membrane Science*, 468, pp. 276-307.
<https://doi.org/10.1016/j.memsci.2014.05.060>
- Ward, A. J., Arola, K., Brewster, E. T., et al. (2018) 'Nutrient recovery from wastewater through pilot scale electrodialysis', *Water. Res.*, 135, pp. 57-65.
<https://doi.org/10.1016/j.watres.2018.02.021>

- Wasewar, K. L., Heesink, A. B. M., Versteeg, G. F., et al. (2002) 'Reactive extraction of lactic acid using alamine 336 in MIBK: equilibria and kinetics', *J. Biotechnol.*, 97, pp. 59-68. [https://doi.org/10.1016/S0168-1656\(02\)00057-3](https://doi.org/10.1016/S0168-1656(02)00057-3)
- Wasewar, K. L., Pangarkar, V. G., Heesink, A. B. M., et al. (2003) 'Intensification of enzymatic conversion of glucose to lactic acid by reactive extraction', *Chem. Eng. Sci.*, 58, pp. 3385-3393. [https://doi.org/10.1016/S0009-2509\(03\)00221-5](https://doi.org/10.1016/S0009-2509(03)00221-5)
- Wei, Y., Ding, A., Dong, L., et al. (2015) 'Characterisation and coagulation performance of an inorganic coagulant—poly-magnesium-silicate-chloride in treatment of simulated dyeing wastewater', *Colloids. Surf. A Physicochem. Eng. Asp.*, 470, pp. 137-141. <https://doi.org/10.1016/j.colsurfa.2015.01.066>
- Weng, Y.-H., Wei, H.-J., Tsai, T.-Y., et al. (2009) 'Separation of acetic acid from xylose by nanofiltration', *Sep. Purif. Technol.*, 67, pp. 95-102. <https://doi.org/10.1016/j.seppur.2009.03.030>
- Werber, J. R., Deshmukh, A. & Elimelech, M. (2016) 'The critical need for increased selectivity, not increased water permeability, for desalination membranes', *Environ. Sci. Technol. Lett.*, 3, pp. 112-120. <https://doi.org/10.1021/acs.estlett.6b00050>
- Xie, Y. & Liu, S. (2015) 'Purification and concentration of paulownia hot water wood extracts with nanofiltration', *Sep. Purif. Technol.*, 156, pp. 848-855. <https://doi.org/10.1016/j.seppur.2015.11.012>
- Xiong, B., Richard, T. L. & Kumar, M. (2015) 'Integrated acidogenic digestion and carboxylic acid separation by nanofiltration membranes for the lignocellulosic carboxylate platform', *J. Membr. Sci.*, 489, pp. 275-283. <https://doi.org/10.1016/j.memsci.2015.04.022>
- Xu, F., Li, Y., Ge, X., et al. (2018a) 'Anaerobic digestion of food waste—Challenges and opportunities', *Bioresour. Technol.*, 247, pp. 1047-1058. <https://doi.org/10.1016/j.biortech.2017.09.020>
- Xu, F., Li, Y., Ge, X., et al. (2018b) 'Anaerobic digestion of food waste – Challenges and opportunities', *Bioresour. Technol.*, 247, pp. 1047-1058. <https://doi.org/10.1016/j.biortech.2017.09.020>
- Xu, Y., Yuan, D., Bao, J., et al. (2018c) 'Nanofibrous membranes with surface migration of functional groups for ultrafast wastewater remediation', *J. Mater. Chem. A.*, 6, pp. 13359-13372. <https://doi.org/10.1039/C8TA04005B>
- Xu, Y., Yuan, D., Guo, Y., et al. (2022) 'Superhydrophilic and polyporous nanofibrous membrane with excellent photocatalytic activity and recyclability for wastewater remediation under visible light irradiation', *Chemical Engineering Journal*, 427, pp. 131685. <https://doi.org/10.1016/j.cej.2021.131685>
- Yadav, V., Sarker, A., Yadav, A., et al. (2022) 'Integrated biorefinery approach to valorize citrus waste: A sustainable solution for resource recovery and environmental management', *Chemosphere*, 293, pp. 133459. <https://doi.org/10.1016/j.chemosphere.2021.133459>

- Yagy, D., Ohishi, T., Igarashi, T., et al. (2013) 'Recovery of acetic acid from dilute aqueous solutions using catalytic dehydrative esterification with ethanol', *Chemosphere.*, 91, pp. 61-67. <https://doi.org/10.1016/j.chemosphere.2012.11.078>
- Yam-Cervantesa, M., Aguilar-Vegaa, M., Santiago-Garcíaa, J. L., et al. (2020) 'Methylene blue removal from aqueous solutions by sulfonated polymeric porous sorbents', *Desalin. Water. Treat.*, 184, pp. 367-374. <https://doi.org/10.5004/dwt.2020.25388>
- Yang, G., Jahan, M. S., Ahsan, L., et al. (2013a) 'Recovery of acetic acid from pre-hydrolysis liquor of hardwood kraft-based dissolving pulp production process by reactive extraction with triisooctylamine', *Bioresour. Technol.*, 138, pp. 253-258. <https://doi.org/10.1016/j.biortech.2013.03.164>
- Yang, W., Li, X., Pan, B., et al. (2013b) 'Effective removal of effluent organic matter (EfOM) from bio-treated coking wastewater by a recyclable aminated hyper-cross-linked polymer', *Water. Res.*, 47, pp. 4730-4738. <https://doi.org/10.1016/j.watres.2013.05.032>
- Yao, M., Woo, Y. C., Ren, J., et al. (2019) 'Volatile fatty acids and biogas recovery using thermophilic anaerobic membrane distillation bioreactor for wastewater reclamation', *J. Environ. Manage.*, 231, pp. 833-842. <https://doi.org/10.1016/j.jenvman.2018.11.009>
- Yar, A., Haspulat, B., Üstün, T., et al. (2017) 'Electrospun TiO₂/ZnO/PAN hybrid nanofiber membranes with efficient photocatalytic activity', *RSC Adv.*, 7, pp. 29806-29814. 10.1039/C7RA03699J
- Yasin, O., Zelal, I. & Nadir, D. (2020) 'Acetic acid and methanol recovery from dimethyl terephthalate process wastewater using pressure membrane and membrane distillation processes', *J. Water. Process. Eng.*, 38, pp. 101532. <https://doi.org/10.1016/j.jwpe.2020.101532>
- Yesil, H., Taner, H., Nigiz, F. U., et al. (2020) 'Pervaporative separation of mixed volatile fatty acids: a study towards integrated VFA production and separation', *Waste, Biomass. Valor.*, 11, pp. 1737-1753. <https://doi.org/10.1007/s12649-018-0504-6>
- Yesil, H., Tugtas, A. E., Bayrakdar, A., et al. (2014) 'Anaerobic fermentation of organic solid wastes: volatile fatty acid production and separation', *Water. Sci. Technol.*, 69, pp. 2132-2138. <https://doi.org/10.2166/wst.2014.132>
- Yin, D.-m., Mahboubi, A., Wainaina, S., et al. (2021a) 'The effect of mono- and multiple fermentation parameters on volatile fatty acids (VFAs) production from chicken manure via anaerobic digestion', *Bioresource Technology*, 330, pp. 124992. <https://doi.org/10.1016/j.biortech.2021.124992>
- Yin, D.-m., Mahboubi, A., Wainaina, S., et al. (2021b) 'The effect of mono- and multiple fermentation parameters on volatile fatty acids (VFAs) production from chicken manure via anaerobic digestion', *Bioresour. Technol.*, 330, pp. 124992. <https://doi.org/10.1016/j.biortech.2021.124992>
- Yin, Z., Yang, C., Long, C., et al. (2017) 'Influence of surface properties of RO membrane on membrane fouling for treating textile secondary effluent',

- Environ. Sci. Pollut. Res.*, 24, pp. 16253-16262.
<https://doi.org/10.1007/s11356-017-9252-6>
- Young, M. N., Krajmalnik-Brown, R., Liu, W., et al. (2013) 'The role of anaerobic sludge recycle in improving anaerobic digester performance', *Bioresour. Technol.*, 128, pp. 731-737. <https://doi.org/10.1016/j.biortech.2012.11.079>
- Yousuf, A., Bonk, F., Bastidas-Oyanedel, J.-R., et al. (2016) 'Recovery of carboxylic acids produced during dark fermentation of food waste by adsorption on Amberlite IRA-67 and activated carbon', *Bioresour. Technol.*, 217, pp. 137-140. <https://doi.org/10.1016/j.biortech.2016.02.035>
- Yu, L., Guo, Q., Hao, J., et al. (2000) 'Recovery of acetic acid from dilute wastewater by means of bipolar membrane electrodialysis', *Desalination.*, 129, pp. 283-288. [https://doi.org/10.1016/S0011-9164\(00\)00068-0](https://doi.org/10.1016/S0011-9164(00)00068-0)
- Yuan, Y., Hu, X., Chen, H., et al. (2019) 'Advances in enhanced volatile fatty acid production from anaerobic fermentation of waste activated sludge', *Sci. Total. Environ.*, 694, pp. 133741. <https://doi.org/10.1016/j.scitotenv.2019.133741>
- Yue, X., Huang, J., Jiang, F., et al. (2019) 'Synthesis and characterization of cellulose-based adsorbent for removal of anionic and cationic dyes', *Journal of Engineered Fibers and Fabrics*, 14, pp. 1558925019828194. [10.1177/1558925019828194](https://doi.org/10.1177/1558925019828194)
- Zacharof, M.-P. & Lovitt, R. W. (2013a) 'Complex Effluent Streams as a Potential Source of Volatile Fatty Acids', *Waste and Biomass Valorization*, 4, pp. 557-581. [10.1007/s12649-013-9202-6](https://doi.org/10.1007/s12649-013-9202-6)
- Zacharof, M.-P. & Lovitt, R. W. (2013b) 'Complex effluent streams as a potential source of volatile fatty acids', *Waste, Biomass. Valor.*, 4, pp. 557-581. <https://doi.org/10.1007/s12649-013-9202-6>
- Zacharof, M.-P. & Lovitt, R. W. (2013c) 'Recovery of volatile fatty acids (VFA) from complex waste effluents using membranes', *Water. Sci. Technol.*, 69, pp. 495-503. <https://doi.org/10.2166/wst.2013.717>
- Zacharof, M.-P., Mandale, S. J., Oatley-Radcliffe, D., et al. (2019) 'Nutrient recovery and fractionation of anaerobic digester effluents employing pilot scale membrane technology', *Journal of Water Process Engineering*, 31, pp. 100846. <https://doi.org/10.1016/j.jwpe.2019.100846>
- Zacharof, M.-P., Mandale, S. J., Williams, P. M., et al. (2016) 'Nanofiltration of treated digested agricultural wastewater for recovery of carboxylic acids', *J. Clean. Prod.*, 112, pp. 4749-4761. <https://doi.org/10.1016/j.jclepro.2015.07.004>
- Zacharof, M. P. & Lovitt, R. W. Year. Published. The recovery of volatile fatty acids (VFA) from mixed effluent streams using membrane technology: a literature review. 4th international symposium on energy from biomass and waste. Iwwg-international waste working group, 2012 San Servolo, Venice, Italy.
- Zacharof, M. P. & Lovitt, R. W. (2014) 'Recovery of volatile fatty acids (VFA) from complex waste effluents using membranes', *Water. Sci. Technol.*, 69, pp. 495-503. <https://doi.org/10.2166/wst.2013.717>

- Zamani, F., Chew, J. W., Akhondi, E., et al. (2015) 'Unsteady-state shear strategies to enhance mass-transfer for the implementation of ultrapermeable membranes in reverse osmosis: A review', *Desalination*, 356, pp. 328-348. <https://doi.org/10.1016/j.desal.2014.10.021>
- Zan, F., Iqbal, A., Lu, X., et al. (2022) "Food waste-wastewater-energy/resource" nexus: Integrating food waste management with wastewater treatment towards urban sustainability', *Water Research*, 211, pp. 118089. <https://doi.org/10.1016/j.watres.2022.118089>
- Zhang, B., Zhang, L. L., Zhang, S. C., et al. (2005a) 'The Influence of pH on Hydrolysis and Acidogenesis of Kitchen Wastes in Two-phase Anaerobic Digestion', *Environmental Technology*, 26, pp. 329-340. <https://doi.org/10.1080/09593332608618563>
- Zhang, G., Lu, S., Zhang, L., et al. (2013a) 'Novel polysulfone hybrid ultrafiltration membrane prepared with TiO₂-g-HEMA and its antifouling characteristics', *Journal of Membrane Science*, 436, pp. 163-173. <https://doi.org/10.1016/j.memsci.2013.02.009>
- Zhang, G., Lu, S., Zhang, L., et al. (2013b) 'Novel polysulfone hybrid ultrafiltration membrane prepared with TiO₂-g-HEMA and its antifouling characteristics', *J. Membr. Sci.*, 436, pp. 163-173. <https://doi.org/10.1016/j.memsci.2013.02.009>
- Zhang, Q., Wang, H., Fan, X., et al. (2015) 'A controlled wet-spinning and dip-coating process for preparation of high-permeable TiO₂ hollow fiber membranes', *Water Science and Technology*, 73, pp. 725-733. 10.2166/wst.2015.543
- Zhang, S., Qu, Y., Liu, Y., et al. (2005b) 'Experimental study of domestic sewage treatment with a metal membrane bioreactor', *Desalination*, 177, pp. 83-93. <https://doi.org/10.1016/j.desal.2004.10.034>
- Zhang, S., Wang, P., Fu, X., et al. (2014a) 'Sustainable water recovery from oily wastewater via forward osmosis-membrane distillation (FO-MD)', *Water Res.*, 52, pp. 112-121. <https://doi.org/10.1016/j.watres.2013.12.044>
- Zhang, W.-d., Sun, W., Yang, J., et al. (2009) 'The study on pervaporation behaviors of dilute organic solution through PDMS/PTFE composite membrane', *Appl. Biochem. Biotechnol.*, 160, pp. 156. <https://doi.org/10.1007/s12010-009-8582-3>
- Zhang, W., Xu, Y., Yu, Z., et al. (2014b) 'Separation of acetic acid/water mixtures by pervaporation with composite membranes of sodium alginate active layer and microporous polypropylene substrate', *J. Membr. Sci.*, 451, pp. 135-147. <https://doi.org/10.1016/j.memsci.2013.09.027>
- Zhang, X., Scott, J., Sharma, B. K., et al. (2018a) 'Advanced treatment of hydrothermal liquefaction wastewater with nanofiltration to recover carboxylic acids', *Environ. Sci. Water. Res. Technol.*, 4, pp. 520-528. <https://doi.org/10.1039/C8EW00007G>
- Zhang, X., Scott, J., Sharma, B. K., et al. (2018b) 'Advanced treatment of hydrothermal liquefaction wastewater with nanofiltration to recover

- carboxylic acids', *Environ. Sci.: Water. Res. Technol.*, 4, pp. 520-528. <https://doi.org/10.1039/C8EW00007G>
- Zhang, Y. & Angelidaki, I. (2015) 'Bioelectrochemical recovery of waste-derived volatile fatty acids and production of hydrogen and alkali', *Water. Res.*, 81, pp. 188-195. <https://doi.org/10.1016/j.watres.2015.05.058>
- Zhang, Z., Xu, Z., Song, X., et al. (2020) 'Membrane processes for resource recovery from anaerobically digested livestock manure effluent: Opportunities and challenges', *Curr. Pollut. Rep.*, 6, pp. 123-136. <https://doi.org/10.1007/s40726-020-00143-7>
- Zhao, C., Xue, J., Ran, F., et al. (2013) 'Modification of polyethersulfone membranes—a review of methods', *Prog. Mater. Sci.*, 58, pp. 76-150. <https://doi.org/10.1016/j.pmatsci.2012.07.002>
- Zhao, L. & Ho, W. S. W. (2014) 'Novel reverse osmosis membranes incorporated with a hydrophilic additive for seawater desalination', *J. Membr. Sci.*, 455, pp. 44-54. <https://doi.org/10.1016/j.memsci.2013.12.066>
- Zhao, R., Wang, Y., Li, X., et al. (2015a) 'Water-insoluble sericin/ β -cyclodextrin/PVA composite electrospun nanofibers as effective adsorbents towards methylene blue', *Colloids and Surfaces B: Biointerfaces*, 136, pp. 375-382. <https://doi.org/10.1016/j.colsurfb.2015.09.038>
- Zhao, R., Wang, Y., Li, X., et al. (2015b) 'Synthesis of β -Cyclodextrin-Based Electrospun Nanofiber Membranes for Highly Efficient Adsorption and Separation of Methylene Blue', *ACS Applied Materials & Interfaces*, 7, pp. 26649-26657. 10.1021/acsami.5b08403
- Zhao, X.-x., Fan, X.-l., Xue, Z.-x., et al. (2017) 'Simultaneous production of hydrogen and volatile fatty acids from anaerobic digestion of *Macrocyctis pyrifera* biomass residues', *Journal of Central South University*, 24, pp. 1281-1287. <https://doi.org/10.1007/s11771-017-3533-6>
- Zheng, G., Jiang, J., Wang, X., et al. (2020) 'Nanofiber membranes by multi-jet electrospinning arranged as arc-array with sheath gas for electro dialysis applications', *Materials & Design*, 189, pp. 108504. <https://doi.org/10.1016/j.matdes.2020.108504>
- Zheng, X., Ni, C., Xiao, W., et al. (2022) 'Ionic liquid grafted polyethersulfone nanofibrous membrane as recyclable adsorbent with simultaneous dye, heavy metal removal and antibacterial property', *Chemical Engineering Journal*, 428, pp. 132111. <https://doi.org/10.1016/j.cej.2021.132111>
- Zheng, X., Yinguang, C. & Chenchen, L. (2010) 'Waste activated sludge alkaline fermentation liquid as carbon source for biological nutrients removal in anaerobic followed by alternating aerobic-anoxic sequencing batch reactors', *Chin. J. Chem. Eng.*, 18, pp. 478-485. [https://doi.org/10.1016/S1004-9541\(10\)60246-7](https://doi.org/10.1016/S1004-9541(10)60246-7)
- Zhou, F., Li, K., Hang, F., et al. (2022) 'Efficient removal of methylene blue by activated hydrochar prepared by hydrothermal carbonization and NaOH activation of sugarcane bagasse and phosphoric acid', *RSC Advances*, 12, pp. 1885-1896. 10.1039/D1RA08325B

- Zhou, F., Wang, C. & Wei, J. (2013a) 'Separation of acetic acid from monosaccharides by NF and RO membranes: performance comparison', *J. Membr. Sci.*, 429, pp. 243-251. <https://doi.org/10.1016/j.memsci.2012.11.043>
- Zhou, F., Wang, C. & Wei, J. (2013b) 'Simultaneous acetic acid separation and monosaccharide concentration by reverse osmosis', *Bioresour. Technol.*, 131, pp. 349-356. <https://doi.org/10.1016/j.biortech.2012.12.145>
- Zhou, T., Li, J., Guo, X., et al. (2019) 'Freestanding PTFE electrospun tubular membrane for reverse osmosis brine concentration by vacuum membrane distillation', *Desalin. Water Treat.*, 165, pp. 63-72. <https://doi.org/10.5004/dwt.2019.24499>
- Zhu, J., Qin, L., Uliana, A., et al. (2017) 'Elevated performance of thin film nanocomposite membranes enabled by modified hydrophilic mofs for nanofiltration', *ACS. Appl. Mater. Interfaces.*, 9, pp. 1975-1986. <https://doi.org/10.1021/acsami.6b14412>
- Zhu, X., Cheng, X., Luo, X., et al. (2020a) 'Ultrathin thin-film composite polyamide membranes constructed on hydrophilic poly(vinyl alcohol) decorated support toward enhanced nanofiltration performance', *Environ. Sci. Technol.*, 54, pp. 6365-6374. <https://doi.org/10.1021/acs.est.9b06779>
- Zhu, X., Leininger, A., Jassby, D., et al. (2021a) 'Will membranes break barriers on volatile fatty acid recovery from anaerobic digestion?', *ACS. EST. Engg.*, 1, pp. 141-153. <https://doi.org/10.1021/acsestengg.0c00081>
- Zhu, Y., Galier, S. & Balmann, H. R.-d. (2020b) 'Nanofiltration of solutions containing organic and inorganic salts: Relationship between feed and permeate proportions', *J. Membr. Sci.*, 613, pp. 118380. <https://doi.org/10.1016/j.memsci.2020.118380>
- Zhu, Y., Galier, S. & Roux-de Balmann, H. (2021b) 'Description of the variation of retention versus pH in nanofiltration of organic acids', *J. Membr. Sci.*, 637, pp. 119588. <https://doi.org/10.1016/j.memsci.2021.119588>
- Zhu, Y., Galier, S. & Roux-de Balmann, H. (2021c) 'Description of the variation of retention versus pH in nanofiltration of organic acids', *Journal of Membrane Science*, 637, pp. 119588. <https://doi.org/10.1016/j.memsci.2021.119588>
- Zhu, Y., Yi, B., Yuan, Q., et al. (2018) 'Removal of methylene blue from aqueous solution by cattle manure-derived low temperature biochar', *RSC Adv.*, 8, pp. 19917-19929. 10.1039/C8RA03018A
- Zielińska, M. & Galik, M. (2017) 'Use of Ceramic Membranes in a Membrane Filtration Supported by Coagulation for the Treatment of Dairy Wastewater', *Water, Air, & Soil Pollution*, 228, pp. 173. 10.1007/s11270-017-3365-x
- Zinder, S. H., Anguish, T. & Cardwell, S. C. (1984) 'Selective inhibition by 2-bromoethanesulfonate of methanogenesis from acetate in a thermophilic anaerobic digester', *Applied and Environmental Microbiology*, 47, pp. 1343-1345. <https://doi.org/10.1128/aem.47.6.1343-1345.1984>
- Zulaikha, S., Lau, W. J., Ismail, A. F., et al. (2014) 'Treatment of restaurant wastewater using ultrafiltration and nanofiltration membranes', *Journal of*

References

Water Process Engineering, 2, pp. 58-62.
<https://doi.org/10.1016/j.jwpe.2014.05.001>